AFIT/GE/EN/91D-14

AD-A243 792

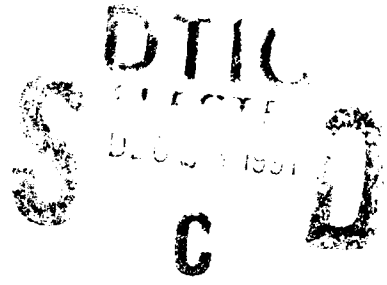

PROPORTIONAL PLUS INTEGRAL CONTROL OF AIRCRAFT FOR AUTOMATED MANEUVERING FORMATION FLIGHT

THESIS

John L. Dargan
Captain, USAF

AFIT/GE/EN/91D-14

Approved for public release; distribution unlimited

91-19042

91 12 24 074

December 1991 Master's Thesis

Proportional Plus Integral Control of Aircraft for Automated Maneuvering Formation Flight

John L. Dargan
Captain, USAF

Air Force Institute of Technology
WPAFB OH 45433-6583

AFIT/GE/ENG/91D-14

WL/FIGX
WPAFB OH 45433

Approved for Public Release; Distribution Unlimited.

In this study an automated formation control system for a lead and wing aircraft flight is developed. The proposed formation control system is capable of controlling like or dissimilar aircraft in maneuvering formation flight. Thus, two versions of the C-130 aircraft, the C-130A and the C-130B, are modelled. The C-130B has superior performance characteristics to that of the C-130A. The wing aircraft continuously measures lead aircraft position with an ideal on-board relative position sensor, maneuvering to maintain relative position. External formation guidance is assumed to be released in a single data burst, consisting of formation geometry and nominal separation commands for each aircraft in the formation. No continuous communication is assumed between formation aircraft. Simulation of the formation control system reveals that a controller is needed to alleviate the steady state errors in separation distance after a formation maneuver is executed. Hence, a Proportional plus Integral formation system control has been developed, which allows aircraft with differing performance capabilities to safely and effectively execute all maneuvers evaluated in the study. Moreover, the formation control system is shown to satisfactorily operate independent of the aircraft or formation configuration being flown. There is zero steady state error for all maneuver and separation distance responses, and the transients are such that no collision occurs between the aircraft in the formation. Open loop and controlled time responses, as well as flight path responses, are presented for comparison.

Formation Control System, Automated Control Systems, PI Control, Formation Flight Control, 183

Unclassified Unclassified Unclassified UL

AFIT/GE/EN/91D-14

PROPORTIONAL PLUS INTEGRAL CONTROL OF AIRCRAFT FOR AUTOMATED MANEUVERING FORMATION FLIGHT

THESIS

Presented to the Faculty of the School of Engineering
of the Air Force Institute of Technology
Air University
In Partial Fulfillment of the
Requirements for the Degree of
Master of Science in Electrical Engineering

John L. Dargan, B.S.E.E.
Captain, USAF

December 1991

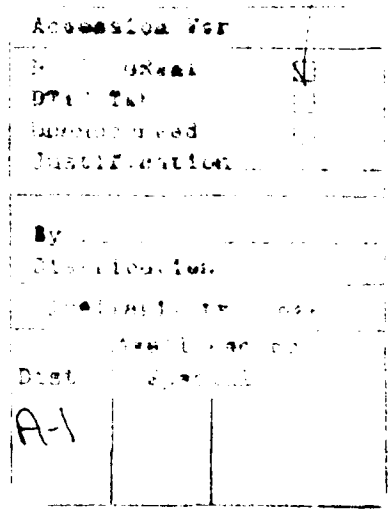

Approved for public release; distribution unlimited

Preface

I would like to extend my sincere gratitude to Dr. D'Azzo and Dr. Pachter for their time, guidance, and interest, without which this research would not have been completed. I would especially like to share the accomplishment of this research with my wife, JenRa, my father in-law and mother in-law, Raymond and Jeannette Jackson, and my parents, John H. and Ernestine Dargan. The love and support of my wife, while not apparent in the text of this document, was greatly needed and was sincerely appreciated throughout the duration of this endeavor. I am grateful to my in-laws for the numerous times they performed tasks that were rightfully mine, particularly home improvement tasks, because I was buried in thesis research. Their assistance and support is sincerely appreciated. I also am grateful for the long-distance support and encouragement given by my parents throughout this endeavor. Although they never saw first hand what was involved in this research, their concern, encouragement, and interest was extremely beneficial.

John L. Dargan

Table of Contents

List of Figures

List of Tables

Abstract

In this study an automated formation control system for a lead and wing aircraft flight is developed. The proposed formation control system is capable of controlling like or dissimilar aircraft in maneuvering formation flight. Thus, two versions of the C-130 aircraft, the C-130A and the C-130B, are modelled. The C-130B has superior performance characteristics to that of the C-130A.

The wing aircraft continuously measures lead aircraft position with an ideal on-board relative position sensor, maneuvering to maintain relative position. External formation guidance is assumed to be released in a single data burst, consisting of formation geometry and nominal separation commands for each aircraft in the formation. No continuous communication is assumed between formation aircraft.

Simulation of the formation control system reveals that a controller is needed to alleviate the steady state errors in separation distance after a formation maneuver is executed. Hence, a Proportional plus Integral formation system control has been developed, which allows aircraft with differing performance capabilities to safely and effectively execute all maneuvers evaluated in the study. Moreover, the formation control system is shown to satisfactorily operate independent of the aircraft or formation configuration being flown. There is zero steady state error for all maneuver and separation distance responses, and the transients are such that no collision occurs between the aircraft in the formation. Open loop and controlled time responses, as well as flight path responses, are presented for comparison.

PROPORTIONAL PLUS INTEGRAL CONTROL OF AIRCRAFT FOR AUTOMATED MANEUVERING FORMATION FLIGHT

I. INTRODUCTION

1.1 Overview of the Thesis

The introduction and general background to the formation control problem considered in this research are provided in Chapter I. A literature search on formation flight and formation flight control systems is provided in Chapter II. Technical aspects, control theory background, and the formation control system simulation development are described in Chapter III. The design of the proportional plus integral controller is described in Chapter IV. A thorough evaluation of formation control system performance in which the performance of the lead aircraft is superior to that of the wing aircraft is presented in Chapter V. A thorough evaluation of the formation control system performance in which the lead aircraft and wing aircraft both have similar superior performance is presented in Appendix A. An evaluation of formation control system performance in which the lead aircraft has a degraded performance capability compared to the wing aircraft is presented in Appendix B, and an evaluation of formation control system performance in which the lead aircraft and wing aircraft both have degraded performance is presented in Appendix C. Overall conclusions and areas requiring further study are presented in Chapter VI.

1.2 Background

Air Force flying missions include air-to-air combat, air-to-ground combat, strategic bombing, refueling, and personnel and cargo transport. Advancements in avionics and computer technology increase mission effectiveness in all of these flying operations. These system enhancements vastly improve the performance of the aircraft and provide the pilot with a better situational awareness. However, pilot workload has increased significantly, leading to pilot saturation, the point where the pilot can no longer assimilate the information that is being presented to him from the cockpit displays or warning systems. For example, pilots flying combat missions in Vietnam could not hear the tones from their missile warning systems because they were so busy with the other tasks involved with combat flying. These tones were indications that a missile could be in pursuit of their aircraft. Eventually, the pilots decided not to turn on the missile warning system since it provided no benefit during the heat of combat (11). Thus, automation of some pilot functions would be of great help.

The Air Force Special Operations Forces (SOF) mission requires a high pilot workload. SOF pilots are tasked to conduct overt, clandestine, or covert missions which can range from routine training missions to highly sensitive missions of national importance (11). These missions entail formation flights and emphasize concealment and secrecy. To decrease the probability of detection, these missions are often flown in close formation at night and at low altitudes with similar or dissimilar aircraft (11). Several formations and maneuvers are flown by the SOF. Figure 1.1 shows a diamond formation, and Figure 1.2 shows a trail formation. The diamond configuration allows good relative visibility between formation aircraft. The trail configuration is an important one with regard to covert operations, as the minimum amount of landmass is overflown; this translates to a reduced probability of detection by ground forces.

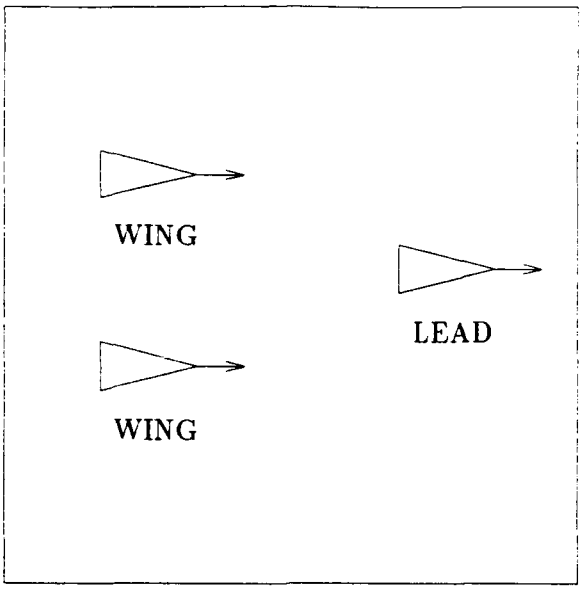

Figure 1.1. Diamond Formation

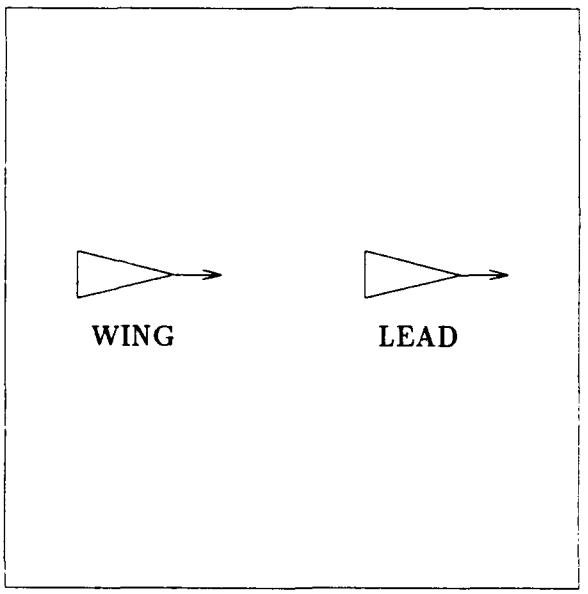

Figure 1.2. Trail Formation

The nature of the SOF missions require that the pilots perform many tasks while flying. Chief among these tasks is maintaining the desired formation while performing a maneuver such as a change in course or change in formation speed. Therefore, the potential for pilot saturation and pilot fatigue is high, and automation of station keeping/formation flying would be most welcome.

Figure 1.3 illustrates a trail formation heading change maneuver. Figure 1.4 illustrates a diamond formation heading change maneuver, Figure 1.5 illustrates an abreast formation heading change maneuver, and Figure 1.6 shows a terrain avoidance maneuver performed by a trail formation.

The particular formation flown during a certain mission segment varies. A long cruise portion of the mission may employ a loose diamond pattern, while penetration segments may require a close trail pattern in order to overfly a narrow threat corridor or valley permitting only single file passage (10:15). Overall, formations can change frequently during a typical mission, in order to optimally meet the demands of a changing environment.

Formation change maneuvers are considered for transition from trail to diamond formations, and from diamond to trail, as shown in Figure 1.7 and Figure 1.8, respectively. Because of the close proximity of the aircraft in the formation and the low altitude, there is little room for pilot error. Therefore, in order to improve the effectiveness of the SOF missions, the problem of pilot fatigue and pilot saturation needs to be addressed.

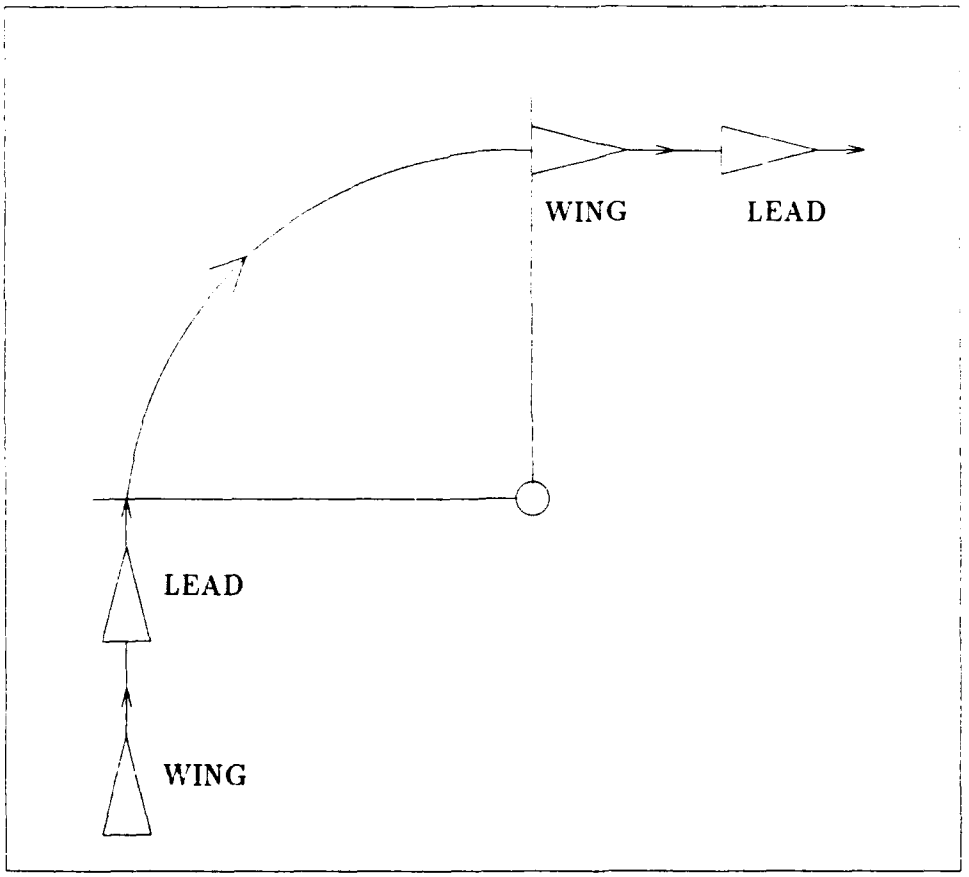

Figure 1.3. 90 Degree Heading Change Maneuver - Trail Formation

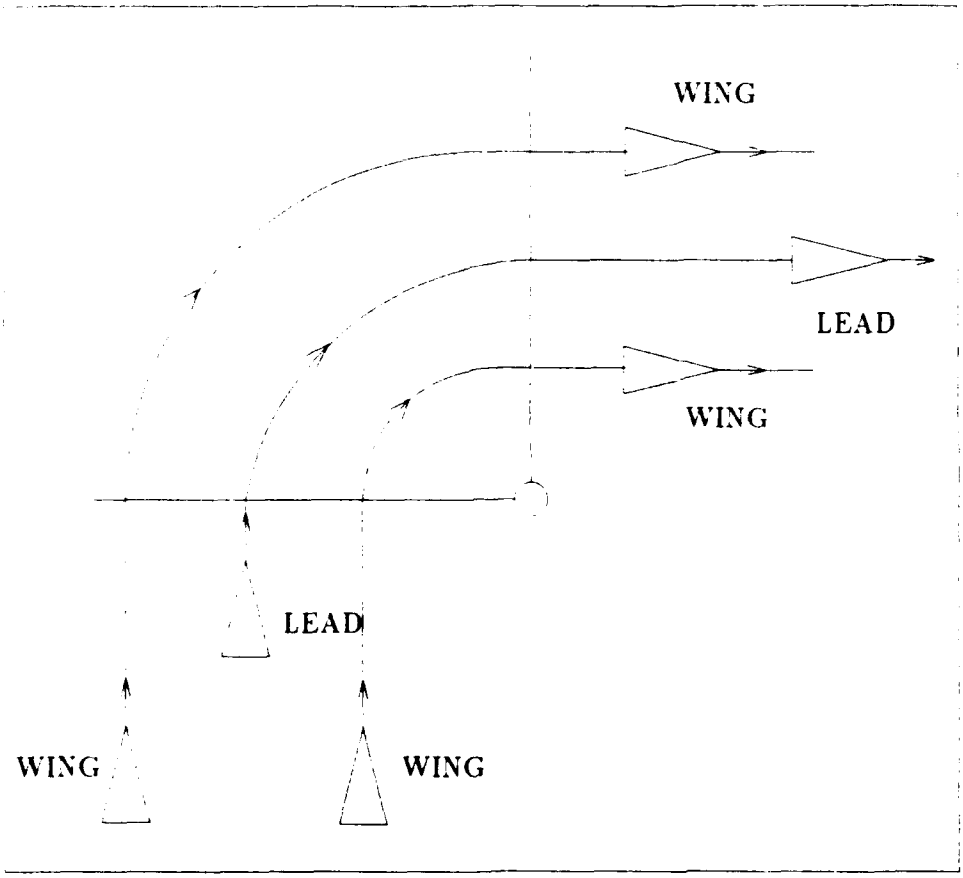

Figure 1.4. 90 Degree Heading Change Maneuver - Diamond Formation

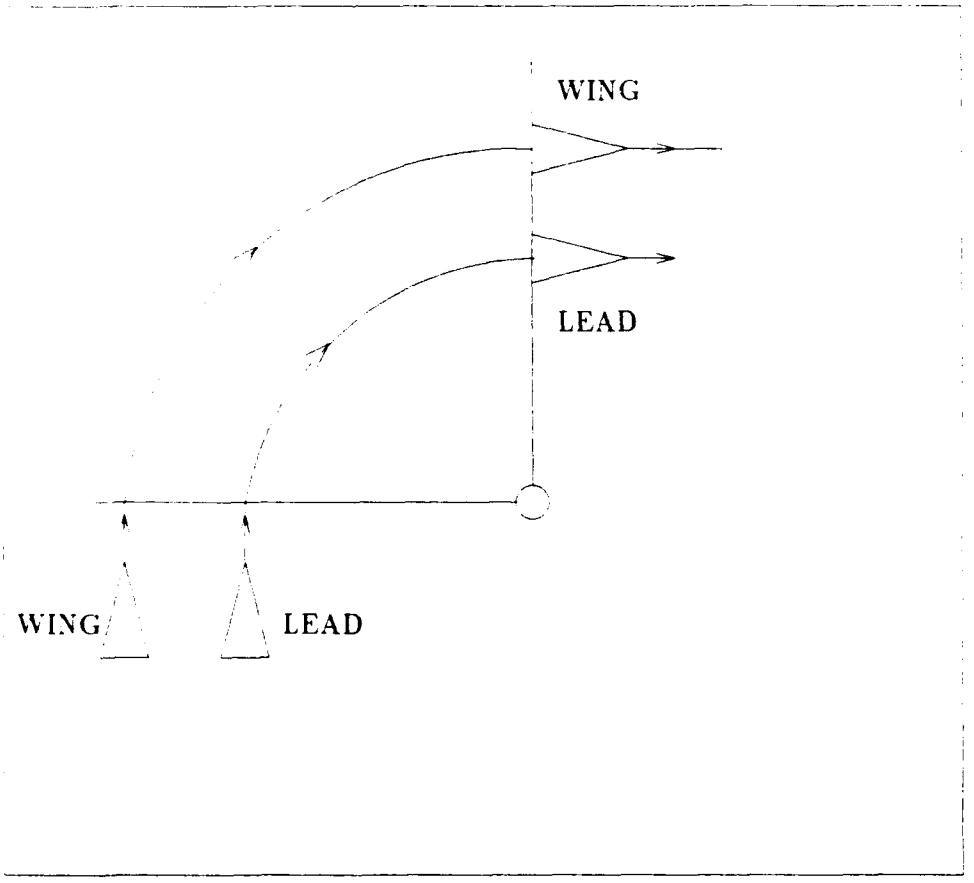

Figure 1.5. 90 Degree Heading Change Maneuver - Abreast Formation

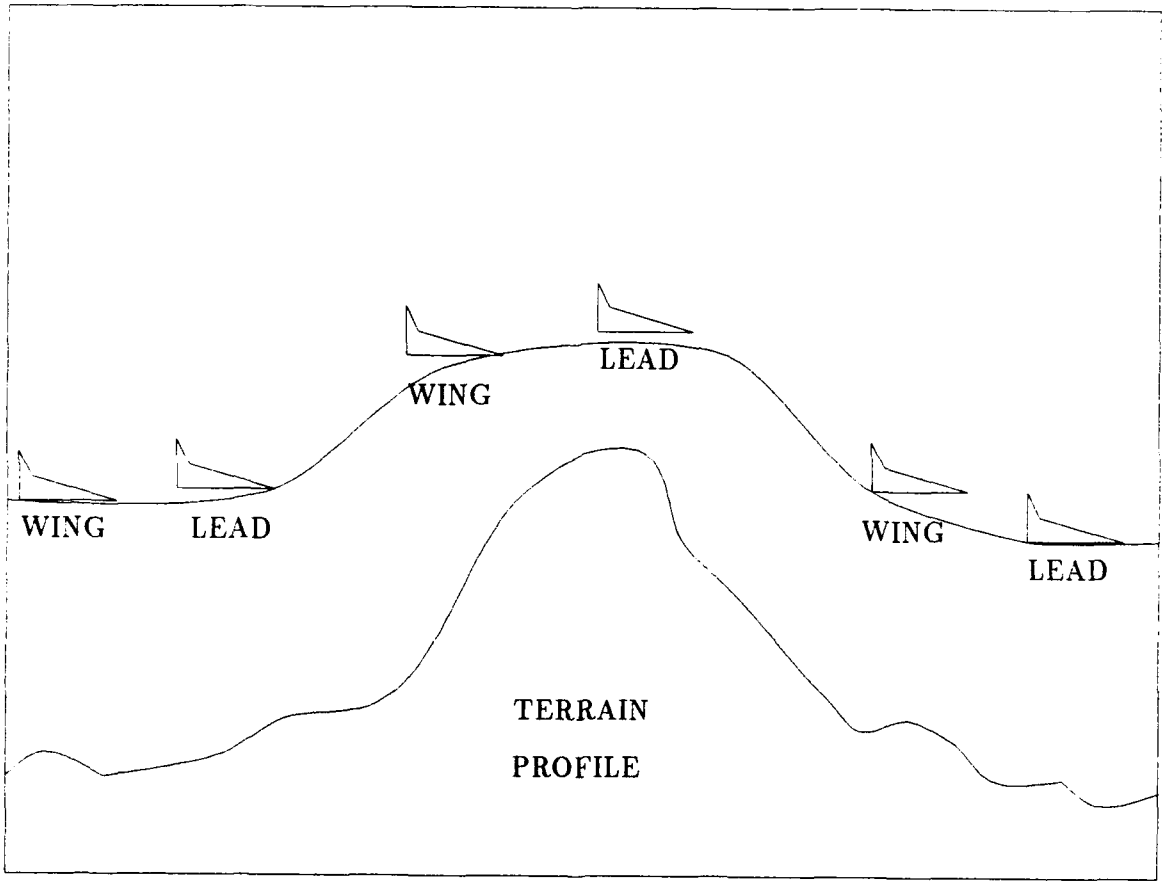

Figure 1.6. Terrain Avoidance Maneuver

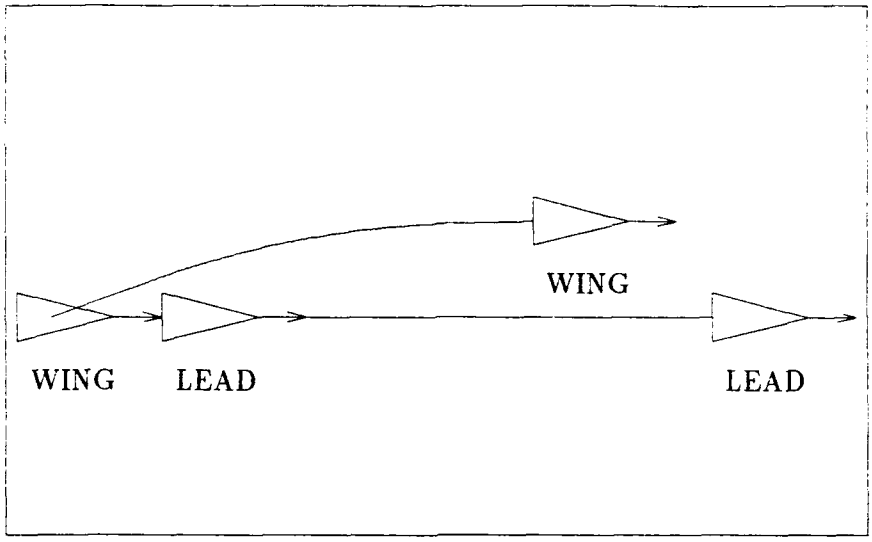

Figure 1.7. Formation Change Maneuver - Trail to Diamond

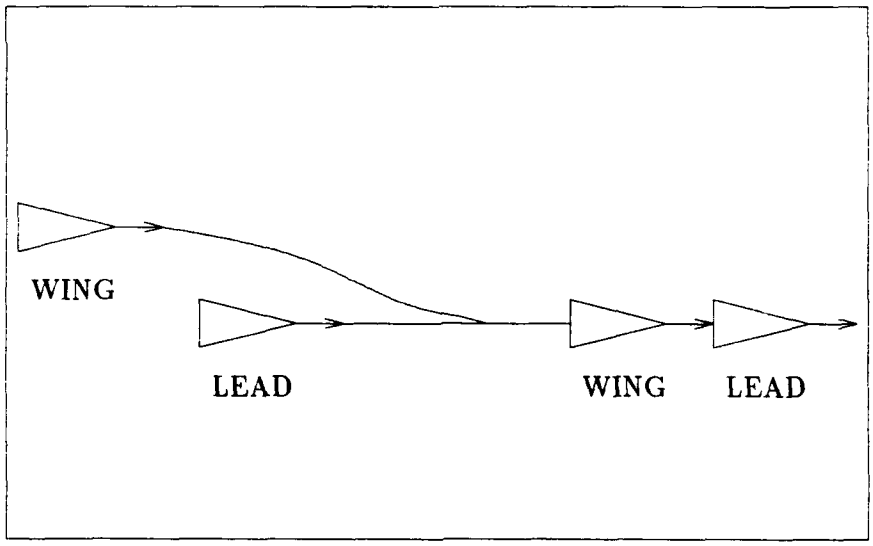

Figure 1.8. Formation Change Maneuver - Diamond to Trail

1.3 Problem Statement

The problem of improving the effectiveness of SOF missions is addressed in this thesis. These missions typically involve reaching the target in a safe and timely

manner, payload delivery, and safe return to base. Mission effectiveness will be enhanced by an automated formation control system that maintains the desired formations throughout the mission. Automated formation control will free the pilots from the background tasks involved with manually maintaining the formation. With such a system, pilot fatigue and saturation will decrease, and the pilots will then be free to concentrate on the other tasks involved with executing the mission. Thus, the purpose of this study is to develop an automated formation control system to control a number of like or dissimilar aircraft in maneuvering formation flight.

1.4 Summary of Current Knowledge

Captain Rohs' recent thesis research (10) at the Air Force Institute of Technology investigated the development of a formation control system capable of controlling a number of like or dissimilar aircraft in maneuvering, formation flight. The system was developed and evaluated through digital computer simulation. The research effort employed diamond and trail formations of like and dissimilar aircraft and used three separate formation maneuvers: (1) a formation turn or heading change, (2) a terrain clearing maneuver such as a ridge crossing, (3) and a change in formation from diamond to trail formation and return to diamond (10:11). Aircraft position was measured in a Cartesian coordinate axis system. One axis was defined for the longitudinal displacement, another axis was for the lateral displacement, and the third axis was for vertical displacement. After a maneuver by the lead aircraft, the wing aircraft senses the new position of the lead aircraft and then reduces the errors simultaneously in each of the three axes, thereby causing the whole aircraft formation to perform the maneuver. This research assumed that formation position was obtained from noiseless and ideal on-board sensors. Rohs concluded that it is possible to control formations of like or dissimilar aircraft with a fully coupled, multivariable control strategy (10:99).

1.5 Research Objective

The objective of this thesis is to determine whether or not the automated formation control system that was developed and simulated by Captain Rohs can be extended to control formations of like or dissimilar aircraft under more realistic conditions.

1.6 Research Questions

The following questions are answered in this thesis.

1. Can an open-loop, uncontrolled formation system maintain the formation and separation distance?
2. Can velocity, heading, and altitude feedback be used to successfully track the commanded formation separation distances and maneuvers with zero steady state error?
3. Can a linear Proportional plus Integral (PI) controller be designed that satisfactorily controls a nonlinear formation control system?
4. Can one set of gains be derived for the PI controller that provides satisfactory formation control for all maneuvers?
5. Does the proportional plus integral controller perform better when formation separation error is controlled, or when both formation separation error and maneuver (velocity and heading) error are controlled?

1.7 Assumptions

In support of the research objective and questions listed earlier, a number of assumptions must be identified, so that this research effort can achieve reasonable results.

The existence of overall formation command guidance is assumed and not addressed as part of this research. It is assumed that formation guidance comes from

pre-flight mission planning, on-board sensors, lead pilot decision, or a combination of these factors. Each aircraft receives the overall formation control input vector as a single data burst and operates on these parameters. This is justified because, currently, pre-flight mission planning is used to determine both the formation maneuvers and separation distances for any mission requiring formation flight.

This research does not require the exact, high order models of the aircraft. Aircraft simulation models are developed which reproduce the overall flight path vector and dynamic responses of the aircraft modelled. Thus, simple, first-order aircraft models are used in this research. This is justified because these first-order models approximately reproduce the required dynamic closed loop behavior of the aircraft with internal control systems or autopilots.

It is assumed that each individual aircraft is capable of automated control to effect the desired flight path control commands necessary to perform the formation maneuver and/or maintain the desired formation. Thus, each aircraft is assumed capable of adjusting its forward velocity to control relative separation along the flight path vector, performing coordinated turns for lateral separation control, and climbing or descending for vertical separation. In other words, the aircraft are equipped with three-channel autopilots.

The wing aircraft is assumed to possess an on-board sensor capable of providing precise position measurements relative to the lead aircraft. Thus, wing aircraft sensor measurement data is used to track the maneuvering of the lead aircraft.

The formation control system developed in this research is comprised of only two aircraft, a lead aircraft (L) and a wing aircraft (W). The lead and wing aircraft may have similar performance characteristics, or dissimilar characteristics.

The initial conditions for all formation maneuvers are straight, level, unaccelerated flight in a constant formation. Formation maneuvers are executed one at a time.

1.8 Scope

The overall objective of determining whether an automated formation control system can operate successfully under realistic simulation conditions is achieved. The formation control system that is designed for this research is developed and simulated through the use of the $MATRIX_x$ CAD tool. Two derivatives of the C-130 aircraft are modelled in this research, the C-130A and C-130B. Also, no specific sensor is modelled in this research. Exact aircraft and sensor models are not used in order to confine this research effort to a reasonable level. In the present formulation, the formation is basically being driven by the lead aircraft maneuvers. Although control of the lead aircraft is an aspect of formation control that must be investigated, this research focuses only on control of the wing aircraft. Therefore, this research addresses the 'inner-loop' of formation control. Finally, this research is not intended to result in the fabrication of the hardware necessary to field an automated formation control system. Thus, hardware specifications such as weight, power requirements, and dimensions are not addressed.

1.9 Standards

The usual control system standards, (3:73-100), are used for this research. Step inputs of various magnitudes are applied to the formation control system, and the resulting system time responses are obtained. In the analysis of these time responses, the transient and steady state behavior of the formation control system are compared. Peak overshoot, settling time, rise time, stability, and steady state error are determined.

1.10 Approach/Methodology

The formation control system that was developed and simulated by Rohs serves as the foundation for this research. The same system models and a similar implementation of the formation control system used by Rohs are also used in this research.

Simulation of the formation control system is accomplished next. The formation geometries and formation maneuvers used in Rohs' research are used as well in this research. However, the geometric modeling has been enhanced to include non-linear dynamics, based on a moving coordinate reference frame that is affixed to the wing aircraft. These formations and maneuvers are described and illustrated in section 1.2.

After verification of the simulation, a PI controller is designed and implemented in the formation control system. The system is then simulated to determine how well the PI controller works.

The premise of using Rohs' formation control system design as a starting point is justified since his research showed that the system worked under the given assumptions. Therefore, since a system has been previously designed and has been shown to work, it is not necessary to start over and design a completely new system.

1.11 Benefits of the Research

This research provides a method of implementing a formation control system which uses a proportional plus integral controller to track formation maneuver commands and separation commands. Currently, the Intra Formation Positioning System (IFPS) program that is sponsored by the Flight Dynamics Laboratory is addressing this very issue of formation flight control. This thesis provides an additional independent approach to formation flight control, and the results provide a benchmark formation control system that performs well. Thus, information and ideas obtained from this thesis may be used in the IFPS program to help solve a real-world problem.

1.12 Materials and Equipment

The only equipment required are the SPARC work-station computers and the $MATRIX_x$ computer aided design tool. This equipment is available for use in the AFIT/ENG computer lab located in room 133 in building 640.

II. LITERATURE REVIEW

2.1 Introduction

The literature dealing with the application of control theory to aircraft formation flight, the development of the equation of Coriolis, Porter's Method for controller design, and the Joint Tactical Information Distribution System (JTIDS) is reviewed. This review gives the background information needed to develop a simulation model of a formation control system for the SOF aircraft.

2.2 U.S. Army Formation Flight Studies

During the mid 1960's, the U.S. Army conducted a formation flight study to determine the feasibility of developing a formation flight control system for Army aircraft. Both automatic and manual operation were considered. The study concluded that a formation flight control system consisting of a sensing/ measuring system, displays and controls, control laws using a lead aircraft-based coordinates geometry, and hybrid analog-digital data processing, offered the best promise for development of a tactical formation flight control system by 1970 (12:147). The study showed that a slave aircraft oriented coordinate system and related control laws were unsatisfactory, due to the sluggish response of the formation flight control system and due to the system's instability in certain situations. However, a formation flight control system based upon a lead aircraft oriented coordinate system and related control laws had sufficient stability and speed of response. Also, it was concluded that autopilots would enhance the performance of the formation flight control system and relieve the pilot of some of the burdensome tasks required during formation flight (12:148).

2.3 Drone Formation Control Systems

In the mid 1960's, the U.S. Navy developed the control laws for a full-scale aircraft drone target, the QF-4. Two drones were flown together to form a two-target formation in straight and level flight at the flight condition of Mach 0.85 and 2,500 feet altitude (6:3). The purpose of the drone automatic formation control system was to present a realistic threat formation for missile weapon system development. The drone formation control system was based upon a lead aircraft and slave aircraft concept. A three axes inertial coordinate system was established for the aircraft. One axis represented the longitudinal direction, another axis represented the lateral direction, and the third axis represented the vertical direction. Initial and desired separation distances in the three inertial axes were given to the slave aircraft at time zero (6:3). The slave aircraft then maneuvered to reduce the errors along all three inertial axes simultaneously. The lead drone aircraft and the slave drone aircraft were controlled by separate controllers. The slave aircraft was maneuvered by its operator to keep the lead aircraft in the center of the field of view of the television tracking camera (6:4).

2.4 The Equation of Coriolis

The rate of change of a vector is different when viewed from different axes systems (1:489). When there are two or more axes systems rotating relative to each other, the need for using the Coriolis equation arises . The equation of Coriolis can be summarized in the following manner. The motion of an object as viewed from a reference frame is equal to the motion as seen from the moving frame, plus the motion resulting from the relative angular velocity of the moving frame with respect to the reference frame (1:489). Figure 2.1 illustrates this concept.

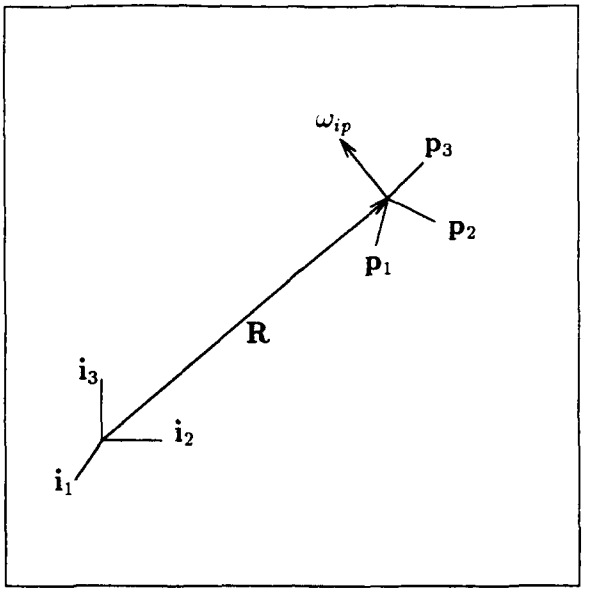

Figure 2.1. Representation of the Equation of Coriolis

Thus, the equation of Coriolis can be written as

$$\dot{\mathbf{R}}_i = \dot{\mathbf{R}}_p + \omega_{ip} \times \mathbf{R} \tag{2.1}$$

$\dot{\mathbf{R}}_i$ is the velocity of the point in question relative to the frame i, $\dot{\mathbf{R}}_p$ is the velocity vector of the point in question relative to the moving frame, and ω_{ip} is the angular velocity of frame p with respect to frame i. The equation of Coriolis is also referred to as the velocity transformation law.

2.5 Porter's Design Method

Output decoupling is an essential requirement in many multi-input multi-output (MIMO) control systems. Some design methods require that all the states must be fed back in order to achieve output decoupling. Depending upon the dimension of the state vector, it may not be physically possible to include enough sensors which will measure all of the states. It may be necessary in this case to

use a state estimator or observer to reconstruct the states, and then feed back these estimated states. However, a control design method which uses only output feedback to generate an error vector avoids the requirement for measuring or reconstructing the entire state vector. One such method is that developed by Brian Porter (8) (9). His method of designing a high gain proportional plus integral controller produces output decoupling and leads to very fast tracking of the command input by the output. The MIMO plant is represented by the standard state and output equations, of the respective forms:

$$\dot{\mathbf{x}}(t) = \mathbf{A}\mathbf{x}(t) + \mathbf{B}\mathbf{u}(t) \tag{2.2}$$

$$\mathbf{y}(t) = \mathbf{C}\mathbf{x}(t) \tag{2.3}$$

A requirement for Porter's design method is that the matrix product **CB** have full rank. When **CB** has full rank the plant is described as regular. When **CB** does not have full rank the plant is described as irregular. In the case of regular plants the controller implements a proportional plus integral control law in the forward loop of the control system. In the case of irregular plants, the proportional plus integral control is augmented with an inner-loop which provides extra measurements for control purposes (3:660-661).

2.6 Joint Tactical Information Distribution System

Operational experience in Vietnam illustrated the importance to air operations of a real-time command and control network. As a result, the need for the Joint Tactical Information Distribution System (JTIDS) was developed. JTIDS is a secure, jam resistant, near real-time information network which provides integrated tactical, communication, identification and navigation data (4:1). Design of JTIDS is based on a pseudo-noise modulated, frequency hopped signal characteristic which provides

data communications on a rigidly structured time division access basis (2:1). Information provided by JTIDS is primarily presented to the pilot on one of the cockpit displays. Since the information is displayed, more than one piece of data can be presented simultaneously. This provides a wide variety of data to the pilot at any given moment. The advantage of JTIDS is increased situational awareness for the pilot, thereby enhancing survivability and effectiveness.

Use of code division multiplex techniques superimposed on the basic Time Division Multiple Access (TDMA) structure allows multi-netted JTIDS operation. Each participating subscriber is assigned to operate on one or more networks and is allocated specific time slots during which it may transmit information on a specific network. Each subscriber may receive information during all time slots not used to transmit (2:2).

In the case where there are two or more fixed and surveyed JTIDS community members, or in the case where there are two or more surveyed members who have accurate knowledge of position such as from GPS, relative navigation of the subscribers in the network can be accomplished. Through periodic reporting of the surveyed members' position, other users could use range measurements from such members to locate themselves in the surveyed members' coordinate system. Relative navigation provides consistency of position location among all elements, as well as the data derived from other sensors whose measurements are made in the JTIDS relative grid (2:3).

JTIDS operates in the 960-1215 MHz frequency range, the same band used for IFF and range measuring equipment. System power is sufficient for line of sight ranges up to 500 nautical miles, and can be extended up to 1200 nautical miles through the use of airborne relays (5:10).

JTIDS gains its jam resistant capability through TDMA, frequency hopping, and direct sequence pseudo-noise. The TDMA architecture divides each 24 hour day into 112.5 epochs. An epoch is 12.8 minutes long and is divided into 98,304 time

slices. The 98,304 time slices are divided into three interleaved sets, each containing 32,768 time slices. Each time slice is 7.8125 ms long. The basic message unit is a time slot which is a subset of the time slice. The details of the time slot are classified (5:10).

JTIDS is capable of distributing data in free text or in a standard message format. The system can handle free text at 28.9 KBPS and standard message formats at 59.5 KBPS. Digitized voice can be handled at 16 KBPS (5:11).

III. SIMULATION DEVELOPMENT

3.1 Aircraft and Formation System Overview

The C-130A and C-130B aircraft models that were developed in Rohs' thesis are used in this research. Rohs developed these models based on information gleaned from extensive conversations with C-130 SOF pilots, aircraft DASH 1 manuals, and from flight test data obtained from the Air Force Flight Test Center. Control surface inputs and aircraft responses are not modelled. The models do however encompass flight path control inputs and responses, such as those considered in autopilot systems. These rudimentary aircraft models are first-order and over-damped and match the overall closed loop velocity, heading, and altitude responses of the respective aircraft. Delays representative of the respective aircraft are listed in Table 3.1 (10:28) for completeness, but they are not used in this work..

Aircraft ownship control inputs that normally correspond to autopilot settings command the formation flight control system of the wing aircraft to a set point, relative to the lead aircraft. Individual aircraft flight path control commands are velocity, magnetic heading, and altitude. The reference parameters used to control the wing aircraft and the formation geometry are the longitudinal, lateral, and vertical separation distances that the wing aircraft is commanded to maintain with respect to the lead aircraft. These separation distances are the rectangular x, y, and z distances coordinatized in the wing aircraft's rotating reference frame. The wing aircraft, through its own formation flight control system, maneuvers to eliminate errors between the commanded position and the actual position relative to the lead aircraft.

3.2 Aircraft Transfer Functions

Equations 3.1 - 3.3 represent the (first order) transfer functions for the velocity, heading, and altitude channels of the C-130. V, H, and h represent velocity, heading, and altitude respectively, while G_V, G_H, and G_h represent the open loop velocity channel constant, heading channel constant, and altitude channel constant respectively. These constants are the reciprocals of the time constants. The C-130A and C-130B aircraft have similar response characteristics, although their limits and capabilities are different. Table 3.1 shows the gains and rate limits of the two aircraft. The onset delay and onset rate are flying qualities characteristics based on a second order time response (7). Onset delay is not used in these first-order models, and with the exception of the velocity channel, neither is onset rate.

Figure 3.1 shows the block diagram of the C-130B aircraft model, and Figure 3.2 shows the unit step response plots for therespective models, where the step input is applied at time t = 0. The solid line of the time response plots represents the velocity response, the dotted line represents the heading response, and the dashed line represents the altitude response. The differences in these time responses are due to the differences in the time constants of the velocity, heading, and altitude channels of the aircraft model. The velocity channel time constant is 0.333 seconds, the heading channel time constant is 0.67 seconds, and the altitude channel time constant is 2 seconds. Both aircraft responses are the same for a unit step input because G_V,G_H, and G_h are the same for both aircraft models.

The performance differences between the C-130A amd C-130B aircraft models are due to the differences in the velocity, heading, and climb rate limits of the two models. A large step input to the respective aircraft models clearly illustrates these performance differences. Figure 3.3 shows the differences in the time responses of the aircraft models for a velocity step input command of 400 ft/sec, a heading step input command of 75 degrees, and an altitude step input command of 650 feet, applied at time t = 0, respectively. The differences occur because the maximum rates of

change for the C-130B are larger than those of the C-130A. This is shown by the limiters contained in the models in Figure 3.1 and by the onset rate contained in Table 3.1.

$$\frac{V(s)}{V_c(s)} = \frac{G_V}{s + G_V} \tag{3.1}$$

$$\frac{H(s)}{H_c(s)} = \frac{G_H}{s + G_H} \tag{3.2}$$

$$\frac{h(s)}{h_c(s)} = \frac{G_h}{s + G_h} \tag{3.3}$$

Table 3.1. Aircraft Model Constants and Rate Limits

Aircraft and Parameter	Onset Delay	Onset Rate	Lower Limit	Upper Limit	G_V	G_H	G_h
C-130A							
Constants					3	1.5	0.5
Velocity	< 1 s	2.5 ft/s^2	304 ft/s	422 ft/s			
Heading	1.5 s	1.5 deg/s^2	-3 deg/s	3 deg/s			
Altitude	1 s	-8.4 ft/s^2 to 1.7 ft/s^2	-42 ft/s	8.5 ft/s			
C-130B							
Constants					3	1.5	0.5
Velocity	< 1 s	3.9 ft/s^2	304 ft/s	422 ft/s			
Heading	1.5 s	2 deg/s^2	-4.7 deg/s	4.7 deg/s			
Altitude	1 s	-8.4 ft/s^2 to 6.6 ft/s^2	-42 ft/s	33 ft/s			

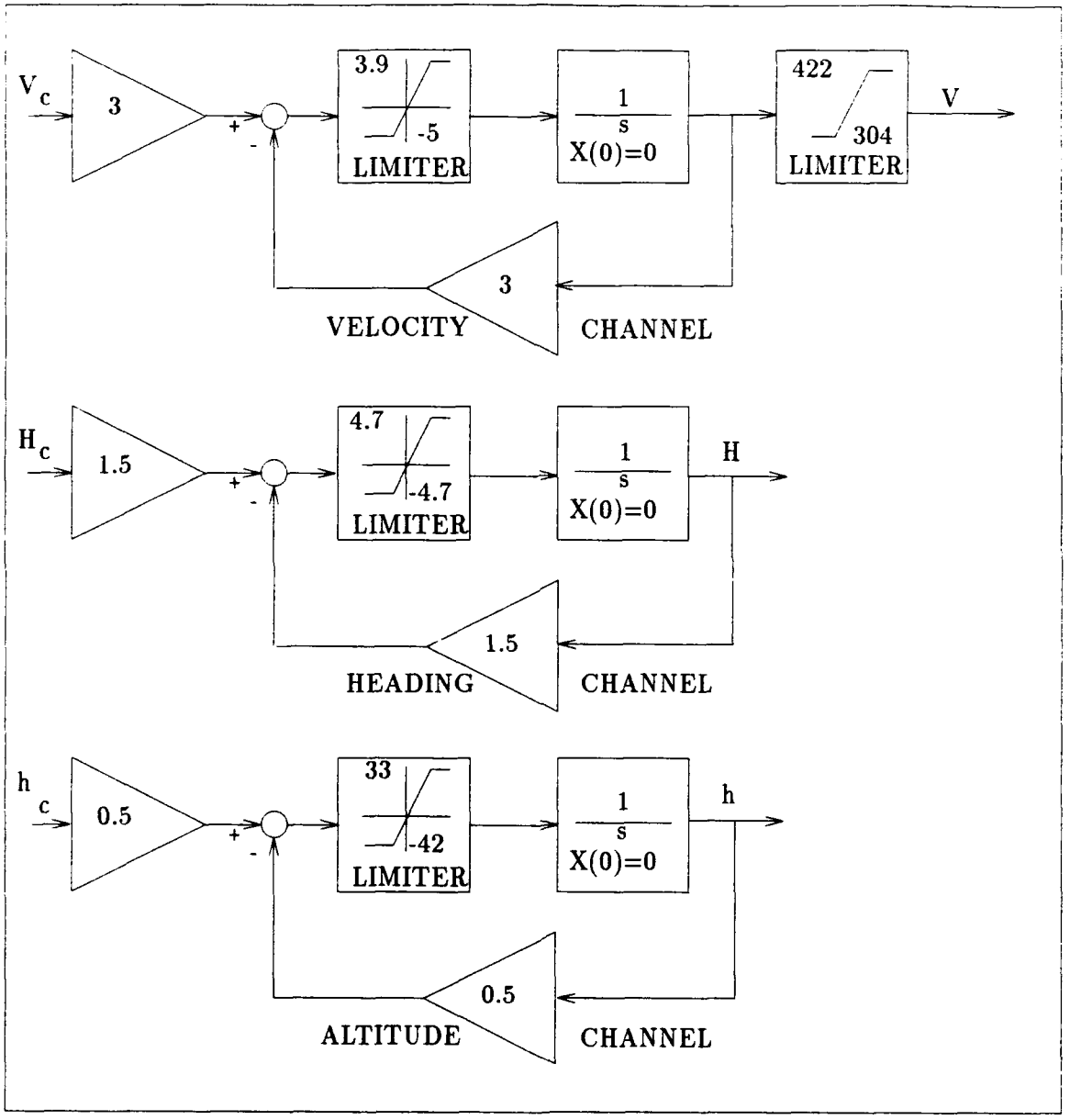

Figure 3.1. C-130B First-Order Aircraft Model With Autopilot

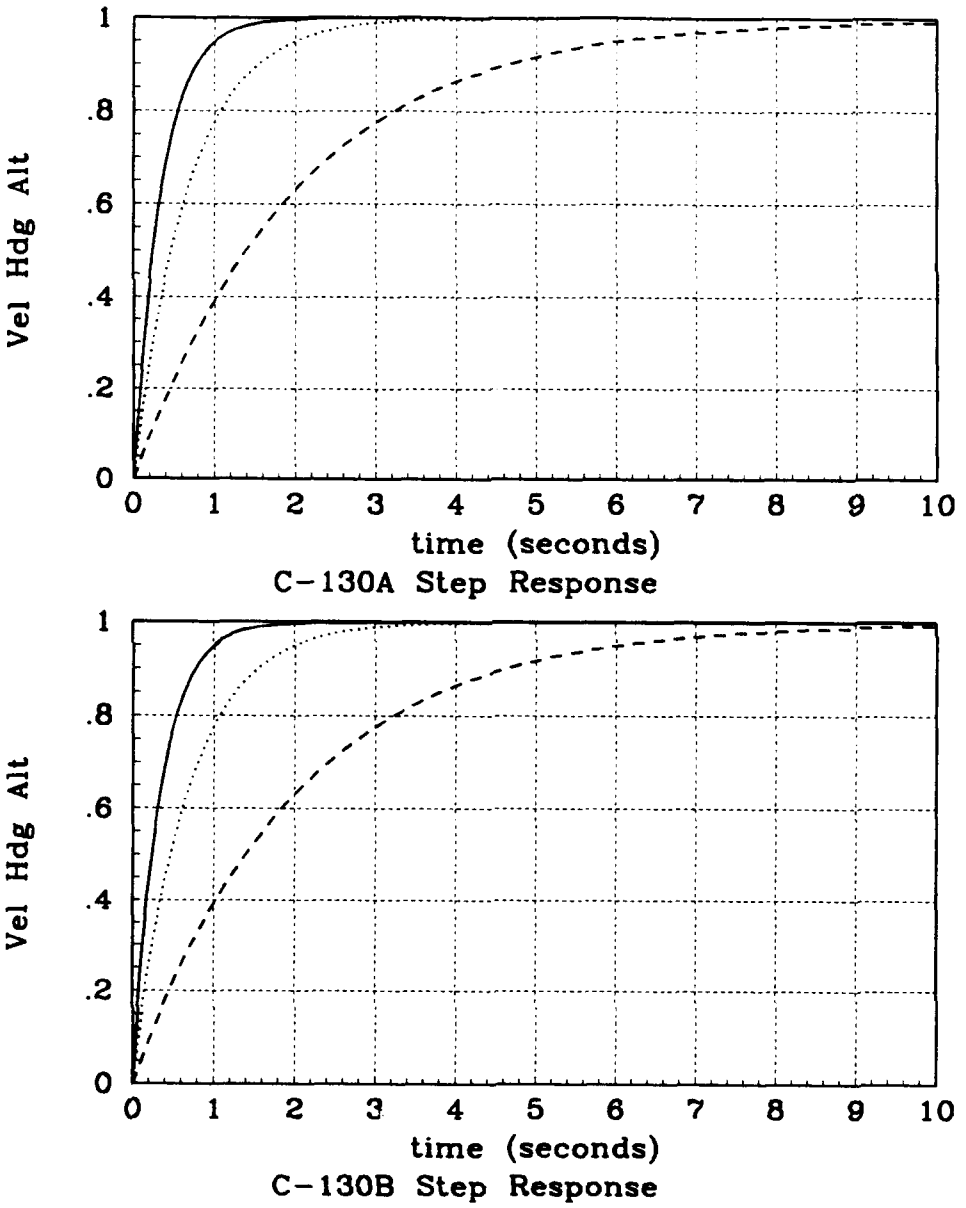

Figure 3.2. C-130 Unit Step Response Samples

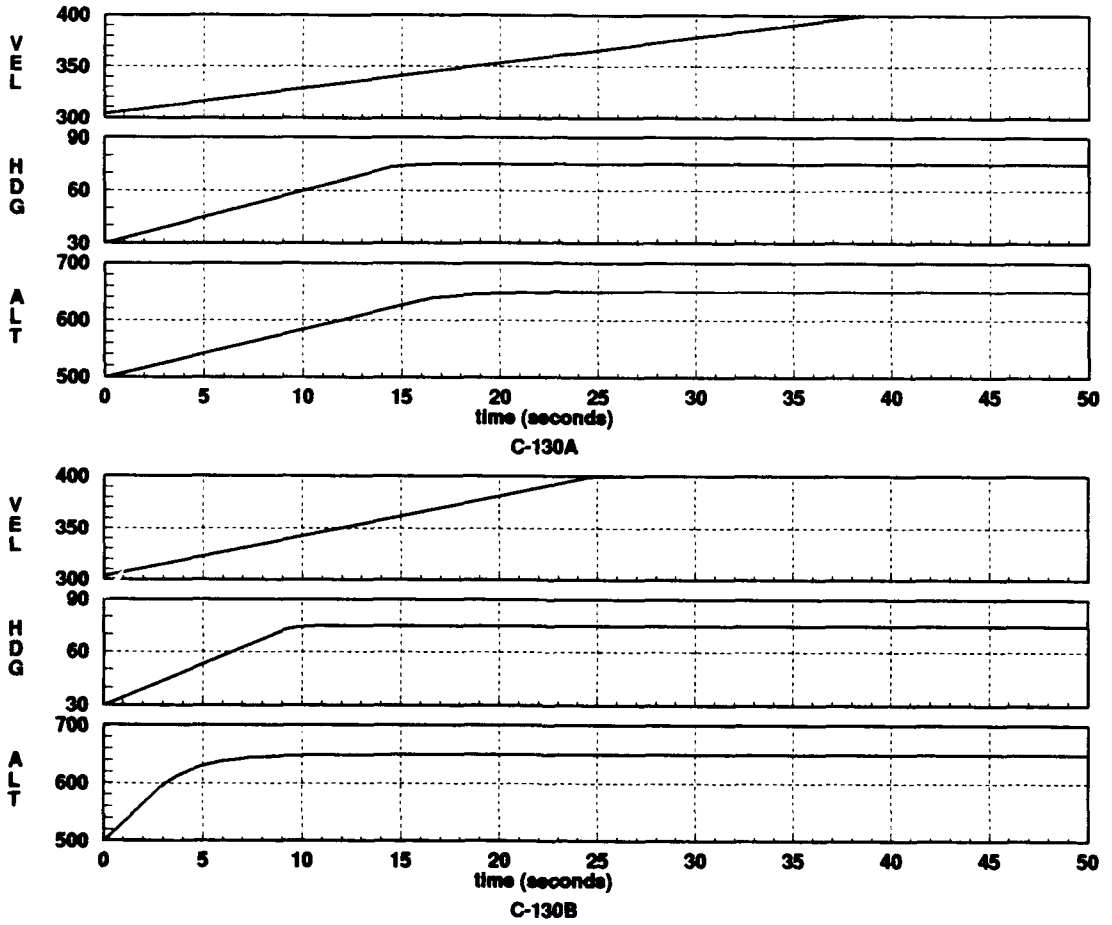

Figure 3.3. C-130 Large Step Response Samples

The aircraft model transfer functions were determined by the over-damped response characteristics and speed of response of the respective aircraft. Longitudinal position along the flight path vector is a direct function of forward velocity. Velocity is determined by flight condition and aircraft parameters, such as engine thrust, spool up time, and propeller pitch. These responses are very fast for a C-130 since it has a constant speed propeller, allowing the engine to operate at a constant speed. Thrust is therefore only a function of propeller pitch which is regulated by a hydraulic controller. Lateral position is a function of directional control or turn response, while vertical position and spacing is varied by altitude control (10:29-30). The respective models were developed by Rohs through comparison with flight test data obtained from the Air Force Flight Test Center and from the DASH 1 manuals. Data used for this verification consisted of time response plots produced during C-130H model systems evaluation by the Dryden Flight Research Facility. Velocity and acceleration limits were determined through pilot interviews and the MC-130 DASH 1 Flight Manual (10:34).

Plots of flight data provided turn, climb and descent rates, and time responses for maneuvers initiated and controlled by the autopilot system. These results show complete, actual closed loop system responses of the aircraft to a control input. Comparing the operating limits and capabilities of the two C-130 models shows the differences in turn, climb, and descent rate capability and forward acceleration. Such differences are of major concern for a formation control system for controlling a formation of mixed aircraft. These differences could allow one aircraft to outmaneuver another within the formation, resulting in either an aircraft that loses the formation, or worse, a collision within the formation. Therefore, formation level control must account for these performance differences to prevent aircraft from being forced to maneuver outside of their individual operational envelope.

3.3 Aircraft Sensor Measurements

To implement a formation control system, the wing aircraft would require an on-board sensor capable of providing relative position information in the wing aircraft's reference frame. This on-board sensor could extract this position information from elevation angle, azimuth angle, and separation range measurements of the lead aircraft. Figures 3.4 - 3.5 show that relative position is completely defined by these three parameters. Only elevation angle is required in the vertical plane, the azimuth and elevation angles determine horizontal position, and range is needed in both planes. These raw measurements are transformed into rectangular longitudinal, lateral, and vertical separation distances in the wing aircraft rotating reference frame. These created "displacement measurements" are referred to as "pseudo-measurements" in the Kalman Filtering literature.

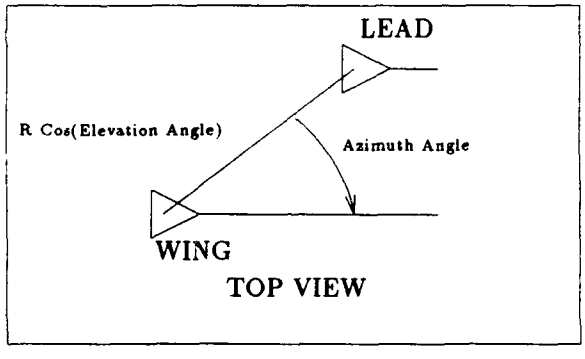

Figure 3.4. Wing Aircraft Azimuth Measurements

3.4 Formation Coordinate System

In this research, two possible reference frames are considered, an inertial reference frame and a rotating reference frame centered on the wing aircraft.

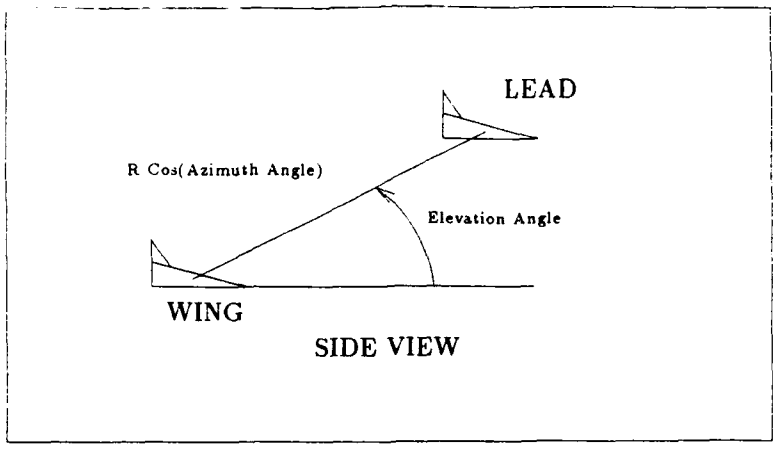

Figure 3.5. Wing Aircraft Elevation Measurements

The inertial frame has a stationary origin, with latitude, longitude, and altitude as its axes. This system is used for navigation and is best used over long distances. Figure 3.6 depicts the lead and wing aircraft in an inertial reference frame.

The rotating aircraft reference frame origin is affixed to the wing aircraft, with its x axis aligned with the aircraft's direction of flight, the y axis perpendicular and extending laterally to the right, and the z axis down (toward the earth). Since this reference frame rotates with the wing aircraft, it is always oriented in the direction of flight of the wing aircraft. By referencing the lead aircraft's position from the wing aircraft's instantaneous axes, relative position between the two aircraft can be readily obtained. Figure 3.7 depicts the lead and wing aircraft in the rotating wing aircraft reference frame. Note that the velocity vector of the wing aircraft is in the x axis direction.

Because the rotating wing aircraft reference frame provides the distance measurements that an actual wing aircraft on-board sensor would provide, this reference frame is chosen for this research.

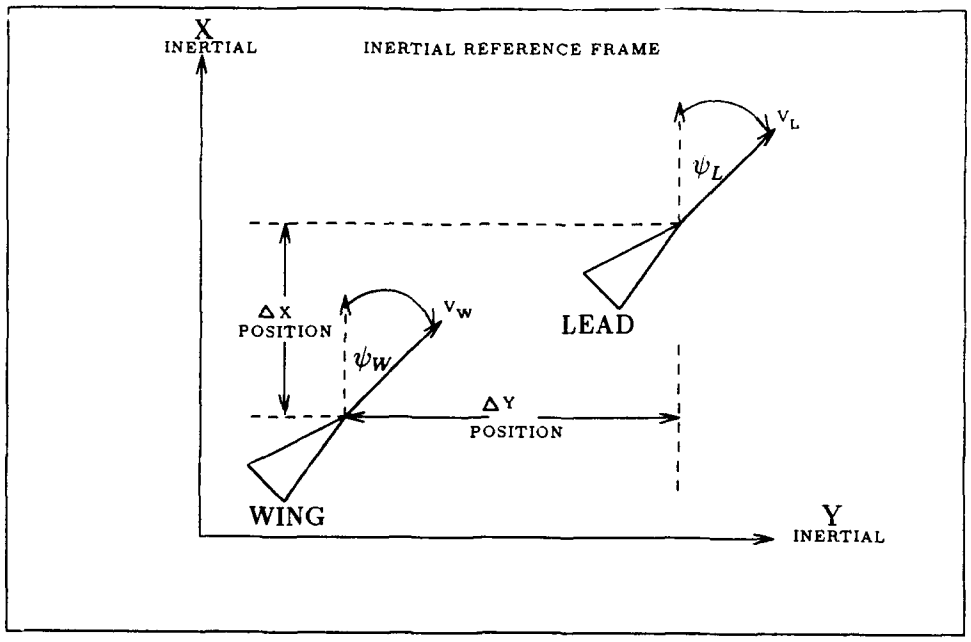

Figure 3.6. Inertial Reference Frame

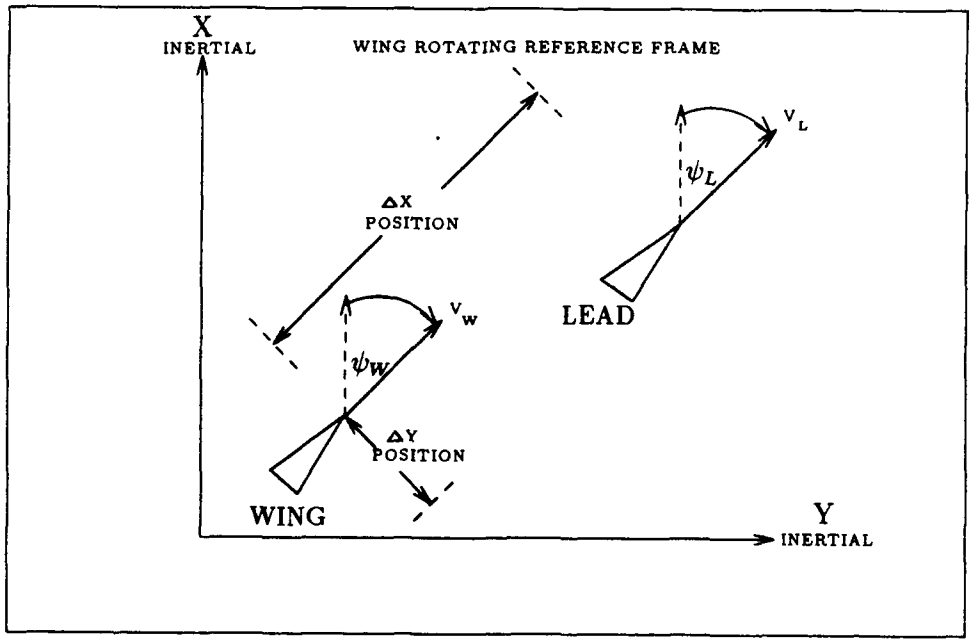

Figure 3.7. Wing Aircraft Reference Frame

3.5 Formation Control Strategy

For this research a two tiered control strategy is employed. The upper tier is for control of the formation as a whole, and the lower tier is for control of the individual aircraft within the formation. Formation level guidance is provided to all formation aircraft. These guidance inputs include formation velocity, magnetic heading, altitude, and the particular formation to be flown. The formation itself is defined by a commanded longitudinal separation distance, Δx, a lateral separation distance, Δy, and a vertical separation distance, Δz. Figure 3.8 illustrates the formation control strategy.

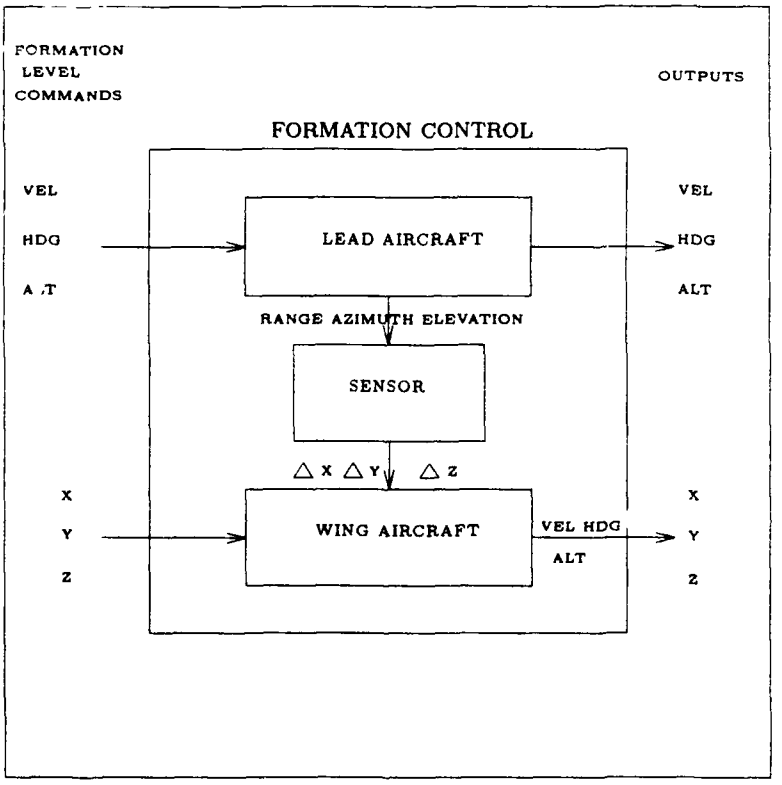

Figure 3.8. Formation Control Strategy

The commanded formation velocity is resolved in the wing aircraft's reference frame, as are the commanded separation distances. The lead aircraft uses commanded formation velocity, heading, and altitude for aircraft guidance, while the wing aircraft maneuvers to maintain its respective commanded separation distances from the lead aircraft. The wing aircraft on-board sensor measurements track lead aircraft position relative to the wing aircraft. An error is formed by differencing the commanded separation distances with the actual separation distances measured by the on-board sensor. This error is used to create the control inputs to the wing aircraft for tracking the lead aircraft's position.

3.6 Formation Kinematic Equations Development

The kinematic equations that represent the relative positioning between the lead and wing aircraft are developed and implemented in a $MATRIX_x$ simulation of the formation control system. Thus, these equations calculate the positioning information in the wing aircraft's rotating reference frame that would be provided by an on-board sensor in an actual formation control system. Development of the formation control system kinematic equations is based on the diagram shown in Figure 3.9.

The wing aircraft's mass center is located at **W**, and the lead aircraft's mass center is located at **L**. The position vector of **L** relative to **W** is $(x\hat{X}_W, y\hat{Y}_W, z\hat{Z}_W)$, where:

- $x\hat{X}_W$ is the component of the lead aircraft's position in the wing aircraft's x axis direction
- $y\hat{Y}_W$ is the component of the lead aircraft's position in the wing aircraft's y axis direction
- $z\hat{Z}_W$ is the component of the lead aircraft's position in the wing aircraft's z axis direction

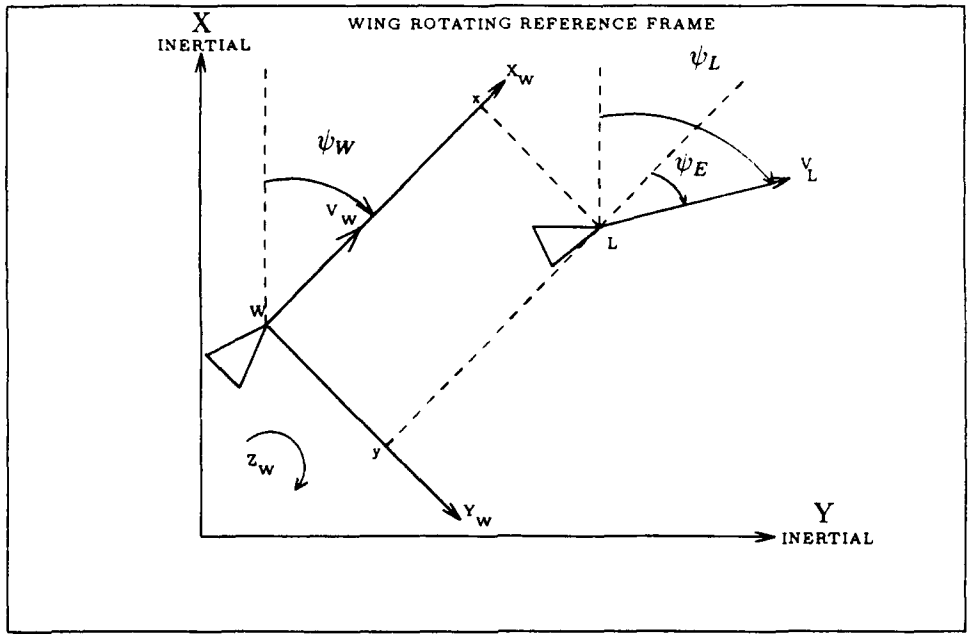

Figure 3.9. Relative Motion Diagram

The heading error is $\psi_E = \psi_L$ - ψ_W. The magnitude of the inertial linear velocities of the mass centers of the wing aircraft and lead aircraft are V_W and V_L respectively. The magnitude of the inertial angular velocities of the mass centers of the wing aircraft and lead aircraft are ω_W and ω_L respectively. An equation which relates the position of the lead aircraft with respect to the wing aircraft is needed. Equations 3.4 - 3.14 show the intermediate steps for determining this kinematic relationship.

$$\mathbf{V}_L^L = \begin{bmatrix} V_L \\ 0 \\ 0 \end{bmatrix} \tag{3.4}$$

$$\mathbf{V}_W^W = \begin{bmatrix} V_W \\ 0 \\ 0 \end{bmatrix} \tag{3.5}$$

$$\mathbf{L}^W = \begin{bmatrix} x \\ y \\ z \end{bmatrix} \tag{3.6}$$

$$\mathbf{W}^W = \begin{bmatrix} 0 \\ 0 \\ 0 \end{bmatrix} \tag{3.7}$$

where:

- $\mathbf{V}_L^L$ is the inertial velocity of the lead aircraft resolved in its own reference frame
- $\mathbf{V}_W^W$ is the inertial velocity of the wing aircraft resolved in its own reference frame
- $\mathbf{L}^W$ is the position vector of the lead aircraft in the wing aircraft's reference frame
- $\mathbf{W}^W$ is the position vector of the wing aircraft in its own reference frame

Since the **W** reference frame and the **L** reference frame both rotate about the z axis, the angle between **L** and **W** is ψ_E. Therefore, to relate the **L** reference frame to the **W** reference frame requires that a Direction Cosine Matrix be calculated, as shown in Equation 3.8:

$$\mathbf{C}_L^W = \begin{bmatrix} \cos\psi_E & -\sin\psi_E & 0 \\ \sin\psi_E & \cos\psi_E & 0 \\ 0 & 0 & 1 \end{bmatrix} \tag{3.8}$$

The linear velocity of the lead aircraft may be transformed into the wing aircraft reference frame by use of Equation 3.9. Since both reference frames rotate about the z axis, the angular velocities, ω_L, and ω_W are in the same direction.

$$\mathbf{V}_L^W = \mathbf{C}_L^W \mathbf{V}_L^L = \begin{bmatrix} V_L \cos\psi_E \\ V_L \sin\psi_E \\ 0 \end{bmatrix} \tag{3.9}$$

$$\omega_W^W = \begin{bmatrix} 0 \\ 0 \\ \dot{\psi}_W \end{bmatrix} \tag{3.10}$$

where:

- $\mathbf{V}_L^W$ is the inertial velocity of the lead aircraft resolved in the wing aircraft's coordinate frame
- ω_W^W is the angular velocity of the wing aircraft resolved in its own coordinate frame

The velocity of the lead aircraft with respect to the wing aircraft may be computed using the velocity transformation law:

$$\mathbf{V}_{WL}^W = \mathbf{V}_L^W - \omega_W^W \times \mathbf{L}^W - \mathbf{V}_W^W + \omega_W^W \times \mathbf{W}^W \tag{3.11}$$

Since $\mathbf{W}$ is always at the origin of the wing aircraft reference frame, Equation 3.11 reduces to Equation 3.12.

$$\mathbf{V}_{WL}^{W} = \mathbf{V}_{L}^{W} - \omega_{W}^{W} \times \mathbf{L}^{W} - \mathbf{V}_{W}^{W} \tag{3.12}$$

$$\mathbf{V}_{WL}^{W} = \begin{bmatrix} V_L \cos\psi_E \\ V_L \sin\psi_E \\ 0 \end{bmatrix} - \begin{bmatrix} 0 \\ 0 \\ \dot{\psi}_W \end{bmatrix} \times \begin{bmatrix} x \\ y \\ z \end{bmatrix} - \begin{bmatrix} V_W \\ 0 \\ 0 \end{bmatrix} \tag{3.13}$$

$$\mathbf{V}_{WL}^{W} = \begin{bmatrix} V_L \cos\psi_E \\ V_L \sin\psi_E \\ 0 \end{bmatrix} - \begin{bmatrix} -\dot{\psi}_W y \\ \dot{\psi}_W x \\ 0 \end{bmatrix} - \begin{bmatrix} V_W \\ 0 \\ 0 \end{bmatrix} \tag{3.14}$$

The velocity of the lead aircraft with respect to the wing aircraft has a component in the wing x axis, or longitudinal, direction and a component in the wing y axis, or lateral, direction. Examining these two components independently in Equations 3.15 - 3.16 yields the equations of relative velocity between the lead and wing aircraft. Integrating these two equations with respect to time yields the equations of relative position between the lead and wing aircraft.

$$\dot{x} = V_L \cos\psi_E + \dot{\psi}_W y - V_W \tag{3.15}$$

$$\dot{y} = V_L \sin\psi_E - \dot{\psi}_W x \tag{3.16}$$

Since the only angular rate accounted for in the aircraft models is $\dot{\psi}$, there is no component of the velocity in the z axis, or vertical, direction. Thus, a $\dot{z}$ equation is not needed.

3.7 Aircraft Longitudinal (X) Channel Maneuvering

The longitudinal channel involves the longitudinal separation distance between the lead and wing aircraft, as well as the longitudinal relative velocity between the two. The lead aircraft responds to the formation-level velocity command, while the wing aircraft responds to the formation longitudinal separation command. As the separation distance increases or decreases from its commanded value, the wing aircraft's velocity is varied above or below the commanded nominal value so that the commanded separation distance is maintained. An increase in x separation, as when the lead is accelerating away from the wing aircraft, causes an increase in the wing aircraft's velocity in an attempt to null out the error in separation distance. A decrease in separation distance, as when the lead is decelerating, causes a decrease in the wing aircraft's velocity in an attempt to null out the error in separation distance. A rearrangement of Equation 3.15 yields the following relationships for V_L and V_W in the wing aircraft reference frame longitudinal axis, $\hat{X}_W$:

$$V_L \hat{X}_W = (V_L \cos\psi E + \dot{\psi}_W y)\hat{X}_W \tag{3.17}$$

$$V_W \hat{X}_W = V_W \hat{X}_W \tag{3.18}$$

where:

- $V_L \hat{X}_W$ is the component of the lead aircraft's velocity in the wing aircraft's x axis direction
- $V_W \hat{X}_W$ is the component of the wing aircraft's velocity in its own x axis direction

3.8 Aircraft Lateral (Y) Channel Maneuvering

The lateral channel involves the lateral separation distance between the lead and wing aircraft, as well as the relative heading angle between the two. The lead aircraft responds to the formation level heading command, while the wing aircraft responds to the formation lateral separation command. The wing aircraft employs lateral coordinated turn maneuvers, to maintain the nominal lateral separation. This allows the wing aircraft to track the lead aircraft through heading changes, or to change formation spacing based on a new formation level commanded separation distance. A rearrangement of Equation 3.16 yields the following relationships for V_L and V_W in the wing aircraft reference frame lateral axis, $\hat{Y}_W$:

$$V_L \hat{Y}_W = (V_L \sin \psi_E - \dot{\psi}_W x)\hat{Y}_W \tag{3.19}$$

$$V_W \hat{Y}_W = 0 \tag{3.20}$$

where:

- $V_L \hat{Y}_W$ is the component of the lead aircraft's velocity in the wing aircraft's y axis direction
- $V_W \hat{Y}_W$ is the component of the wing aircraft's velocity in its own y axis direction

3.9 Aircraft Vertical (Z) Channel Maneuvering

The vertical channel involves the vertical separation distance between the lead and wing aircraft. This vertical separation distance also represents the altitude differential of the two aircraft. The lead aircraft responds to the formation level altitude command, while the wing aircraft responds to the formation vertical separation command. The wing aircraft employs vertical maneuvers, a climb or a descent, to

maintain the target vertical position. The relationship for relative vertical positioning of the two aircraft is shown in Equation 3.21:

$$z\hat{Z}_W = z_W\hat{Z}_W - z_L\hat{Z}_L = z_W\hat{Z}_W - z_L\hat{Z}_W \tag{3.21}$$

3.10 Simulation Implementation

The state equations representing the formation kinematics and the aircraft models are given in Equations 3.22 - 3.29. Note that the state equations representing the lead and wing altitude are decoupled from the other equations, whereas the equation representing the wing heading is coupled in the $\dot{x}$ and $\dot{y}$ equations.

$$\dot{x} = V_L \cos\psi_E + \dot{\psi}_W y - V_W \tag{3.22}$$

$$\dot{y} = V_L \sin\psi_E - \dot{\psi}_W x \tag{3.23}$$

$$\dot{V_W} = -3V_W + 3V_{W_c} \tag{3.24}$$

$$\dot{V_L} = -3V_L + 3V_{L_c} \tag{3.25}$$

$$\dot{\psi_W} = -1.5\psi_W + 1.5\psi_{W_c} \tag{3.26}$$

$$\dot{\psi_L} = -1.5\psi_L + 1.5\psi_{L_c} \tag{3.27}$$

$$\dot{h_W} = -0.5h_W + 0.5h_{W_c} \tag{3.28}$$

$$\dot{h_L} = -0.5h_L + 0.5h_{L_c} \tag{3.29}$$

where:

- V_{W_c} and V_{L_c} are the velocity input commands to the wing and lead aircraft, respectively
- ψ_{W_c} and ψ_{L_c} are the heading angle input commands to the wing and lead aircraft, respectively
- h_{W_c} and h_{L_c} are the altitude input commands to the wing and lead aircraft, respectively

These state equations are coded into $MATRIX_x$ through the *System Build* feature of $MATRIX_x$. *System Build* allows the state equations to be implemented in a graphical block diagram format (frequency domain representation). The $\dot{\psi}_W$, $\dot{V}_W$, and $\dot{h}_W$ equations are coded in one block to represent the wing aircraft model. The $\dot{\psi}_L$, $\dot{V}_L$, and $\dot{h}_L$ equations are coded in a separate block to represent the lead aircraft model. The $\dot{x}$ and $\dot{y}$ equations are coded in a block simulating kinematics of the lead and wing aircraft configuration. This block outputs the (x,y) separation of the wing and lead aircraft. Thus, the formation control strategy diagram shown in Figure 3.8 is simulated as shown in Figure 3.10. Since the altitude channel is decoupled, Figure 3.10 only depicts simulation in the horizontal (x,y) plane.

The velocity, heading, and altitude commands are input to the lead aircraft model as step inputs, and the x, y, z commands are input to the wing aircraft model as step inputs. The description of the methodology for longitudinal, lateral, and vertical maneuvering described earlier is obeyed in the $MATRIX_x$ formation control system simulation.

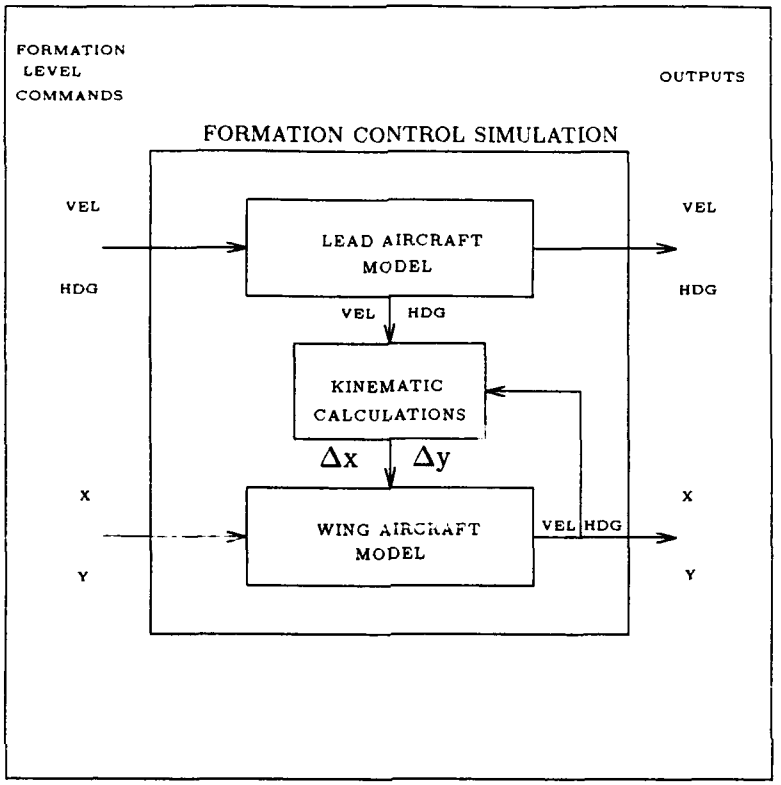

Figure 3.10. Formation Control Simulation Strategy

3.11 Validation of Formation Kinematic Equations

Simulations of the formation control system are accomplished in this section to verify that the kinematic equations derived in the previous section are correct. Two representative test simulations are included. These verification simulations are accomplished by putting the same formation maneuver commands into the lead aircraft and wing aircraft simultaneously, while excluding the x and y inputs to the wing aircraft. This will then exercise the Δx and Δy calculations of the kinematic equations used in the simulation of the formation control system. A diagram depicting the simulation implementation for verification of the kinematic equations is shown in Figure 3.11. This implementation is for the sole purpose of validating the kinematic

equations. Table 3.2 lists the initial conditions and commanded maneuvers of the test simulations.

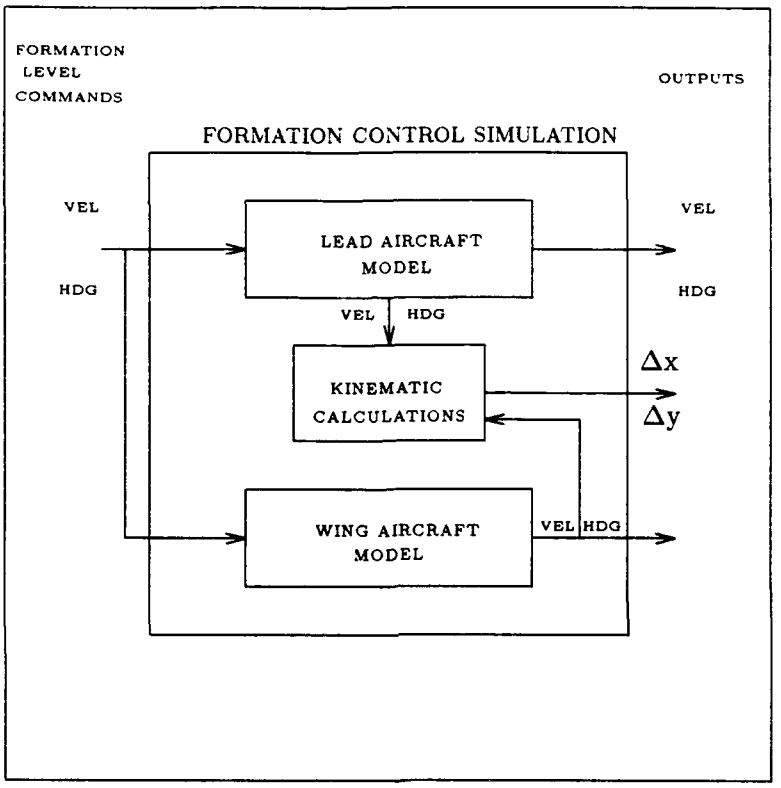

Figure 3.11. Formation Control Simulation for Validation of Kinematic Equations

Table 3.2. Simulation Test Inputs and Initial Conditions

Simulation Number	Commanded Parameter Input	Parameter Output Initial Condition	Formation
1	H_W = 90 deg	H_W = 0 deg Δx = 4298 ft Δy = 0 ft	Trail
2	H_W = 90 deg	H_W = 0 deg Δx = 0 ft Δy = 4298 ft	Abreast

For simulation run number 1, the lead and wing aircraft are in a trail formation separated by 4,298 feet. The lead and wing aircraft are commanded to perform a 90 degree heading change. The expected result is that at the completion of the heading change, the aircraft will be in a line abreast formation separated by 4,298 feet. An examination of Figure 3.12 shows that the expected result is indeed obtained.

For simulation run number 2, the lead and wing aircraft are in a line abreast formation separated by 4,298 feet. The lead and wing aircraft are commanded to perform a 90 degree heading change. The expected result is that at the completion of the heading change, the aircraft will be in a trail formation where they are 4,298 feet apart. An examination of Figure 3.13 shows that the expected result is obtained.

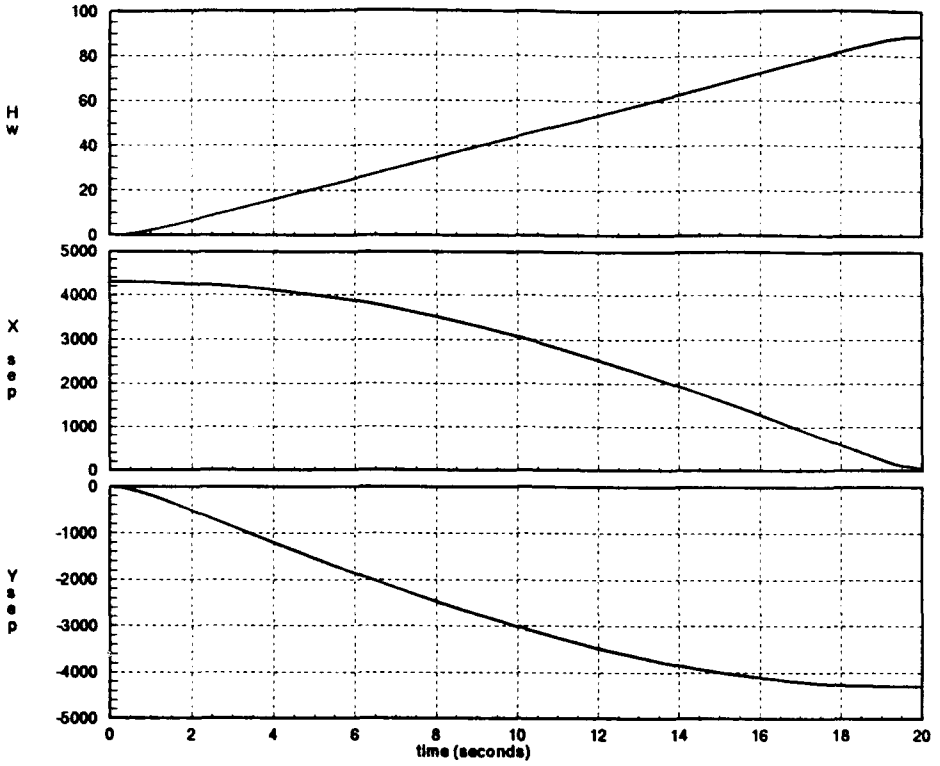

Figure 3.12. Simulation 1 Responses

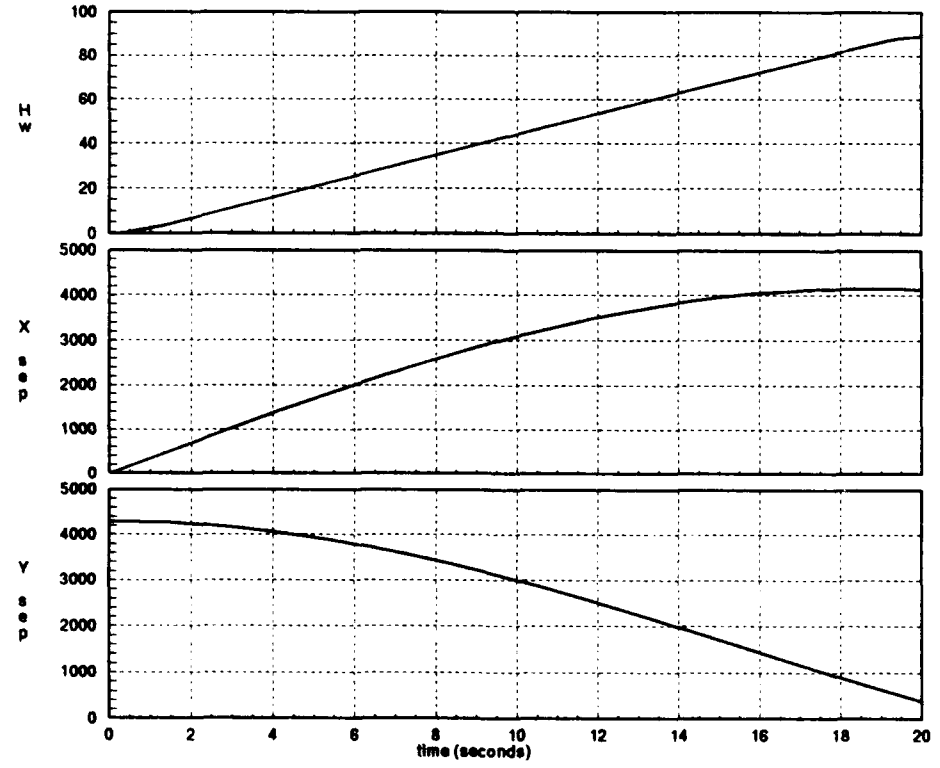

Figure 3.13. Simulation 2 Responses

3.12 Open Loop Formation Control

The justification of the need for some type of controller in an automated formation system is accomplished in this section. An initial thought about automated formation control might lead to the notion that formation control can be accomplished in an open-loop manner, by commanding both aircraft to perform the same maneuver. Figure 3.14 shows a block diagram of an open-loop implementation for the formation control system.

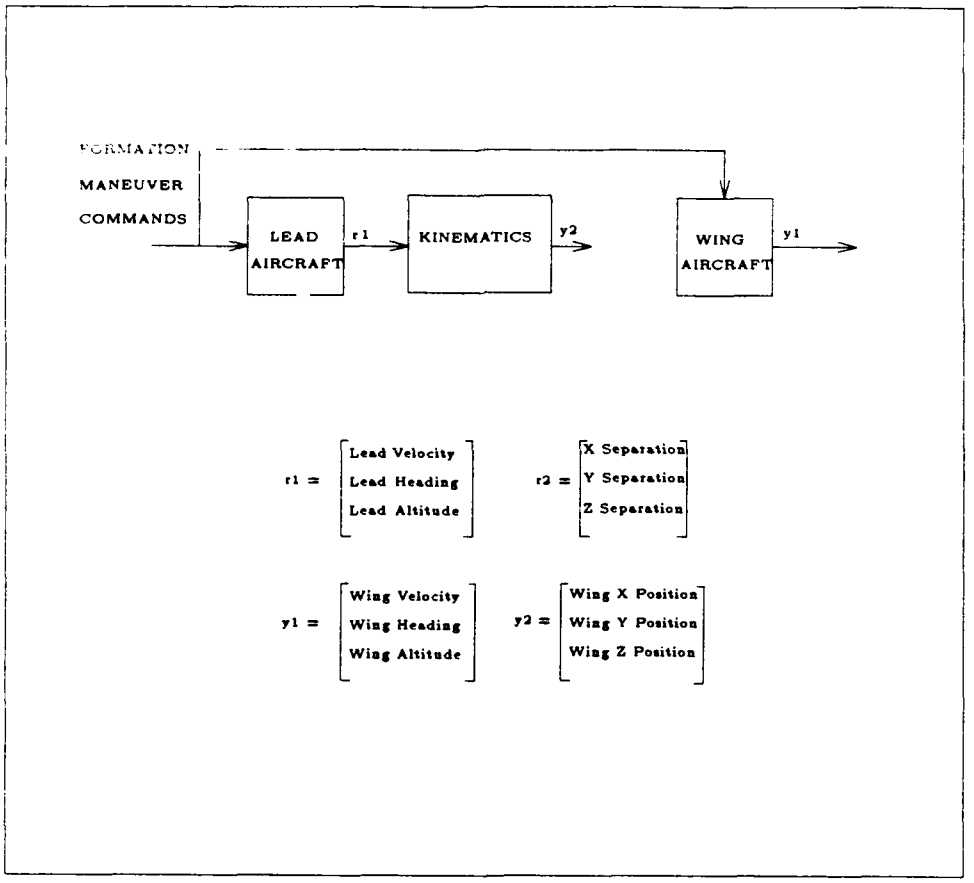

Figure 3.14. Block Diagram of Open-Loop Formation Control System

An evaluation of open-loop operation shows that the commanded formation maneuver of velocity, heading, or altitude can be tracked with zero steady state error.

However, the formation separation distances are not maintained after the formation's maneuver has been completed. A representative example of this is shown in the time response plot shown in Figure 3.15.

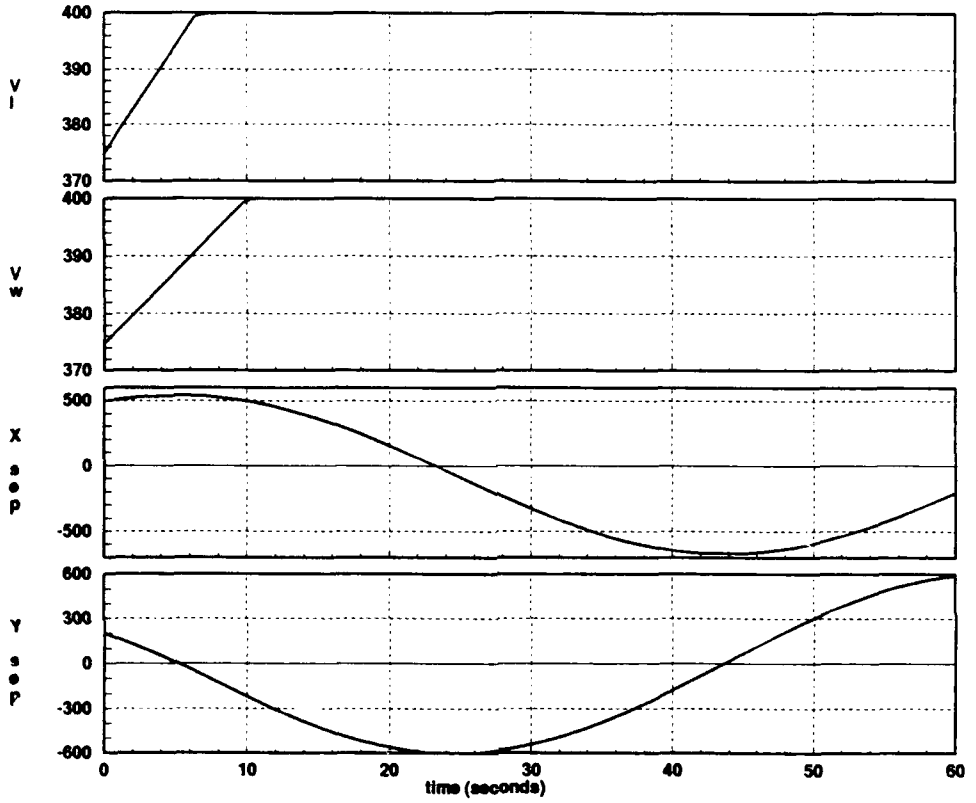

Figure 3.15. Open-Loop Response to a V_L (Input) Change from 375 to 400 ft/sec

In this example the formation is commanded to accelerate from a velocity of 375 ft/sec to 400 ft/sec. However, the initial longitudinal separation of 500 feet and lateral separation of 200 feet are not maintained in the new steady state. Therefore, additional control must be applied to the formation system to alleviate this problem. A good point to begin for applying additional control to the system is to feedback some of the states. This method is addressed in the next section.

3.13 Formation System Performance Using Velocity, Heading, and Altitude Feedback

The performance of the formation control system using velocity, heading, and altitude feedback is evaluated in this section. This type of formation control system implementation, as shown in Figure 3.16, uses feedback without a cascade compensator in the loop.

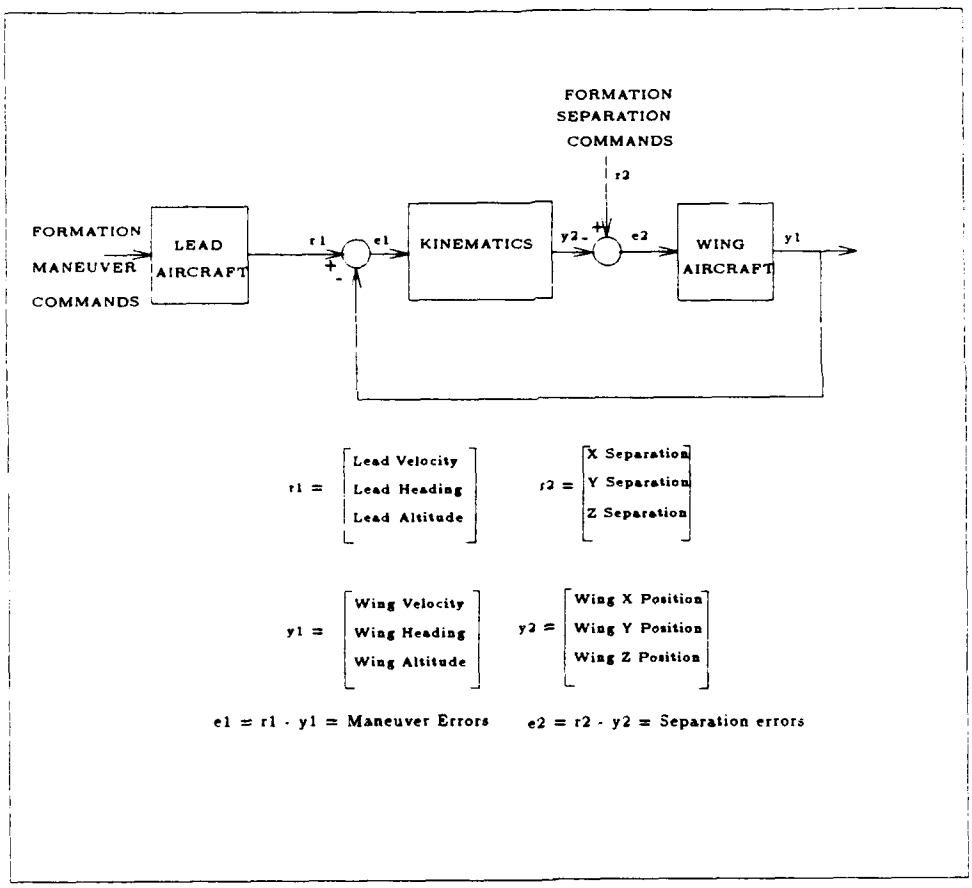

Figure 3.16. Block Diagram of Formation Control System Using Velocity, Heading, and Altitude Feedback

The performance of the formation system using V, H, and h feedback is evaluated for a system comprised of dissimilar aircraft in which one aircraft has inferior performance. A system comprised of dissimilar aircraft is a more challenging test for the formation system, as opposed to a system comprised of similar aircraft. In the case of dissimilar aircraft, there is the chance that one aircraft may outmaneuver another, less capable, aircraft. If the less capable aircraft is in the lead position, it may maneuver at will since the more maneuverable wing aircraft is capable of matching the lead's maneuvering. However, if the lead aircraft is more capable than the wing aircraft, the lead aircraft could possibly outmaneuver and/or outrun and lose the wing aircraft, or worse, cause a collision. Time response plots for the formation maneuver commands and separation commands are shown in the following figures and are briefly analyzed below. Table 3.3 lists the definitions of the variables on the time response plots. Table 3.4 should be referred to for initial conditions and input magnitudes for these plots.

Table 3.3. Variable Definitions

Variable Name: Text	Variable Name: Time Plots	Definition
V_L	V_l	Velocity of lead aircraft
V_W	V_w	Velocity of wing aircraft
H_L	H_l	Heading angle of lead aircraft
H_W	H_w	Heading angle of wing aircraft
h_L	Alt_l	Altitude of lead aircraft
h_W	Alt_w	Altitude of wing aircraft
Δx	$XSep$	Longitudinal separation distance
Δy	$Ysep$	Lateral separation distance
Δz	$Zsep$	Vertical separation distance

Table 3.4. Test Inputs and Initial Conditions

Commanded Parameter Input	Parameter Output Initial Condition	Response Plots
V_L = 400 ft/sec	V_L = 375 ft/sec V_W = 375 ft/sec Δx = 500 ft	Figure 3.17
Δx = 450 ft	V_L = 375 ft/sec V_W = 375 ft/sec Δx = 500 ft	Figure 3.18
H_L = 35 deg	H_L = 30 deg H_W = 30 deg Δy = 200 ft Δx = 500 ft V_L = 375 ft/sec V_W = 375 ft/sec	Figure 3.19
Δy = 150 ft	H_L = 30 deg H_W = 30 deg Δy = 200 ft Δx = 500 ft V_L = 375 ft/sec V_W = 375 ft/sec	Figure 3.20
A_L = 550 ft	A_L = 500 ft A_W = 500 ft Δz = 0 ft	Figure 3.21
Δz = -50 ft	A_L = 500 ft A_W = 500 ft Δz = 0 ft	Figure 3.22
H_L = -45 deg	H_L = 30 deg H_W = 30 deg Δy = 200 ft Δx = 500 ft V_W = 375 ft/sec	Figure 3.23

3.13.1 V_L **and** Δ**x Commands** Maneuvering in the longitudinal axis is effected by inputs of Formation velocity, (V_L), and longitudinal separation, (Δx). Responses for these two inputs are shown in Figures 3.17 - 3.18 respectively.

Analysis of the longitudinal channel response to a V_L input shows that the wing aircraft is able to attain the commanded formation velocity of 400 ft/sec. However, there is an overshoot of 10 ft/sec in the velocity response. The Δx response peaks at 560 feet, but fails to return to its initial commanded value of 500 feet. Therefore, a controller is needed to make the velocity response smoother and to make the Δx response have zero steady state error.

Analysis of the longitudinal channel response to a Δx input shows that the wing aircraft is able to accelerate and then return to its initial commanded velocity while attaining the commanded reduction in separation to 450 feet. This good response occurs because of the inherent integral control in the kinematic relationship between velocity and position.

3.13.2 ψ_L **and** Δ**y Commands** Maneuvering in the lateral axis is effected by inputs of formation heading, (H_L), or (ψ_L), and lateral separation, (Δy). Responses for these two inputs are shown in Figures 3.19 - 3.20 respectively.

Analysis of the lateral channel response to a H_L input shows that the wing aircraft has a first order response and is able to attain the commanded heading angle of 35 degrees. However, the initial commanded Δy is not maintained in steady state. Therefore, a controller is needed to make the Δy response have zero steady state error.

Analysis of the lateral channel response to a Δy input shows that the wing aircraft attains the commanded Δy value of 150 feet, while the H_W response maintains its initial commanded heading angle in steady state. This good response occurs because of the inherent integral control in the kinematic relationship between velocity in the y direction and position in the y direction.

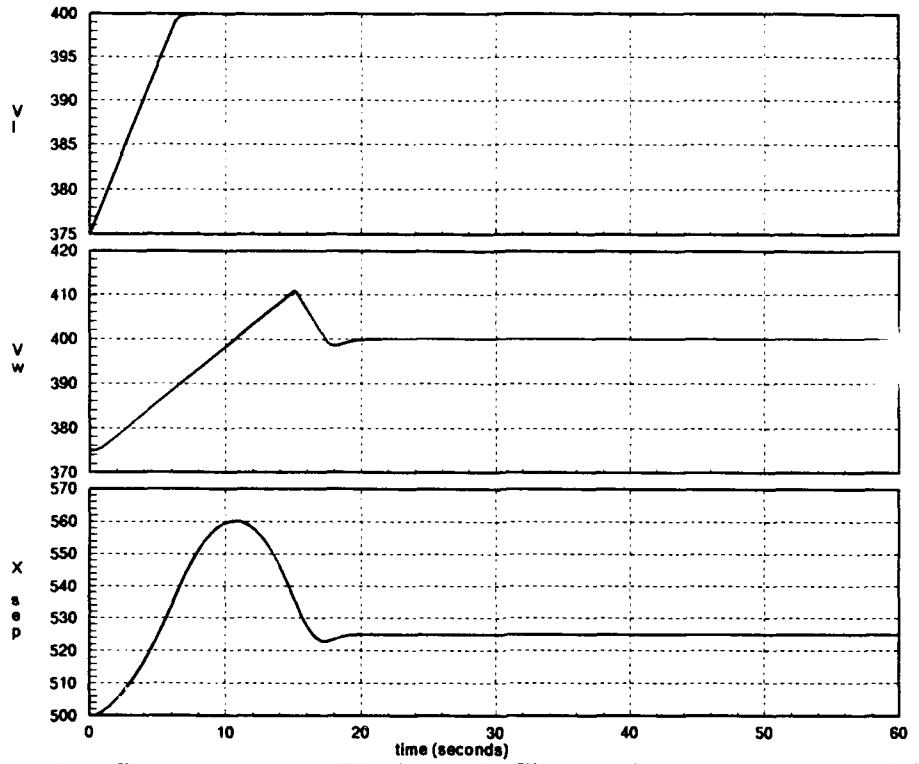

Figure 3.17. Response to a V_L (Input) Change from 375 to 400 ft/sec Using Feedback

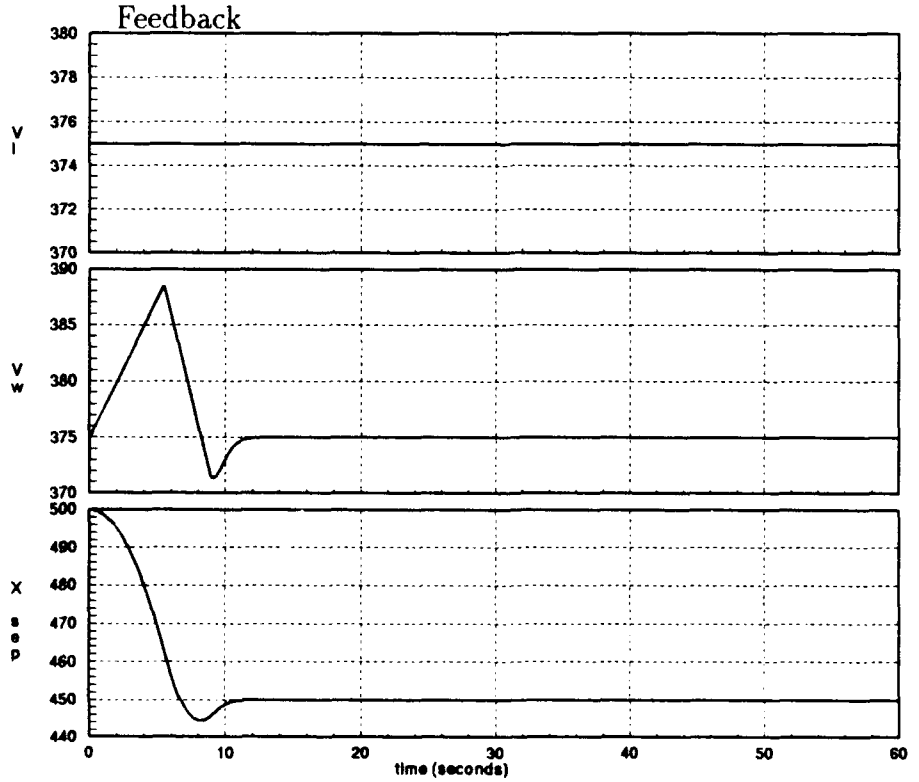

Figure 3.18. Response to a Δx Input Change from 500 to 450 Feet Using Feedback

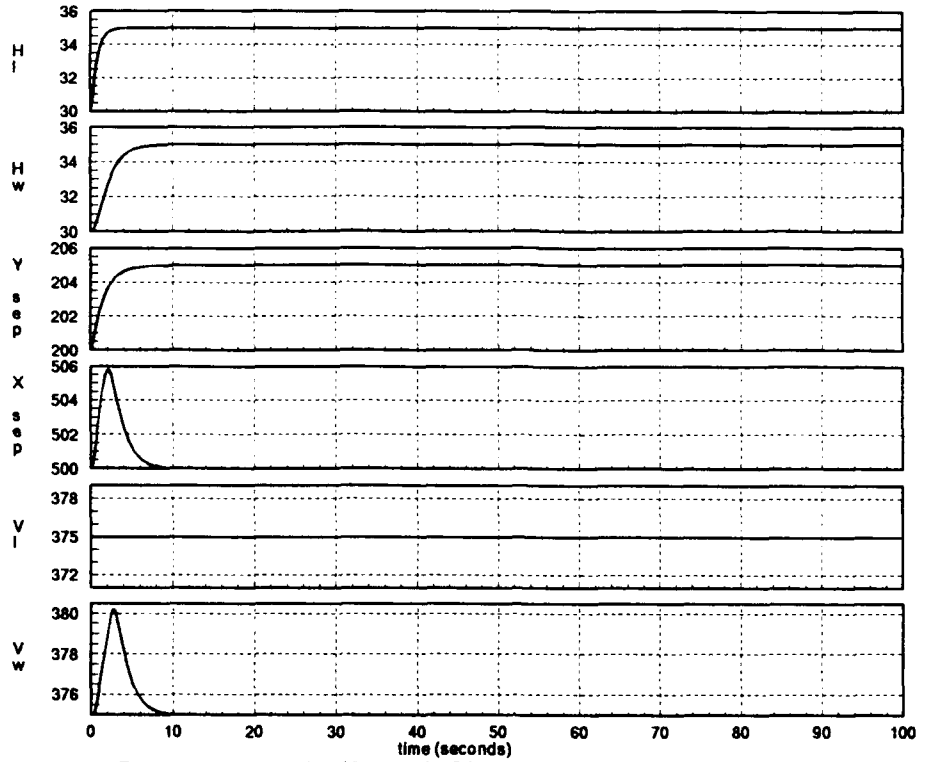

Figure 3.19. Response to H_L (Input) Change from 30 to 35 Degrees Using Feedback

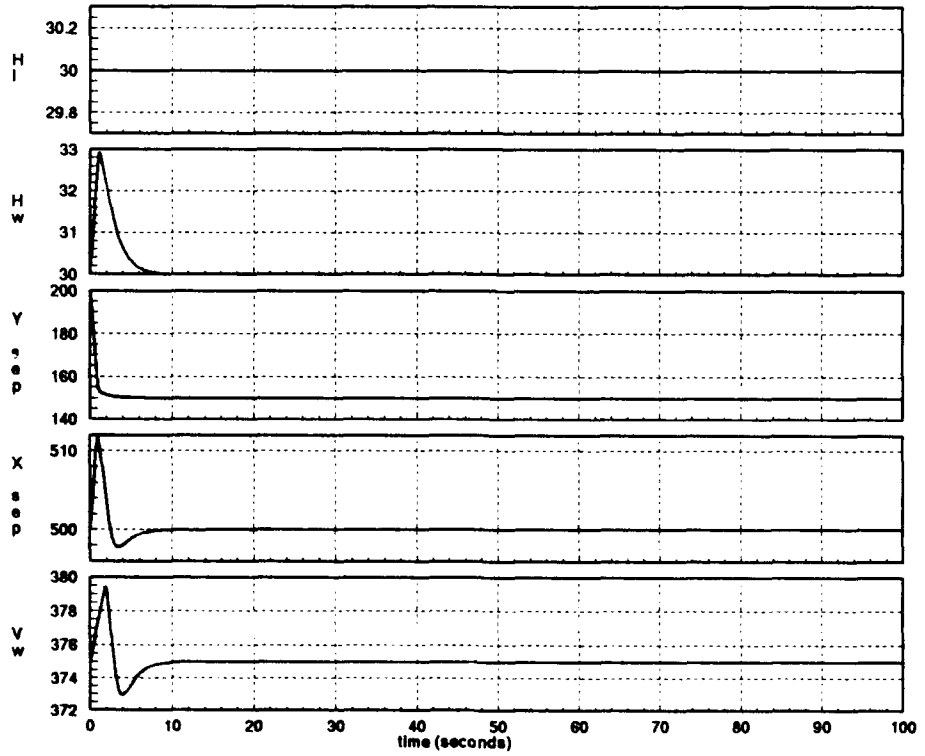

Figure 3.20. Response to Δy Input Change from 200 to 150 Feet Using Feedback

3.13.3 **Altitude and Δz Commands** Maneuvering in the vertical axis is effected by inputs of formation altitude, (h_L), and vertical separation, (Δz). Responses for these two inputs are shown in Figures 3.21 - 3.22 respectively.

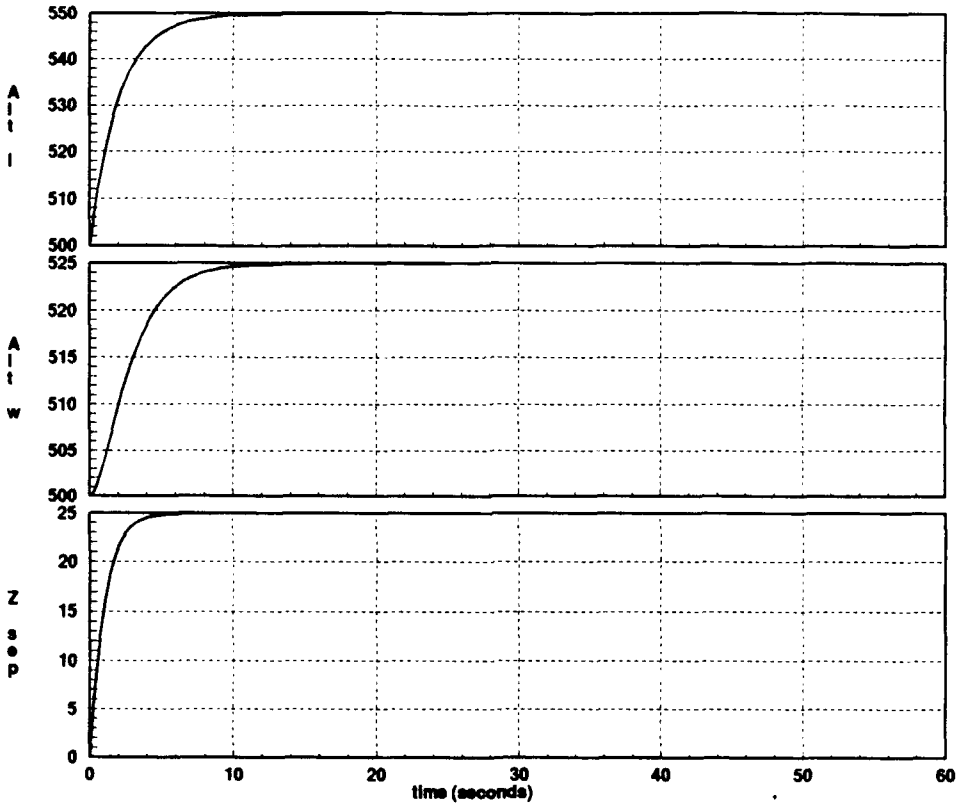

Figure 3.21. Response to an h_L (Input) Change From 500 to 550 Feet Using Feedback

Analysis of the vertical channel response to an h_L input shows that the wing aircraft cannot attain the commanded value of 550 feet. Therefore, additional control is required to eliminate this steady state error.

Analysis of the vertical channel response to a Δz input shows that the wing aircraft cannot attain the commanded Δz value of -50 feet. Therefore, additional control is required to eliminate this steady state error.

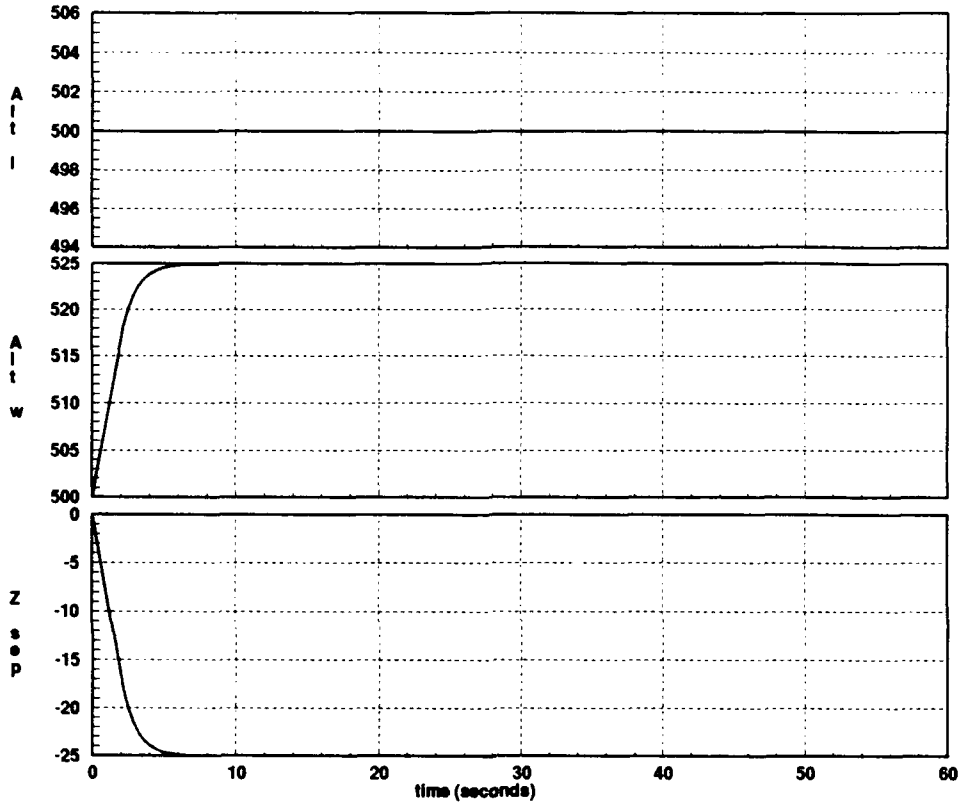

Figure 3.22. Response to a Δz Input Change from 0 to -50 Feet Using Feedback

3.13.4 **Large Heading Commands** Responses for a heading change of -45 degrees are shown in Figure 3.23. Analysis of the lateral channel response to a large heading maneuver into the wing aircraft shows that additional control is needed to smooth out the responses and to eliminate the steady state error in the Δy response.

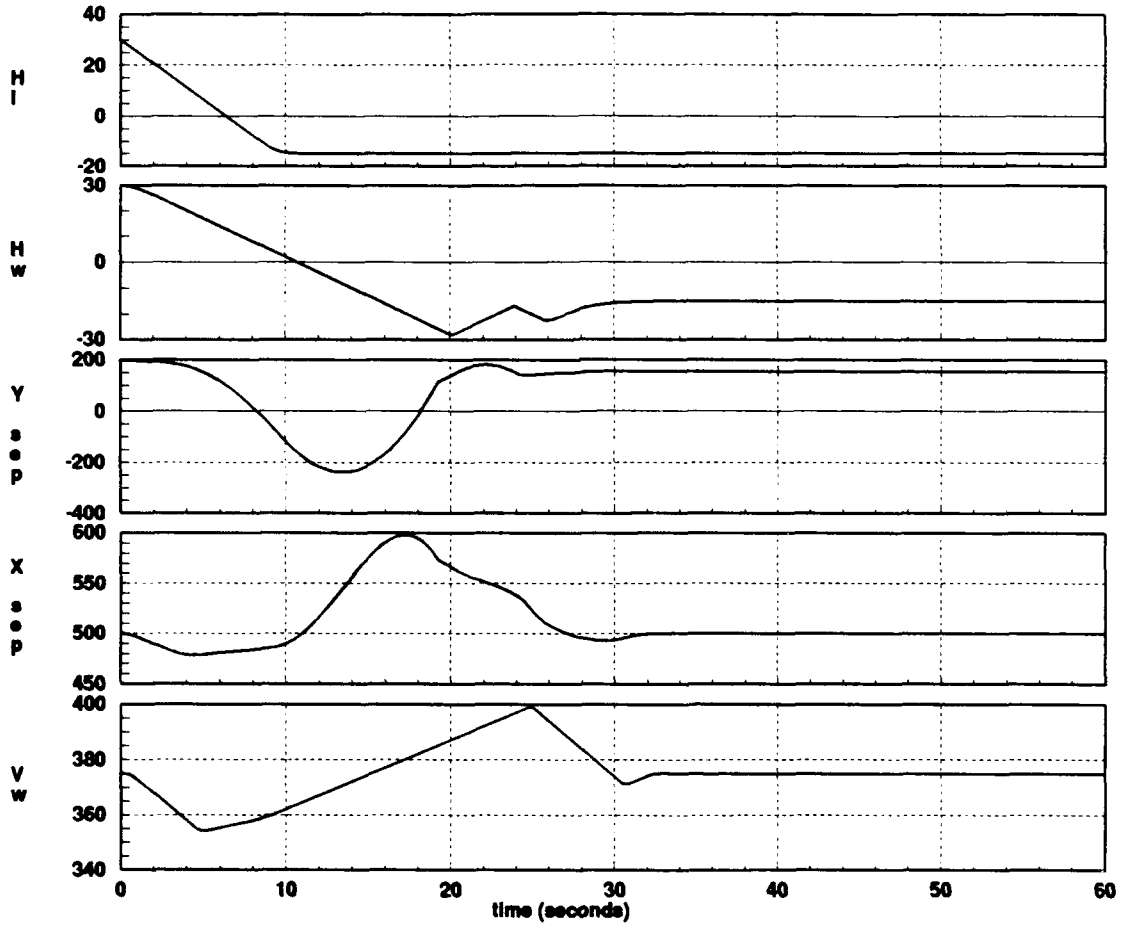

Figure 3.23. Response to an H_L (Input) Change from 30 to -15 Degrees Using Feedback

3.14 Measures of Merit

An examination of the formation system with velocity, heading, and altitude feedback illustrates that additional control is needed to make the system track the commanded inputs and to eliminate all tracking errors. Therefore, the measures of merit for this research are based on the formation control system's transient behavior and steady state error performance. The formation control system will be considered to perform satisfactorily if it is able to track all commanded inputs with zero steady state error and if its transient behavior is such that "collisions" between the lead and wing aircraft are avoided during the transients.

IV. Formation Controller Design

The aircraft models and the formation kinematics render the formation control system nonlinear. Simulations of the open loop performance and the state feedback performance of the formation control system in the previous chapter indicate that additional control is needed to eliminate the steady state error of the system in all three channels. Although there is concern for the transient behavior of the formation control system, a high priority is that good steady state performance is achieved so that the formation is maintained after a maneuver has been executed. Therefore, since the controller needs to reduce the steady state error to zero, which is tantamount to formation holding, the practical choice for a controller is a Proportional plus Integral (PI) controller. Thus, a linear PI controller is designed in this chapter that subsequently is added to the nonlinear formation control system simulation.

4.1 Design Method Overview

A PI controller operates on the error between the system input command signal and the system's output. Proportional and integral action is used to drive the error to zero. Thus, PI compensation uses the error and its integral. A large input is supplied by the controller to the system when either the magnitude or integral of that error is large. As the error returns to zero, so does the system input produced by the controller. Key to this controller operation are the gains used in the proportional and integral paths of the controller. The objective is to achieve decoupling of control and reference states through the judicious selections of the gains.

In formation flight, separation between the lead aircraft and wing aircraft is inherently determined by the maneuvering of those aircraft, through the basic kinematics of the situation. Therefore, the PI controller must decouple the effects of individual aircraft controls. The objective of the controller design is to determine

one set of gains for the PI controller that achieves decoupling of control and reference states for all formation maneuver and separation commands.

A reexamination of Figure 3.16 indicates that there are two sources of errors in the Formation Control System. These are the formation maneuver errors and the formation separation errors. Thus, a PI controller could be used to control both sets of errors. An initial step is to design a PI controller where only the formation separation errors are controlled, as shown in Figure 4.1.

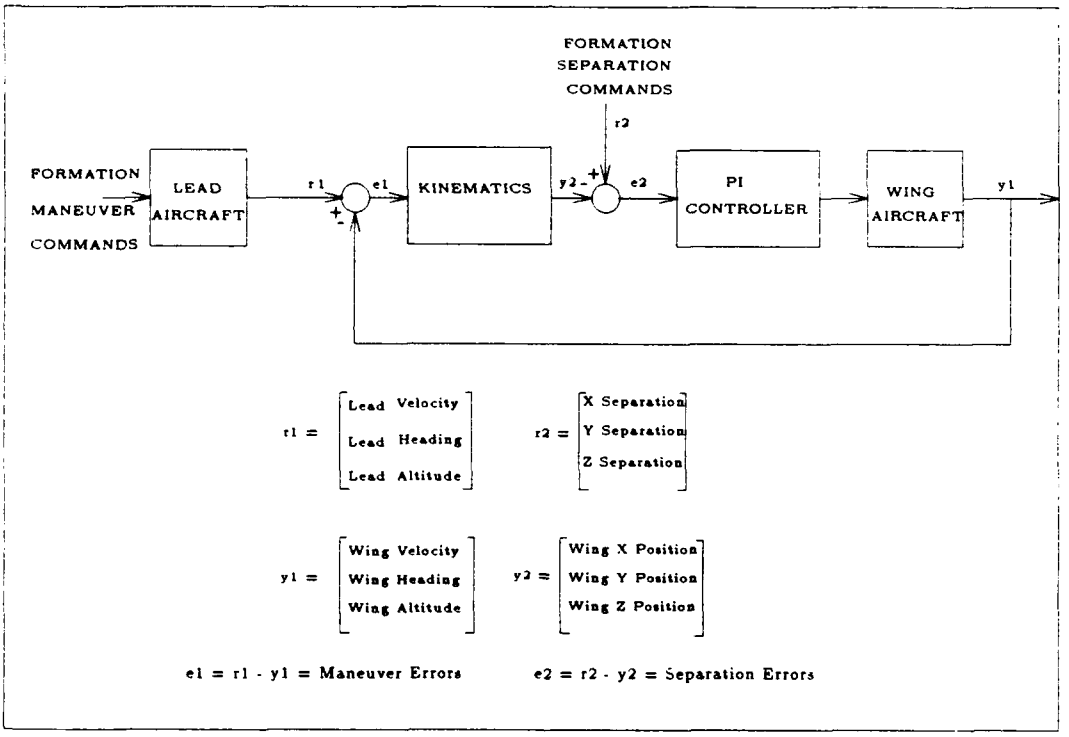

Figure 4.1. Closed Loop Formation Control System Block Diagram

It is evident, based upon the problem set up and the kinematic relationships, that if the formation separation errors are driven to zero, then the commanded formation maneuvers are tracked in steady state. Since the vertical channel of the formation system is decoupled from the longitudinal and lateral channels, a PI controller is first developed to control formation separation error in the vertical, or z axis. Next,

a PI controller is developed to control formation separation error in the longitudinal and lateral axes, or (x,y) plane, and, finally, a PI controller is developed to control a mixture of formation maneuver errors and formation separation errors in the (x,y) plane.

4.2 PI Control of Formation Separation Error in the Z Plane

Figure 4.2 shows a PI controller that controls Δz_E, or separation error in the z axis. The control law for the formation control system vertical channel is given in Equation 4.1,

$$h_{WC}(t) = (K_{z_p})\Delta z_E + (K_{z_I}) \int_0^t \Delta z_E \, dt \tag{4.1}$$

where:

- h_{WC} is the wing aircraft altitude command from the PI controller
- K_{z_p} and K_{z_I} are the z channel proportional and integral gains, respectively
- Δz_E is the separation in the z channel

A trial and error approach is used for obtaining the values of K_{z_p} and K_{z_I} that give the best responses to a given input to the formation control system. These vertical channel closed loop tests are performed on a formation comprised of dissimilar aircraft, and the same test conditions used for the vertical channel tests of the formation system with V, H, and h feedback are used again. Therefore, Table 3.4 may be referenced for these inputs and initial conditions. The gain values which provide the best system responses are as follows:

- $K_{z_p} = 1$
- $K_{z_I} = 0.5$

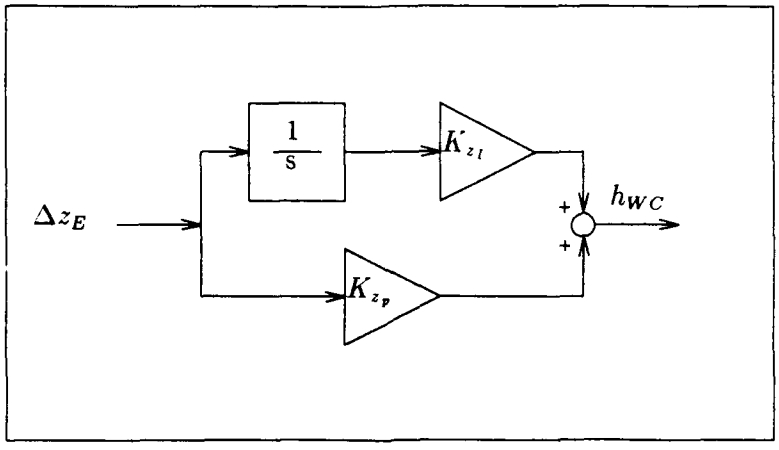

Figure 4.2. Vertical Channel PI Controller

The controlled vertical channel's response to an h_L input is shown in Figure 4.3. An analysis of this response shows that the wing aircraft attains the commanded formation altitude of 550 ft with no overshoot and with zero steady state error. A comparison of this response to the response of the formation system with just feedback, for the same input, Figure 3.21, shows that performance has been significantly improved since the steady state error has been driven to zero..

The controlled vertical channel response to a Δz input is shown in Figure 4.4. An analysis of this response shows that the wing aircraft attains the commanded Δz separation with no overshoot and with zero steady state error. A comparison of this response to the response of the formation system for the same input, Figure 3.22, shows that, once again, performance has been significantly improved.

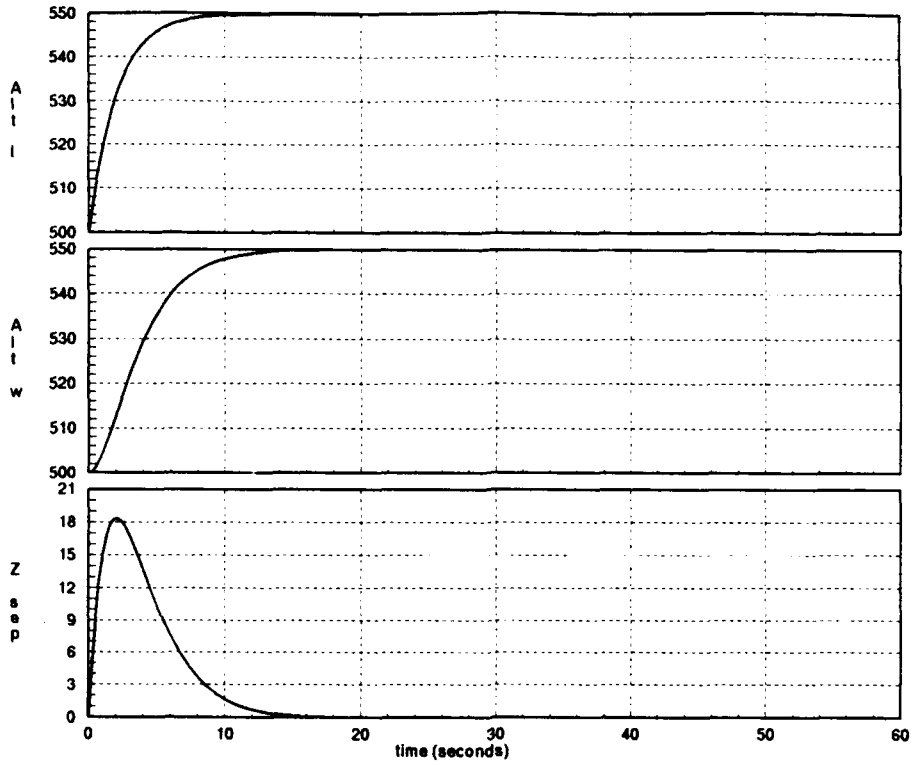

Figure 4.3. Controlled Vertical Response to an h_L (Input) Change, from 500 to 550 Feet

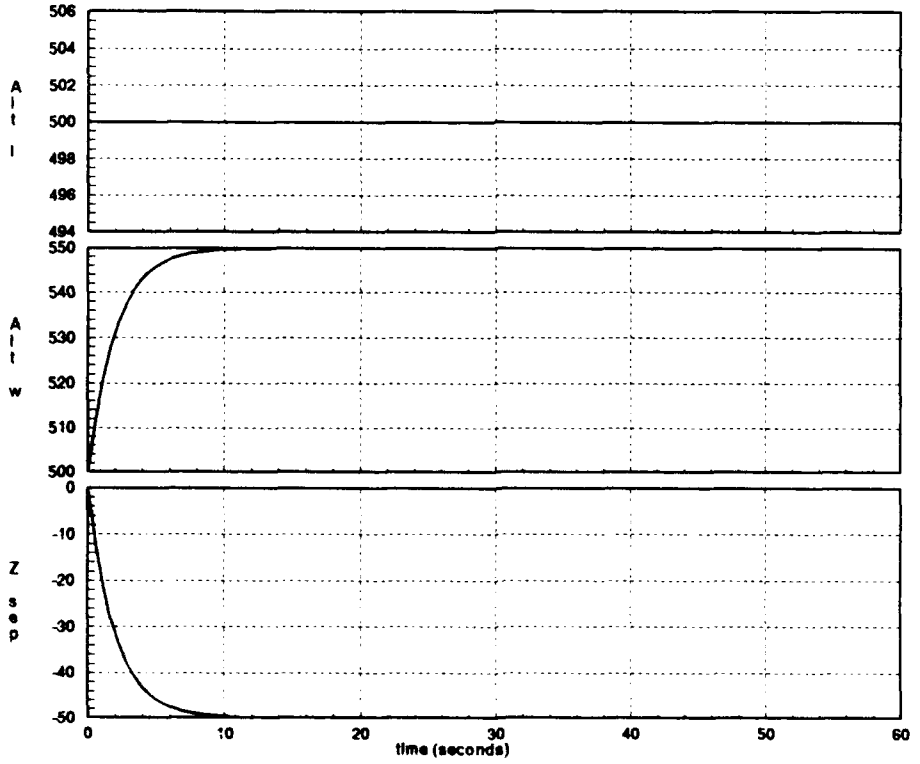

Figure 4.4. Controlled Vertical Channel Response to a Δz Input Change of -50 Feet

Thus, the PI control on the vertical separation error achieves the goal of obtaining zero steady state error in the vertical channel.

4.3 PI Control of Formation Separation Error in the X-Y Plane

Figure 4.5 depicts a PI controller that operates on the separation error in the longitudinal and lateral channels.

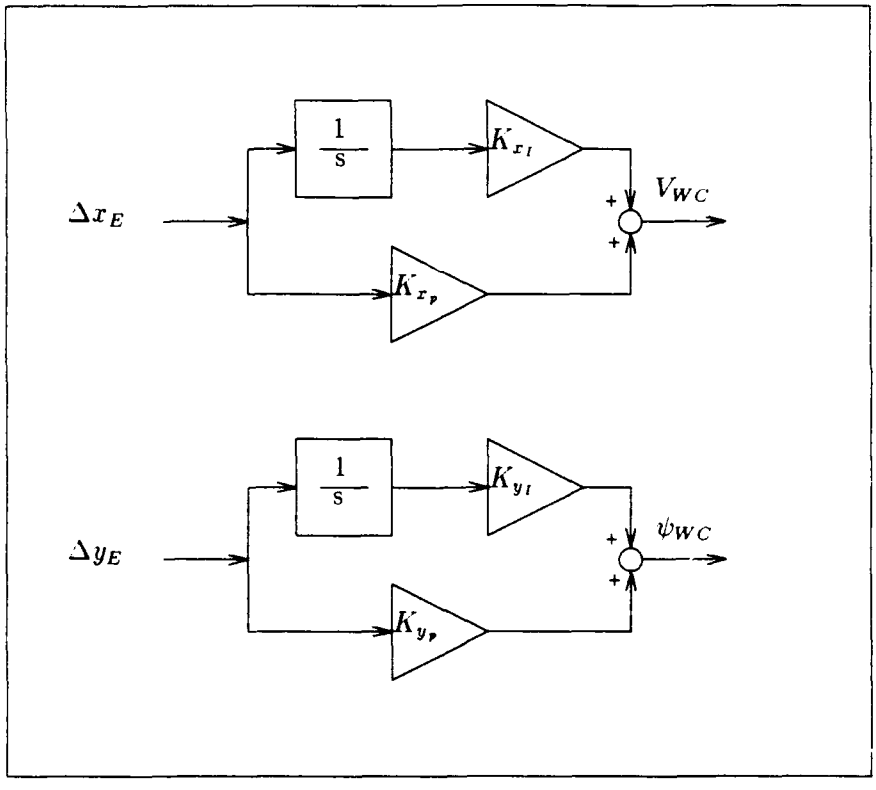

Figure 4.5. Longitudinal and Lateral Channel Separation Error PI Controller

The control laws for the horizontal plane of the formation control system with a PI controller in the loop are given in Equations 4.2 and 4.3.

$$V_{WC}(t) = (K_{x_p})\Delta x_E(t) + (K_{x_I}) \int_0^t \Delta x_E \, dt \tag{4.2}$$

$$\psi_{WC}(t) = (K_{y_p})\Delta y_E(t) + (K_{y_I}) \int_0^t \Delta y_E \, dt \tag{4.3}$$

where:

- V_{WC} is the wing aircraft velocity command from the PI controller
- ψ_{WC} is the wing aircraft heading command from the PI controller
- Δx_E and Δy_E are the respective x and y channel separation errors
- K_{x_p} and K_{x_I} are the x channel proportional and integral gains
- K_{y_p} and K_{y_I} are the y channel proportional and integral gains

A trial and error approach is used for obtaining the values of Kx_p, Kx_I, Ky_p, and Ky_I that give the best responses to a given input to the formation control system. These formation control system tests are performed on a formation comprised of dissimilar aircraft. With the exception of the vertical channel, these tests are performed for the same conditions as the tests of the formation system with just feedback. Therefore, Table 3.4 may be referenced for these inputs and initial conditions. The gain values which provide the best system responses are as follows:

- $K_{x_p} = 0.2$
- $K_{x_I} = 0.015$
- $K_{y_p} = 0.2$
- $K_{y_I} = 0.009$

The controlled longitudinal response to a V_L input is shown in Figure 4.6. An analysis of this response shows that the wing aircraft attains the commanded formation velocity of 400 ft/sec with an overshoot of 6 ft/sec.

A comparison of this response to the response of the formation system with feedback for the same input, Figure 3.17, indicates that the controlled wing velocity response has less overshoot and is slower. Because the controlled velocity response is slower, the Δx response has a larger overshoot, 90 ft, than the Δx response of the formation with feedback. However, the Δx response does achieve zero steady state error.

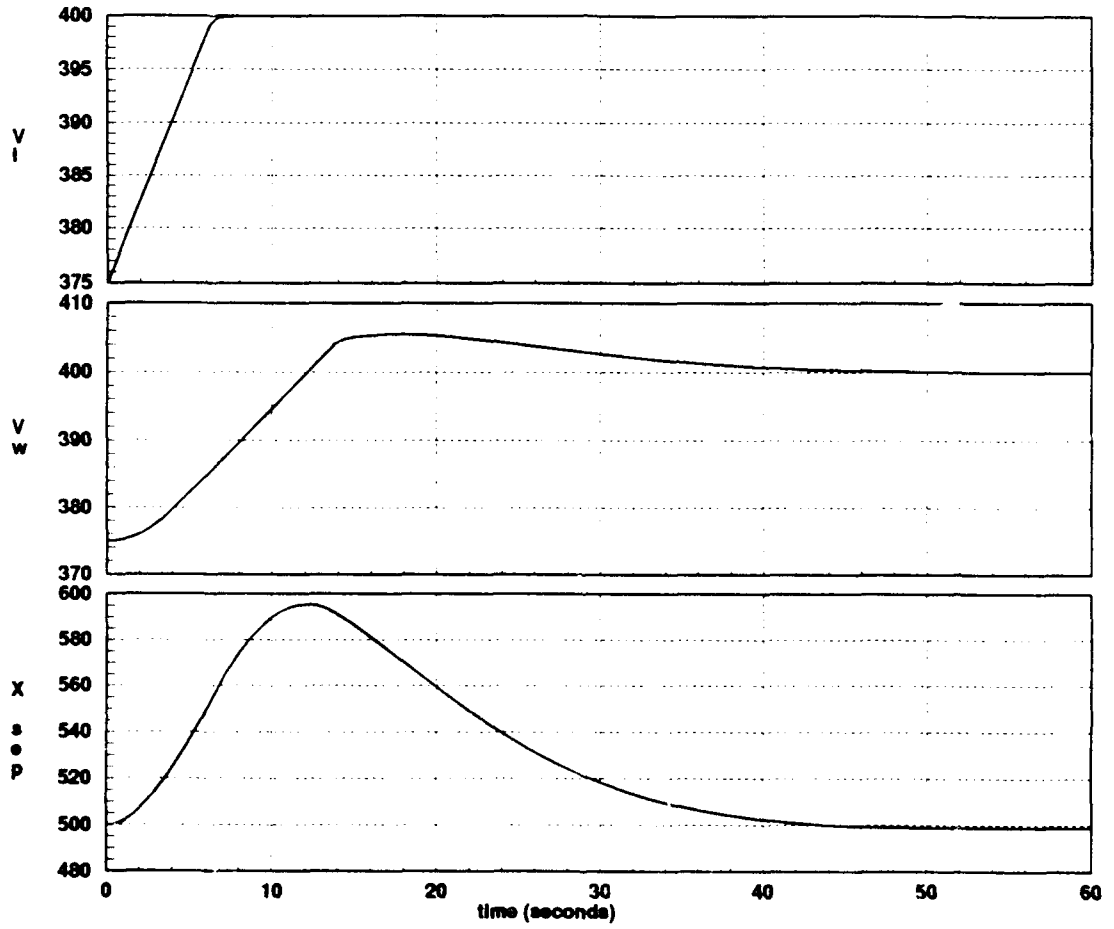

Figure 4.6. Controlled Longitudinal Channel Response to V_L (Input) Change, from $V_L = 375$ to 400 ft/sec

The controlled longitudinal channel response to a Δx response is shown in Figure 4.7. A comparison of this response to the response of the formation system with feedback for the same input, Figure 3.18, shows that an improvement in overshoot is obtained for the wing aircraft velocity response. The Δx response is slower than that of the formation system with feedback, but zero steady state error is achieved.

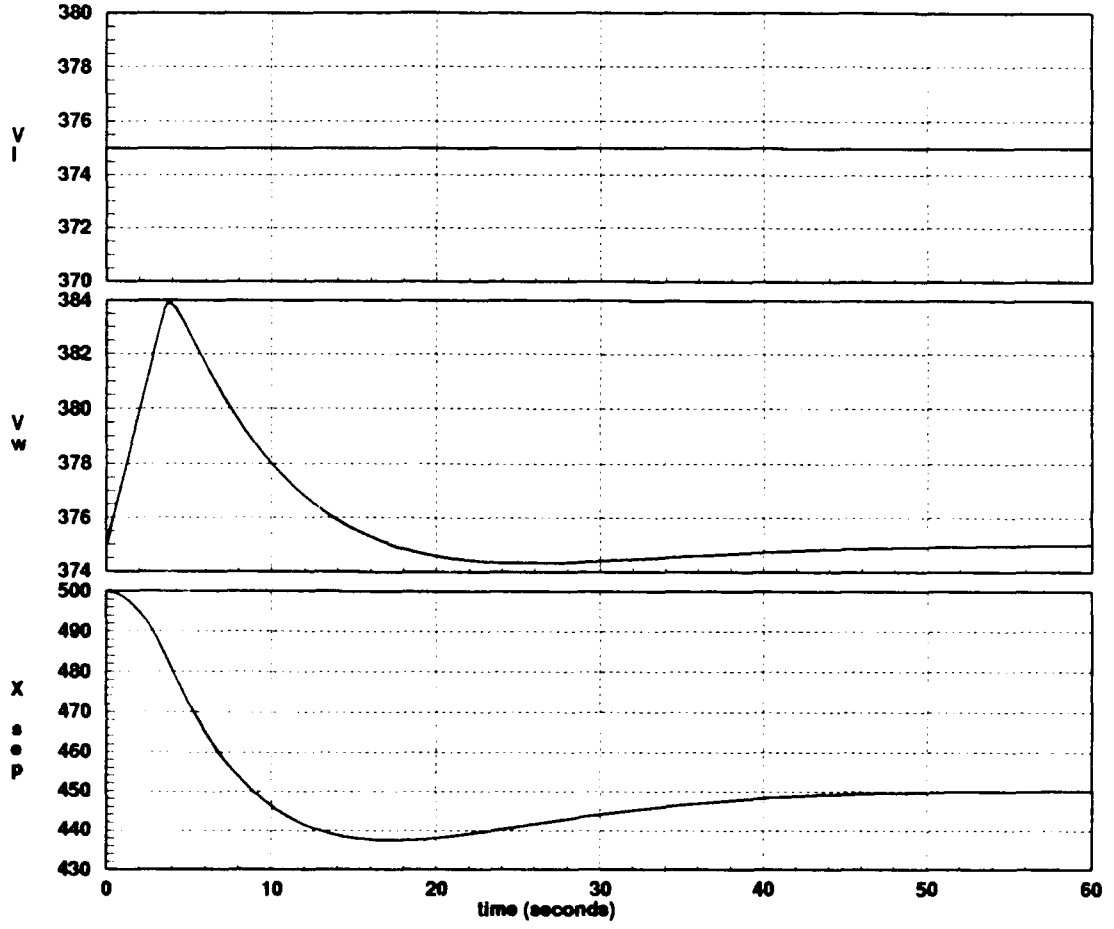

Figure 4.7. Controlled Longitudinal Channel Response to Δx Input Change, from $\Delta x = 500$ to 450 Feet

The controlled lateral response to an H_L input is shown in Figure 4.8. A comparison of this response to the response of the formation system with feedback for the same input, Figure 3.19, shows that a slight overshoot now occurs in the wing aircraft heading response. The Δy response has an overshoot of 21 ft, but achieves zero steady state error.

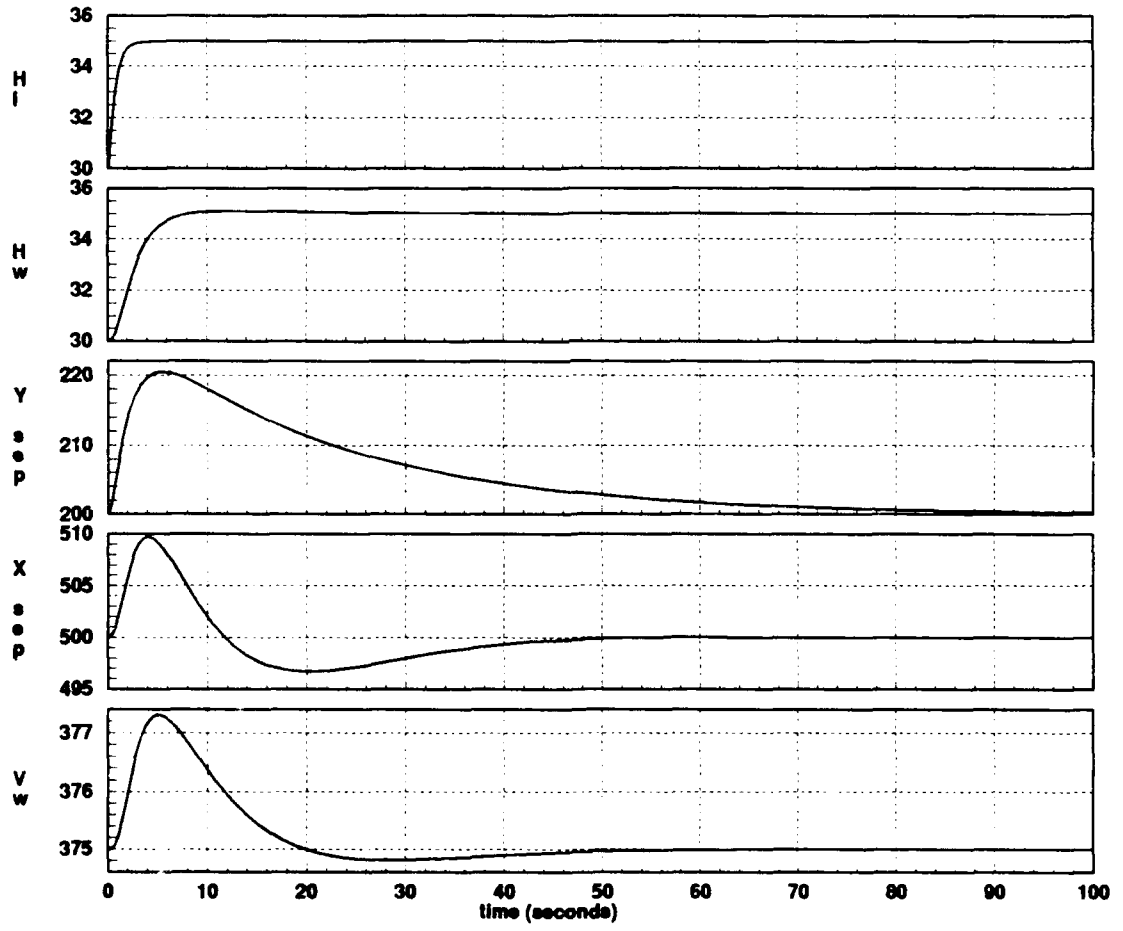

Figure 4.8. Controlled Lateral Channel Response to H_L (Input) Change, from H_L = 30 to 35 Degrees

The controlled lateral channel response to a Δy input is shown in Figure 4.9. A comparison of this response to the response of the system with feedback for the same input, Figure 3.20, shows that a slight improvement in overshoot is obtained for the wing aircraft heading response. The Δy response and the heading response both achieve zero steady state error.

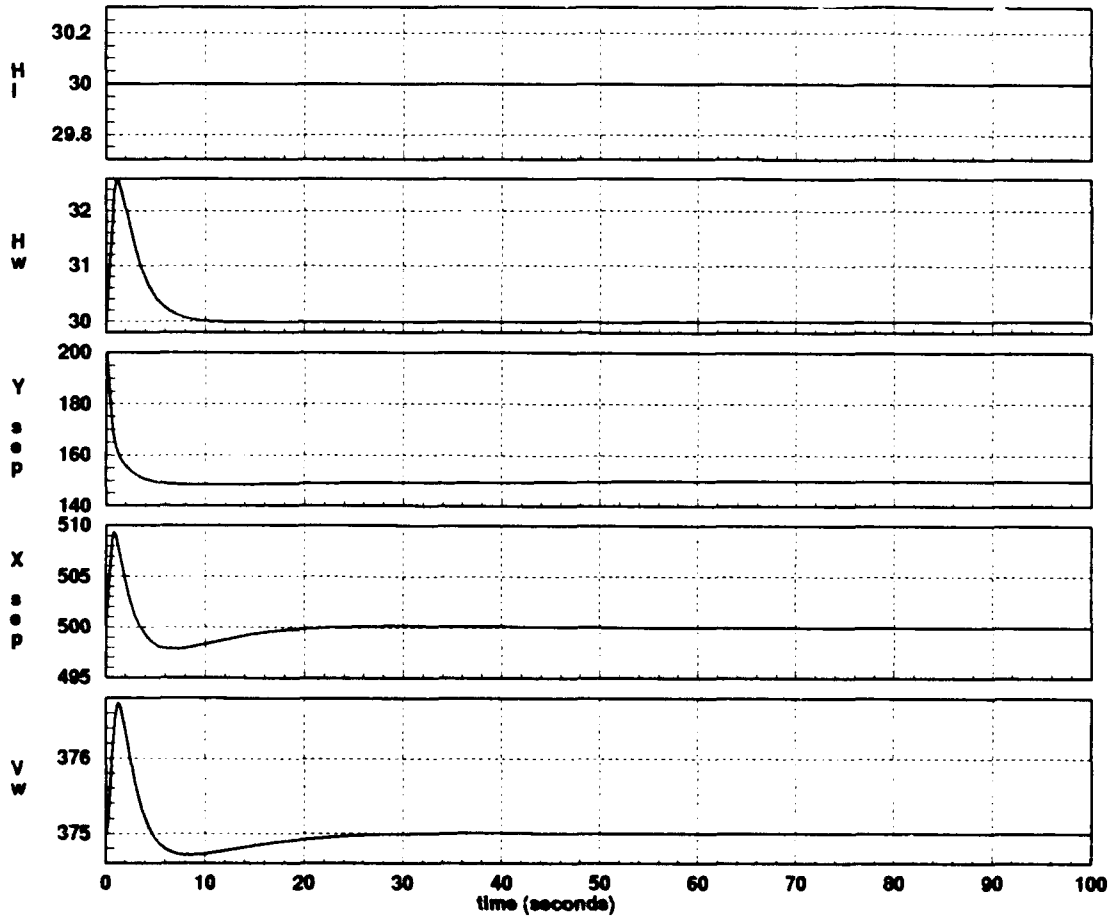

Figure 4.9. Controlled Lateral Channel Response to Δy Input Change, from Δy = 200 to 150 Feet

The controlled lateral channel response to a large H_L input is shown in Figure 4.10. A comparison of this response to the response of the formation system with feedback for the same input, Figure 3.23, shows that only a slight improvement is obtained in the transient behavior of the wing aircraft heading and Δy responses. However, zero steady state error is achieved.

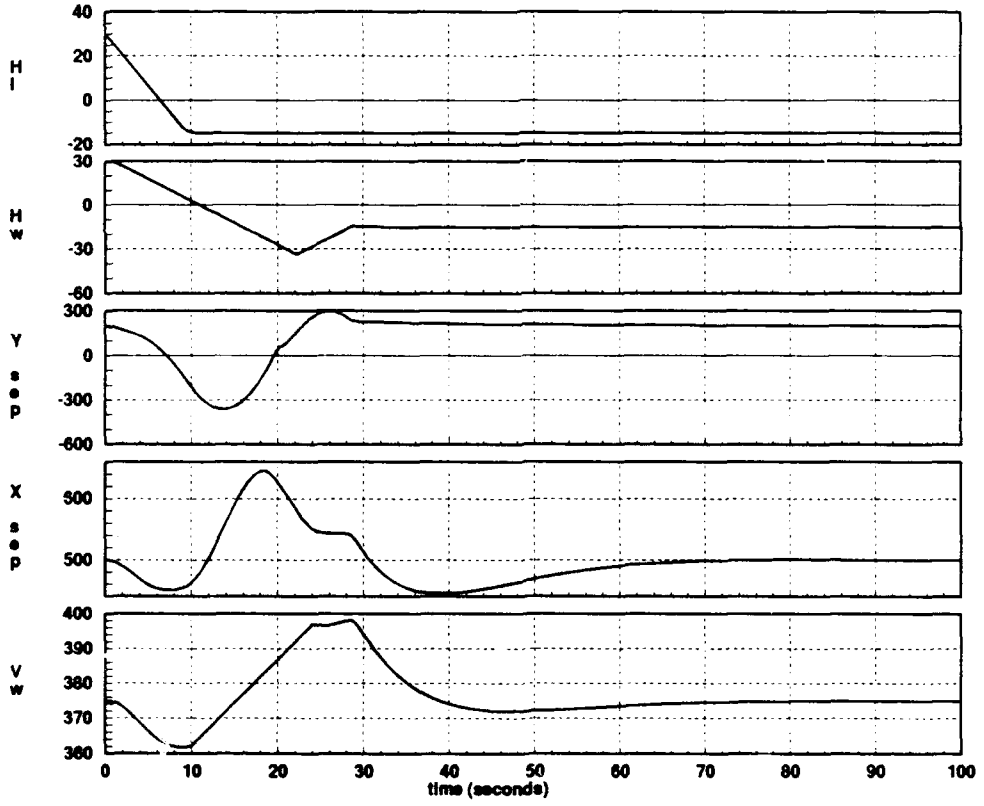

Figure 4.10. Controlled Lateral Channel Response to a Large H_L (Input) Change, from H_L = 30 to -15 Degrees

Thus, PI control on formation separation error in the x y plane achieves the additional control requirements listed in the tests of the formation system with feedback. For a V_L input, the controller smoothes out the wing aircraft velocity response and forces the Δx response to have zero steady state error. Also, the controller forces the Δy response to have zero steady state error for an H_L input. A large H_L input drives the formation system into the nonlinear region of operation. The controller does not provide much improvement in the system transient response for this large input, however, zero steady state error is obtained, as required.

4.4 PI Control Using a Mixture of Formation Separation Errors and Formation Maneuver Errors in the Horizontal Plane

Figure 4.11 shows the formation control system in which separation errors (x and y spacing errors) as well as maneuver errors (velocity and heading errors) are controlled. This type of control is possible through the cascading of a linear mixer with the PI controller. The preceding section describes the design of a PI controller that uses only the maneuver errors as inputs to control the wing aircraft. Thus, the separation errors have no effect on the wing aircraft responses. By combining, or mixing the two types of errors, the wing aircraft responds to both the maneuver and separation commands. Therefore, the previous controller design is henceforth called the unmixed PI controller.

The function of the mixer is to combine velocity error and Δx error for the longitudinal channel and to combine heading error and Δy error for the lateral channel. These outputs from the mixer then respectively feed into the longitudinal and lateral channels of the PI controller. The longitudinal channel mixing is described by Equation 4.4 and the lateral channel mixing is described by Equation 4.5.

$$X_{PI} = K_V V_E + K_X \Delta x_E \tag{4.4}$$

$$Y_{PI} = K_\psi \psi_E + K_Y \Delta y_E \tag{4.5}$$

where:

- X_{PI} is the longitudinal channel input to the PI controller
- K_V is the gain on the velocity error signal, V_E
- K_X is the gain on the x channel separation error signal, Δx_E
- Y_{PI} is the lateral channel input to the PI controller

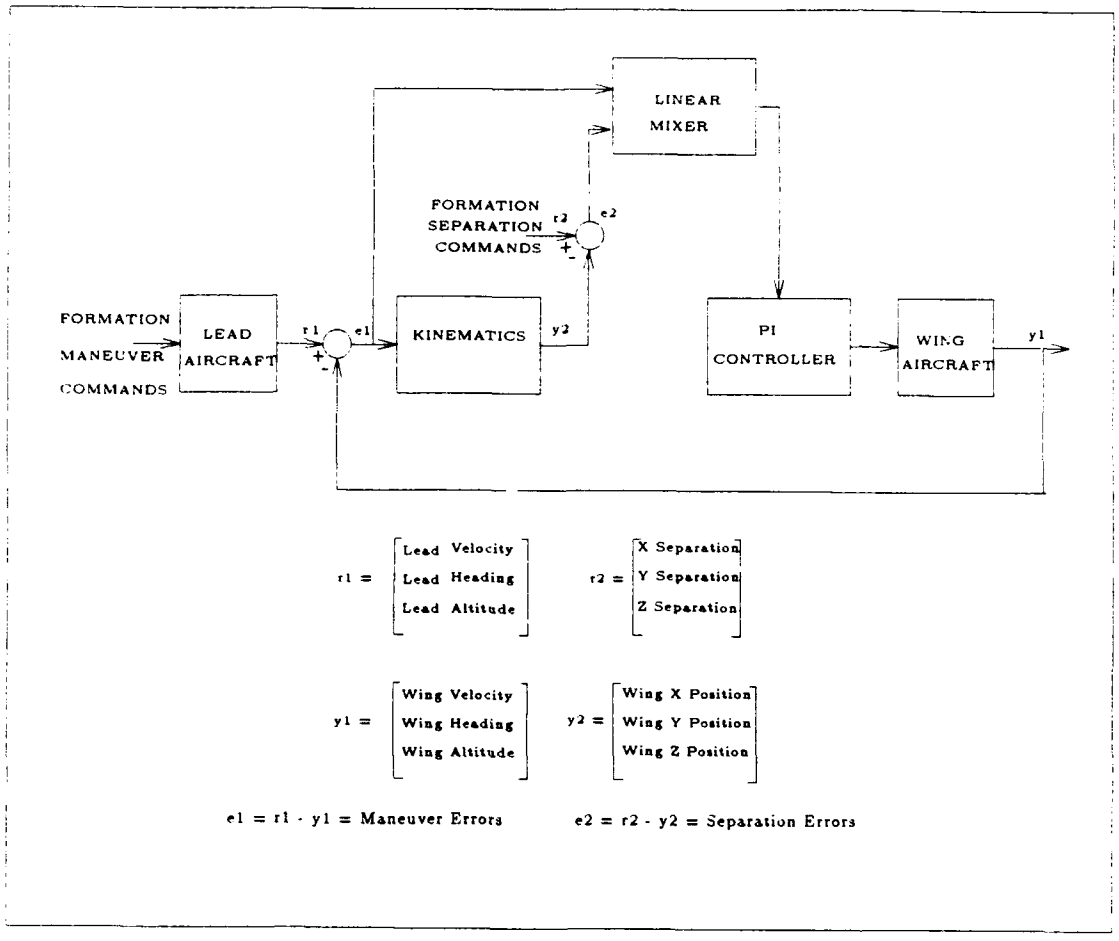

Figure 4.11. Longitudinal and Lateral Channel PI Controller Simulation

- K_ψ is the gain on the heading error signal, ψ_E
- K_Y is the gain on the y channel separation error signal, Δy_E

The resulting control laws for the longitudinal and lateral channels are shown in Equations 4.6 and 4.7.

$$V_{WC}(t) = K_{x_p}[K_V V_E + K_X \Delta x_E] + K_{x_I} \int_0^t [K_V V_E + K_X \Delta x_E]\, dt \qquad (4.6)$$

$$\psi_{WC}(t) = K_{y_p}[K_\psi \psi_E + K_Y \Delta y_E] + K_{y_I} \int_0^t [K_\psi \psi_E + K_Y \Delta y_E]\, dt \qquad (4.7)$$

A trial and error approach is used for obtaining the values of K_{x_p}, K_{x_I}, K_{y_p}, K_{y_I}, K_V, K_X, K_ψ, and K_Y that give the best responses to a given input to the formation control system. As in the previous tests of the formation system with feedback, the closed loop formation control system tests are performed on a formation comprised of dissimilar aircraft. With the exception of the vertical channel, the closed loop tests are performed for the same conditions as the tests of the formation system with feedback. Therefore, Table 3.4 may be referenced for these inputs and initial conditions. The gain values which provide the best system responses are as follows:

- $K_{x_p} = 0.17$, $K_{x_I} = 0.02$, $K_X = 2$, $K_V = 5$
- $K_{y_p} = 0.5$, $K_{y_I} = 0.05$, $K_Y = 1$, $K_\psi = 10$

The controlled longitudinal response to a V_L input using the mixer is shown in Figure 4.12. An analysis of this response indicates that the wing aircraft attains the commanded formation velocity of 400 ft/sec with an overshoot of 6 ft/sec. A comparison of this response with the controlled response for the same input when a mixer is not used, Figure 4.6, shows that the mixed controlled wing velocity response is faster, and the Δx response has less overshoot.

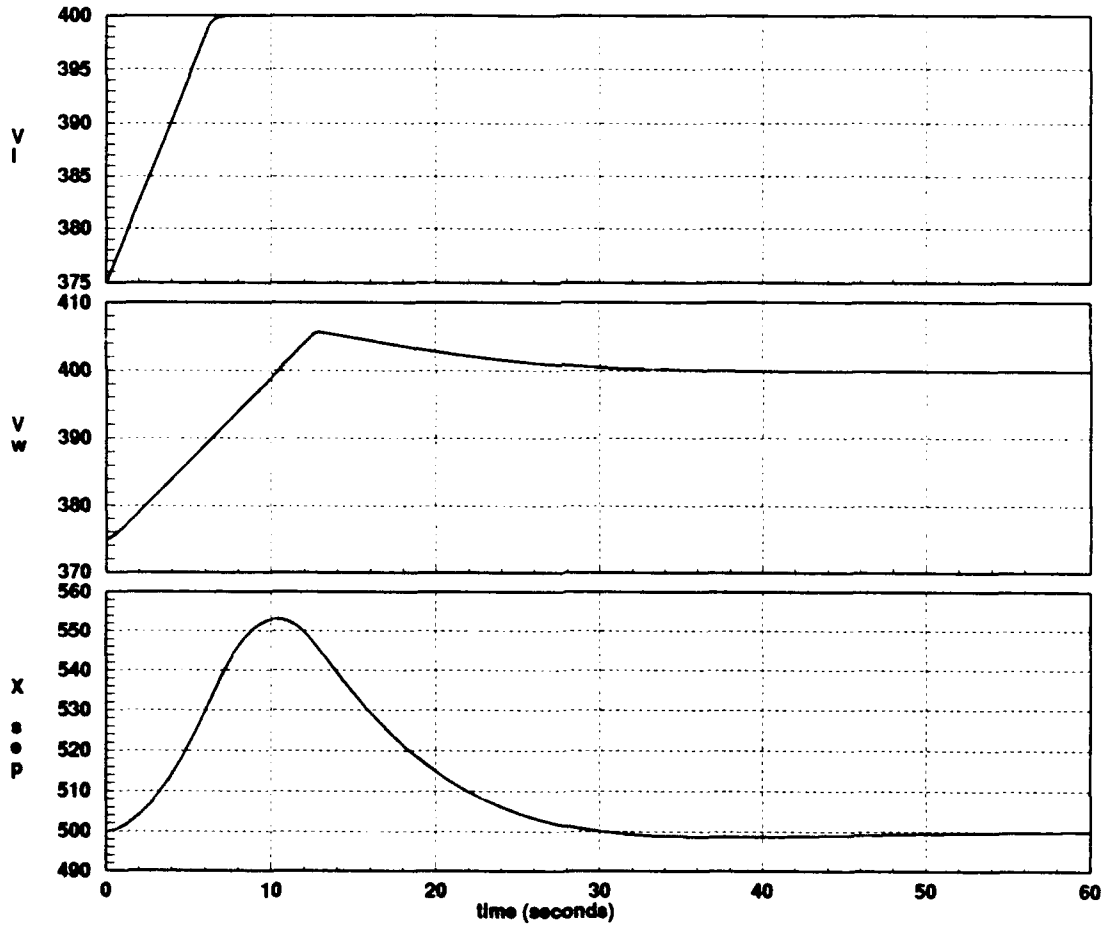

Figure 4.12. Mixed Controlled Longitudinal Channel Response to a V_L (Input) Change with Mixer, from $V_L = 375$ to 400 ft/sec

The mixed controlled longitudinal response to a Δx input is shown in Figure 4.13. An examination of this response indicates that the wing aircraft attains the commanded longitudinal separation, Δx, of 450 ft. A comparison of this response with the unmixed controlled response for the same input, Figure 4.7, illustrates that the mixed controlled wing velocity response is slightly faster and has about 6 ft less of undershoot.

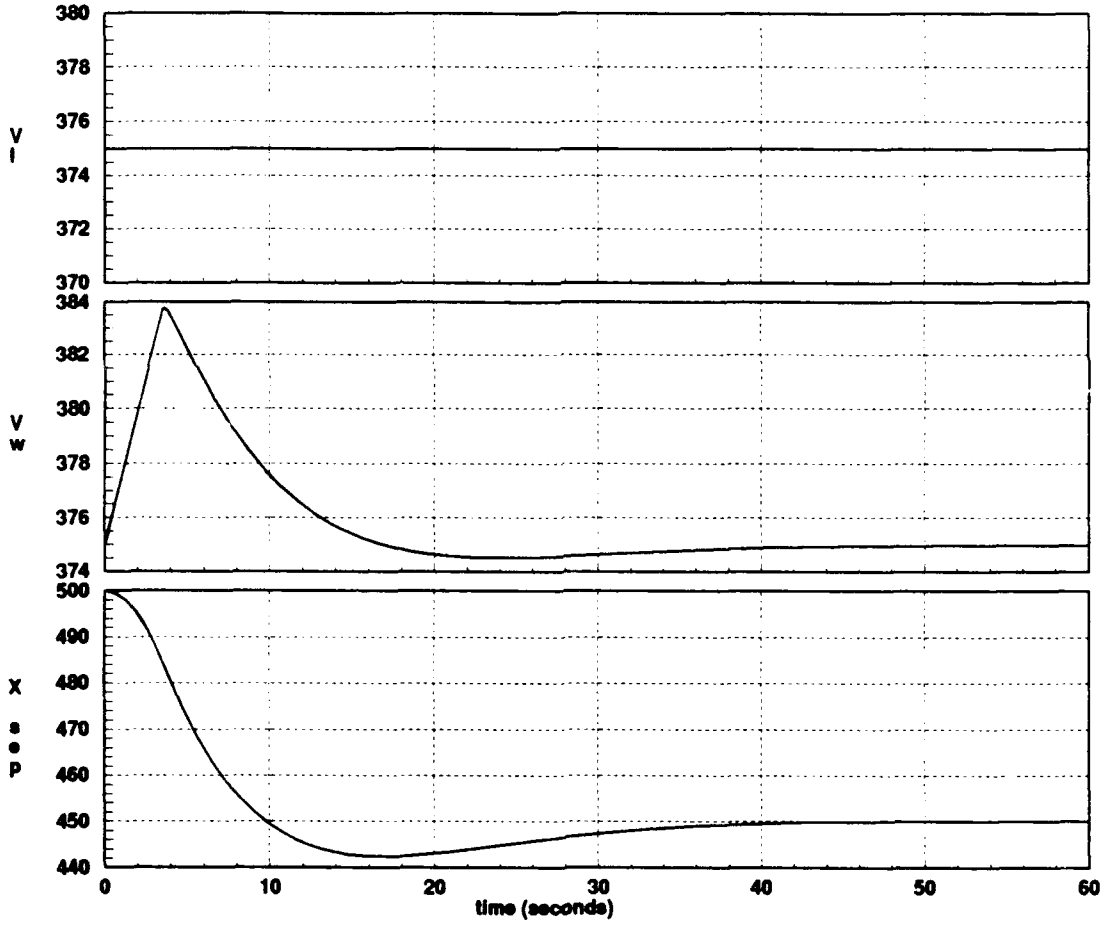

Figure 4.13. Controlled Longitudinal Channel Response to a Δx Input Change, with Mixer, from Δx = 500 to 450 Feet

The mixed controlled lateral response to an H_L input is shown in Figure 4.14. An analysis of this response shows that the wing aircraft attains the commanded H_L input of 35 degrees. A comparison of this response with the unmixed controlled response for the same input, Figure 4.8, shows that the responses are similar. The mixed Δy response does have some undershoot, whereas the unmixed response has none.

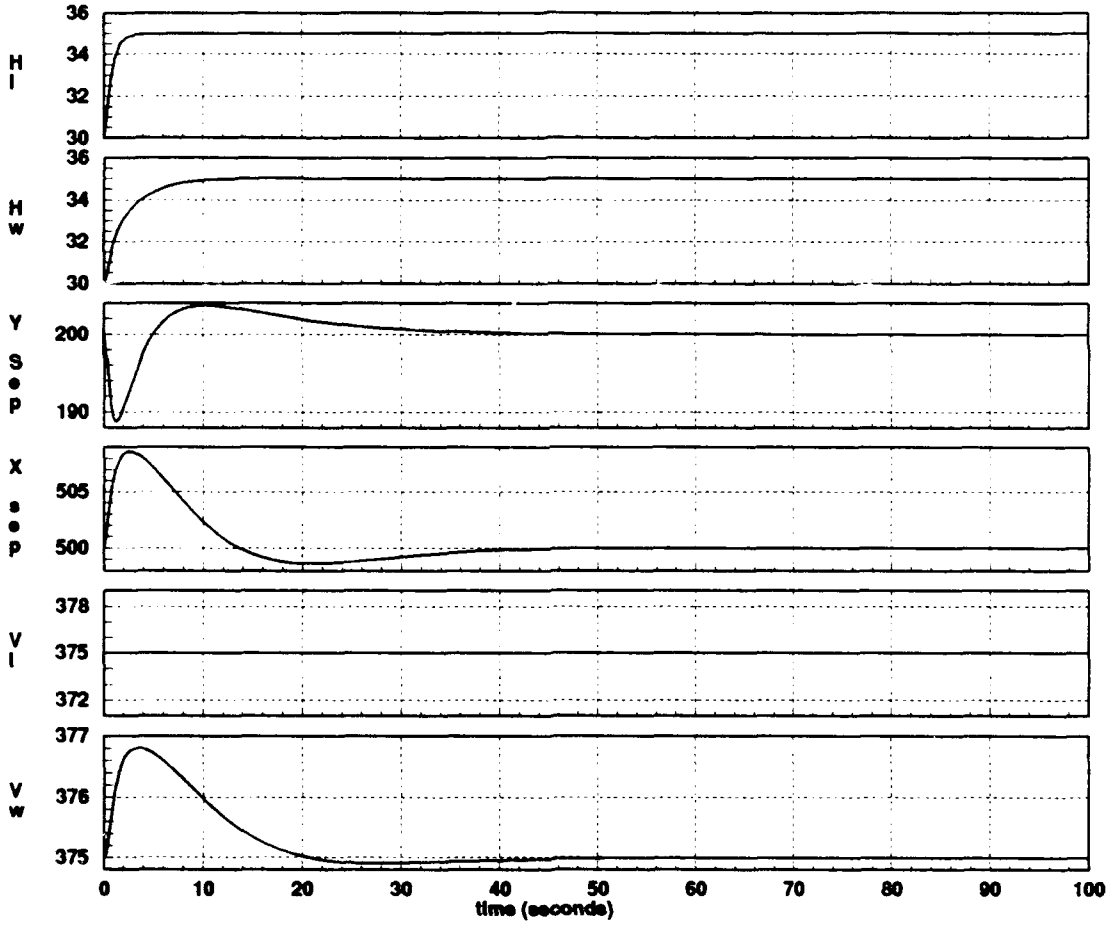

Figure 4.14. Controlled Lateral Channel Response to a H_L (Input) Change, with Mixer, from H_L = 30 to 35 Degrees

The mixed controlled lateral response to a Δy input is shown in Figure 4.15. An examination of this response shows that the wing aircraft attains the commanded Δy of 150 ft. A comparison of this response with the unmixed controlled response for the same input, Figure 4.9, shows that the mixed controlled heading response has less overshoot in the H_W response.

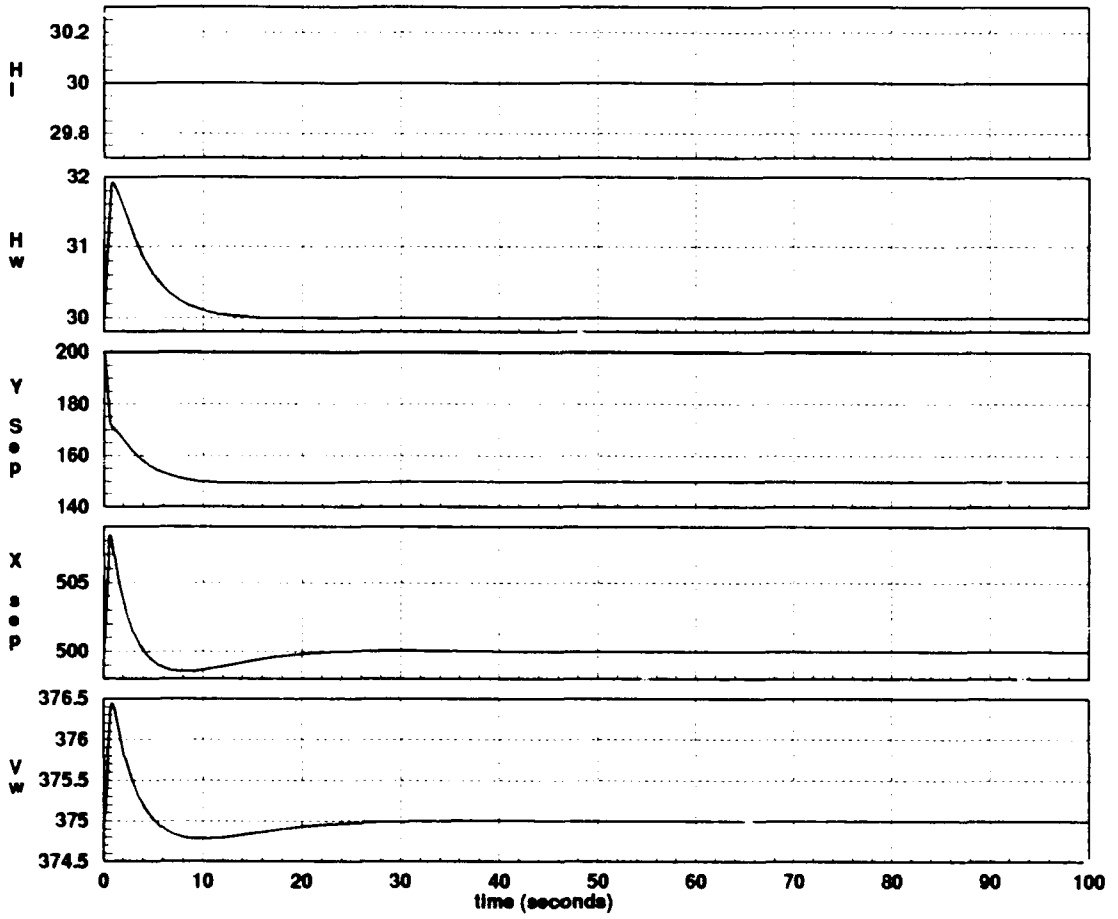

Figure 4.15. Controlled Lateral Channel Response to a Δy Input Change, with Mixer, from Δy = 200 to 150 Feet

The mixed controlled lateral channel response to a large H_L input is shown in Figure 4.16. A comparison of this response to the unmixed controlled response for the same input, Figure 4.10, shows that there is no improvement in the transient behavior of the wing aircraft heading and Δy responses. However, zero steady state error is achieved, as required.

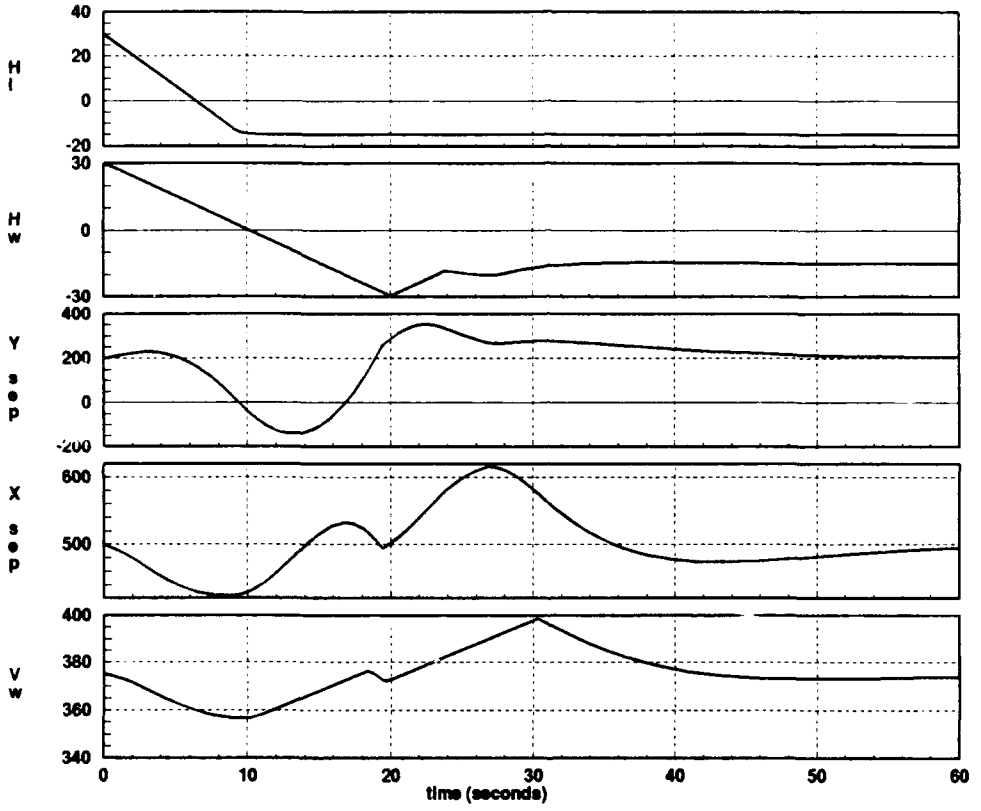

Figure 4.16. Controlled Lateral Channel Response to a Large H_L (Input) Change, with Mixer, from H_L = 30 to -15 Degrees

In this chapter several controllers are developed for the formation control system comprised of a superior performing lead aircraft and an inferior performing wing aircraft. A comparison between the PI controller with a mixer and the PI controller without a mixer shows that the controller with a mixer provides better transient behavior for the longitudinal channel. The amount of overshoot and undershoot is reduced in the longitudinal channel. Little improvement is obtained in the lateral channel through the use of the controller with a mixer. Nonetheless, the controller with a mixer provides better system responses overall. Therefore, this controller is chosen for the formation control system. A performance evaluation of the dissimilar aircraft formation control system, with the PI controller and a mixer, is conducted in the next chapter. A performance evaluation for the same formation control system comprised of similar, superior performing aircraft is given in Appendix A.

V. Formation Control System Performance Evaluation in which the Lead Aircraft's Performance Capability is Superior to the Wing Aircraft's

5.1 Introduction

A representative sample of a thorough evaluation of the closed-loop formation control system with the Mixer/PI controller is included in this chapter. This representative sample is for a formation system comprised of two dissimilar aircraft in which the lead aircraft's performance is superior to that of the wing aircraft. The lead aircraft is a C-130B and the wing aircraft is a C-130A. The results for a formation system comprised of similar aircraft in which both aircraft have superior performance capability are included in Appendix A.

5.2 Performance Evaluations

Time history plots are generated for all tests, and flight path plots are generated for tests that involve a heading change maneuver. The flight path plots are shown in an inertial reference frame with an initial formation heading angle of 0 degrees. The inertial reference frame allows the formation maneuver to be illustrated more clearly. The magnitude of the particular commanded maneuver on the flight path plot is the same as that on the corresponding time history plot. The definitions of the variables on the time response plots are listed in Table 5.1. The solid line on the flight path plots represents the flight path plot of the lead aircraft, and the dashed line represents the flight path plot of the wing aircraft. The initial conditions for the tests are shown in Table 5.2. Table 5.3 lists the tests performed and the location of the results. For the input changes marked with an asterisk in Table 5.3, both time history plots and flight path plots are presented.

Table 5.1. Variable Definitions

Variable Name: Text	Variable Name: Time Plots	Definition
V_L	V_l	Velocity of lead aircraft
V_W	V_w	Velocity of wing aircraft
H_L	H_l	Heading angle of lead aircraft
H_W	H_w	Heading angle of wing aircraft
h_L	Alt_l	Altitude of lead aircraft
h_W	Alt_w	Altitude of wing aircraft
Δx	$XSep$	Longitudinal separation distance
Δy	$Ysep$	Lateral separation distance
Δz	$Zsep$	Vertical separation distance

Table 5.2. Test Initial Conditions

Formation	Parameter	Initial Condition
Diamond	V_L	375 ft/sec
	V_W	375 ft/sec
	H_L	30 deg
	H_W	30 deg
	h_L	500 ft
	h_W	500 ft
	Δx	500 ft
	Δy	200 ft
	Δz	0 ft
Trail	V_L	375 ft/sec
	V_W	375 ft/sec
	H_L	30 deg
	H_W	30 deg
	h_L	500 ft
	h_W	500 ft
	Δx	500 ft
	Δy	0 ft
	Δz	0 ft
Abreast	V_L	375 ft/sec
	V_W	375 ft/sec
	H_L	30 deg
	H_W	30 deg
	h_L	500 ft
	h_W	500 ft
	Δx	0 ft
	Δy	200 ft
	Δz	0 ft

Table 5.3. Formation Control System Simulation Tests

Initial Formation	Final Formation	Commanded Parameter Input	Response Plots
Diamond	Diamond	V_L = 350 ft/sec	Figure 5.1
Diamond	Diamond	Δx = 550 ft	Figure 5.2
Diamond	Diamond	* H_L = 25 deg	Figure 5.3 and 5.4
Diamond	Diamond	* Δy = 250 ft	Figure 5.5 and 5.6
Diamond	Diamond	h_L= 450 ft	Figure 5.7
Diamond	Diamond	Δz = 50 ft	Figure 5.8
Diamond	Diamond	* H_L = 45 deg	Figure 5.9 and 5.10
Diamond	Diamond	* H_L = -45 deg	Figure 5.11, 5.12 and 5.13
Abreast	Abreast	V_L = 400 ft	Figure 5.14
Abreast	Abreast	V_L = 350 ft	Figure 5.15
Abreast	Abreast	* Δy = 300 ft	Figure 5.16 and 5.17
Abreast	Abreast	* Δy = 100 ft	Figure 5.18 and 5.19
Abreast	Abreast	* H_L = -45 deg	Figure 5.20, 5.21
Abreast	Abreast	* H_L = 45 deg	Figure 5.22 and 5.23
Trail	Diamond	* Δy = 200 ft	Figure 5.24 and 5.25
Diamond	Trail	* Δy = 0 ft	Figure 5.26 and 5.27
Trail	Trail	h_L = 850 ft	Figure 5.28

5.2.1 **Diamond Formation Velocity Reduction** For this test the formation is commanded to reduce its velocity from 375 ft/sec to 350 ft/sec. Figure 5.1 shows that the wing aircraft follows the lead aircraft with about three ft/sec of undershoot before attaining the commanded velocity. Due to the delay of the wing aircraft beginning its deceleration, a transient occurs in the longitudinal separation. This transient is smoothly dissipated as the longitudinal separation returns to the commanded value of 500 feet.

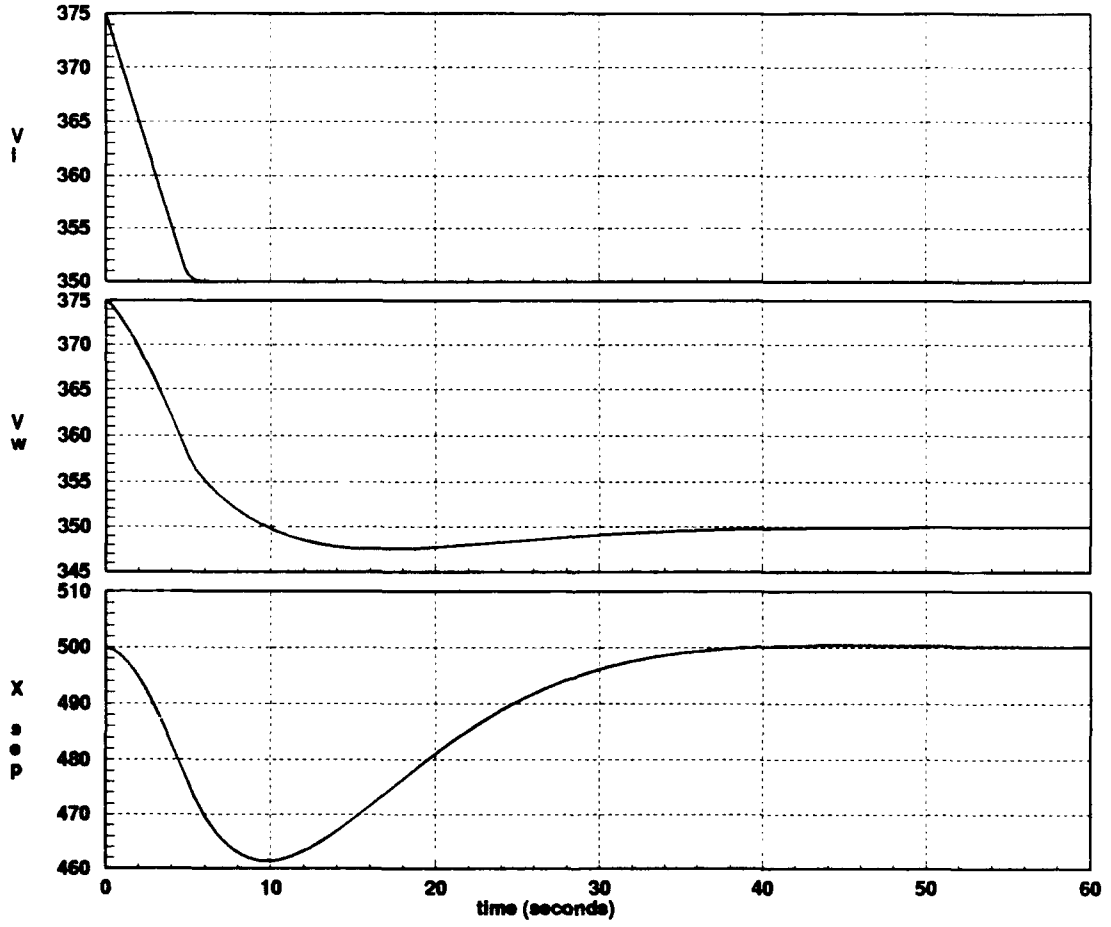

Figure 5.1. Longitudinal Response to a V_L (Input) Change from 375 to 350 ft/sec

5.2.2 **Diamond Formation Longitudinal Separation Increase** The wing aircraft is commanded to increase its longitudinal separation from 500 feet to 550 feet. The wing aircraft initially decreases its velocity to accomplish this command. Then, the wing aircraft returns to the commanded formation velocity of 375 ft/sec in 40 seconds, and it accomplishes the commanded separation increase in 40 seconds with zero steady state error, as shown in Figure 5.2.

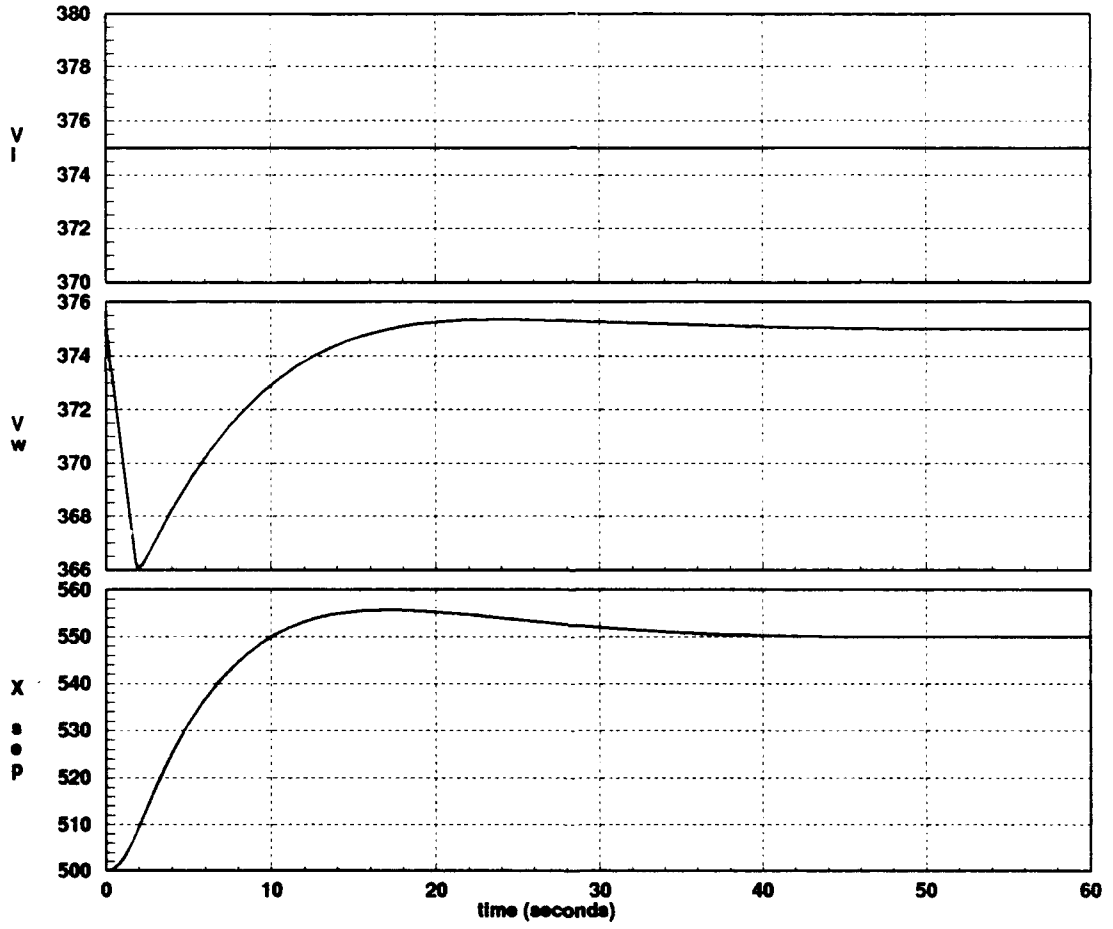

Figure 5.2. Longitudinal Response to a Δx Input Change from 500 to 550 feet

5.2.3 **Diamond Formation Heading Angle Decrease** The formation is commanded a heading change from 30 degrees to 25 degrees as depicted in Figure 5.3. The wing aircraft follows the lead aircraft heading maneuver with no undershoot and zero steady state error. The lead aircraft completes the maneuver in 3 seconds whereas the wing aircraft accomplishes the maneuver in 10 seconds. The lateral separation distance is temporarily increased due to the delay in the wing aircraft performing the commanded maneuver. However, the formation is maintained in steady state, as the longitudinal and the lateral separation distances as well as the wing velocity all return to their respective commanded values. Figure 5.4 illustrates the flight path plot for this maneuver, with an initial heading angle of zero degrees, along with the total separation range, as a function of time.

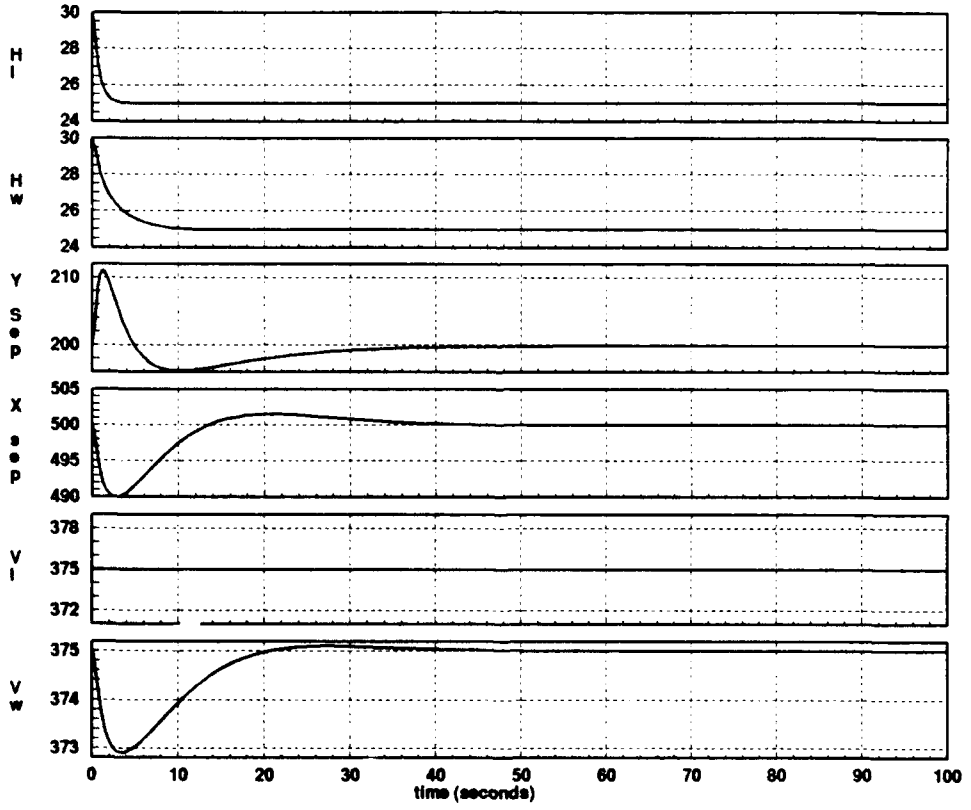

Figure 5.3. Lateral Response to an H_L (Input) Change from 30 to 25 Degrees

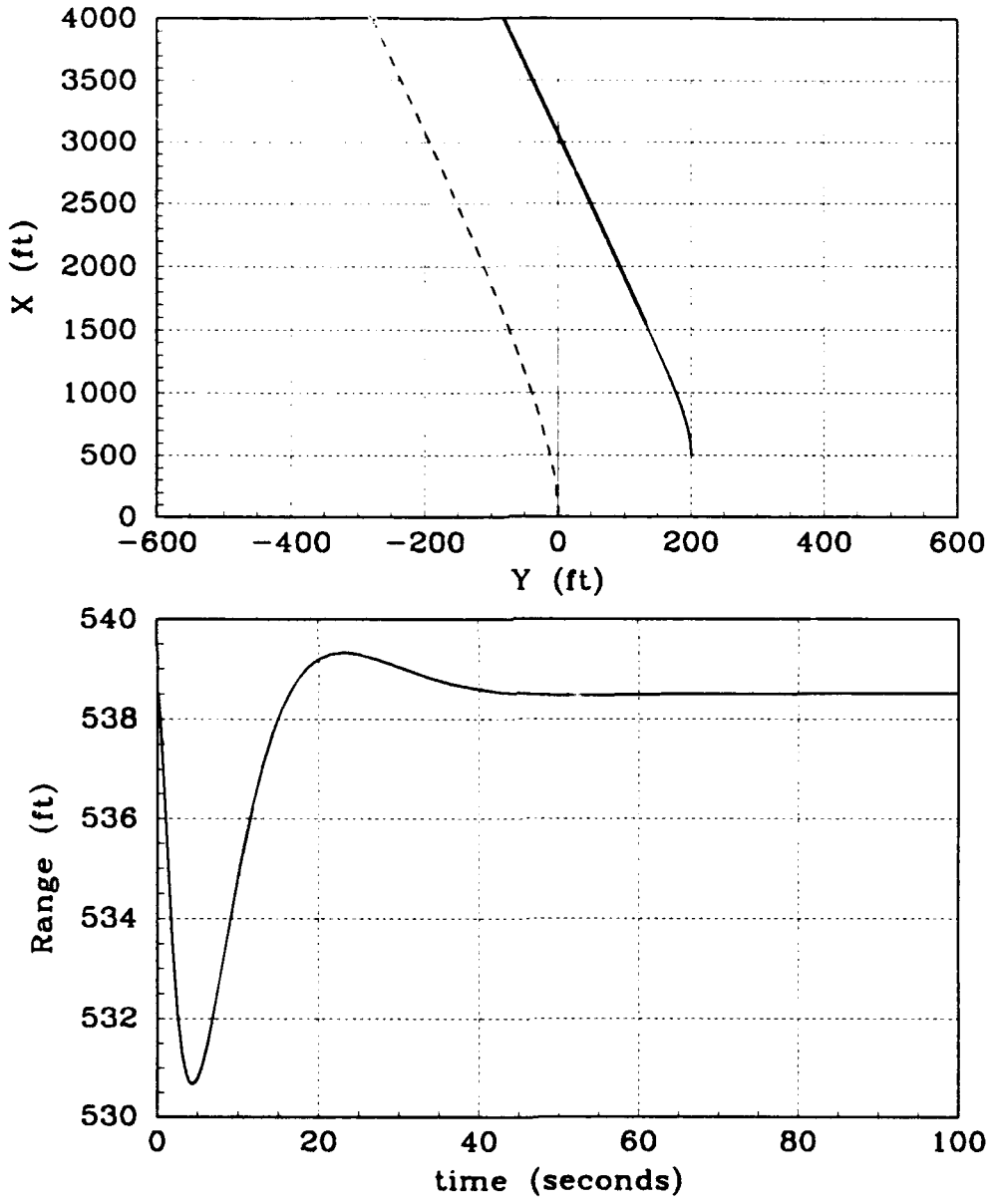

Figure 5.4. Flight Path Plot of an H_L (Input) Change from 0 to -5 Degrees

5.2.4 **Diamond Formation Lateral Separation Increase** Figure 5.5 illustrates that the formation is commanded to increase its lateral separation distance from 200 feet to 250 feet. The wing aircraft accomplishes this command by reducing its heading angle so that the lateral separation distance is increased. After the separation distance is attained, the wing aircraft returns to the commanded formation heading angle of 30 degrees. Thus, the commanded separation distance of 250 feet is attained with zero steady state error, and all other formation commanded values are maintained in steady state. The flight path plot for this commanded maneuver is shown in Figure 5.6, along with the total separation range.

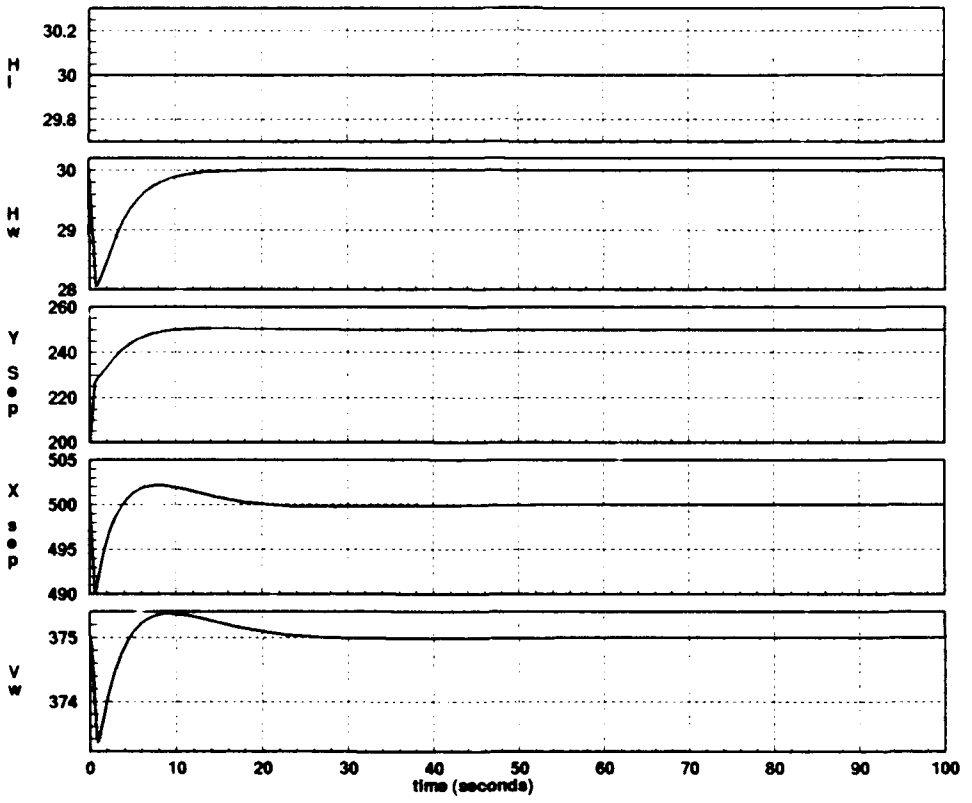

Figure 5.5. Lateral Response to a Δy Input Change from 200 to 250 feet

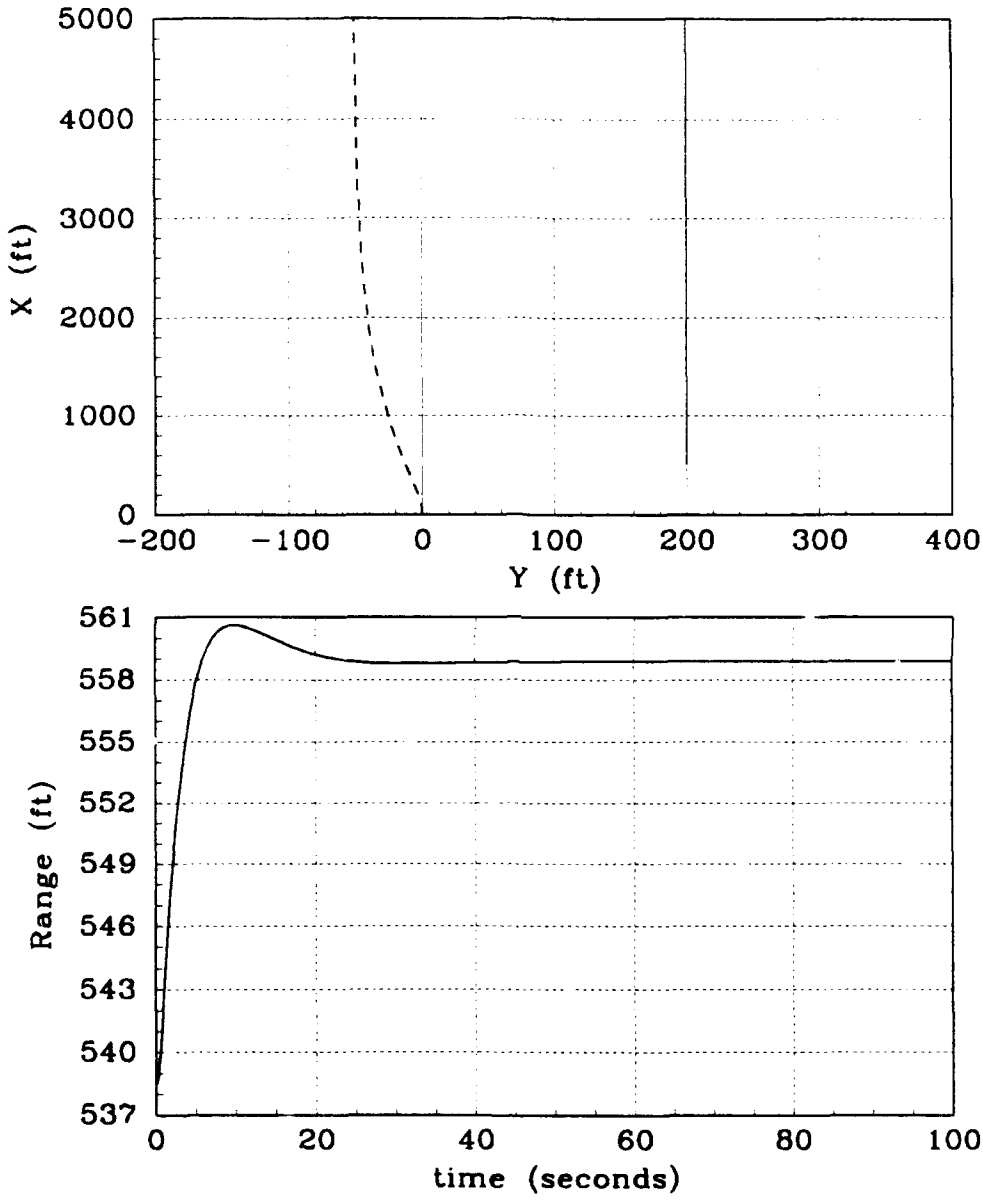

Figure 5.6. Flight Path Plot of a Δy Input from 200 to 250 feet

5.2.5 **Diamond Formation Altitude Decrease** For this test the formation is commanded to decrease its altitude from 500 feet to 450 feet, as shown in Figure 5.7. The lead aircraft performs the command in 10 seconds, whereas the wing aircraft performs the command in 12 seconds. Due to the delay in the wing aircraft's response to the command, a transient occurs in the vertical separation response until both aircraft reach the commanded value. Nonetheless, there is no steady state error in any of the responses.

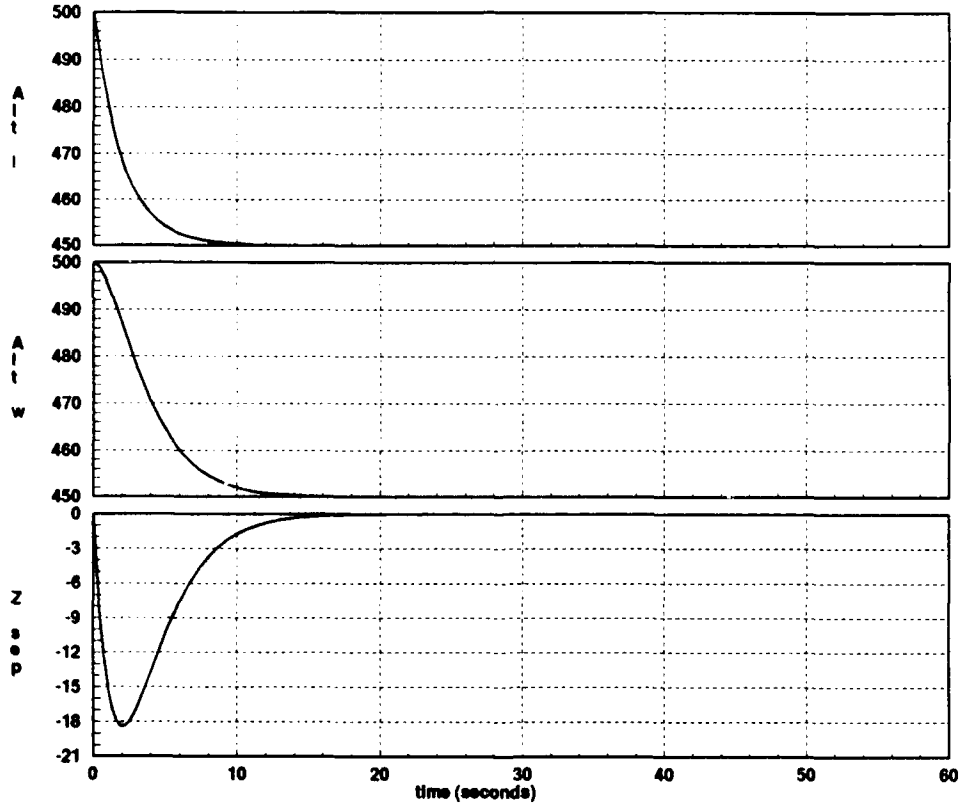

Figure 5.7. Vertical Response to an h_L (Input) Change from 500 to 450 feet

5.2.6 **Diamond Formation Vertical Separation Increase** Figure 5.8 depicts the formation response to a commanded vertical separation change from 0 feet to 50 feet. The wing aircraft increases it altitude from 500 feet to 550 feet so that the commanded vertical separation distance is attained. The wing aircraft performs this maneuver in 10 seconds with zero steady state error.

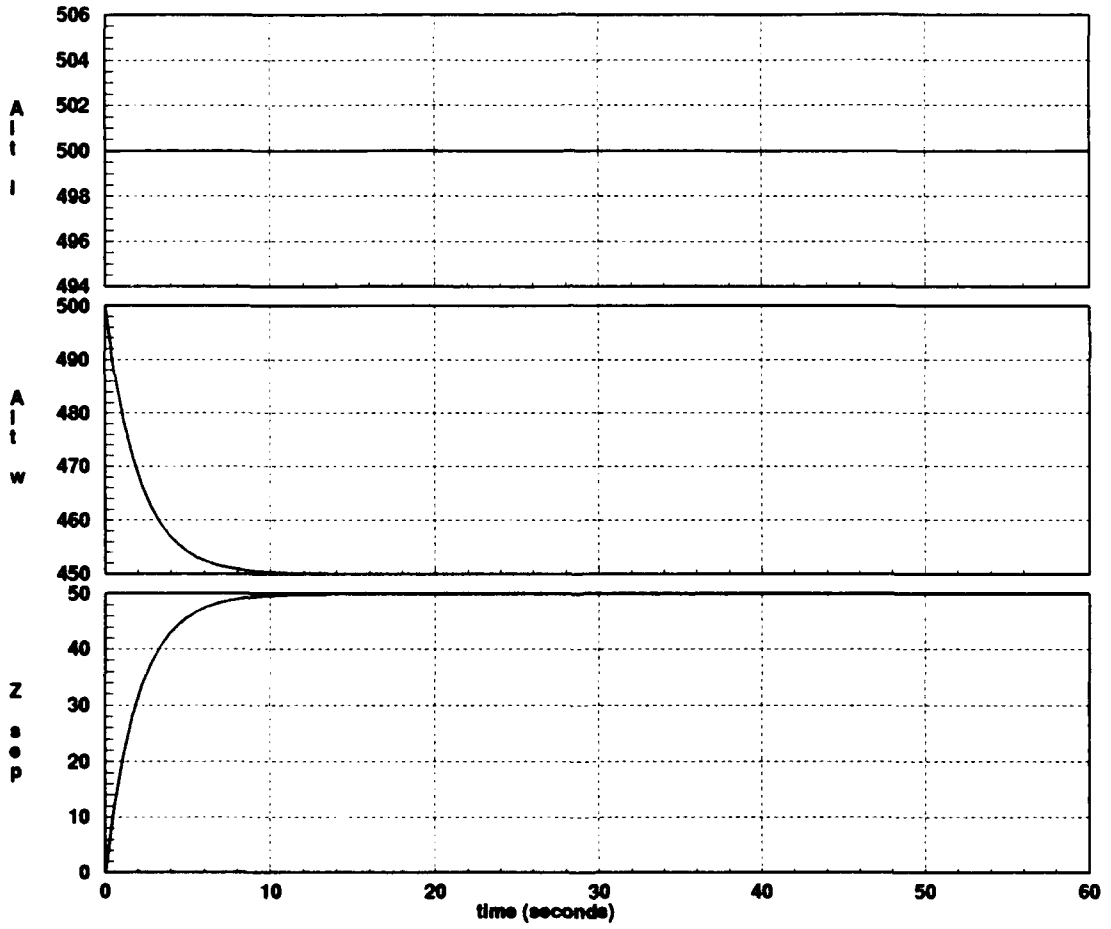

Figure 5.8. Vertical Response to an Δz Input Change from 0 to 50 feet

5.2.7 **Diamond Formation Large Heading Angle Increase** The formation is commanded a heading change from 30 degrees to 75 degrees in this test. Figure 5.8 shows that the wing aircraft heading response reaches a saturation point but still attains the commanded heading angle with no error in steady state. A transient peak amplitude of 420 feet occurs in the lateral separation distance, and a transient peak amplitude of 200 feet occurs in the longitudinal separation distance. This large transient in the lateral separation is due to the superior turn rate capability of the lead aircraft. The lead aircraft out-turns the wing aircraft, thereby increasing the lateral separation distance. However, the formation is maintained as all formation commanded values are maintained with no error in steady state. Figure 5.10 illustrates the flight path plot for this maneuver and the separation range.

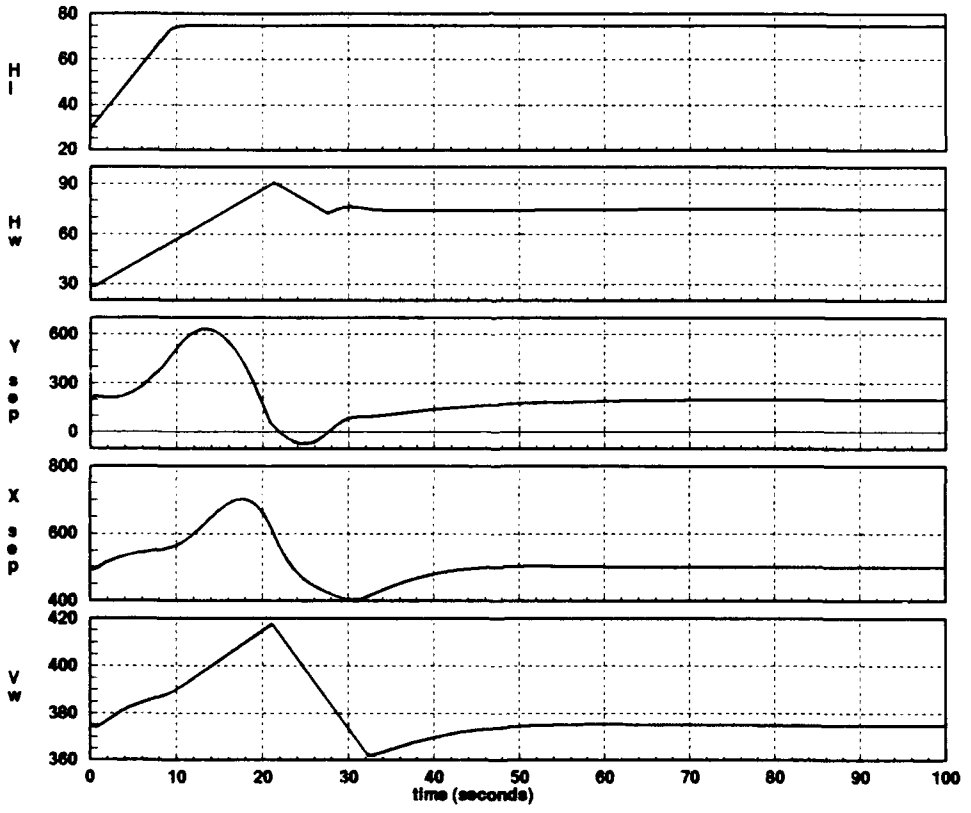

Figure 5.9. Lateral Response to an H_L (Input) Change from 30 to 75 Degrees

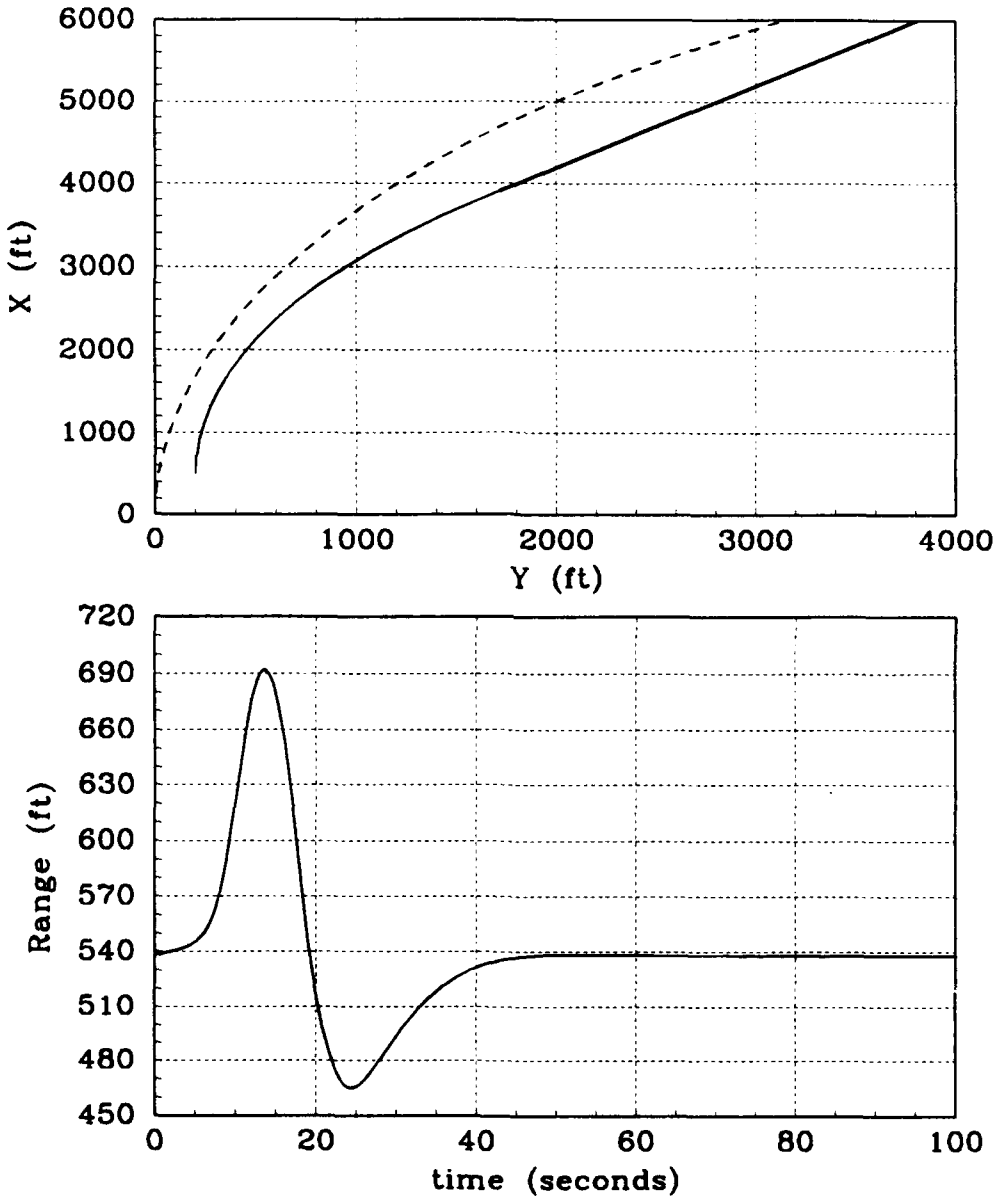

Figure 5.10. Flight Path Plot of an H_L (Input) Change from 0 to 45 Degrees

5.2.8 **Diamond Formation Large Heading Angle Decrease** For this test the formation is commanded a heading change from 30 degrees to -15 degrees. In this case, the superior performing lead aircraft is turning into the wing aircraft. Figure 5.11 illustrates that the wing aircraft heading response has several transients that reach saturation. However, the commanded heading angle is reached with no steady state error. Both the lateral separation distance and longitudinal separation distance have peak transients of about 150 feet. These separation distance transients are less than those obtained in the previous test since the lead aircraft is not turning away from the wing aircraft. The formation is maintained in steady state. Figure 5.12 depicts the flight path plots for this maneuver. Although the paths cross two times, this is not indicative of a collision because the range plot indicates that these crossings do not occur at the same point in time. Figure 5.13 illustrates this further by showing the location of the flight paths at their closest separation range.

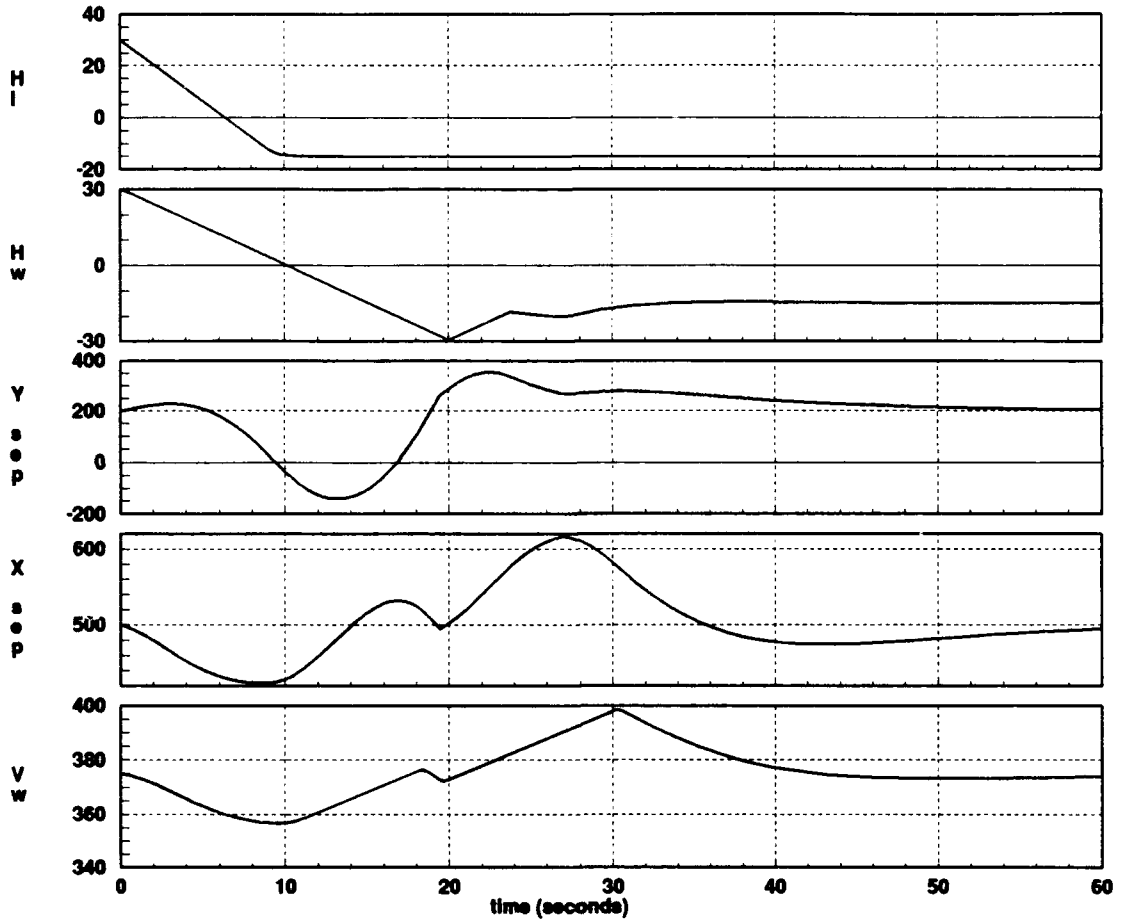

Figure 5.11. Lateral Response to an H_L (Input) Change from 30 to -15 Degrees

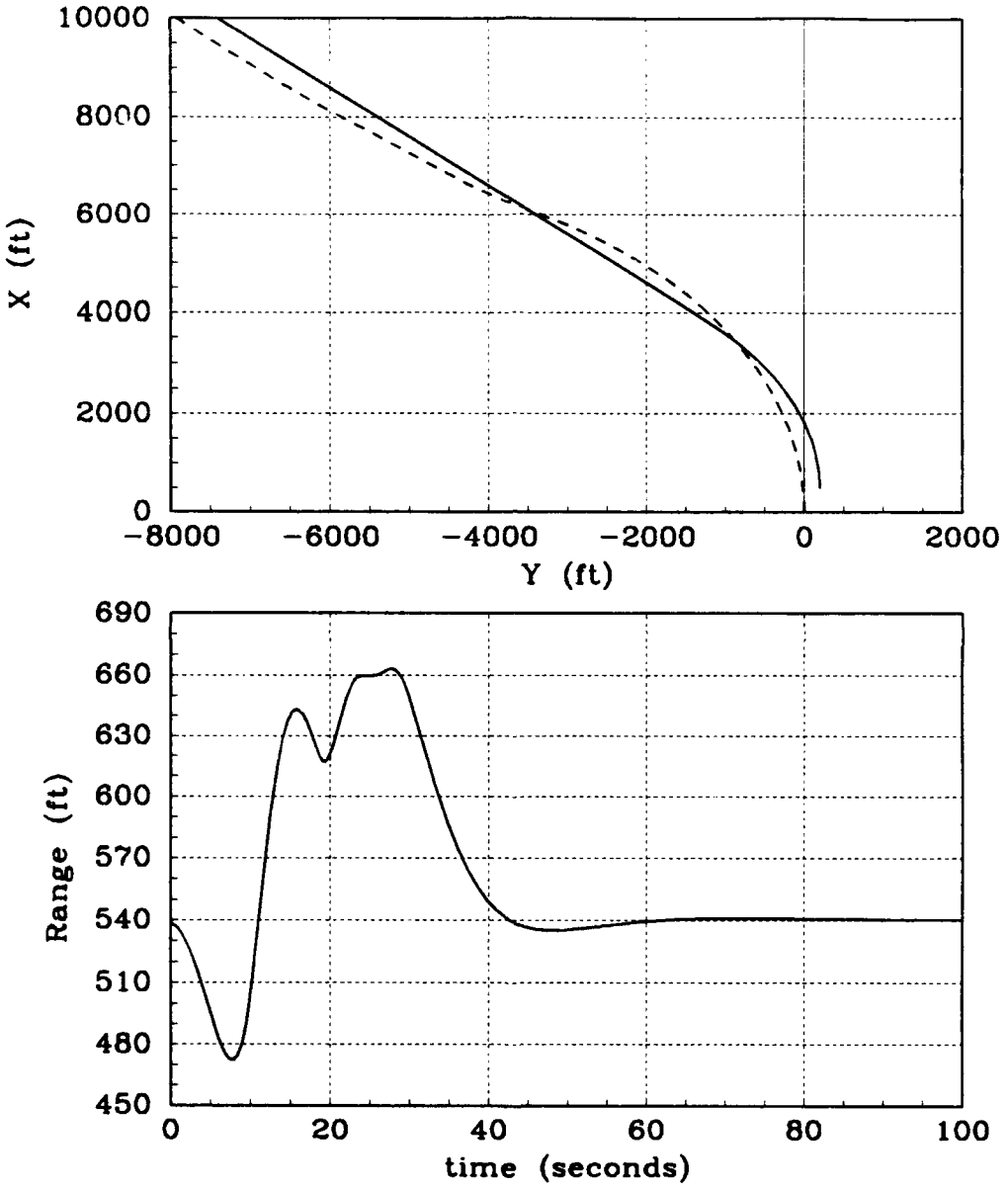

Figure 5.12. Flight Path Plot of an H_L (Input) Change from 0 to -45 Degrees

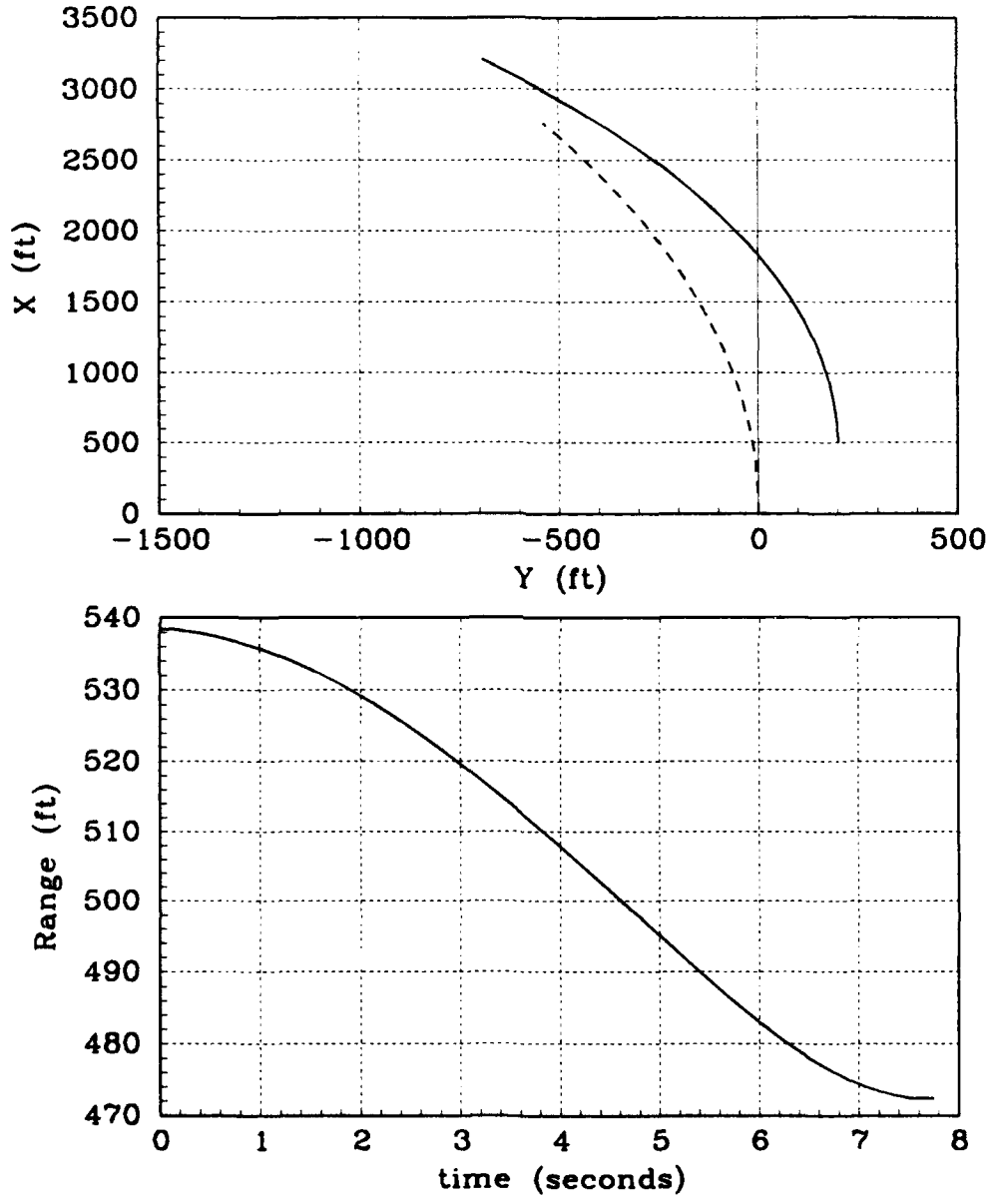

Figure 5.13. Flight Path Plot of the Closest Range for an H_L (Input) Change from 0 to -45 Degrees

5.2.9 **Abreast Formation Velocity Increase** For this test the formation is in a line abreast configuration and is commanded a velocity increase from 375 ft/sec to 400 ft/sec. Due to the delay in the wing aircraft's velocity response, the longitudinal separation distance has a peak overshoot of 54 feet. However, the wing aircraft attains the commanded formation velocity in 32 seconds and the longitudinal separation distance returns to the commanded formation value of 0 feet. Therefore, as shown by Figure 5.14, there is no steady state error.

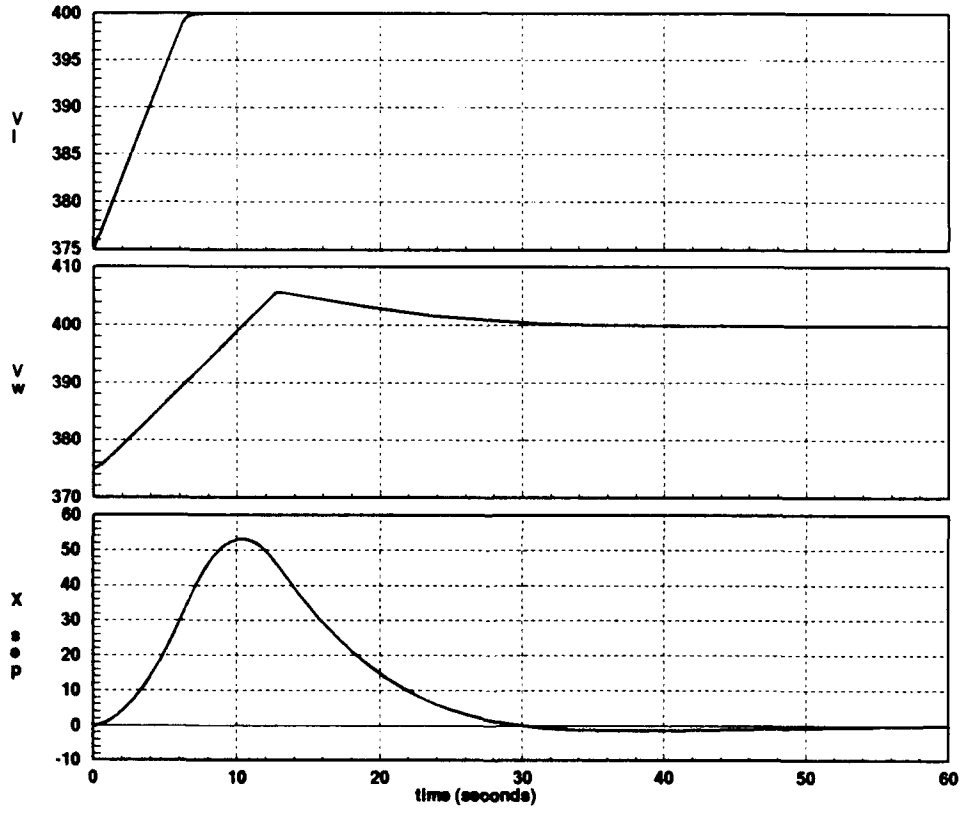

Figure 5.14. Longitudinal Response to a V_L (Input) Change from 375 to 400 ft/sec

5.2.10 **Abreast Formation Velocity Decrease** For a line abreast configuration, the formation is commanded to decrease its velocity from 375 ft/sec to 350 ft/sec. Figure 5.15 illustrates that the wing aircraft velocity response has an undershoot of 3 ft/sec, and the longitudinal separation response has a peak undershoot of 38 feet. This undershoot in longitudinal separation actually means that the wing aircraft overshoots the lead aircraft for the duration of the transient. Nonetheless, there is no steady state error, i.e., the formation is maintained.

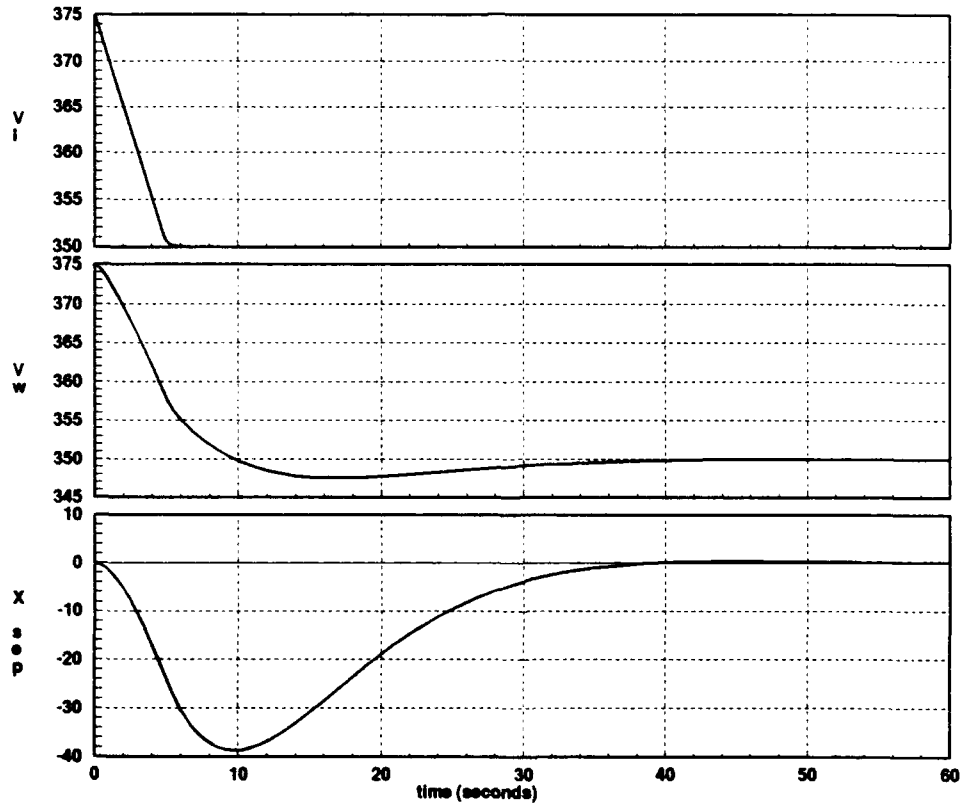

Figure 5.15. Longitudinal Response to a V_L (Input) Change from 375 to 350 ft/sec

5.2.11 **Abreast Formation Lateral Separation Distance Increase** The formation, in a line abreast configuration, is commanded to increase its lateral separation distance from 200 feet to 300 feet. As illustrated in Figure 5.16, the wing aircraft changes its heading angle to effect this lateral separation command. A small overshoot of about 8 feet occurs in the lateral separation response. Overall, the formation is maintained since there is no steady state error. The flight path plot for this maneuver is shown in Figure 5.17.

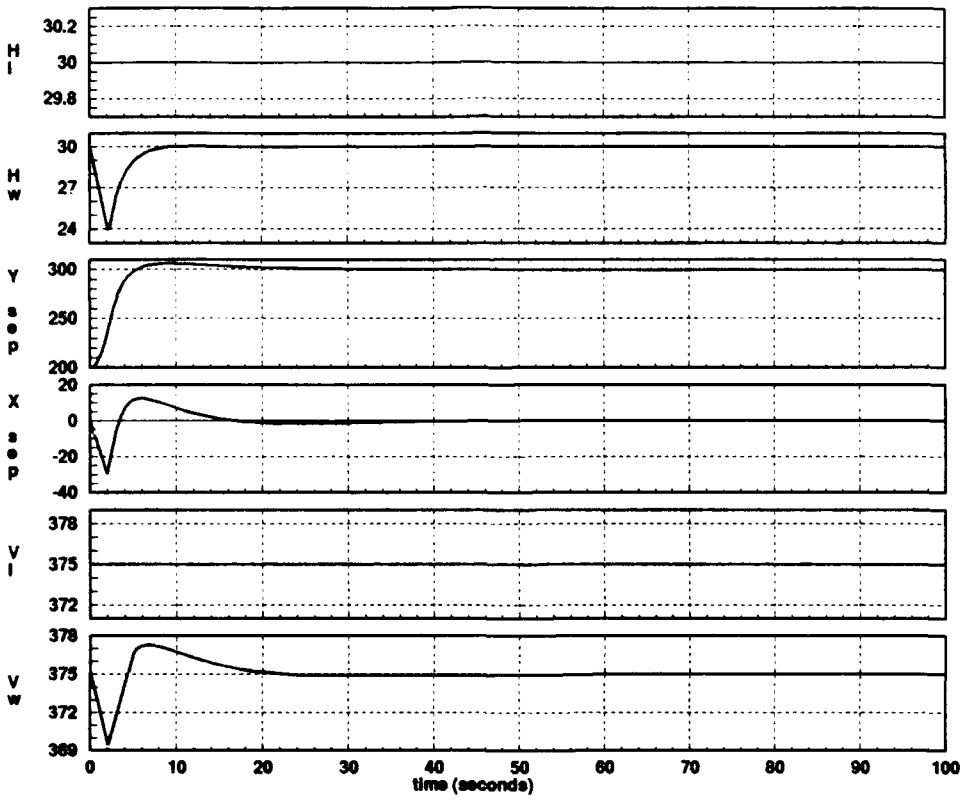

Figure 5.16. Lateral Response to a Δy Input Change from 200 to 300 feet

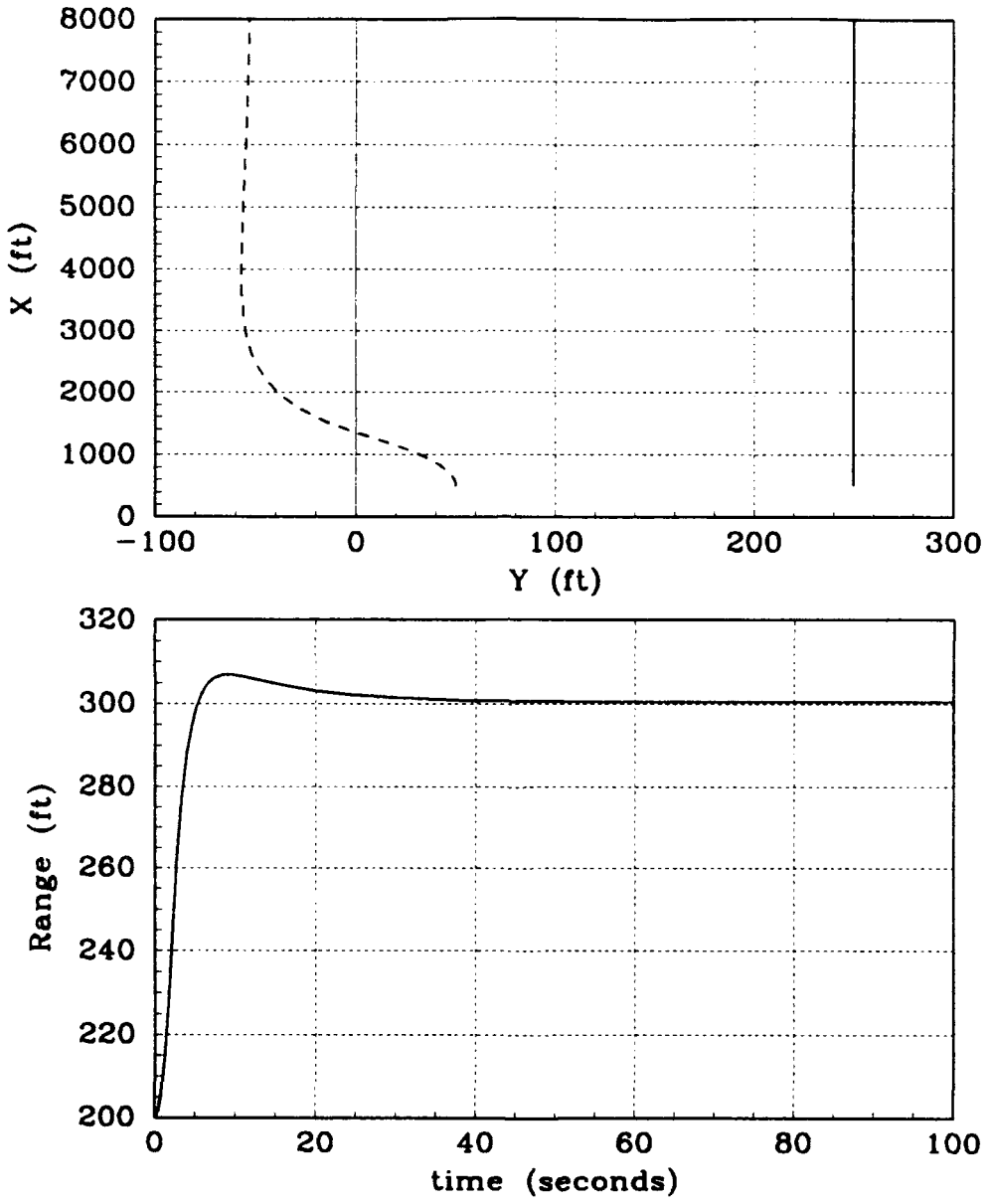

Figure 5.17. Flight Path Plot of a Δy Input Change from 200 to 300 feet

5.2.12 **Abreast Formation Lateral Separation Decrease** The formation, in a line abreast configuration, is commanded to decrease its lateral separation distance from 200 feet to 100 feet. As shown in Figure 5.18, the wing aircraft increases its heading angle to effect this lateral separation command. A small undershoot of about 5 feet occurs in the lateral separation response. However, the formation is maintained since there is no steady state error. Figure 5.19 depicts the flight path plot and total separation range for this maneuver.

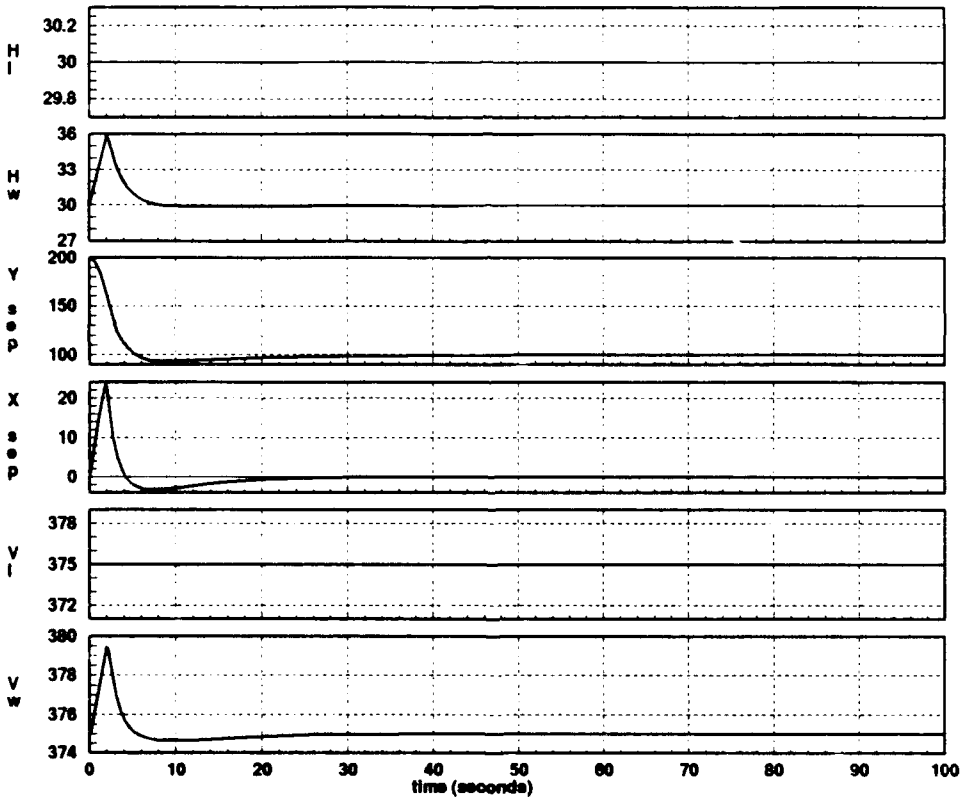

Figure 5.18. Lateral Response to a Δy Input Change from 200 to 100 feet

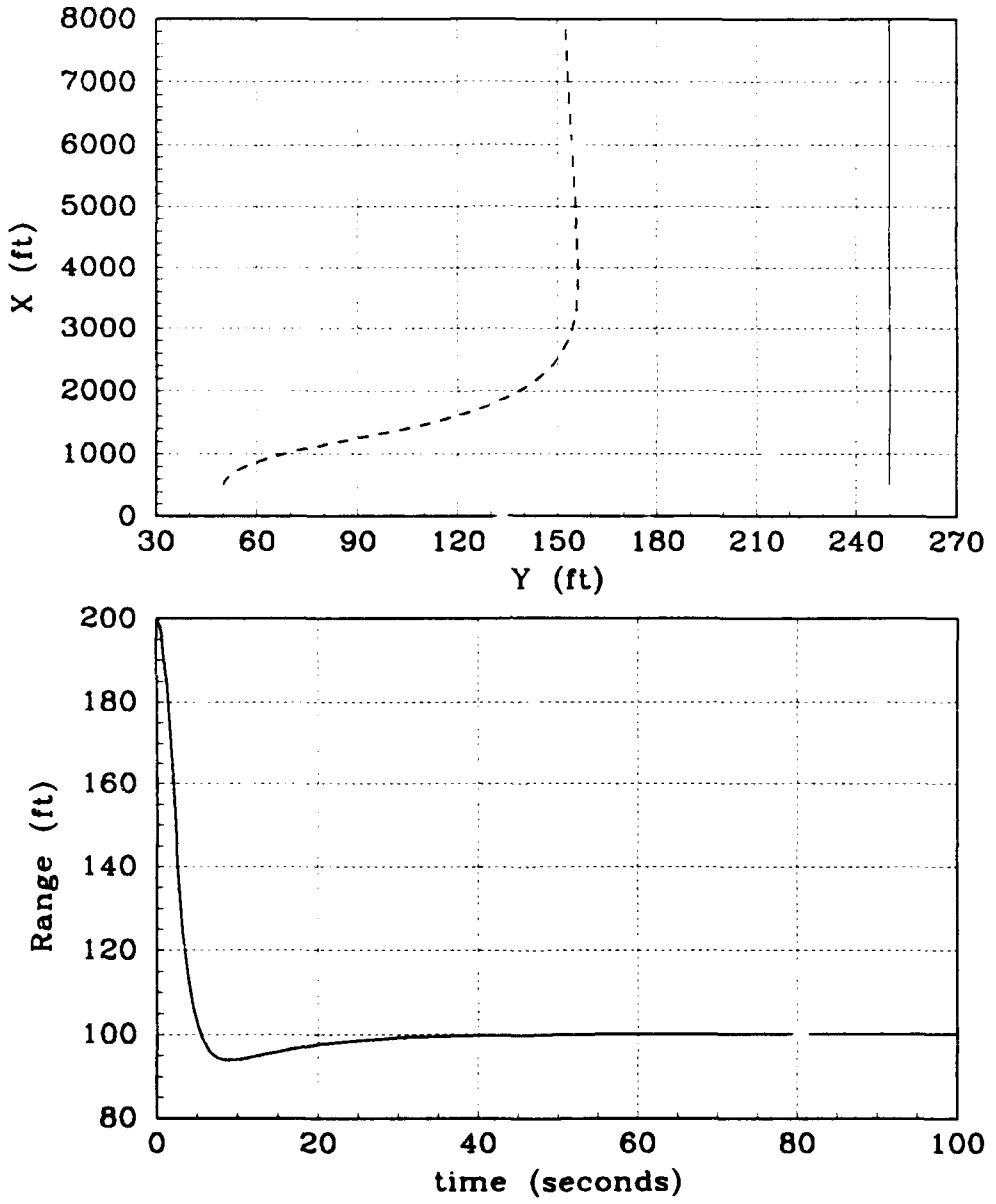

Figure 5.19. Flight Path Plot of a Δy Input Change from 200 to 100 feet

5.2.13 **Abreast Formation Large Heading Angle Decrease** For this test the formation is in a line abreast configuration and is commanded to change its heading from 30 degrees to -15 degrees, as shown in Figure 5.20. To avoid instability in the formation system, a step input heading command is not given to the lead aircraft in this case. Instead, the heading command to the lead aircraft is ramped at a slope equal to the turn rate capability of the wing aircraft. The lead aircraft, with its superior turn rate capability, is turning into the wing aircraft. A peak overshoot of 70 feet occurs in the longitudinal separation distance, that is, the lead aircraft overshoots the wing aircraft in the longitudinal direction for the duration of the transient. The lateral separation response has an undershoot of about 70 feet. This means that the lead aircraft is getting closer to the wing aircraft in the lateral direction. Nonetheless, there is no collision, no steady state error, and the formation is maintained. Figure 5.21 shows the flight path plots and the total separation range for this maneuver. The closest the aircraft come in total separation range is 112 feet.

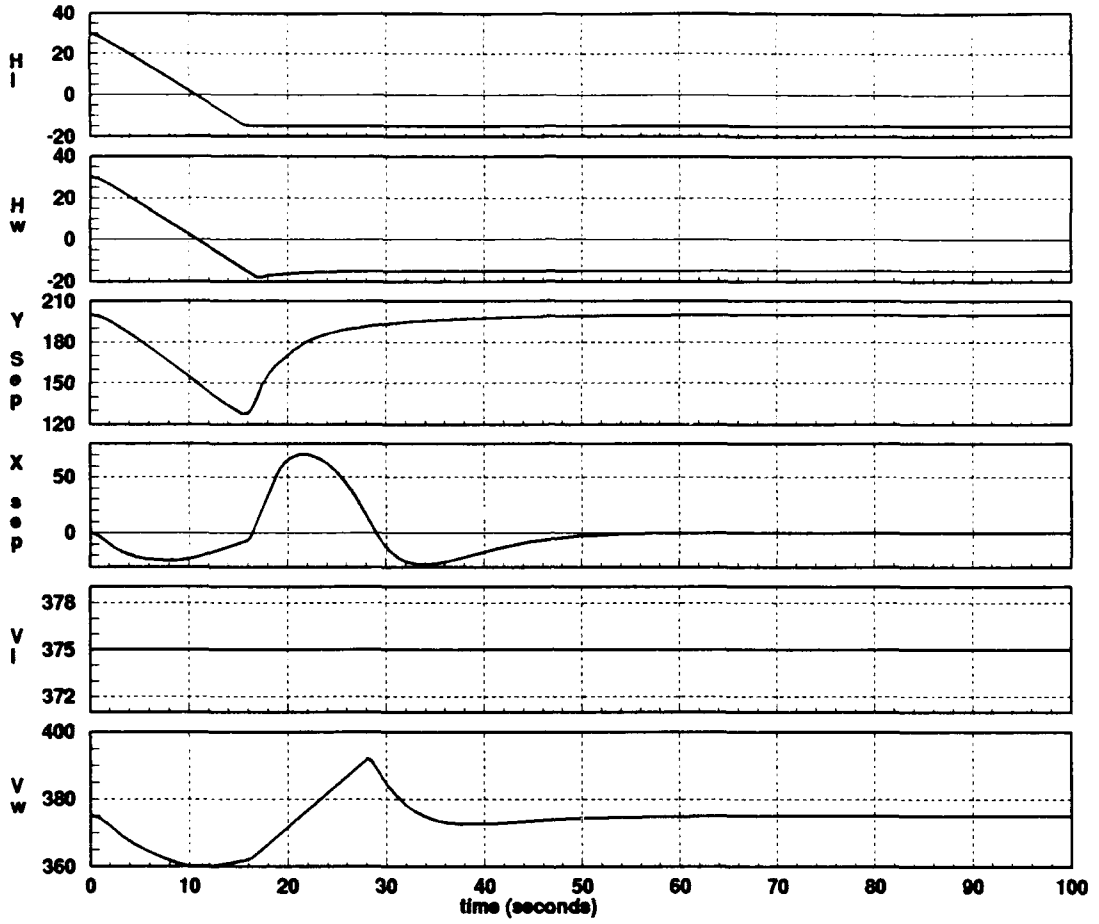

Figure 5.20. Lateral Response to an H_L (Input) Change from 0 to -45 Degrees

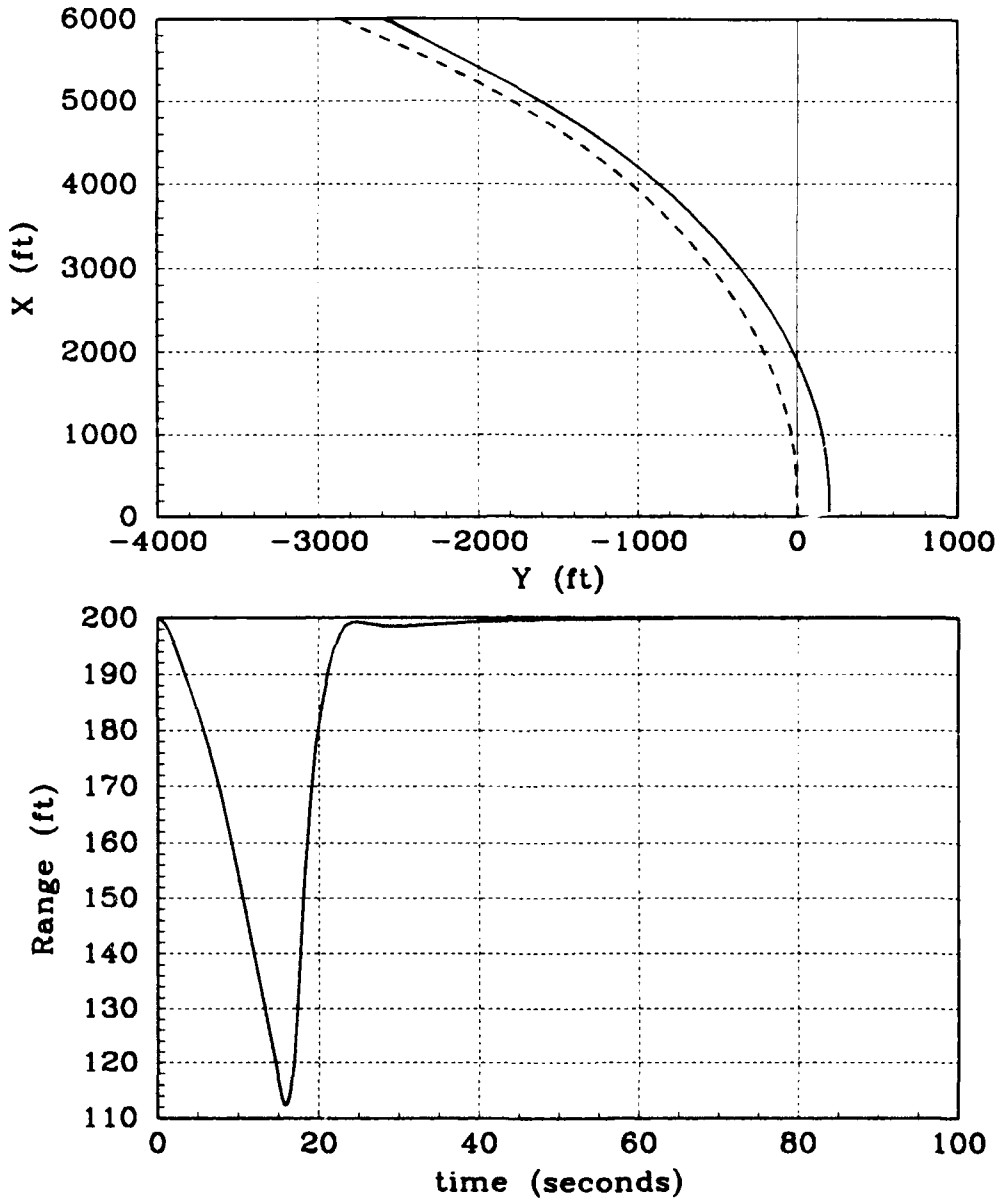

Figure 5.21. Flight Path Plot of an H_L (Input) Change from 0 to -45 Degrees

5.2.14 **Abreast Formation Large Heading Angle Increase** The formation, in a line abreast configuration, is commanded to increase its heading from 30 degrees to 75 degrees. The superior lead aircraft is turning away from the wing aircraft, as shown in Figure 5.22. For the reasons given in the previous test, the heading command is ramped into the lead aircraft. A peak overshoot of 52 feet occurs in the lateral separation response since the wing aircraft can not turn as quickly as the lead aircraft. Overall, the formation is maintained since there is no steady state error. Figure 5.23 illustrates the flight path plots and the total separation range for this maneuver.

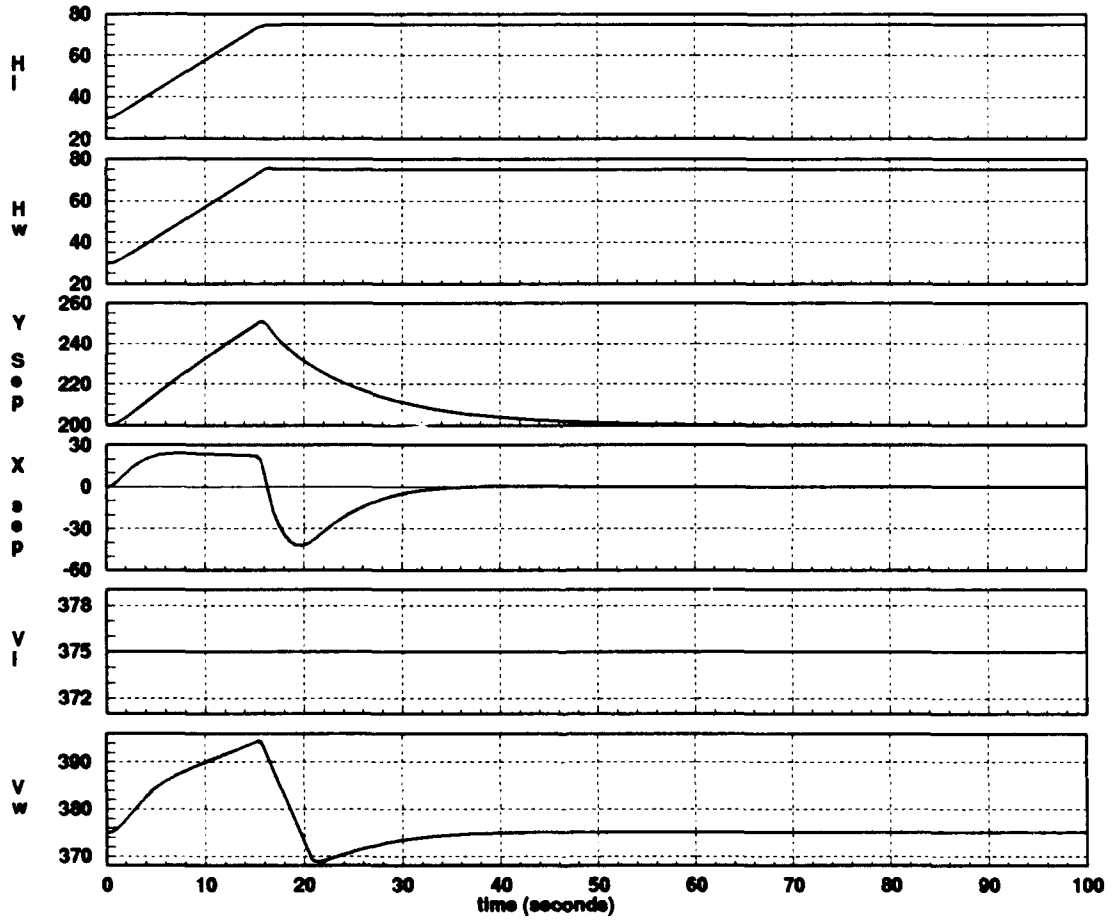

Figure 5.22. Lateral Response to an H_L (Input) Change from 0 to 45 Degrees

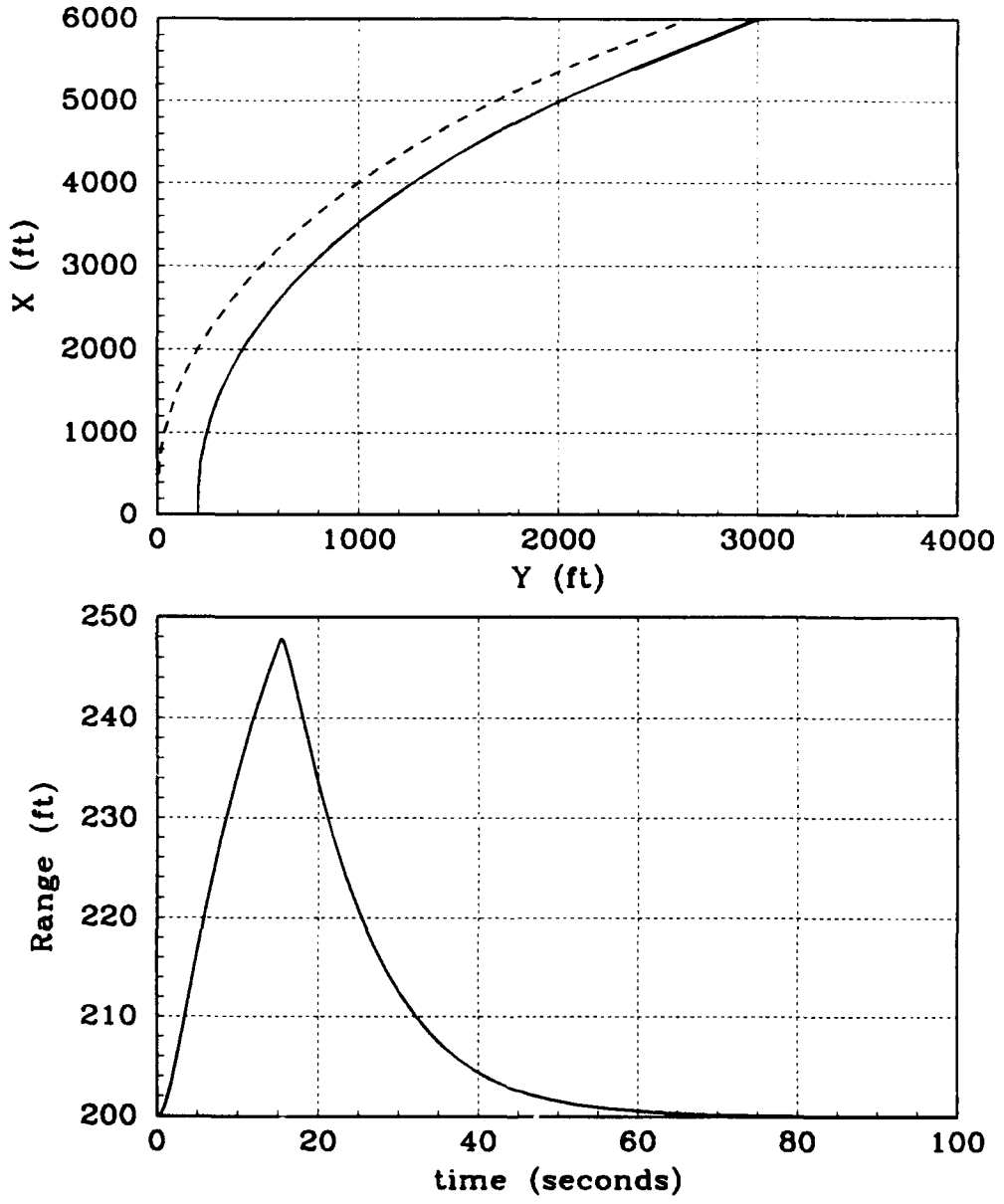

Figure 5.23. Flight Path Plot of an H_L (Input) Change from 0 to 45 Degrees

5.2.15 **Trail Formation to Diamond Formation Maneuver** A trail to diamond configuration maneuver is accomplished in this test. The wing aircraft changes its heading angle to effect the lateral separation distance change necessary to change from a trail configuration to a diamond configuration, as depicted in Figure 5.24. The steady state error for all of the responses is zero; therefore, the new diamond configuration is attained. Figure 5.25 shows the flight path and the total separation range plots for this maneuver.

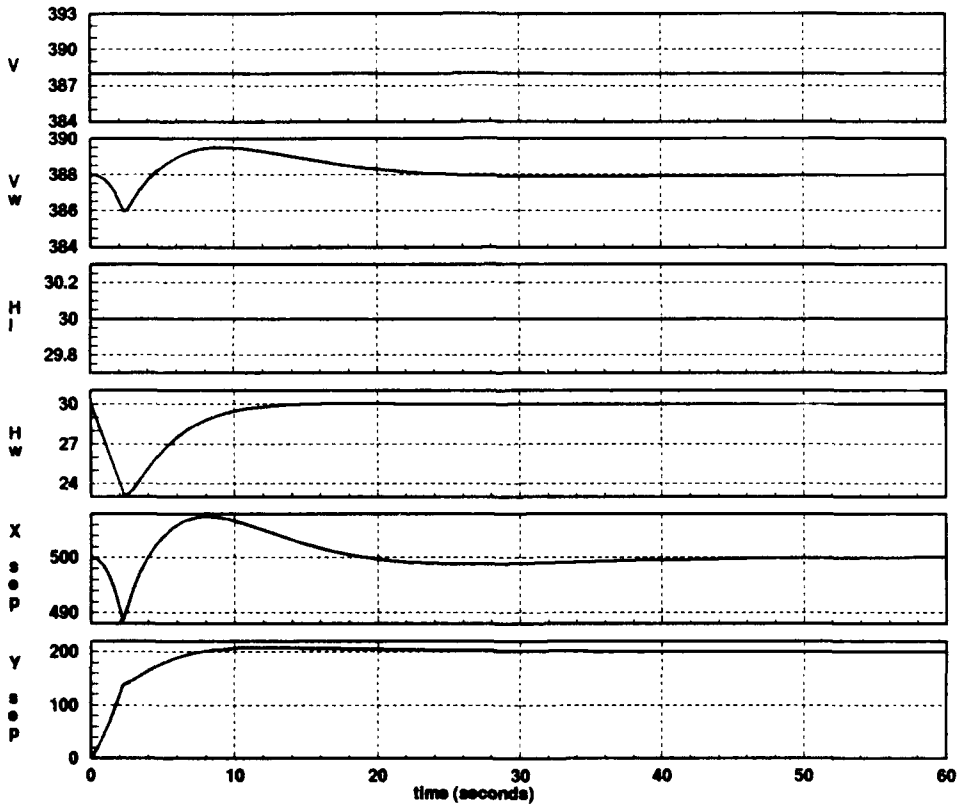

Figure 5.24. Time Response For a Trail to Diamond Formation Change Maneuver

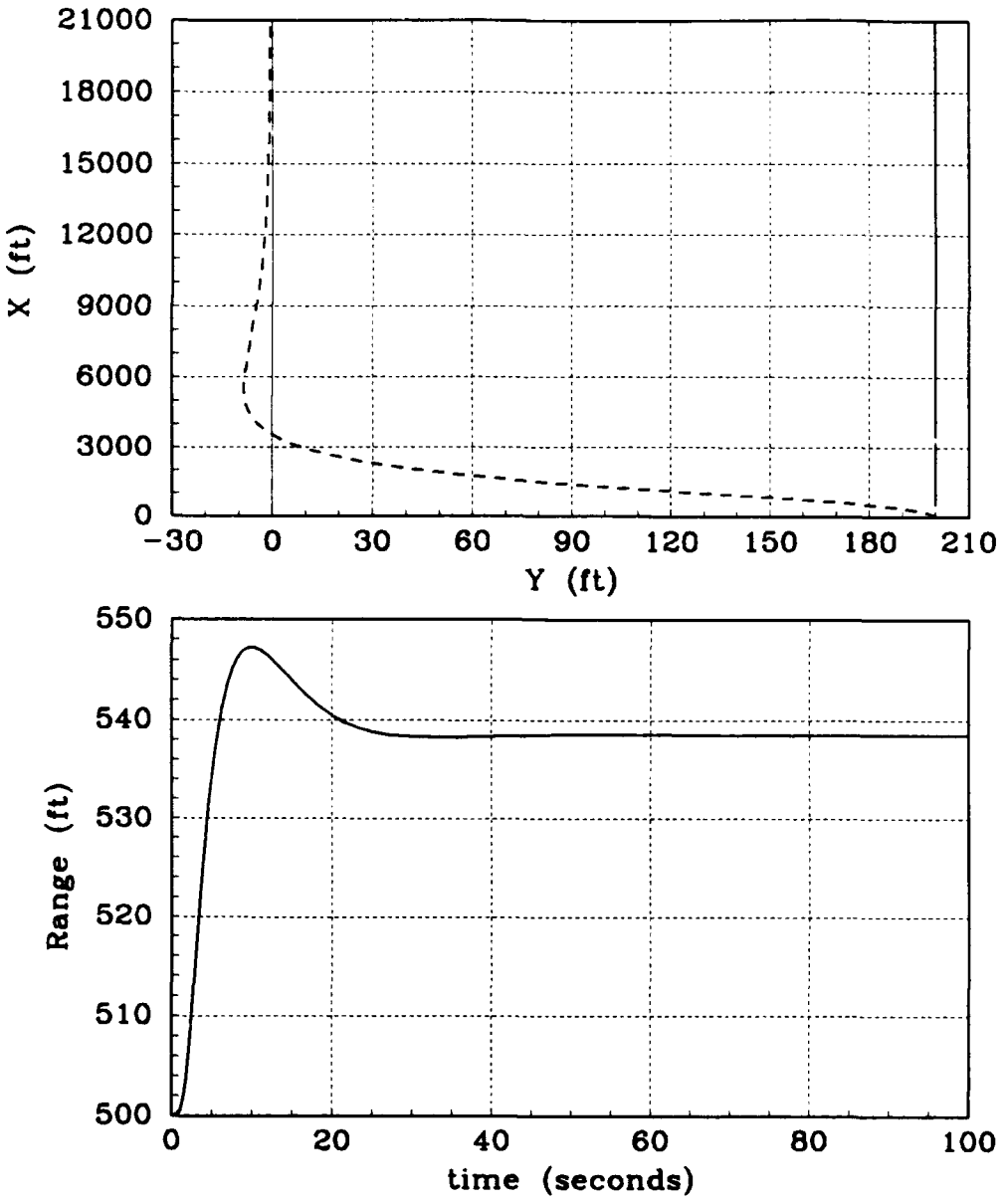

Figure 5.25. Flight Path Plot of Trail to Diamond Formation Change Maneuver

5.2.16 **Diamond Formation to Trail Formation Maneuver** A diamond to trail maneuver is accomplished in this test. The wing aircraft increases its heading angle to effect the lateral separation distance change necessary to go from a diamond configuration to a trail configuration, as shown in Figure 5.26. The steady state error for all of the responses is zero. Therefore, the new trail configuration is attained. Figure 5.27 shows the flight path and the total separation range plots for this maneuver.

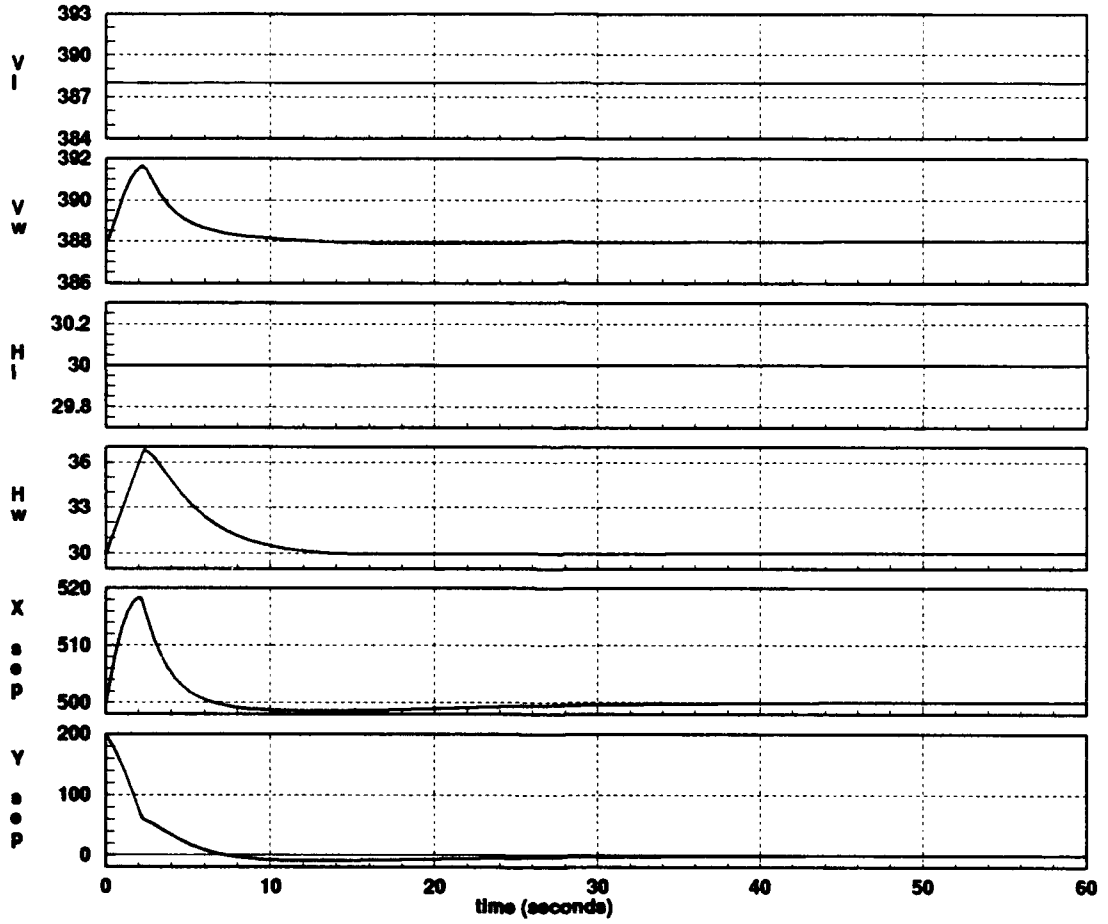

Figure 5.26. Time Response For a Diamond to Trail Formation Change Maneuver

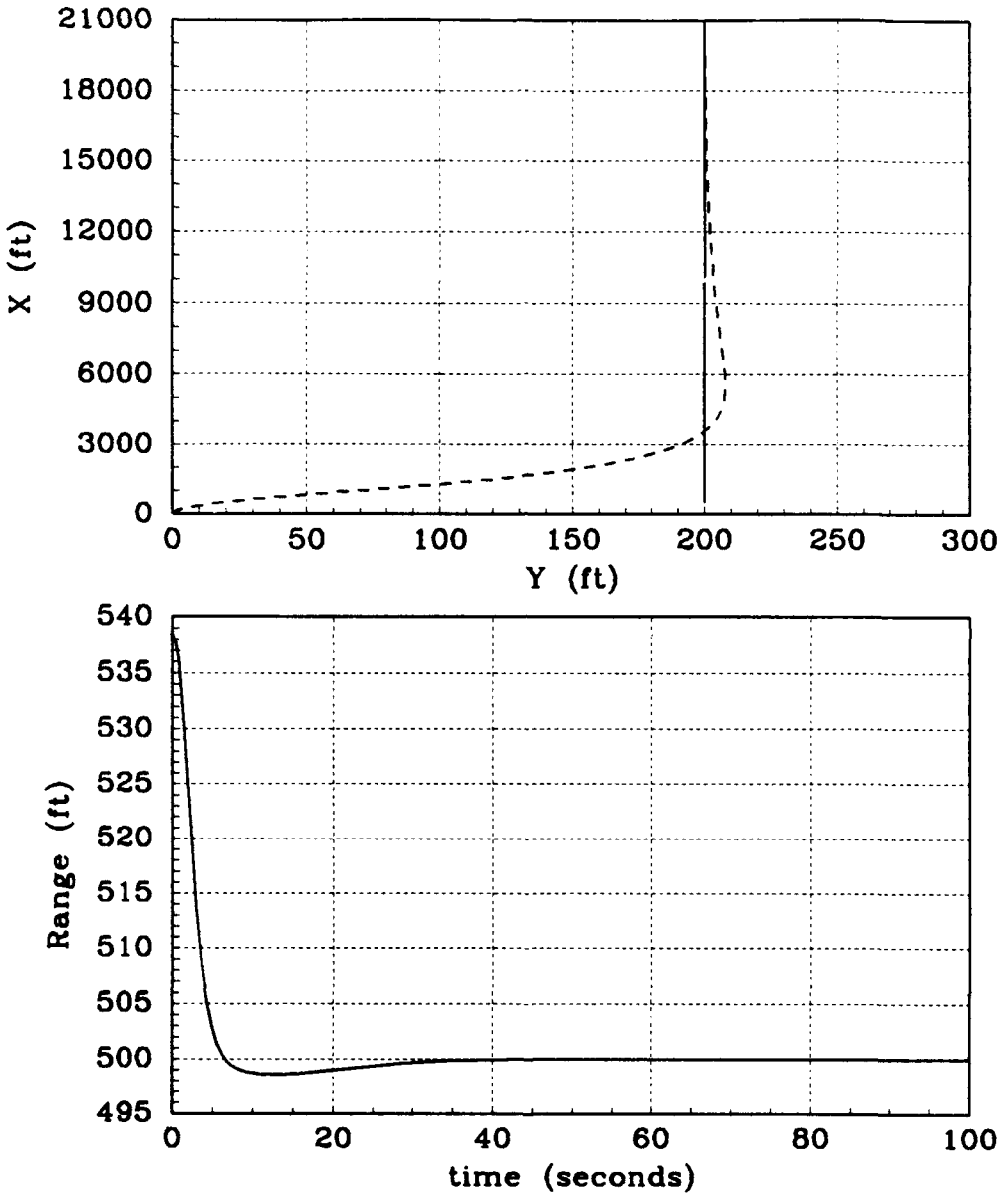

Figure 5.27. Flight Path Plot of a Diamond to Trail Formation Change Maneuver

5.2.17 **Trail Formation Terrain Clearance Maneuver** In this test a terrain clearance maneuver is accomplished. The formation must clear a hill of 600 feet by 250 feet. For this simulation, due to the inferior climb rate capability of the wing aircraft, a step input altitude command is not given to the lead aircraft. Instead, the input to the lead aircraft is ramped at a slope equal to the wing aircraft's climb rate. Thus, the responses shown in Figure 5.28 are obtained. Both the lead aircraft and the wing aircraft clear the hill by the prescribed vertical distance.

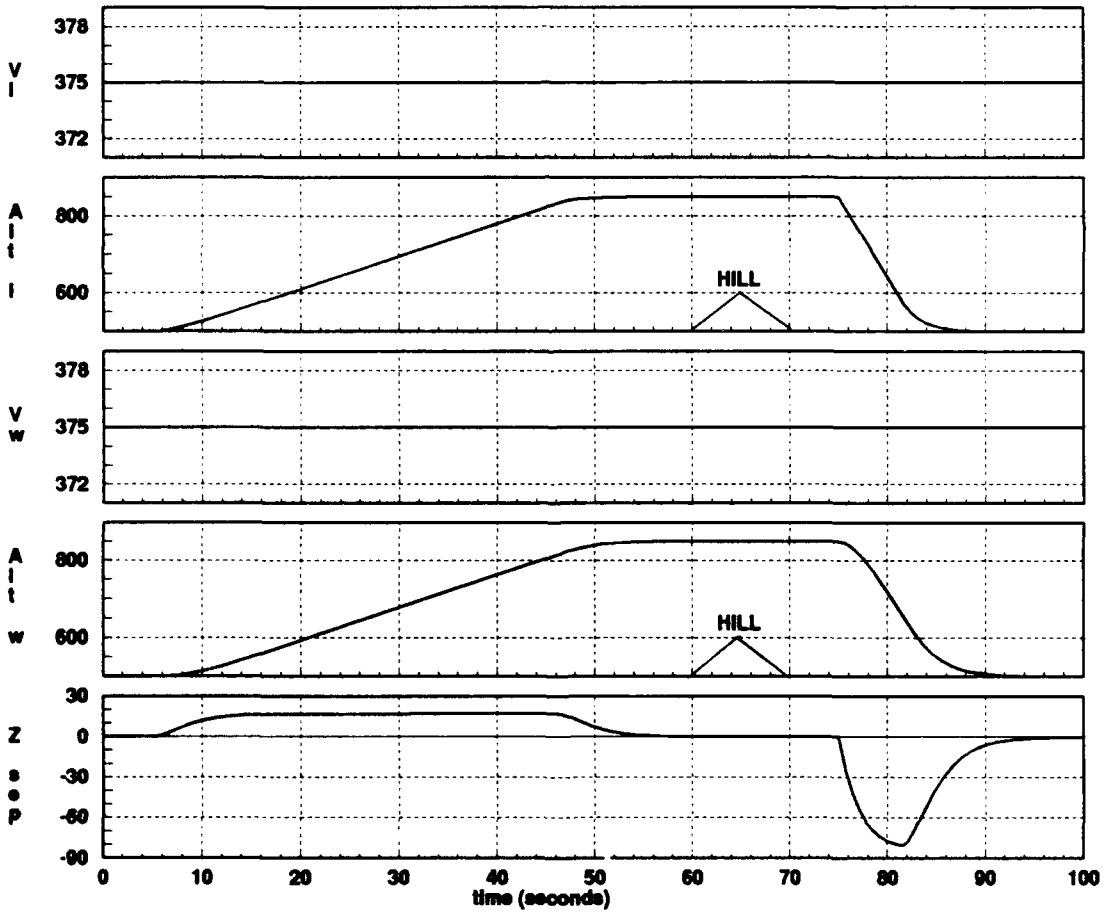

Figure 5.28. Vertical Response to an h_L (Input) Change from 500 to 850 feet

5.3 Summary

The responses in this chapter are for a formation control system comprised of dissimilar aircraft in which the performance of the lead aircraft is superior to the performance of the wing aircraft. The responses for a formation control system comprised of similar aircraft in which the lead aircraft and wing aircraft both have superior performance are presented in Appendix A. The responses for a formation control system comprised of dissimilar aircraft in which the lead aircraft has a degraded performance capability compared to the wing aircraft are presented in Appendix B, and the responses for a formation control system comprised of similar aircraft in which the lead and wing aircraft both have degraded performance are presented in Appendix C.

VI. Analysis and Conclusions

6.1 Analysis of Results

The objective of this research was to determine whether or not the automated formation control system that was developed and simulated by Captain Rohs could be extended to control formations of like or dissimilar aircraft under more realistic conditions. This objective has been met.

It was shown that a formation control system for a formation comprised of like or dissimilar aircraft, that maintains the desired formation and separation distances in steady state, while producing sufficiently small transients that do not cause collisions among the aircraft, can be developed. For the formation control system simulation, step inputs representing the formation's commanded velocity, heading, and altitude are provided to the lead aircraft, and step inputs representing the commanded formation separation distances are provided to the wing aircraft. Formation control is accomplished without providing additional control to the lead aircraft to restrict the lead aircraft's maneuvering. However, when the formation is comprised of dissimilar aircraft in which the lead aircraft has superior performance capability to that of the wing aircraft, the performance difference must be taken into account for two particular "large" maneuvers. The first maneuver is the -45 degree heading turn maneuver, and the second is the 850 foot terrain avoidance maneuver. For these two maneuvers, the lead aircraft's input commands, representing the commanded formation heading and altitude, respectively, are given as ramped up inputs instead of step inputs to the lead aircraft. Use of a step input in these two cases results in an unstable response.

6.2 Open Loop Formation Operation

As shown in Chapter III, an open loop formation system does not perform well. Although the particular maneuver commanded is accomplished by the lead

and wing aircraft, formation geometry (spacing) is not maintained in the process. Thus, feedback control is needed to help maintain the formation.

6.3 Formation Operation with Velocity, Heading, and Altitude Feedback

Simulation of the formation control system using velocity, heading, and altitude feedback in Chapter III shows that velocity, heading, and altitude commands can be tracked by the lead and wing aircraft. However, a steady state error is introduced in the formation spacing geometry. On the other hand, a commanded separation distance can be tracked by the formation, while maintaining the commanded velocity, heading, and altitude in steady state.

6.4 Formation Operation with PI control of Separation Error

Simulation of the formation control system using PI control on separation error is accomplished in Chapter IV. The results of these simulations show that velocity, heading, and altitude commands can be attained by the lead and wing aircraft while maintaining formation spacing, and that a commanded separation distance can be attained while maintaining the commanded velocity, heading, and altitude in steady state.

6.5 Formation Operation with PI Control Using a Mix of Separation Error and Maneuver Error in the Horizontal Plane

Results from simulation of the formation system with PI control using a mix of separation (x and y separation) and maneuver (velocity and heading) error shows that a better transient response is obtained while maintaining the same steady state response as in the case where only PI control on separation error is used. Thus, this controller performs the best overall.

6.6 Conclusions

The following conclusions are drawn from the results of this study.

1. An open-loop formation control system cannot maintain the commanded formation or separation distance. There is the danger of a collision among the aircraft, or, a less capable wing aircraft could peel off the formation.
2. A formation system using velocity and heading feedback can be used to successfully track the commanded formation separation distances. However, station keeping is not possible with this system, since a steady state separation distance error exists after a velocity, heading, or altitude command is executed.
3. A linear PI controller can be designed that addresses the deficiencies outlined in (1) and (2) above and satisfactorily controls a nonlinear formation control system.
4. One set of gains can be derived for the PI controller in (3) that provides satisfactory control for the formation system for all maneuvers.
5. A formation system with PI control of separation error can successfully track both formation maneuver commands (velocity and heading) and formation separation commands with zero steady state error.
6. A formation system with PI control using a mix of separation and maneuver error can also successfully track formation maneuver commands and formation separation commands with zero steady state error. Moreover, there is a better transient response with PI control using a mix of separation and maneuver error than with PI control using only separation error. Hence, the employment of a mixer which uses combined maneuver and separation actuating signals is recommended.

6.7 Recommendations for Further Study

Additional research in the area of formation flight control is needed in the following areas. This work will in part address the limitations and assumptions made for this research. These areas are described below.

1. An overdamped second order lead aircraft input should be used instead of the ramped up step input in order to eliminate the discontinuity at the ramp saturation value.
2. A second wing aircraft should be added to the formation system to evaluate the dynamics between the two wing aircraft as well as that between the wing and the lead aircraft.
3. Control could be applied to the lead aircraft to restrict lead aircraft maneuvering in order not to stress the formation control system.
4. A theoretical determination of the parameters needed for the formation control design problem should be accomplished.
5. Higher order, more elaborate aircraft models should be incorporated into the formation system for evaluation. This would provide a more thorough investigation of formation control with more realistic aircraft models.
6. Actual sensor models should be used in the formation control system to allow evaluation of particular sensors used.
7. Noise should be incorporated into the sensor model to evaluate its affect on formation stability as well.
8. Time delays should be incorporated into the formation control system sensor models to evaluate their affect on formation stability.
9. A pilot model should be added to the formation control system to determine which channels are best suited for manual control and which are best suited for automated control.

6.8 Summary

The results of this research show that a PI controller can be developed for automated maneuvering flight that successfully maintains the formation without collision among the aircraft. The potential for collision increases when the wing aircraft has inferior performance capability compared to the lead aircraft. However, the controller developed in this research provides satisfactory transient and steady state behavior for the formation system so that collisions are avoided and zero steady state error is obtained. Finally, the formation may be comprised of like or dissimilar aircraft.

Appendix A. **Results for a Formation System Comprised of Similar Aircraft in which the Lead Aircraft and Wing Aircraft Both Have Superior Performance Capability**

For the sake of completeness the results for a formation system comprised of similar aircraft are included in this Appendix. The lead and wing aircraft are both C-130B models. Time history plots and flight path plots are generated for the same tests and initial conditions that are accomplished in Chapter V. As in chapter five, the flight path plots are shown in an inertial reference frame with an initial formation heading angle of 0 degrees. The solid line on the flight path plots represents the flight path of the lead aircraft, and the dashed line represents the flight path of the wing aircraft. The variable names and definitions are given in Table A.1.

Table A.1. Variable Definitions

Variable Name: Text	Variable Name: Time Plots	Definition
V_L	V_l	Velocity of lead aircraft
V_W	V_w	Velocity of wing aircraft
H_L	H_l	Heading angle of lead aircraft
H_W	H_w	Heading angle of wing aircraft
h_L	Alt_l	Altitude of lead aircraft
h_W	Alt_w	Altitude of wing aircraft
Δx	$XSep$	Longitudinal separation distance
Δy	$Ysep$	Lateral separation distance
Δz	$Zsep$	Vertical separation distance

Table A.2 and Table A.3 list the formation system tests and the initial conditions, respectively. Note that the velocities, V_L and V_W, have an initial value of 388 ft/sec instead of 375 ft/sec for the trail to diamond and diamond to trail maneuvers. For the inputs marked with an asterisk in Table A.2 both time history response plots and flight path plots are shown.

Table A.2. Formation Control System Simulation Tests

Initial Formation	Final Formation	Commanded Parameter Input	Response Plots
Diamond	Diamond	V_L = 400 ft/sec	Figure A.1
Diamond	Diamond	V_L = 350 ft/sec	Figure A.2
Diamond	Diamond	Δx = 550 ft	Figure A.3
Diamond	Diamond	Δx = 450 ft	Figure A.4
Diamond	Diamond	* H_L = 25 deg	Figure A.5
Diamond	Diamond	* H_L = 35 deg	Figure A.6
Diamond	Diamond	* Δy = 250 ft	Figure A.7
Diamond	Diamond	* Δy = 150 ft	Figure A.8
Diamond	Diamond	h_L= 550 ft	Figure A.9
Diamond	Diamond	h_L= 450 ft	Figure A.10
Diamond	Diamond	Δz = 50 ft	Figure A.11
Diamond	Diamond	Δz = -50 ft	Figure A.12
Diamond	Diamond	* H_L = 45 deg	Figure A.13
Diamond	Diamond	* H_L = -45 deg	Figure A.14
Abreast	Abreast	V_L = 400 ft	Figure A.15
Abreast	Abreast	V_L = 350 ft	Figure A.16
Abreast	Abreast	* Δy = 300 ft	Figure A.17
Abreast	Abreast	* Δy = 100 ft	Figure A.18
Abreast	Abreast	* H_L = 45 deg	Figure A.19
Abreast	Abreast	* H_L = -45 deg	Figure A.20
Trail	Diamond	* Δy = 200 ft	Figure A.21
Diamond	Trail	* Δy = 0 ft	Figure A.22
Trail	Trail	h_L = 850 ft	Figure A.23

Table A.3. Test Initial Conditions

Formation	Parameter	Initial Condition
Diamond	V_L	375 ft/sec
	V_W	375 ft/sec
	H_L	30 deg
	H_W	30 deg
	h_L	500 ft
	h_W	500 ft
	Δx	500 ft
	Δy	200 ft
	Δz	0 ft
Trail	V_L	375 ft/sec
	V_W	375 ft/sec
	H_L	30 deg
	H_W	30 deg
	h_L	500 ft
	h_W	500 ft
	Δx	500 ft
	Δy	0 ft
	Δz	0 ft
Abreast	V_L	375 ft/sec
	V_W	375 ft/sec
	H_L	30 deg
	H_W	30 deg
	h_L	500 ft
	h_W	500 ft
	Δx	0 ft
	Δy	200 ft
	Δz	0 ft

A.1 Results Summary

A comparison between the results obtained for a dissimilar formation system configuration in Chapter V in which the lead aircraft has superior performance to that of the wing aircraft and those obtained in this Appendix for a similar formation system configuration in which both aircraft have superior performance capability

is given in Table A.4. Table A.4 lists only those test maneuvers that result in a noticeable difference between the output responses of the two configurations. For these comparisons, the aircraft are in a diamond formation. The similarly configured formation has a better transient response than the dissimilarly configured formation. In several cases, there is an order of magnitude of difference between the overshoot or undershoot of the two configurations. Hence, although both achieve zero steady state error, the transient response of the dissimilar configuration has a higher potential for either causing loss of formation or collisions.

Table A.4. Response Comparison for Dissimilar/Similar Formation System Configuration in a Diamond Formation

Input Parameter Change	Output Variable	Overshoot Dissimilar	Overshoot Similar	Undershoot Dissimilar	Undershoot Similar
V_L = 400 ft/s	Δx	90 ft	38 ft	0 ft	0 ft
H_L = 35 deg	Δy	20 ft	4 ft	0 ft	0 ft
H_L = 75 deg	Δy	420 ft	30 ft	0 ft	0 ft
	Δx	200 ft	40 ft	0 ft	0 ft
	H_W	15 deg	0 deg	0 deg	0 deg
	V_W	43 ft/s	10 ft/s	13 ft/s	1 ft/s
H_L = (-15) deg	Δy	150 ft	28 ft	350 ft	35 ft
	Δx	120 ft	12 ft	100 ft	70 ft
	H_W	0 deg	0 deg	15 deg	0 deg
	V_W	23 ft/s	1 ft/s	17 ft/s	17 ft/s

A comparison of results between a dissimilar and similar configuration in an abreast formation shows that there is not much appreciable difference between the responses of the two configurations. However, for an H_L input change of 45 deg or -45 deg, this input change must be ramped to the lead aircraft for a dissimilar configuration so that a stable formation system response is obtained. However, for a similarly configured formation, the H_L input change can be input as a step input to the lead aircraft. This is also true for an h_L input change of 350 feet. This input

change must be ramped to the lead aircraft for a dissimilar configuration so that the wing aircraft can clear the crest of the terrain. For a similar configuration, the h_L input change can be input as a step input to the lead aircraft.

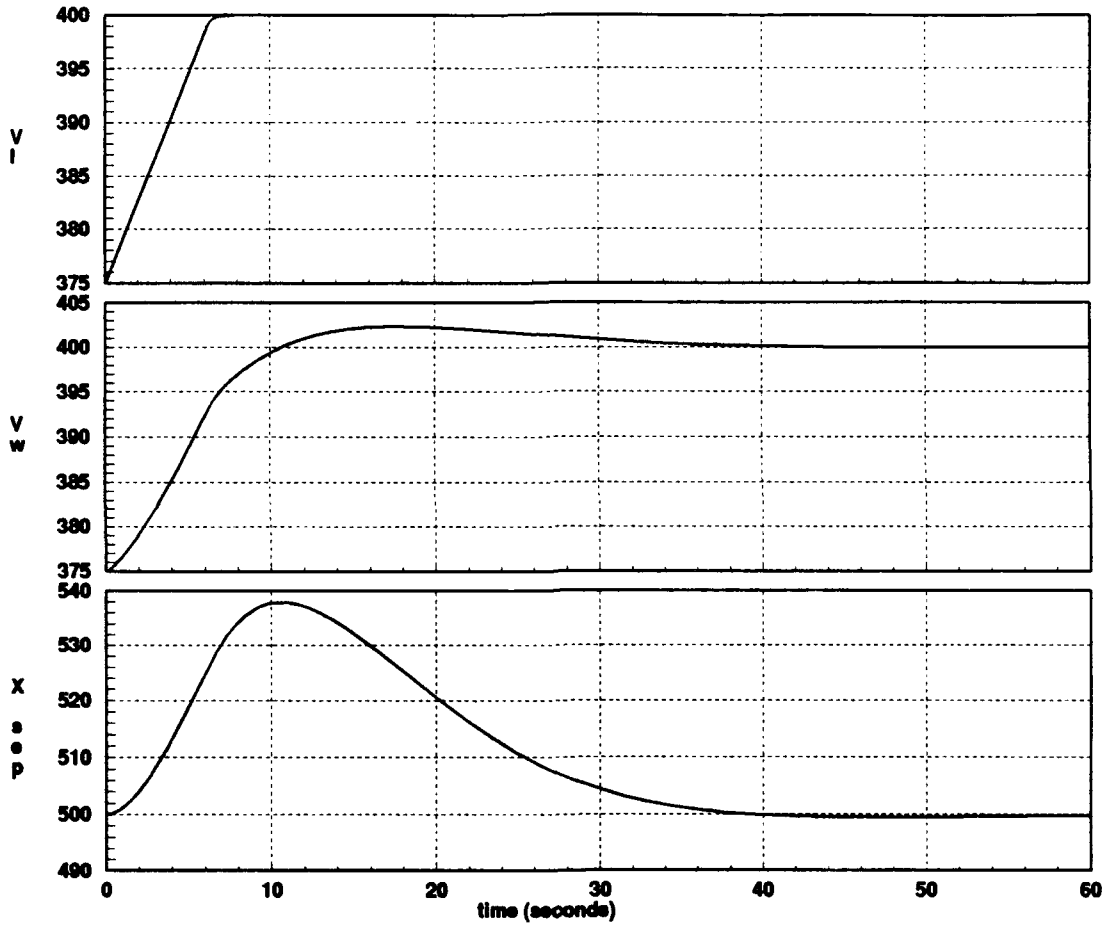

Figure A.1. Longitudinal Response to a V_L (Input) From 375 to 400 ft/sec

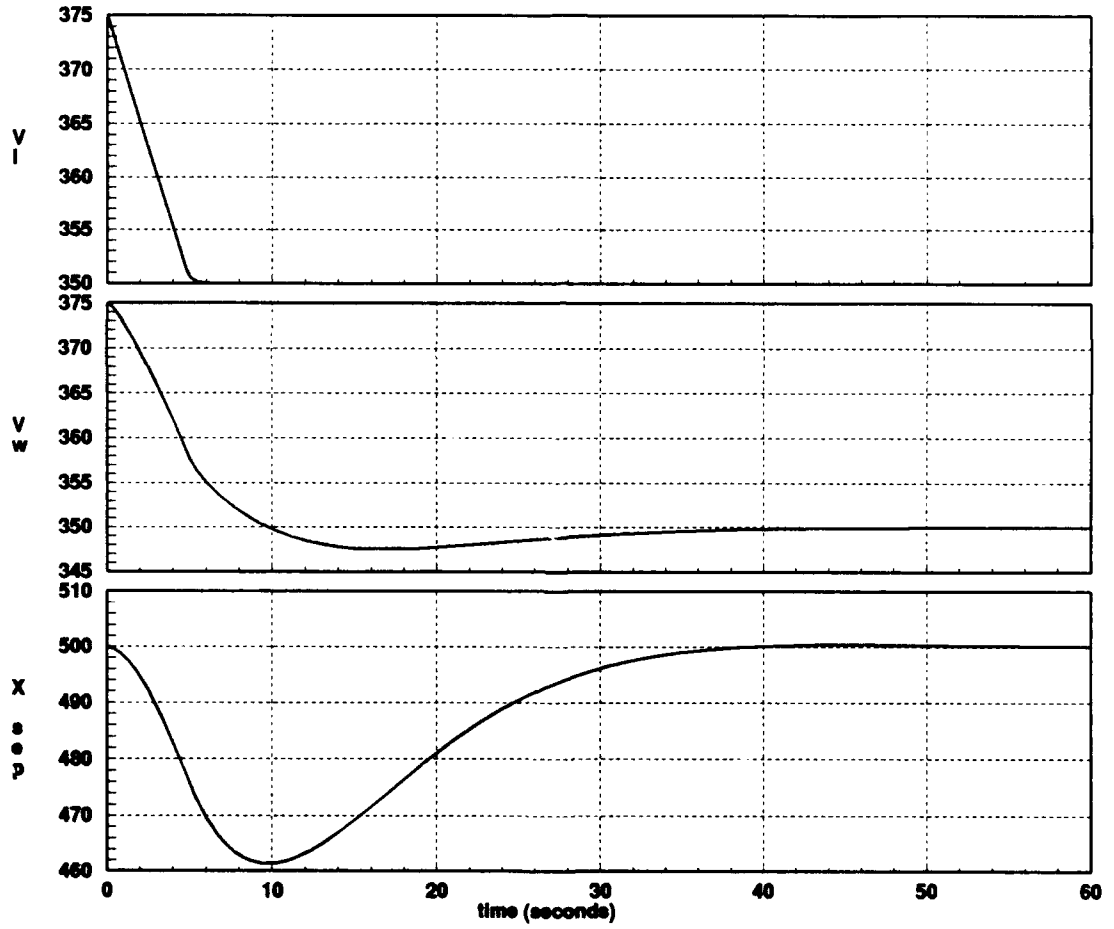

Figure A.2. Time Response for a V_L (Input) From 375 to 350 ft/sec

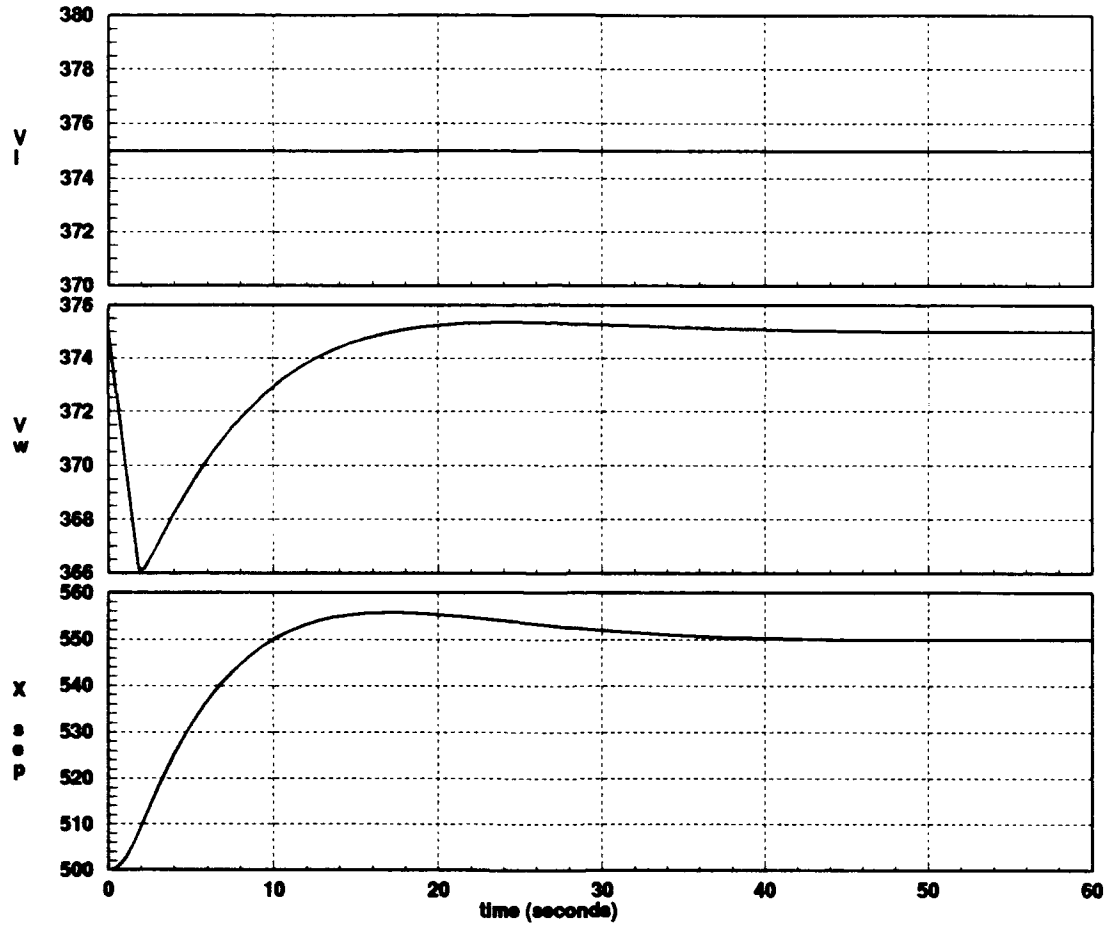

Figure A.3. Time Response for a Δx Input From 500 to 550 ft

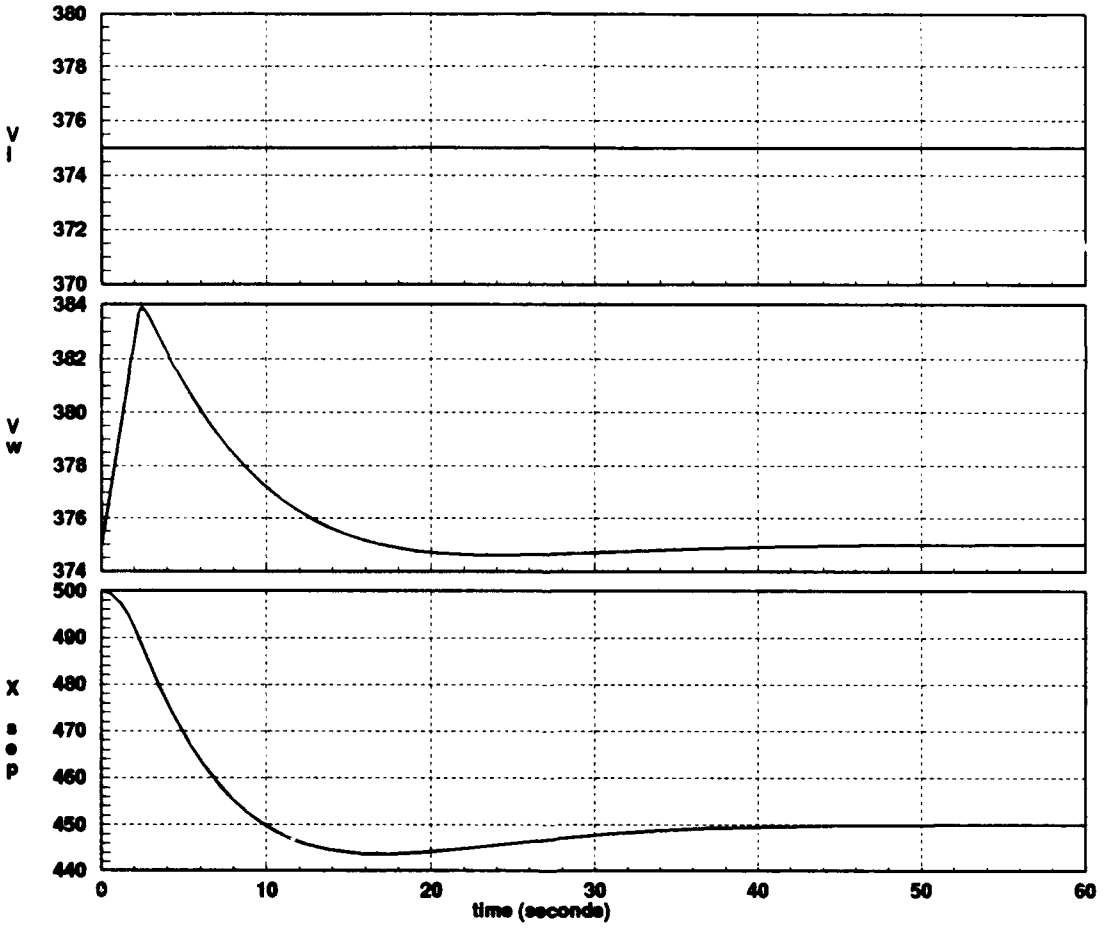

Figure A.4. Time Response for a Δx Input From 500 to 450 ft

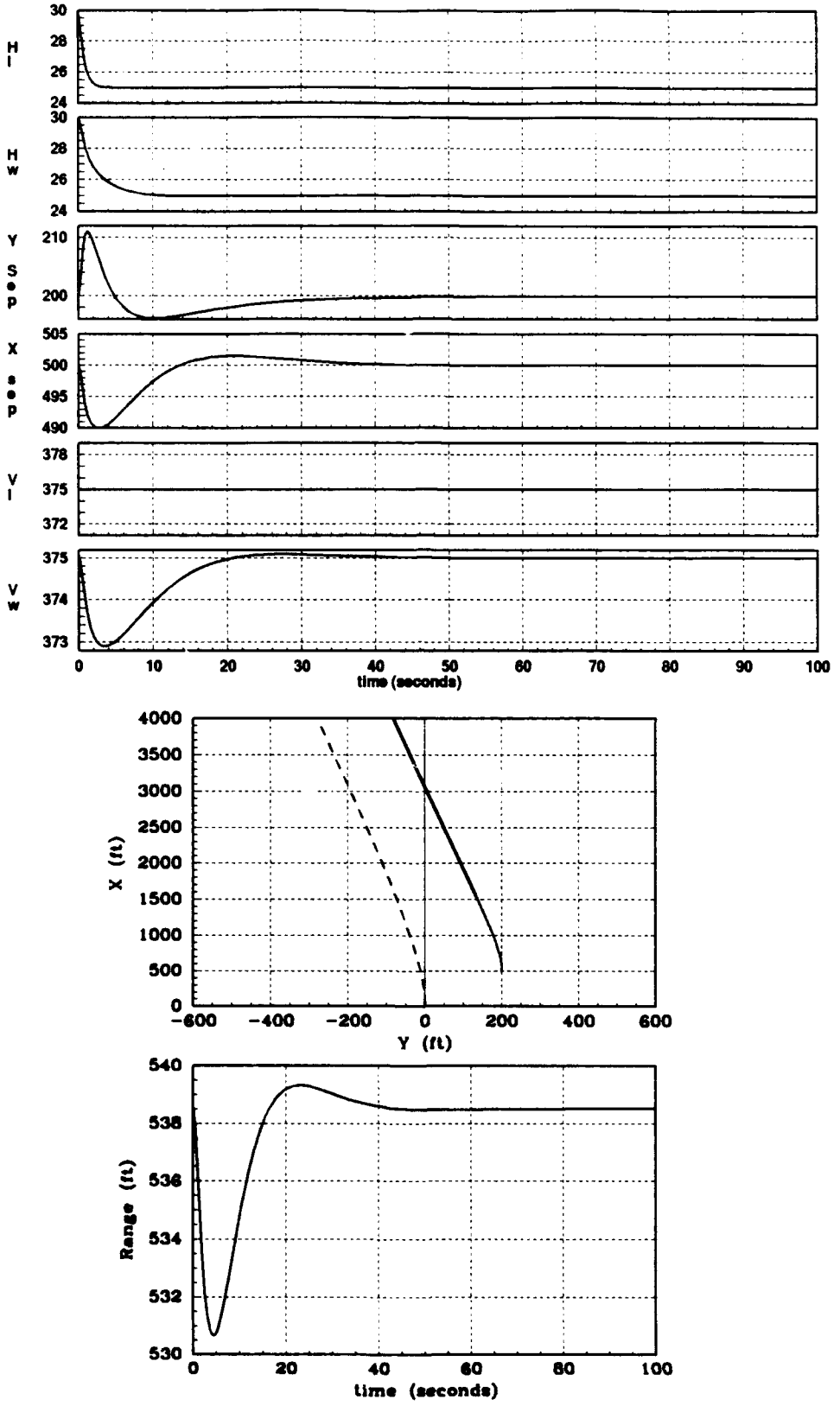

Figure A.5. Time Response and Flight Path Response to an H_L (Input) From 30 to 25 Degrees

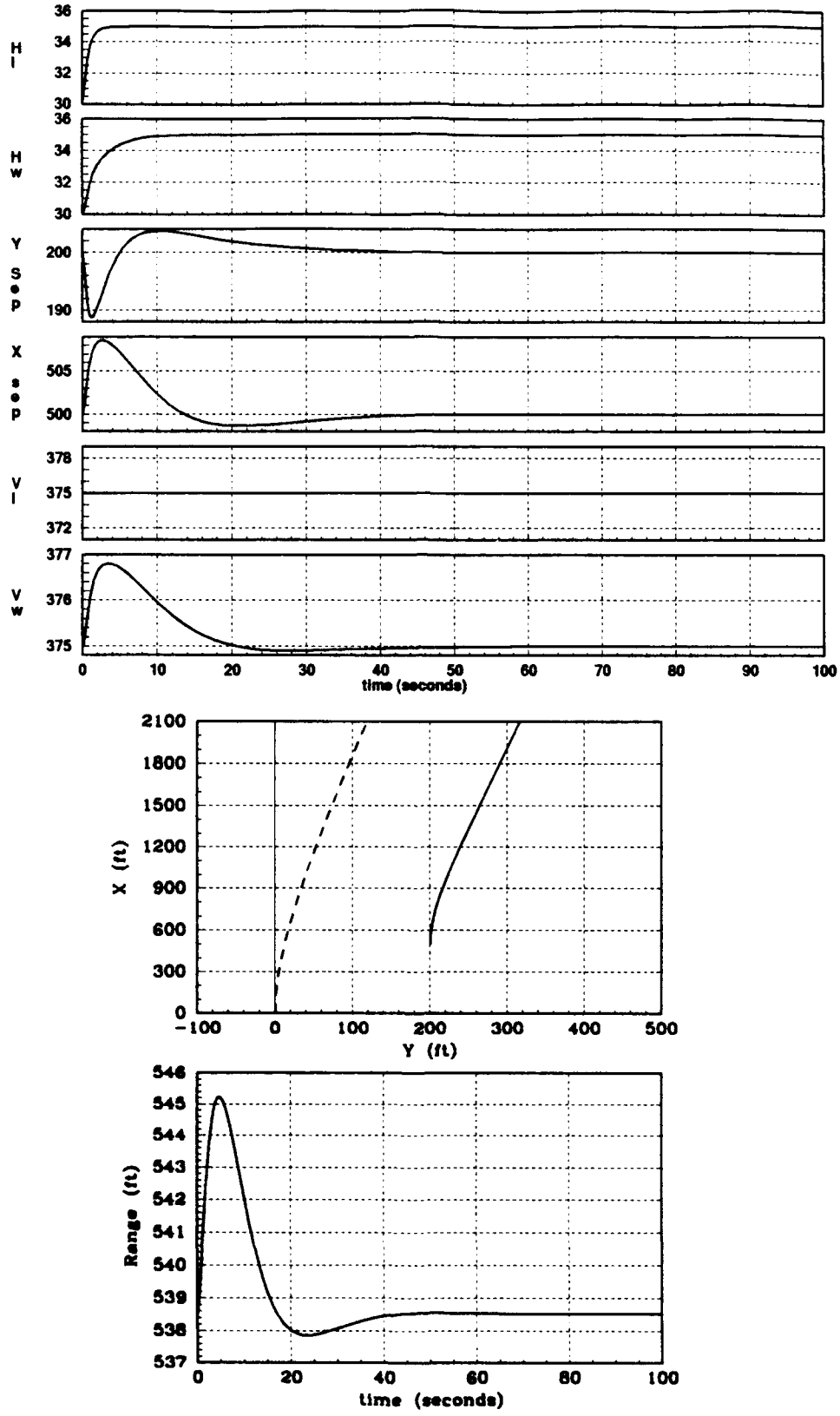

Figure A.6. Time Response and Flight Path Response to an H_L (Input) From 30 to 35 Degrees

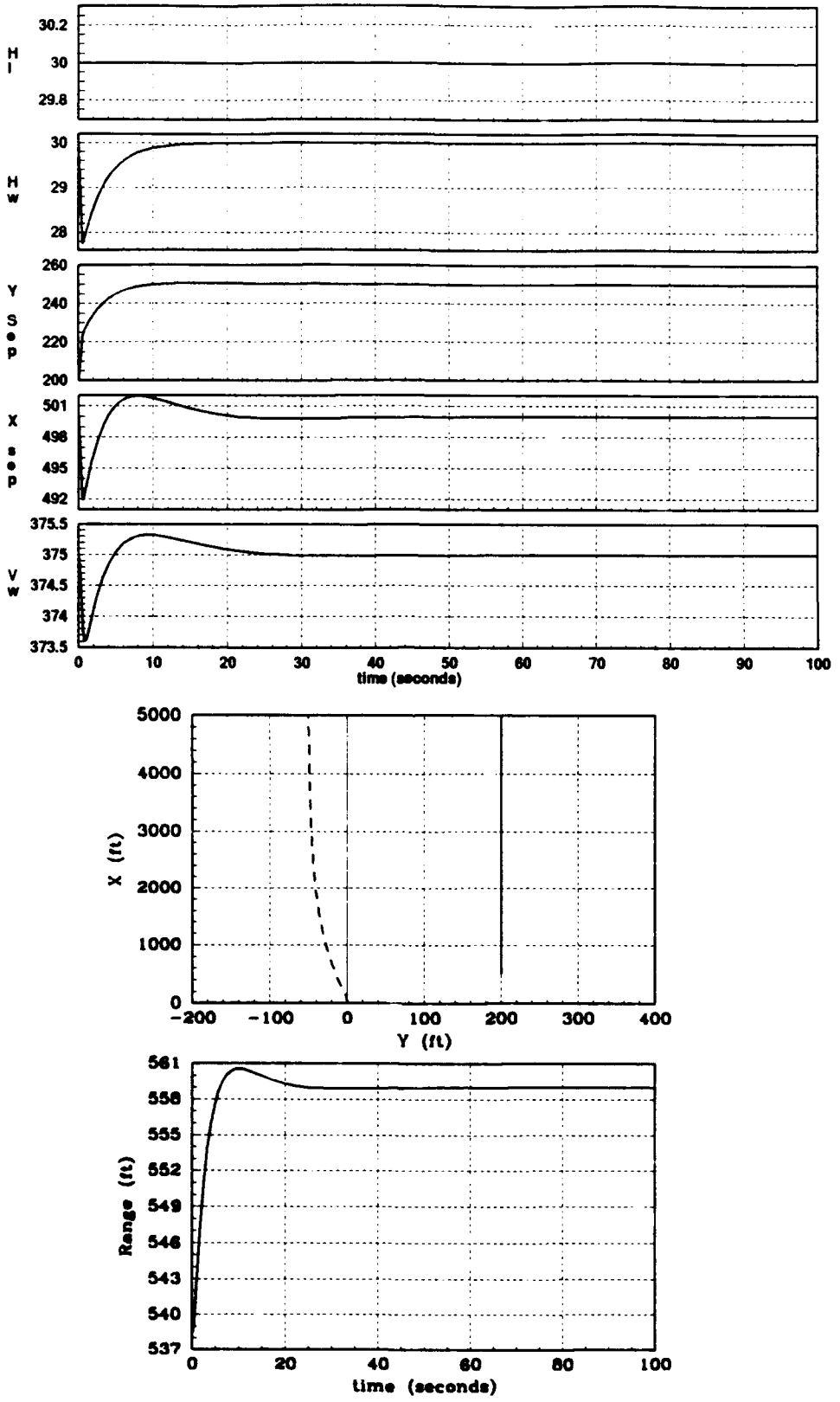

Figure A.7. Time Response and Flight Path Response to a Δy Input From 200 to 250 ft

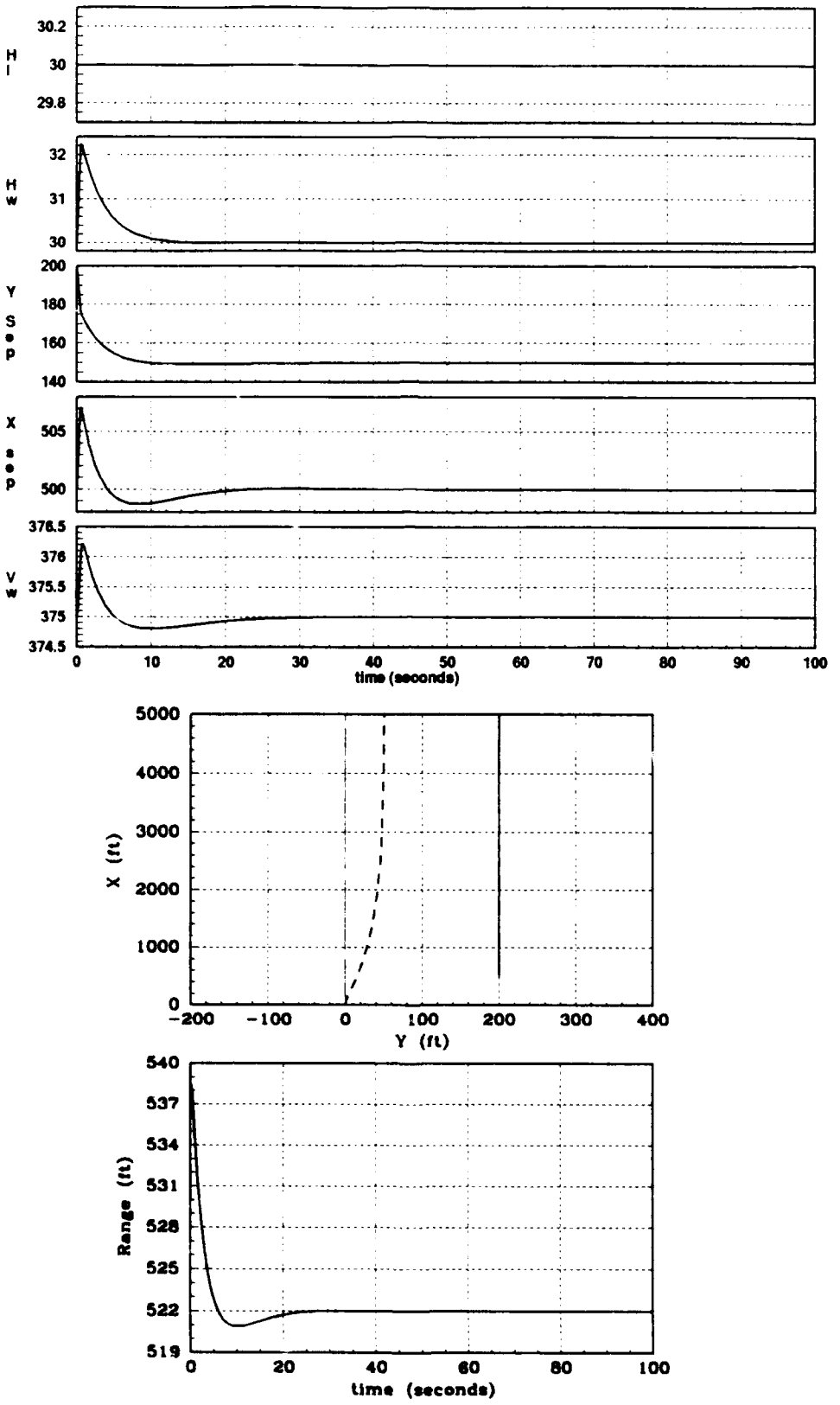

Figure A.8. Time Response and Flight Path Response to a Δy Input From 200 to 150 ft

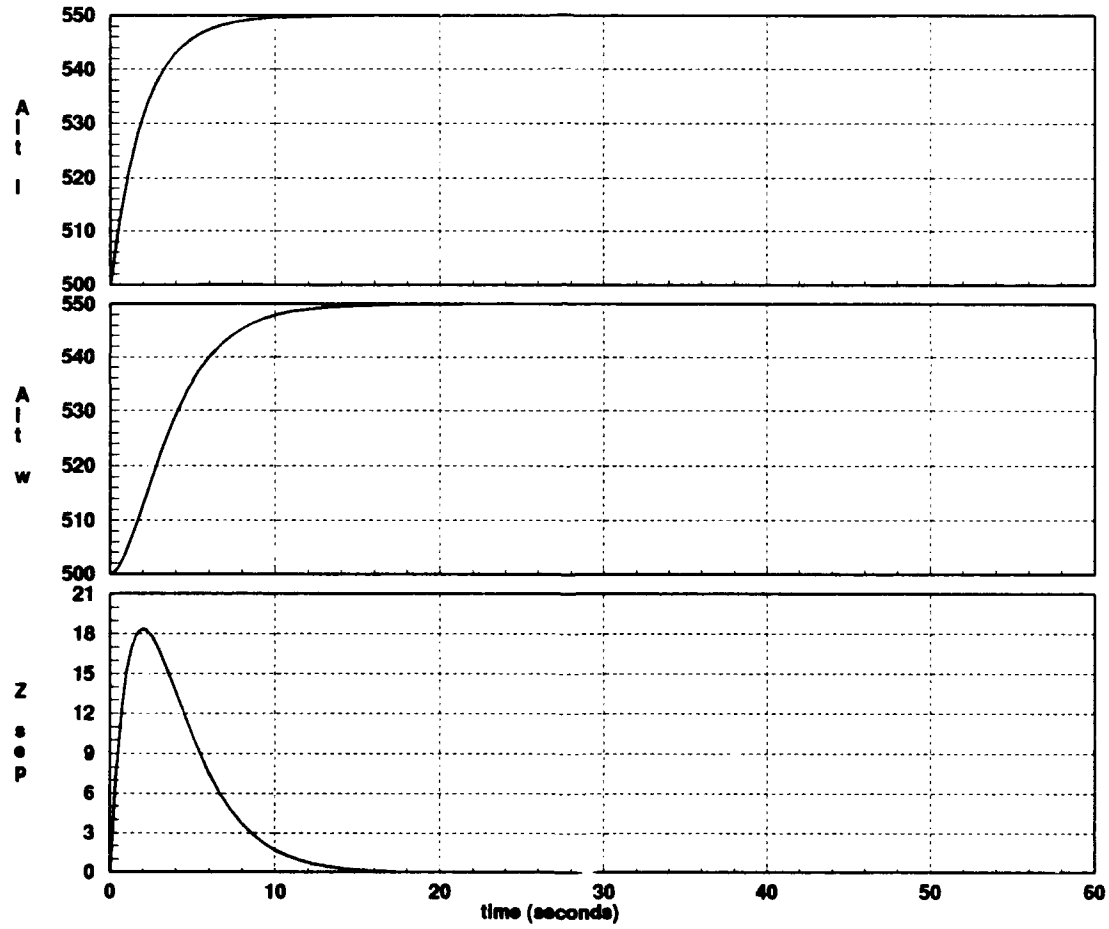

Figure A.9. Time Response for an h_l (Input) From 500 to 550 ft

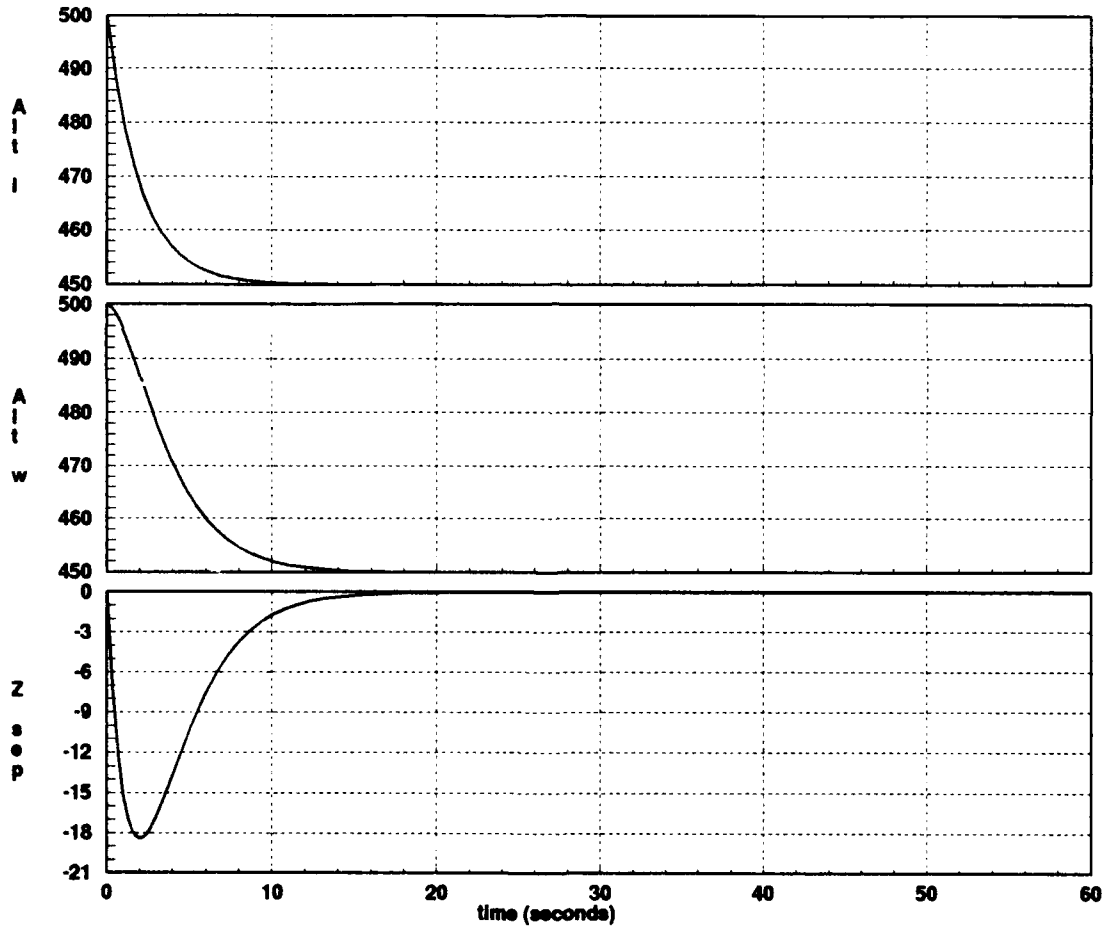

Figure A.10. Time Response for an h_l (Input) From 500 to 450 ft

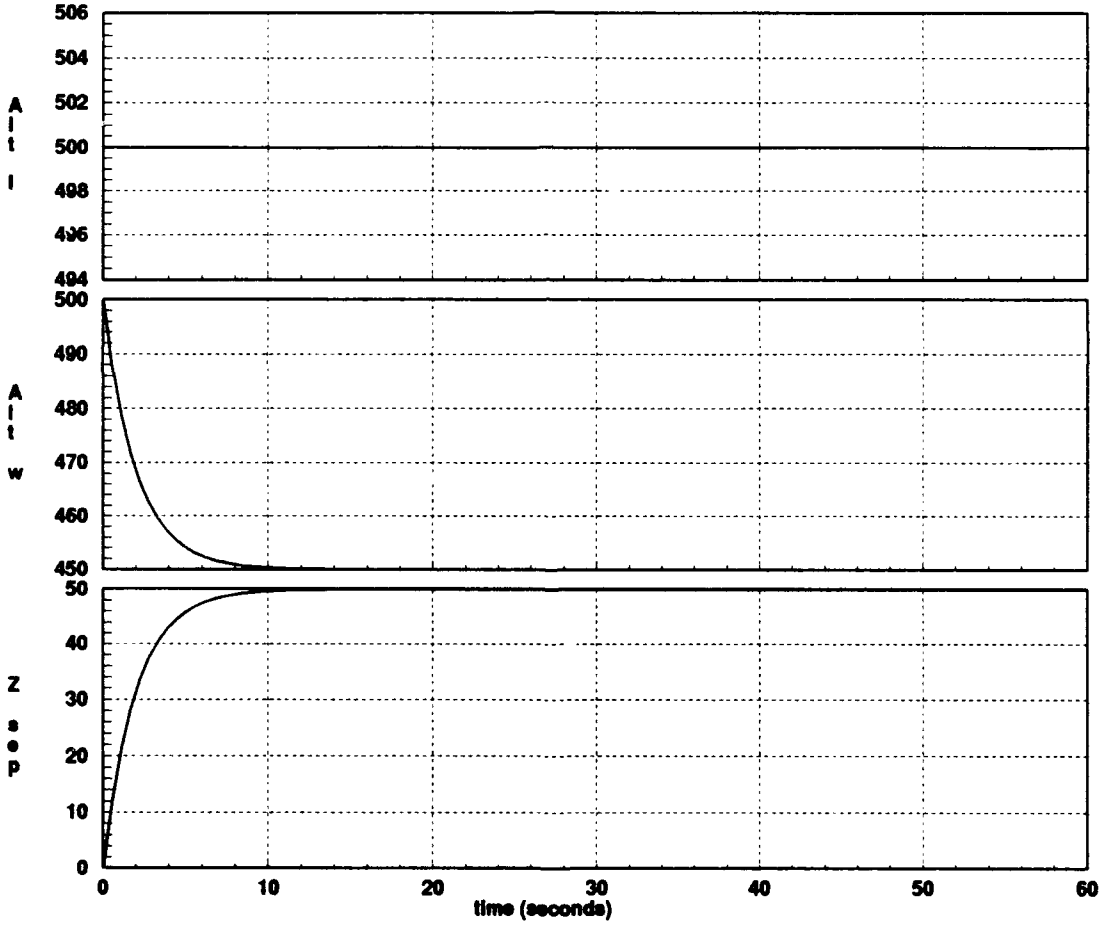

Figure A.11. Time Response for a Δz Input From 0 to 50 ft

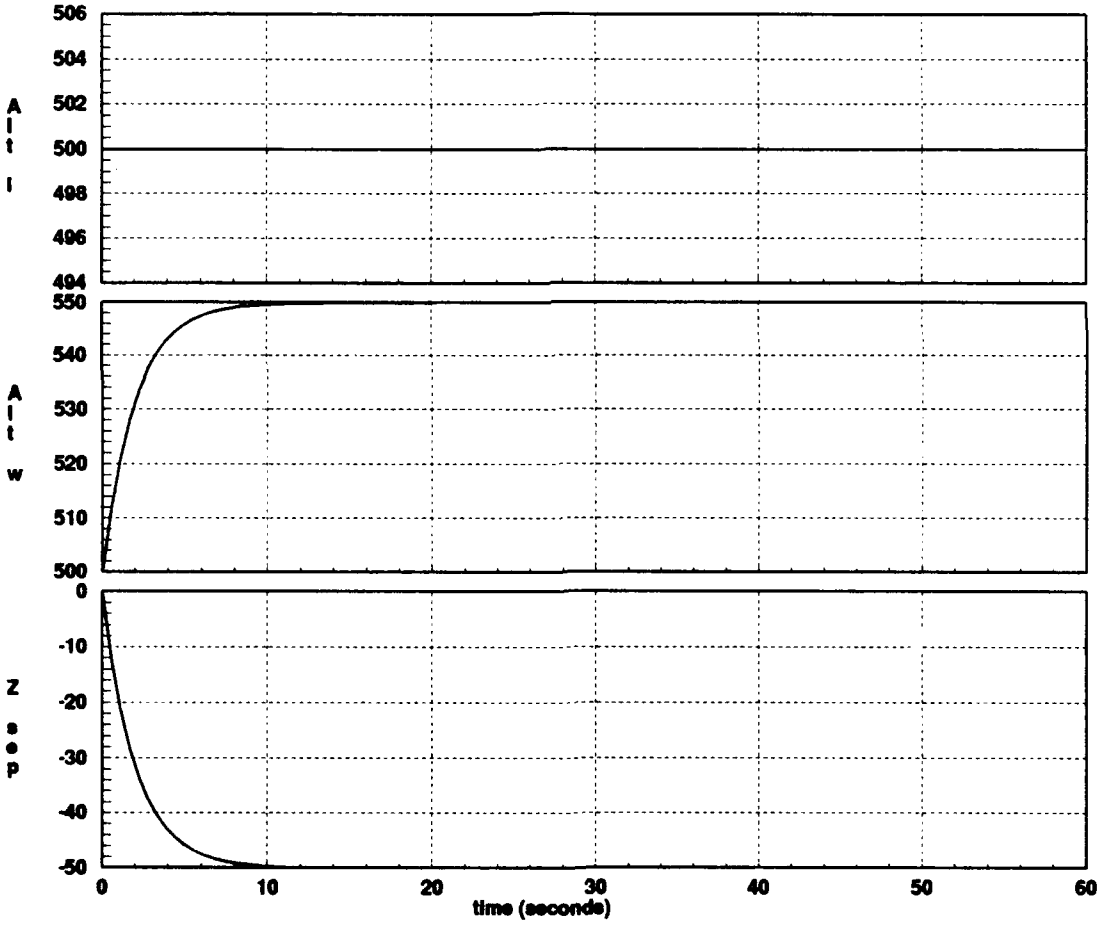

Figure A.12. Time Response for a Δz Input From 0 to -50 ft

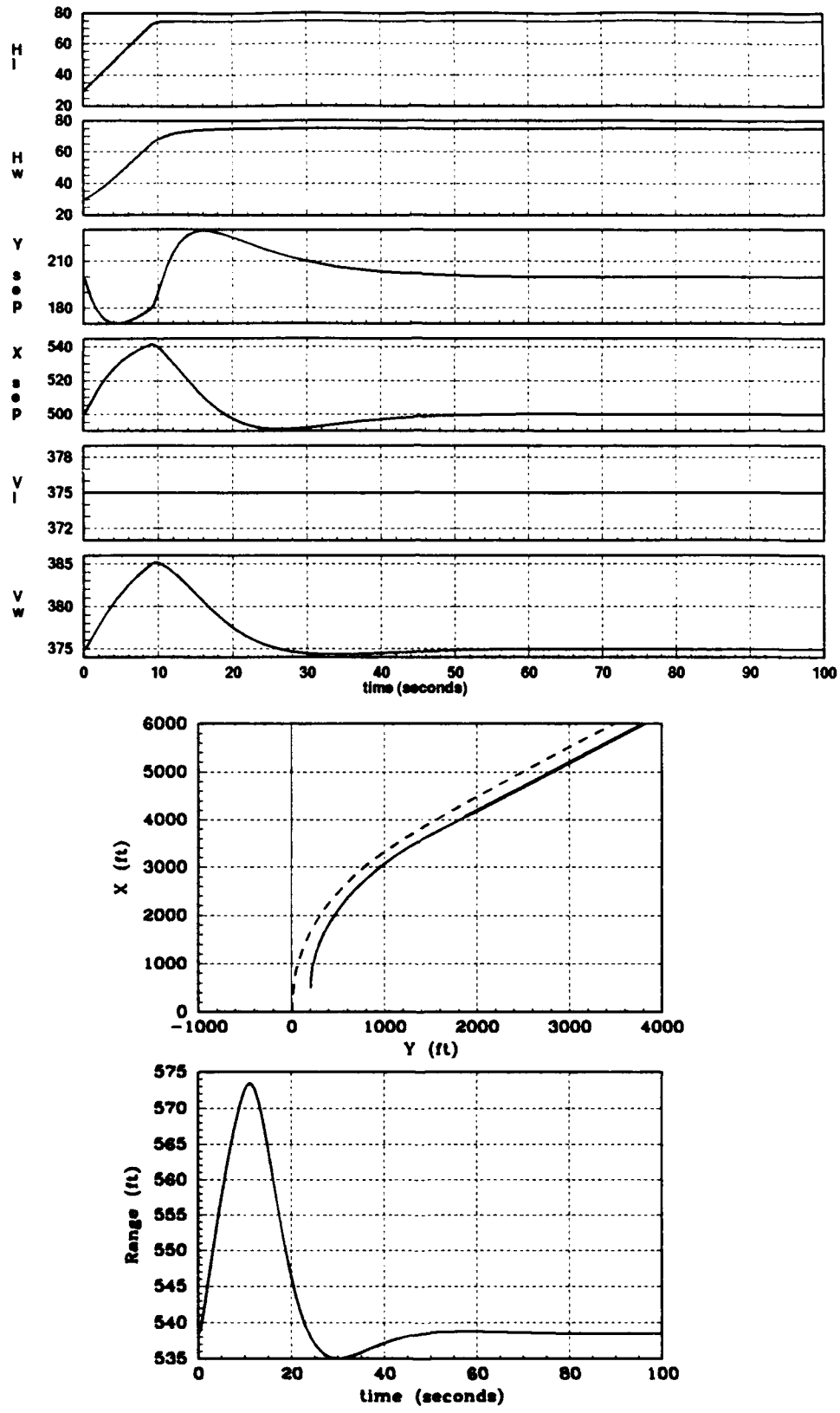

Figure A.13. Time Response and Flight Path Response for an H_L Input From 30 to 75 Degrees

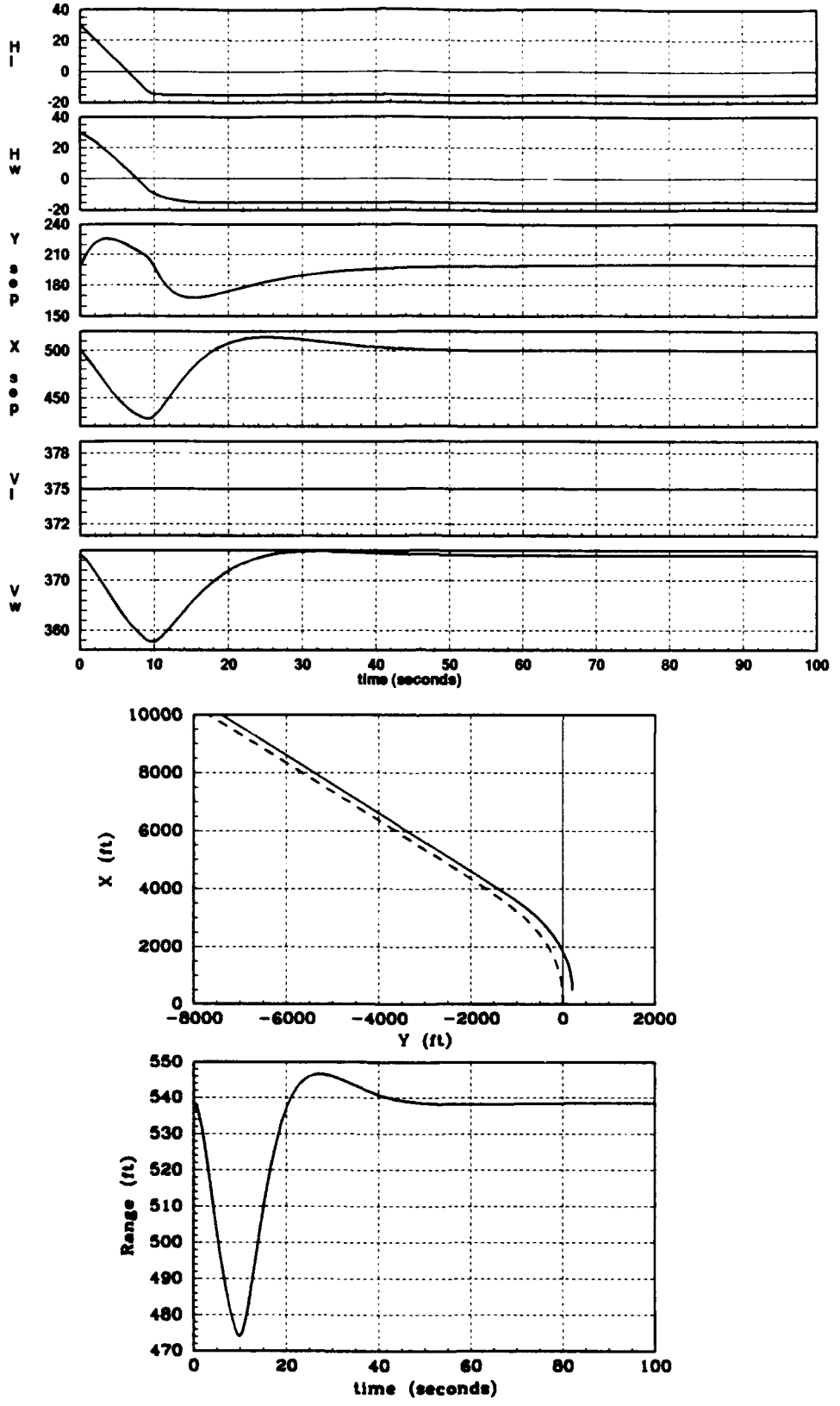

Figure A.14. Time Response and Flight Path Response for an H_L Input From 30 to -15 Degrees

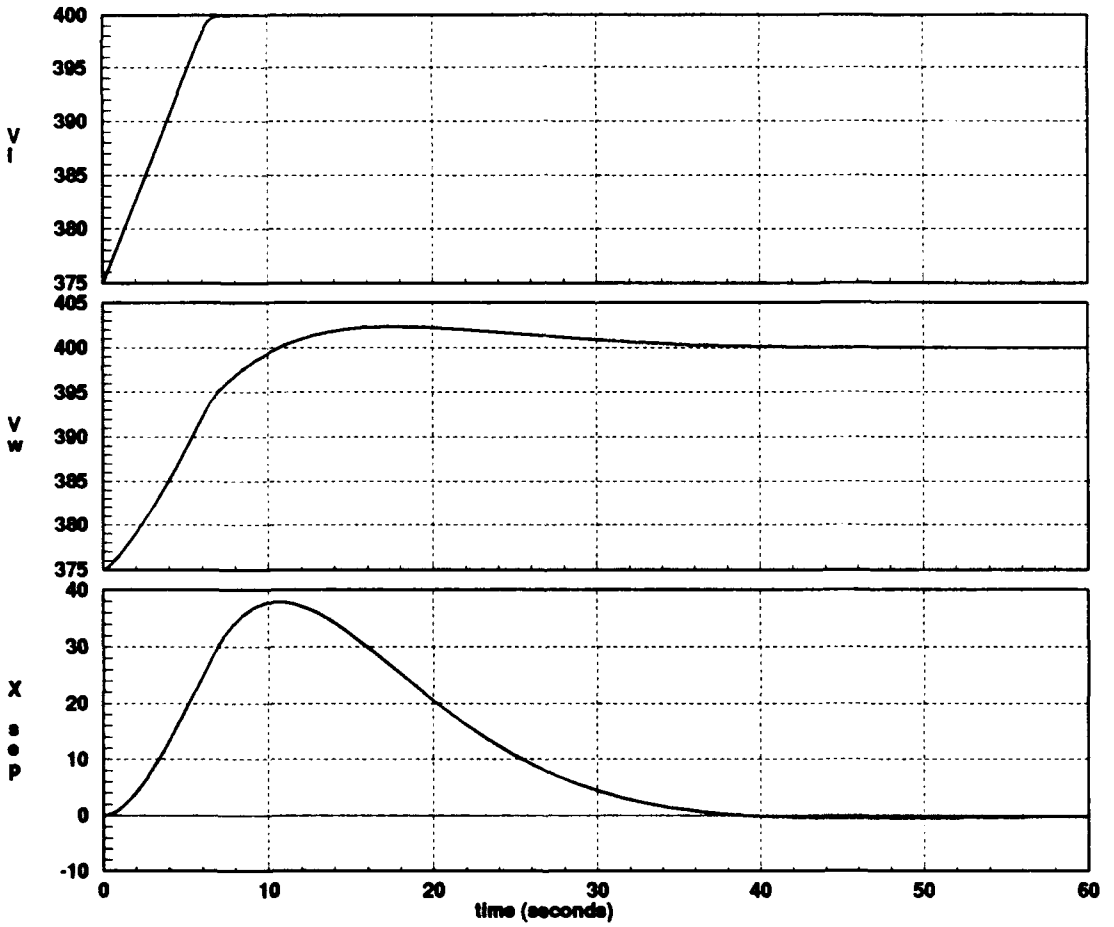

Figure A.15. Time Response for a V_L Input From 375 to 400 ft/sec

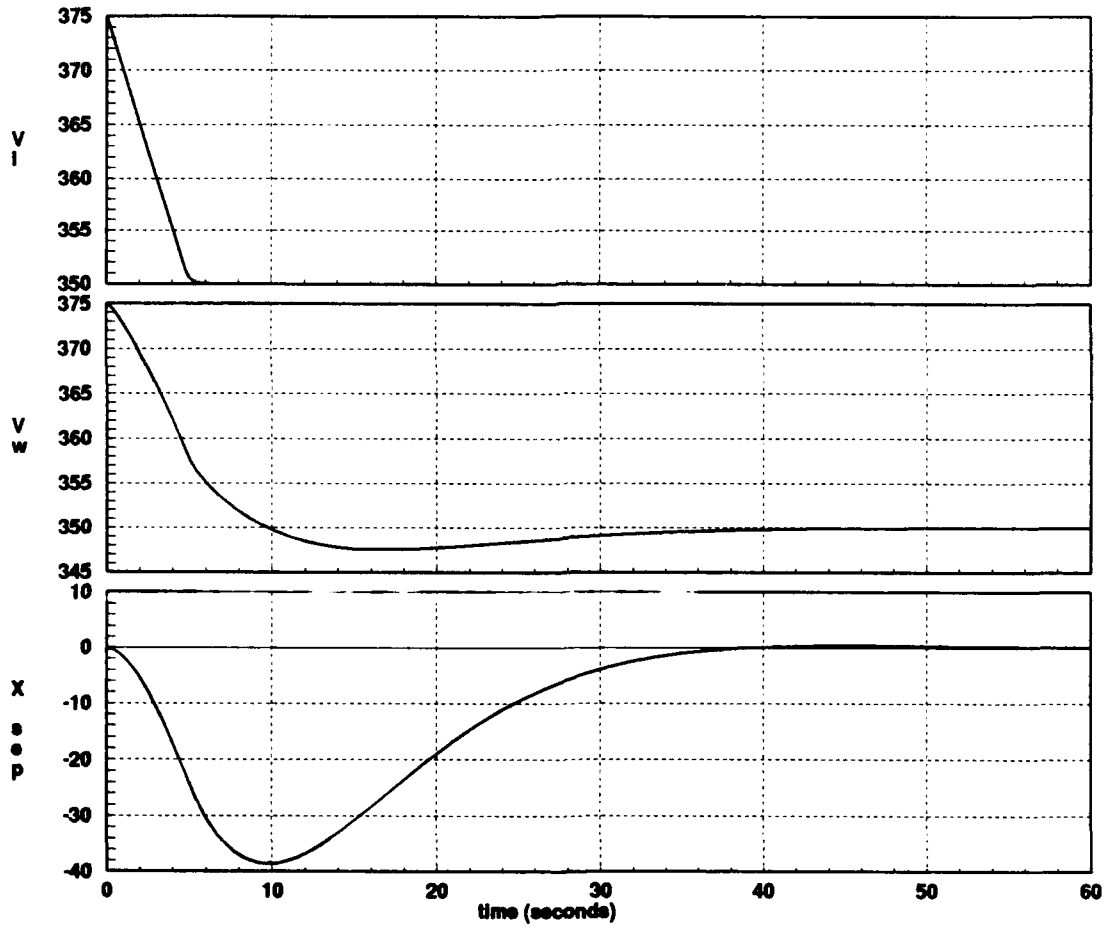

Figure A.16. Time Response for a V_L Input From 375 to 350 ft/sec

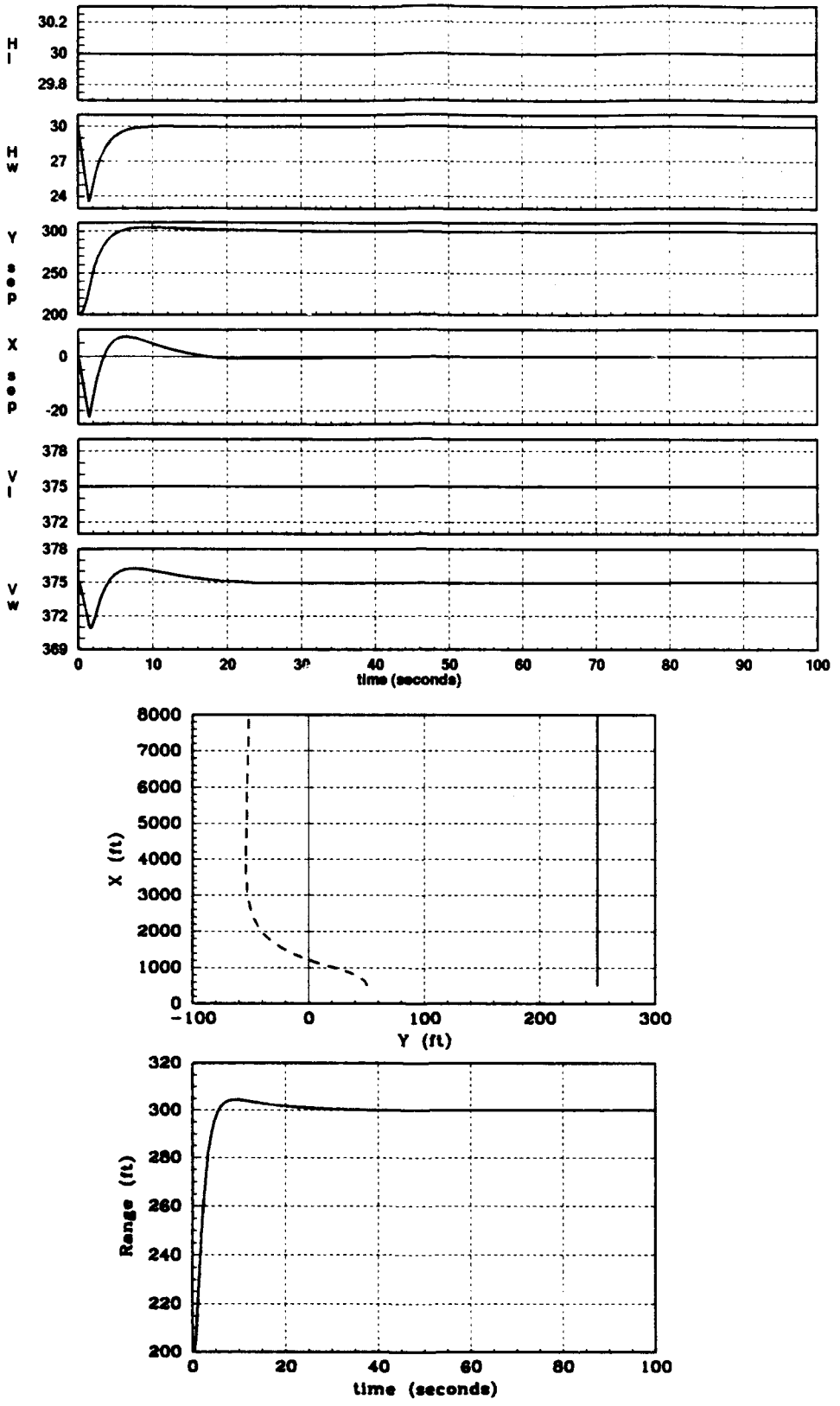

Figure A.17. Time Response and Flight Path Response for a Δy Input From 200 to 300 ft

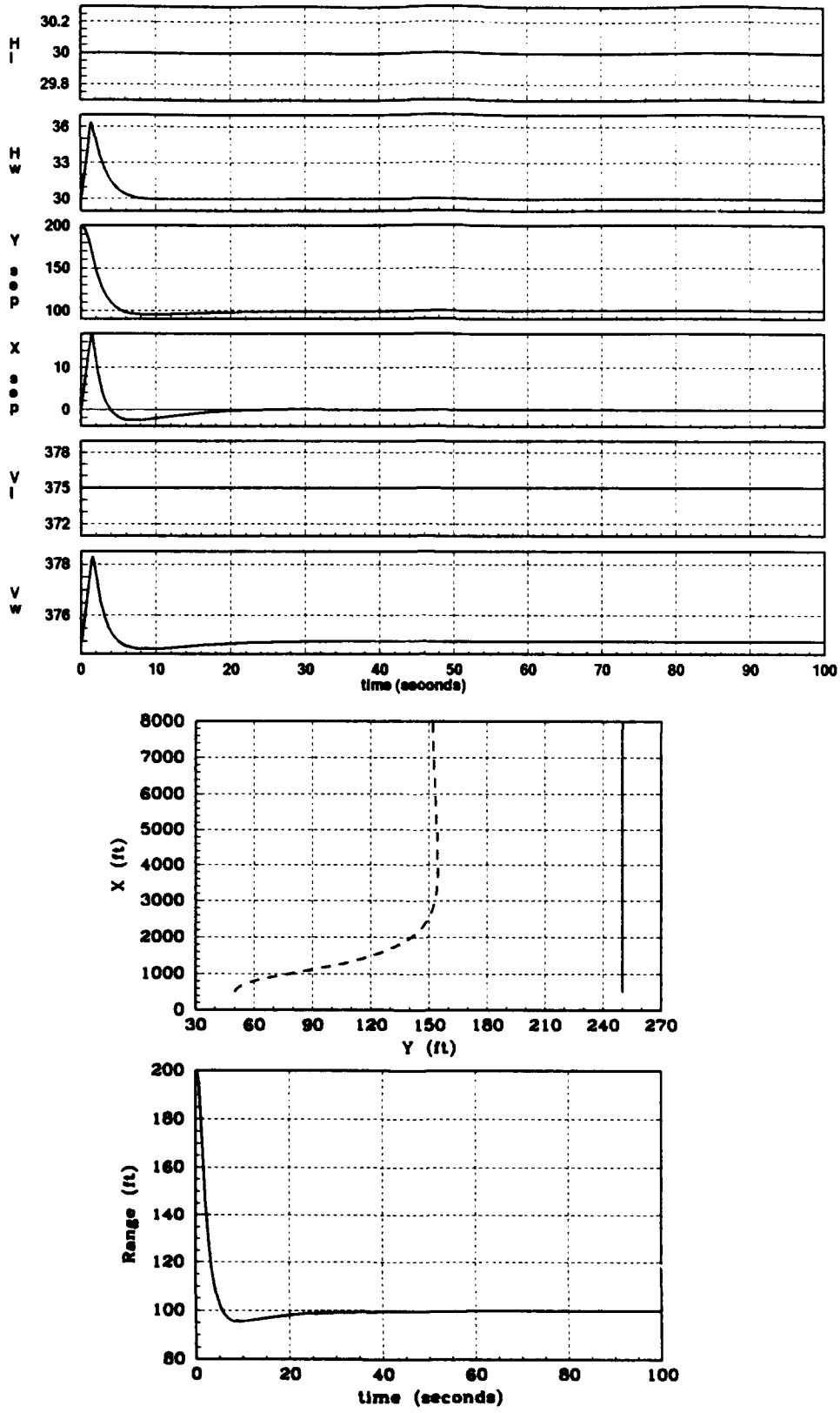

Figure A.18. Time Response and Flight Path Response for a Δy Input From 200 to 100 ft

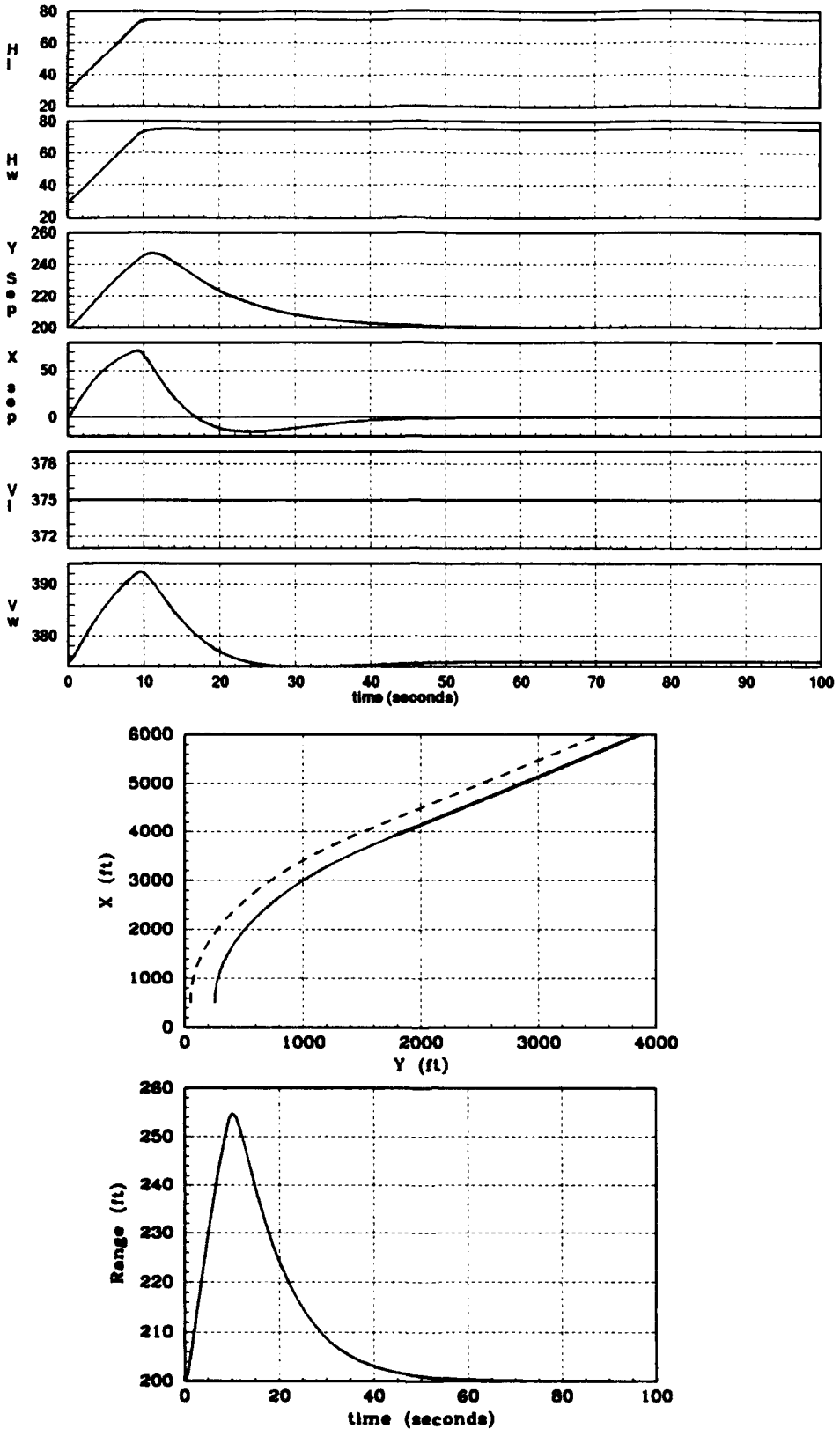

Figure A.19. Time Response and Flight Path Response for an H_L Input From 30 to 75 Degrees

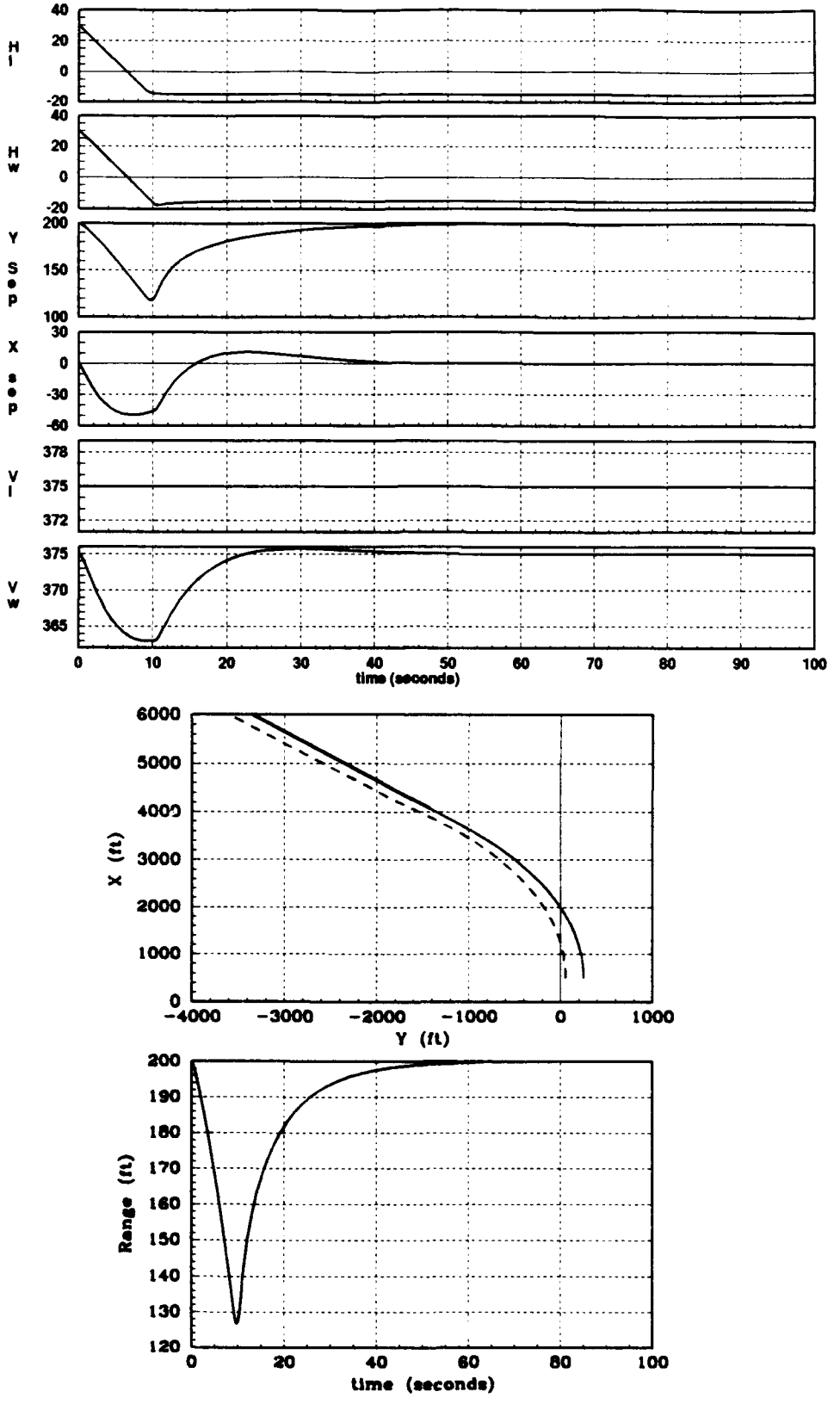

Figure A.20. Time Response and Flight Path Response for an H_L Input From 30 to -15 Degrees

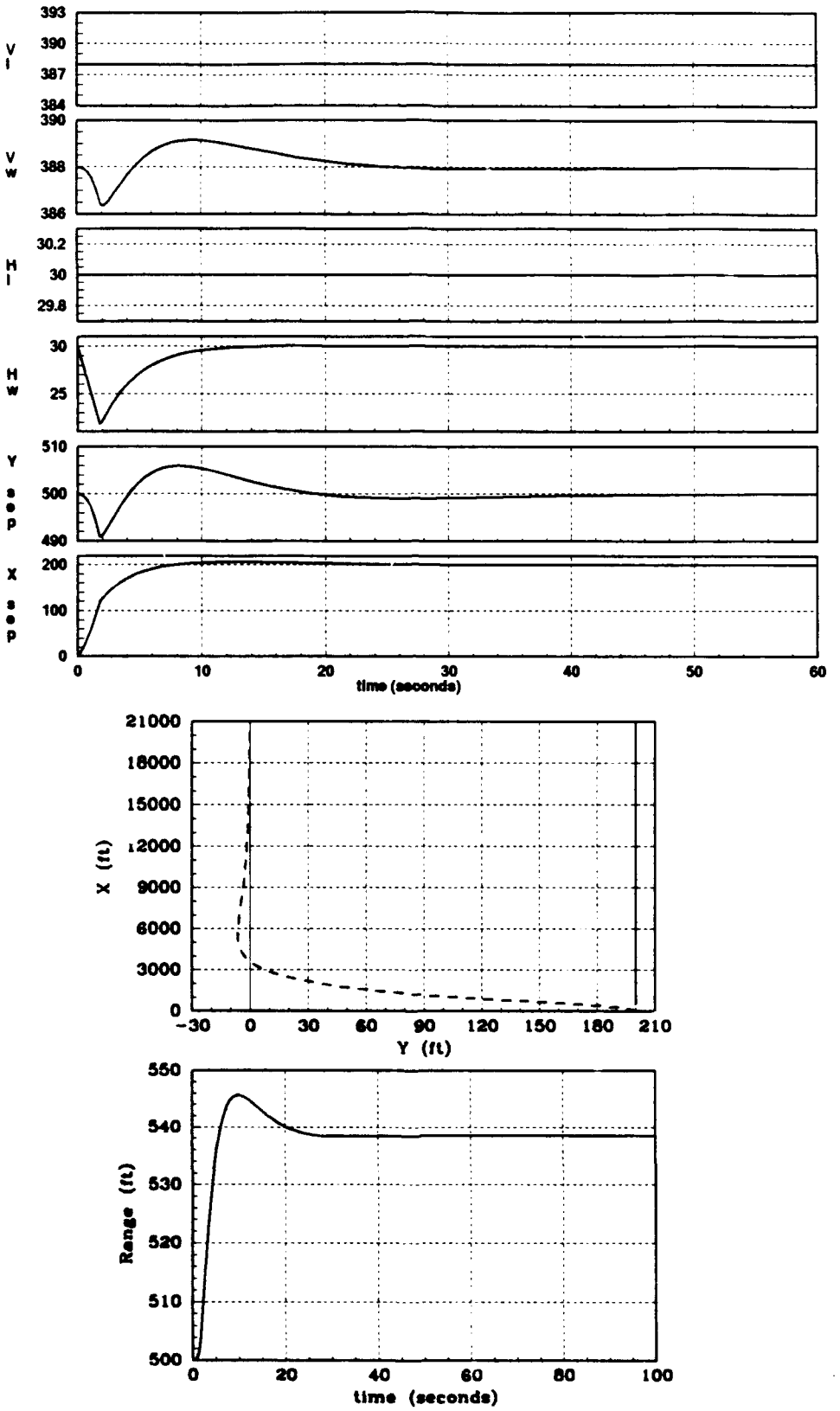

Figure A.21. Time Response and Flight Path Response for a Trail to Diamond Formation Change [Maneuver

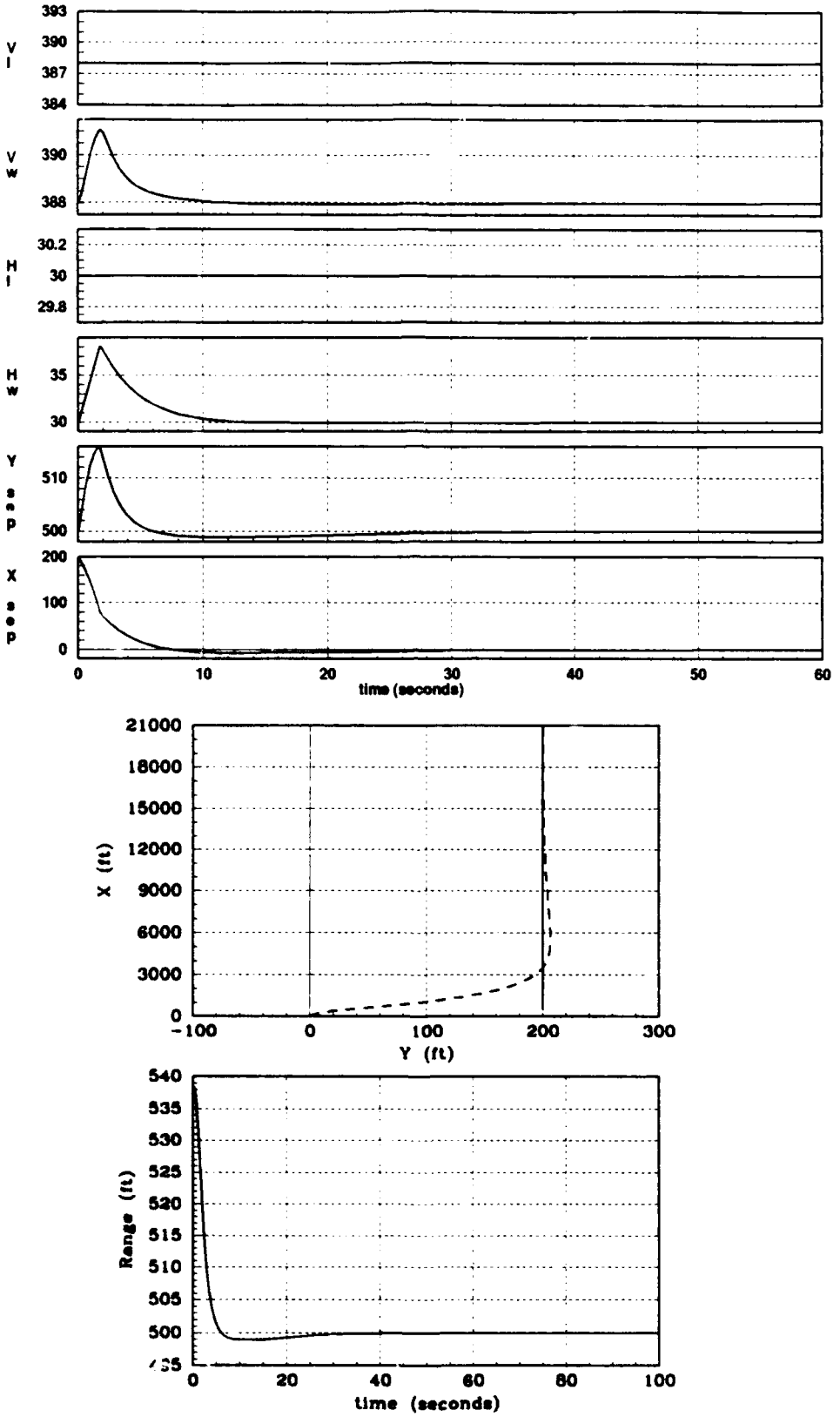

Figure A.22. Time Response and Flight Path Response for a Diamond to Trail Formation Change Maneuver

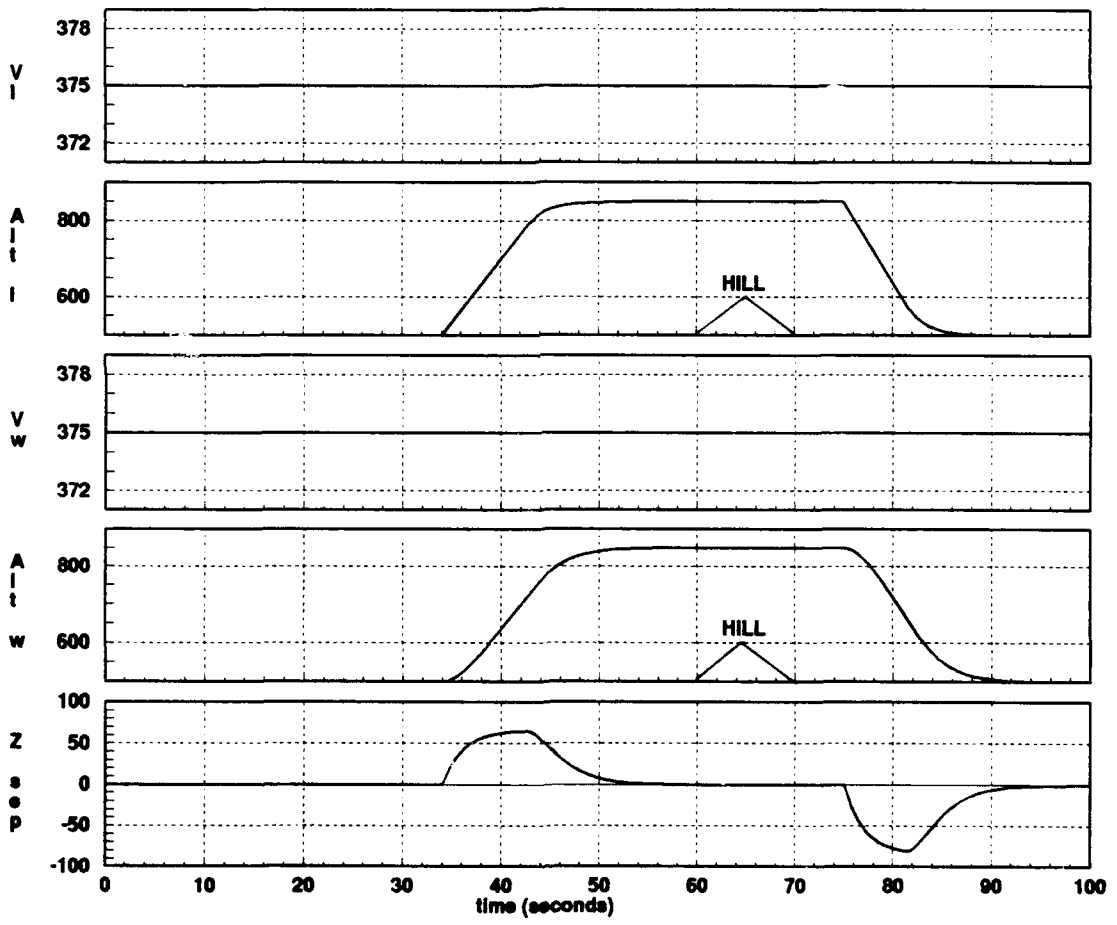

Figure A.23. Time Response for a Terrain Avoidance Maneuver

Appendix B. **Results for a Formation System Comprised of Dissimilar Aircraft in which the Lead Aircraft's Performance Capability is Inferior to the Wing Aircraft's**

The results for a formation comprised of dissimilar aircraft in which the lead aircraft has inferior performance capability to that of the wing aircraft is included in this Appendix. The lead aircraft is a C-130A and the wing aircraft is a C-130B. Time history plots and flight path plots are generated for a select number of the tests accomplished in Chapter V. As in Chapter V, the flight path plots are shown in an inertial reference frame with an initial formation heading angle of 0 degrees. The solid line on the flight path plots represents the flight path of the lead aircraft, and the dashed line represents the flight path of the wing aircraft. The variable names and definitions are given in Table B.1, the tests conducted are shown in Table B.2, and the initial conditions are given in Table B.3.

Table B.1. Variable Definitions

Variable Name: Text	Variable Name: Time Plots	Definition
V_L	V_l	Velocity of lead aircraft
V_W	V_w	Velocity of wing aircraft
H_L	H_l	Heading angle of lead aircraft
H_W	H_w	Heading angle of wing aircraft
h_L	Alt_l	Altitude of lead aircraft
h_W	Alt_w	Altitude of wing aircraft
Δx	$XSep$	Longitudinal separation distance
Δy	$Ysep$	Lateral separation distance
Δz	$Zsep$	Vertical separation distance

Table B.2. Formation Control System Simulation Tests

Initial Formation	Final Formation	Commanded Parameter Input	Response Plots
Diamond	Diamond	V_L = 400 ft/sec	Figure B.1
Diamond	Diamond	V_L = 350 ft/sec	Figure B.2
Diamond	Diamond	Δx = 550 ft	Figure B.3
Diamond	Diamond	Δx = 450 ft	Figure B.4
Diamond	Diamond	Δy = 250 ft	Figure B.5
Diamond	Diamond	Δy = 150 ft	Figure B.6
Diamond	Diamond	* H_L = 45 deg	Figure B.7
Diamond	Diamond	* H_L = -45 deg	Figure B.8
Trail	Trail	h_L = 850 ft	Figure B.9

Table B.3. Test Initial Conditions

Formation	Parameter	Initial Condition
Diamond	V_L	375 ft/sec
	V_W	375 ft/sec
	H_L	30 deg
	H_W	30 deg
	h_L	500 ft
	h_W	500 ft
	Δx	500 ft
	Δy	200 ft
	Δz	0 ft
Trail	V_L	375 ft/sec
	V_W	375 ft/sec
	H_L	30 deg
	H_W	30 deg
	h_L	500 ft
	h_W	500 ft
	Δx	500 ft
	Δy	0 ft
	Δz	0 ft

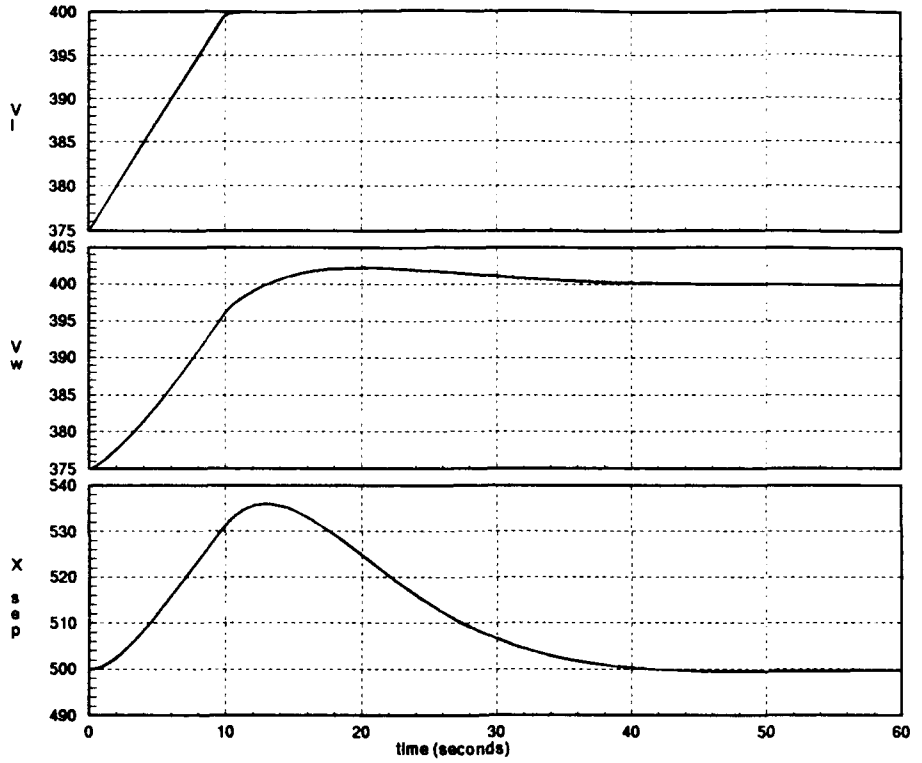

Figure B.1. Controlled Longitudinal Response to a V_L (Input) Change, from 375 to 400 ft/s

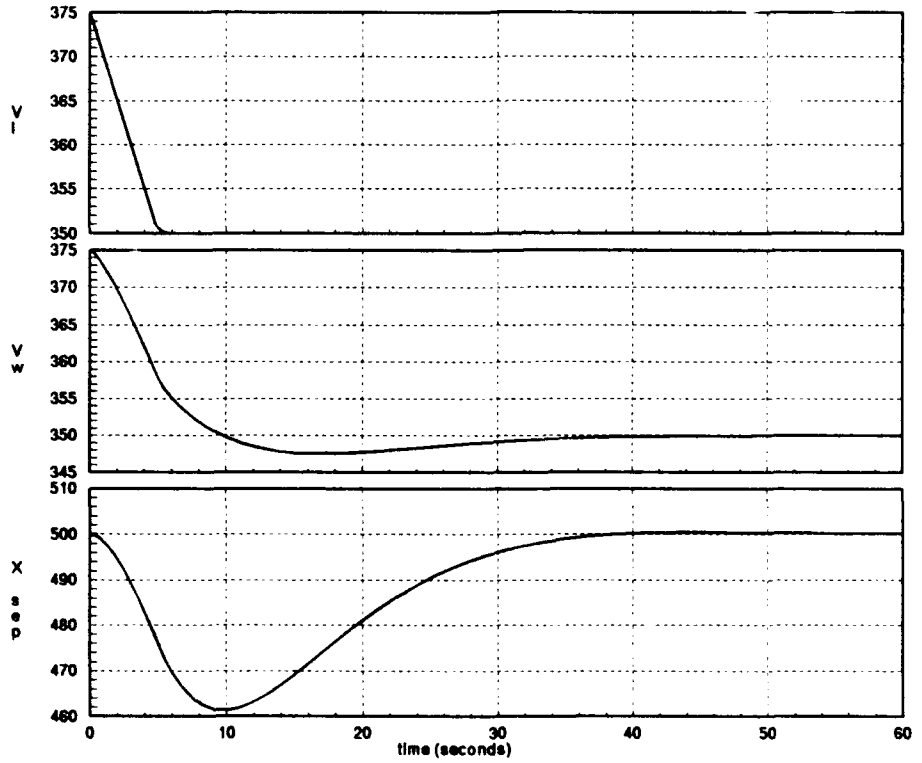

Figure B.2. Controlled Longitudinal Response to a V_L (Input) Change from 375 to 350 ft/s

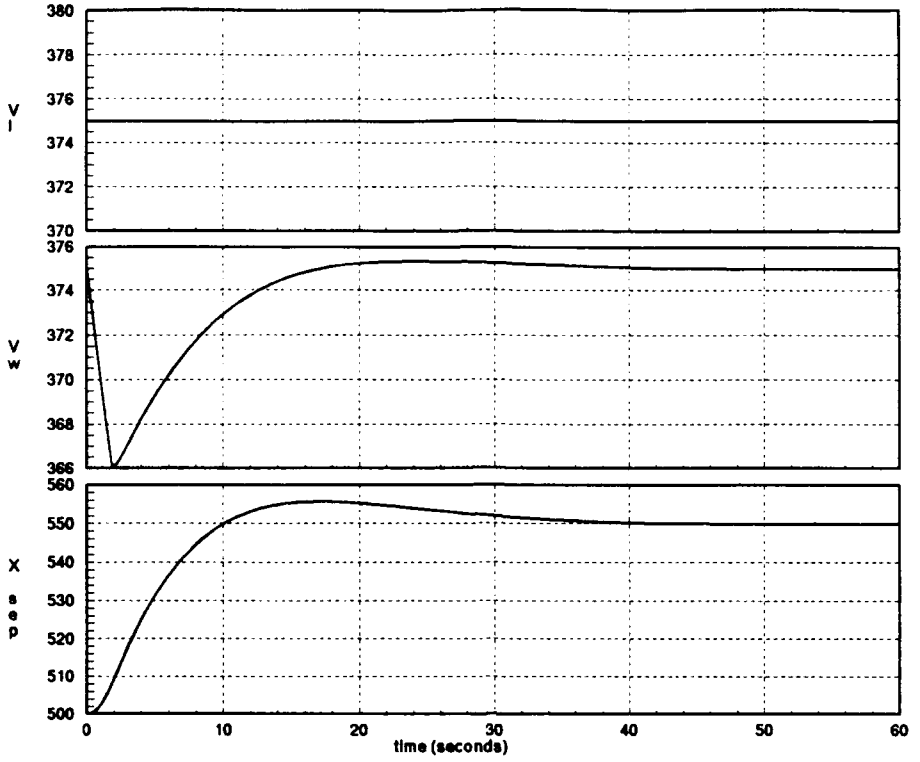

Figure B.3. Controlled Longitudinal Response to a Δx Input Change, from 500 to 550 ft

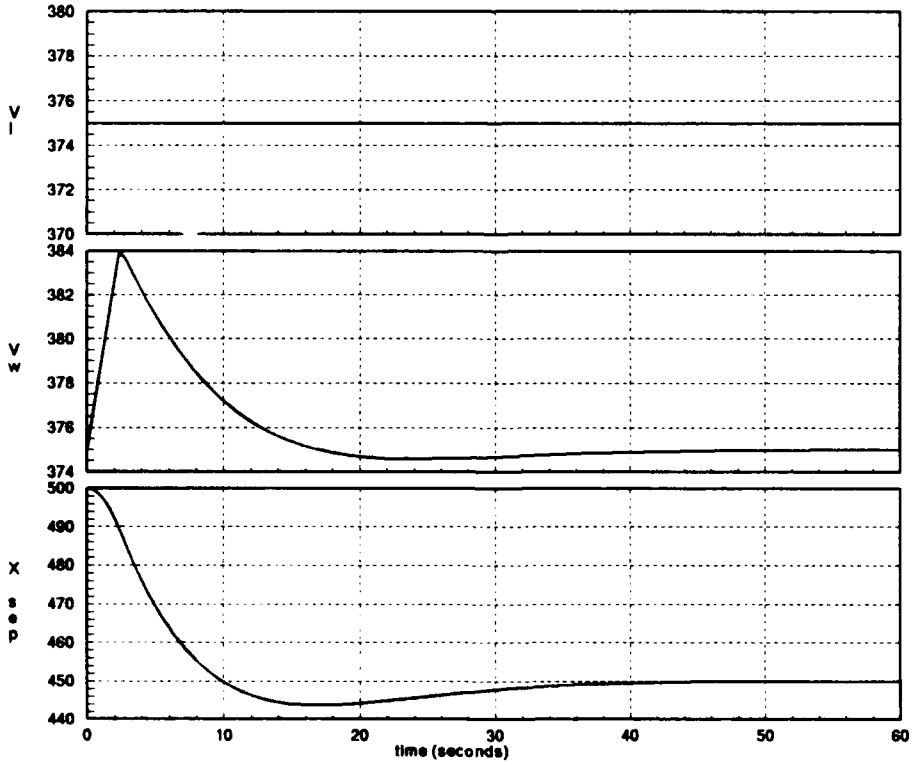

Figure B.4. Controlled Longitudinal Response to a Δx Input Change from 500 to 450 ft

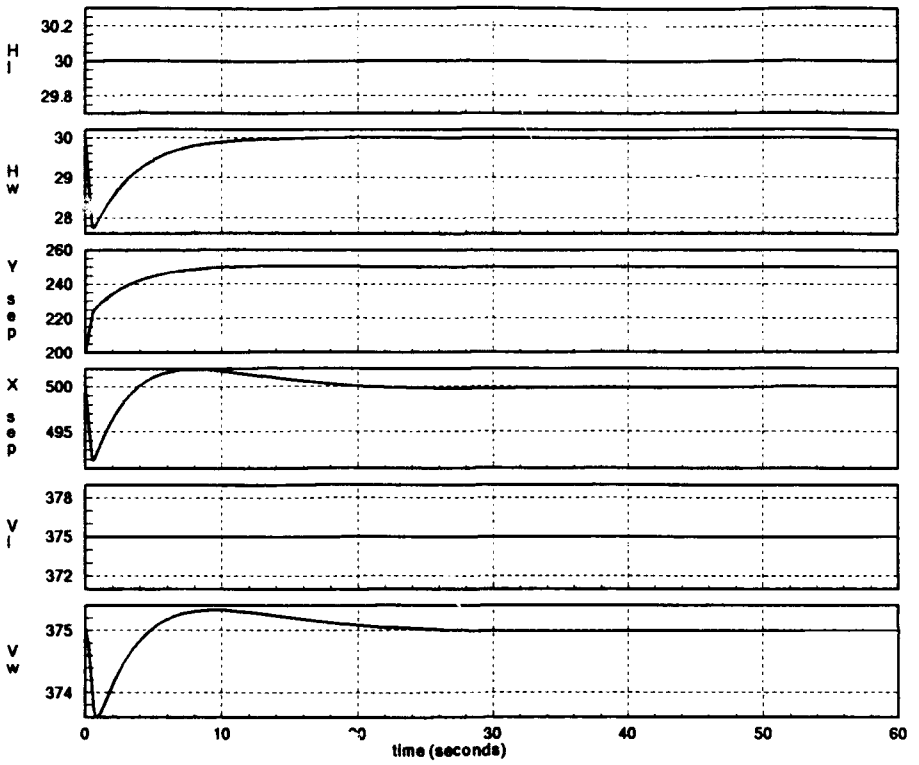

Figure B.5. Controlled Lateral Response to a Δy Input Change, from 200 to 250 ft

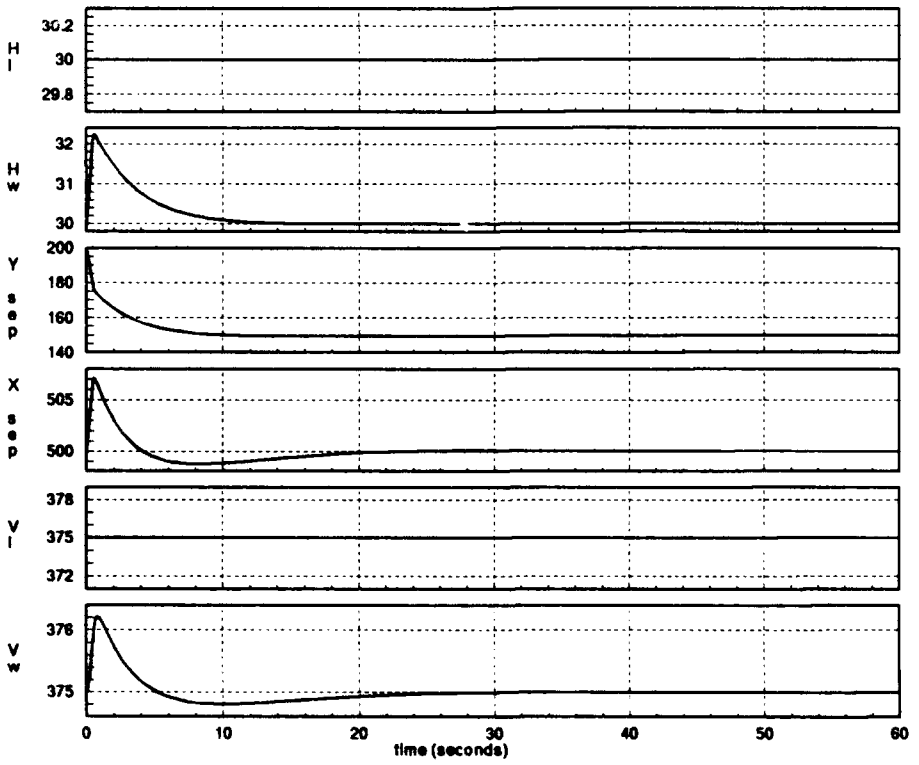

Figure B.6. Controlled Lateral Response to a Δy Input Change from 200 to 150 ft

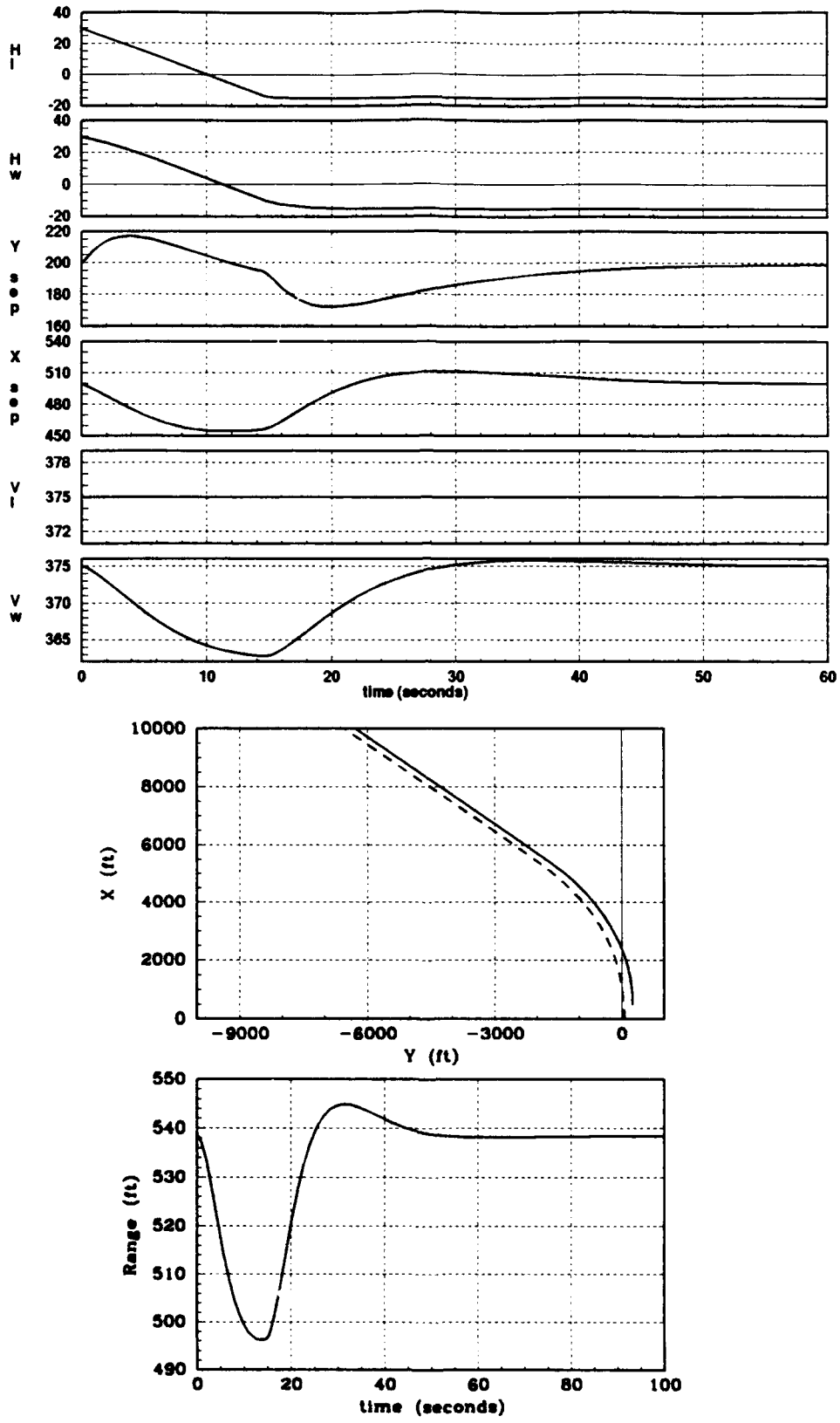

Figure B.7. Time Response and Flight Path Response to an H_L (Input) From 30 to -15 Degrees

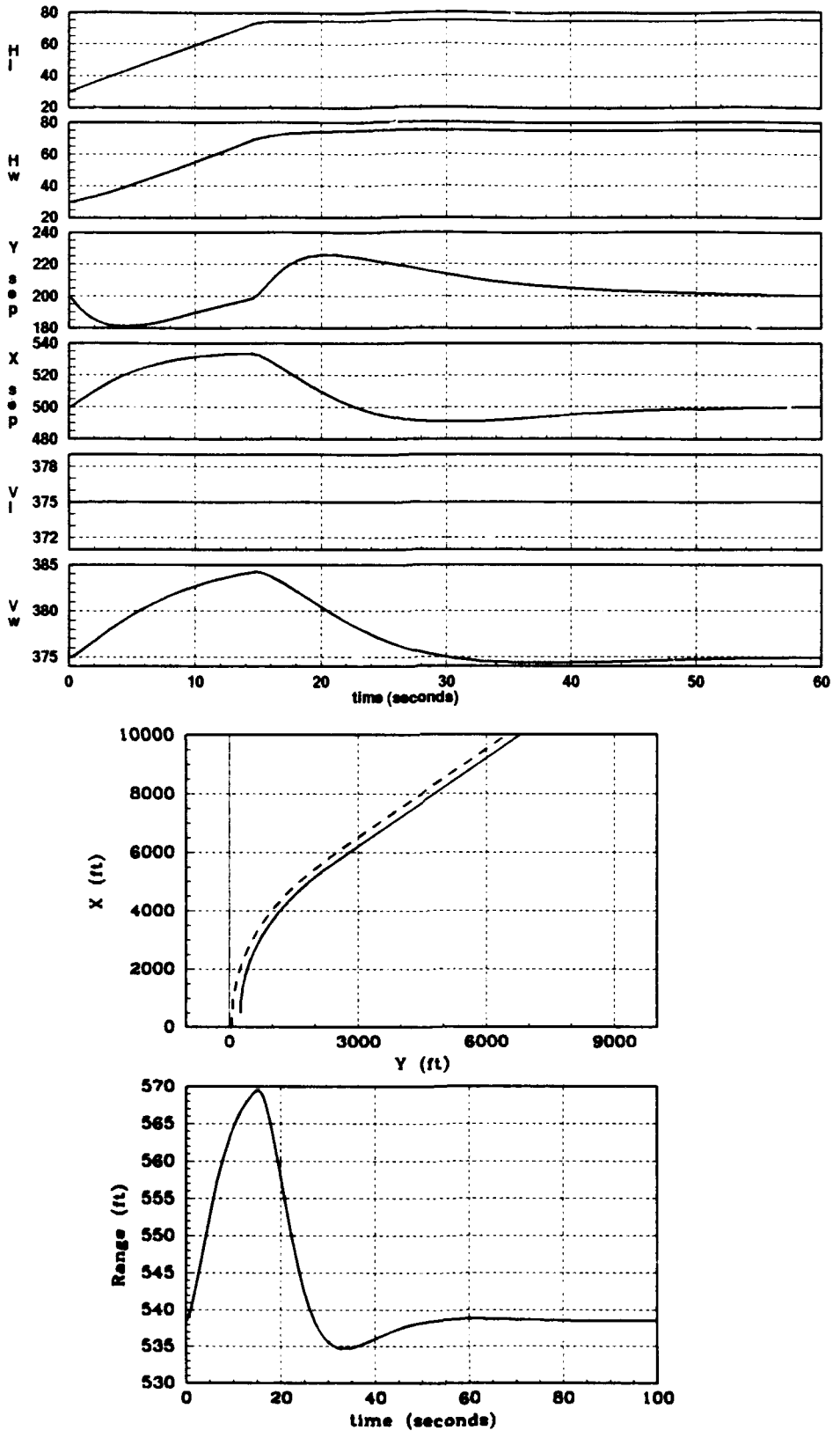

Figure B.8. Time Response and Flight Path Response to an H_L (Input) From 30 to 75 Degrees

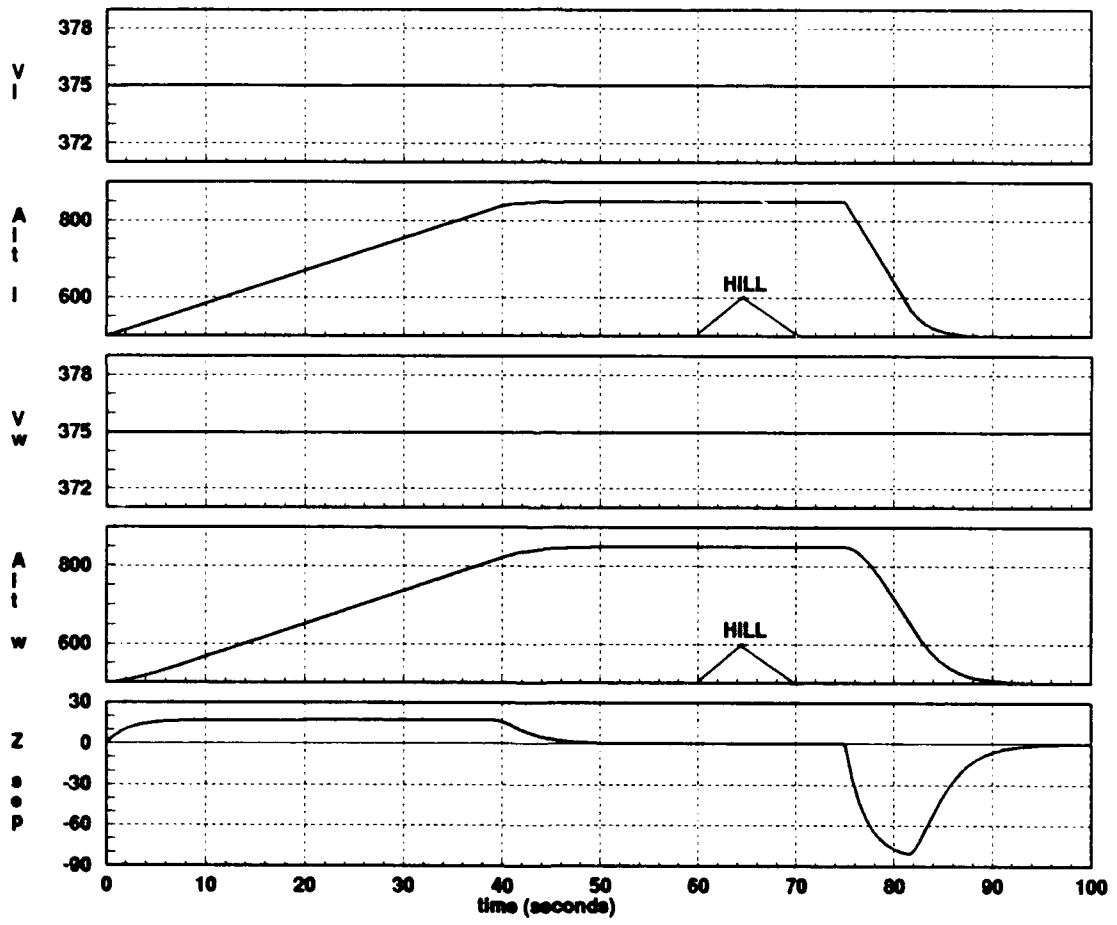

Figure B.9. Time Response for a Terrain Avoidance Maneuver

Appendix C. **Results for a Formation System Comprised of Similar Aircraft in which the Lead and the Wing Aircraft Both Have Inferior Performance Capability**

The results for a formation comprised of similar aircraft in which the lead and wing aircraft both have inferior performance is included in this Appendix. The lead aircraft and wing aircraft are both C-130A models. Time history plots and flight path plots are generated for the same tests accomplished in Appendix B. The flight paths are shown in an inertial reference frame with an initial formation heading angle of 0 degrees. The solid line on the flight path plots represents the flight path of the lead aircraft, and the dashed line represents the flight path of the wing aircraft. The variable names and definitions are given in Table C.1, the tests conducted are shown in Table C.2, and the initial conditions are given in Table C.3.

Table C.1. Variable Definitions

Variable Name: Text	Variable Name: Time Plots	Definition
V_L	V_l	Velocity of lead aircraft
V_W	V_w	Velocity of wing aircraft
H_L	H_l	Heading angle of lead aircraft
H_W	H_w	Heading angle of wing aircraft
h_L	Alt_l	Altitude of lead aircraft
h_W	Alt_w	Altitude of wing aircraft
Δx	$XSep$	Longitudinal separation distance
Δy	$Ysep$	Lateral separation distance
Δz	$Zsep$	Vertical separation distance

Table C.2. Formation Control System Simulation Tests

Initial Formation	Final Formation	Commanded Parameter Input	Response Plots
Diamond	Diamond	V_L = 400 ft/sec	Figure C.1
Diamond	Diamond	V_L = 350 ft/sec	Figure C.2
Diamond	Diamond	Δx = 550 ft	Figure C.3
Diamond	Diamond	Δx = 450 ft	Figure C.4
Diamond	Diamond	Δy = 250 ft	Figure C.5
Diamond	Diamond	Δy = 150 ft	Figure C.6
Diamond	Diamond	* H_L = 45 deg	Figure C.7
Diamond	Diamond	* H_L = -45 deg	Figure C.8
Trail	Trail	h_L = 850 ft	Figure C.9

Table C.3. Test Initial Conditions

Formation	Parameter	Initial Condition
Diamond	V_L	375 ft/sec
	V_W	375 ft/sec
	H_L	30 deg
	H_W	30 deg
	h_L	500 ft
	h_W	500 ft
	Δx	500 ft
	Δy	200 ft
	Δz	0 ft
Trail	V_L	375 ft/sec
	V_W	375 ft/sec
	H_L	30 deg
	H_W	30 deg
	h_L	500 ft
	h_W	500 ft
	Δx	500 ft
	Δy	0 ft
	Δz	0 ft

C.1 **Results Summary**

A comparison between the results in Appendix B in which the lead aircraft has degraded performance capability compared to the wing aircraft and the results in Appendix C in which both aircraft have degraded performance capability reveals that there is little difference in the velocity and Δx time responses. There is a small difference in the Δy responses. The quicker turn rate of the C-130B wing aircraft in Appendix B is evident when the this heading response is compared to that of the C-130A wing aircraft in Appendix C. The settling time for a Δy response to a Δy input change from 200 to 150 feet is 37 seconds in Appendix B and 39 seconds in Appendix C. However, the settling time for a Δy response for a Δy input change from 200 to 250 feet is 42 seconds in both Appendix B and Appendix C. The H_L response for an H_L input change of 45 degrees is similar for both Appendix B and Appendix C as is the H_L response for an H_L input change of -45 degrees. The responses for a terrain avoidance maneuver are similar for both Appendix B and Appendix C. Note that for the terrain avoidance maneuver, the input to the lead aircraft is provided as a step input in both Appendix B and Appendix C.

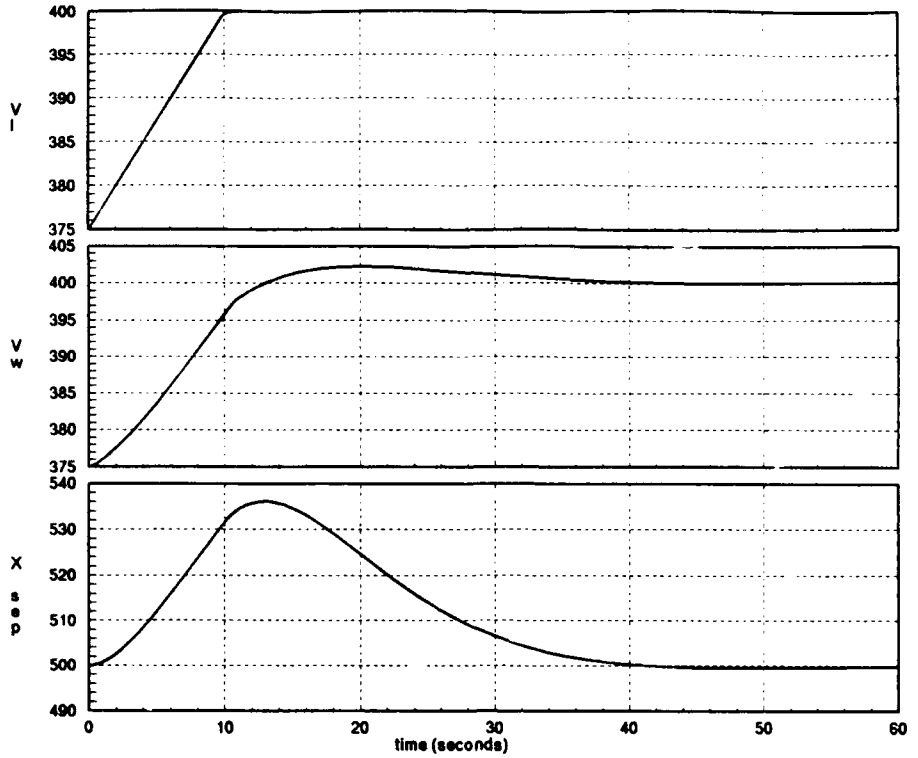

Figure C.1. Controlled Longitudinal Response to a V_L (Input) Change, from 375 to 400 ft/s

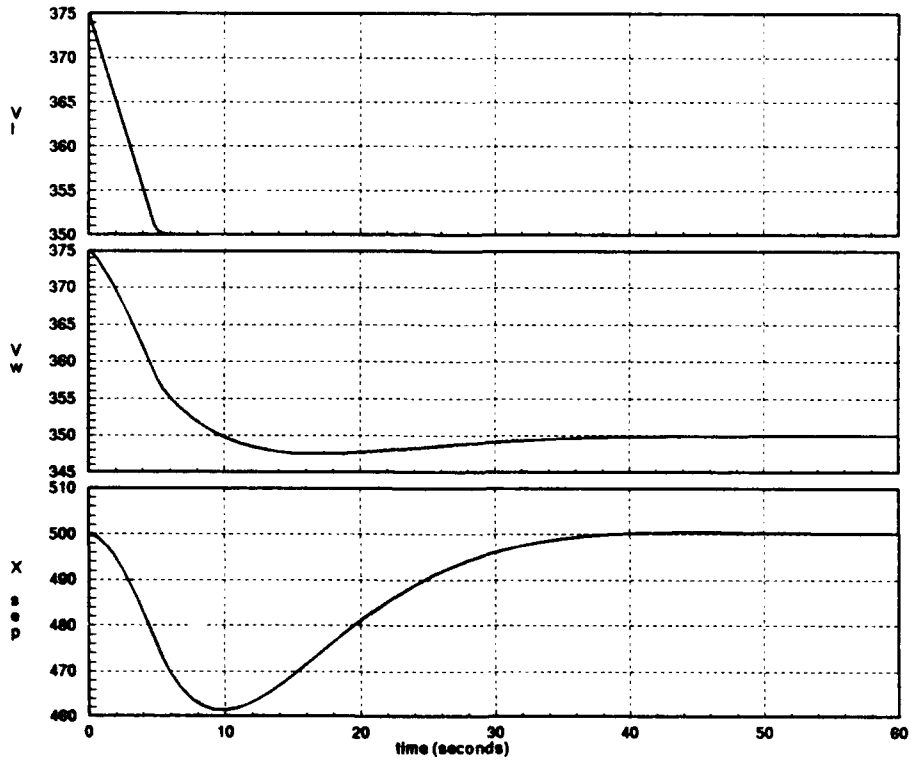

Figure C.2. Controlled Longitudinal Response to a V_L (Input) Change from 375 to 350 ft/s

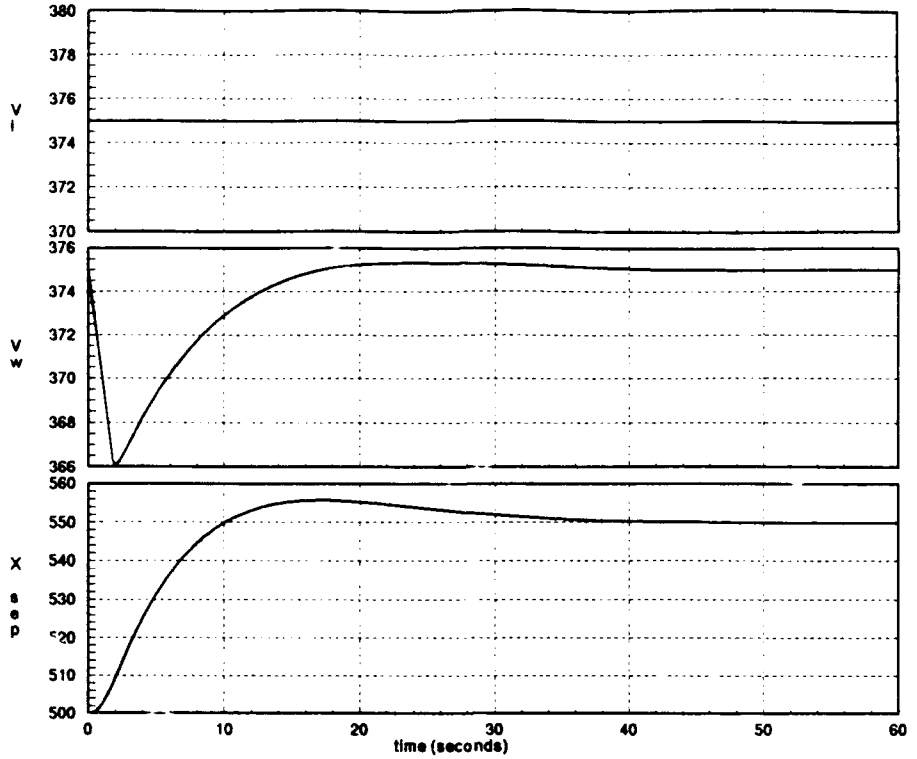

Figure C.3. Controlled Longitudinal Response to a Δx Input Change, from 500 to 550 ft

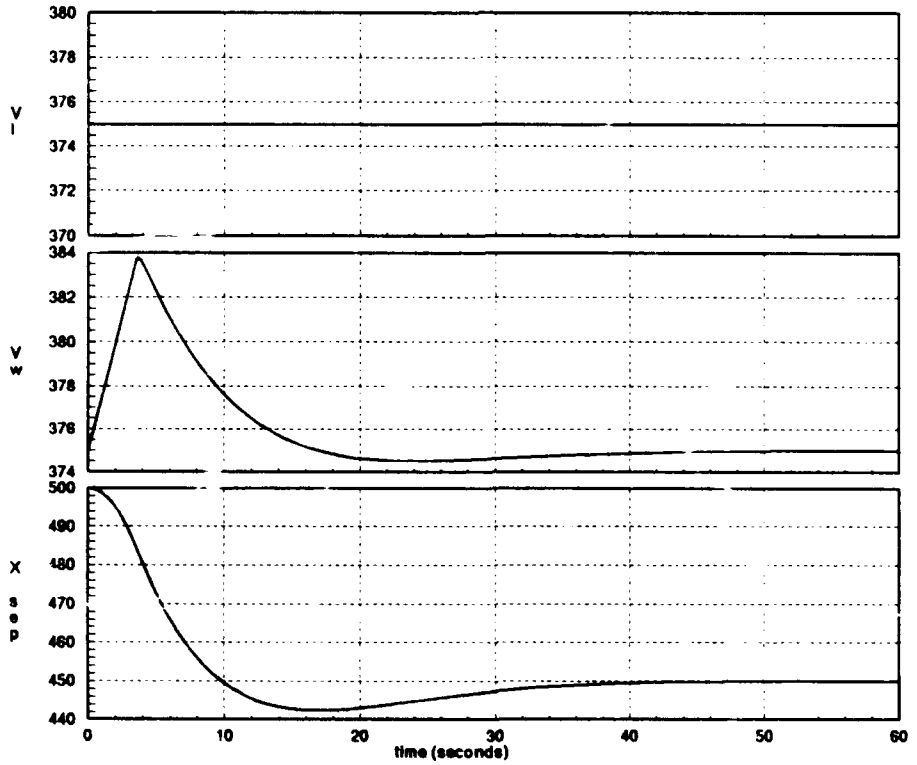

Figure C.4. Controlled Longitudinal Response to a Δx Input Change from 500 to 450 ft

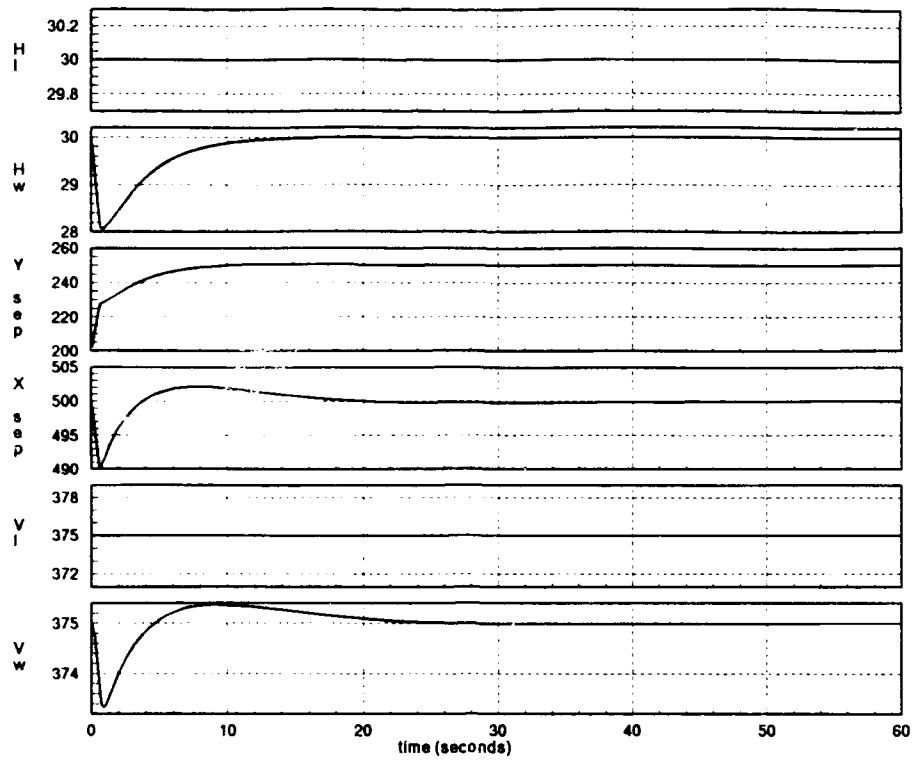

Figure C.5. Controlled Lateral Response to a Δy Input Change, from 200 to 250 ft

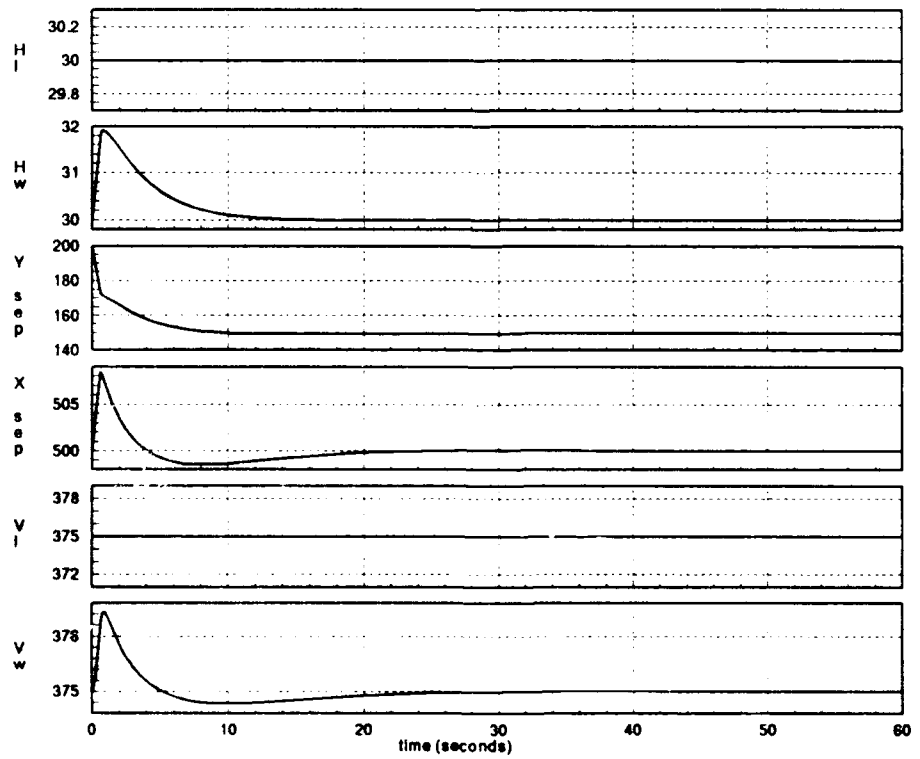

Figure C.6. Controlled Lateral Response to a Δy Input Change from 200 to 150 ft

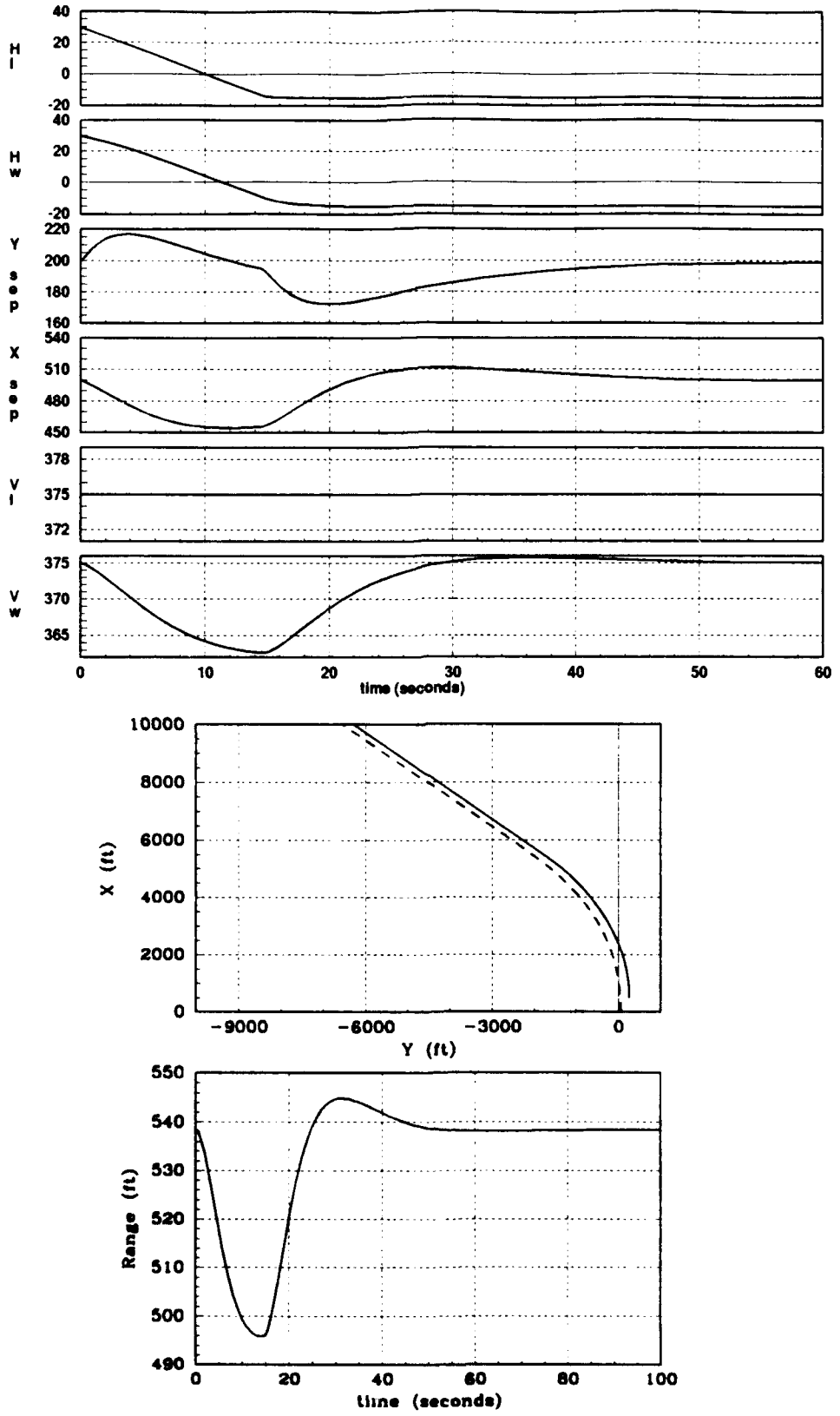

Figure C.7. Time Response and Flight Path Response to an H_L (Input) From 30 to -15 Degrees

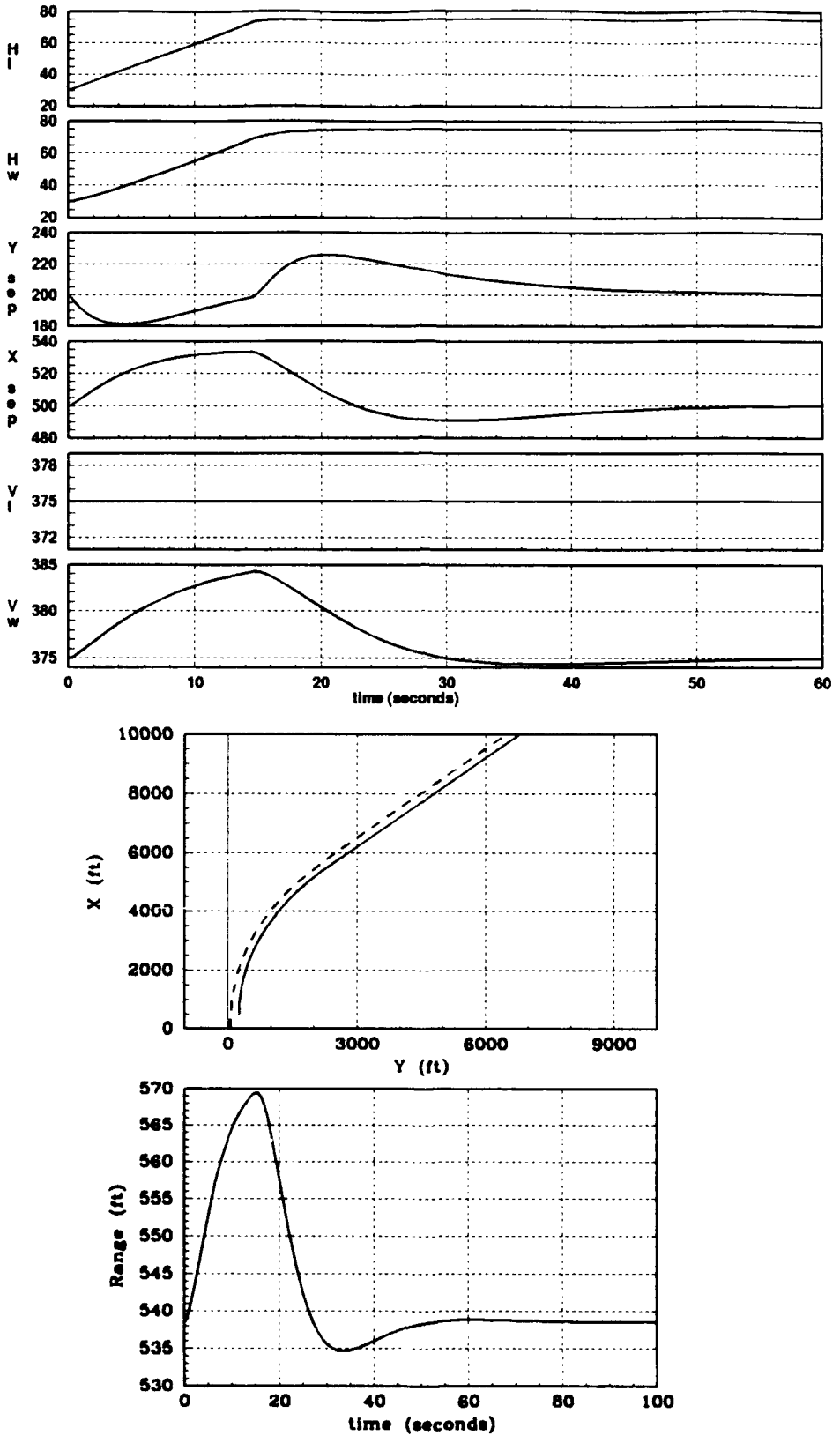

Figure C.8. Time Response and Flight Path Response to an H_L (Input) From 30 to 75 Degrees

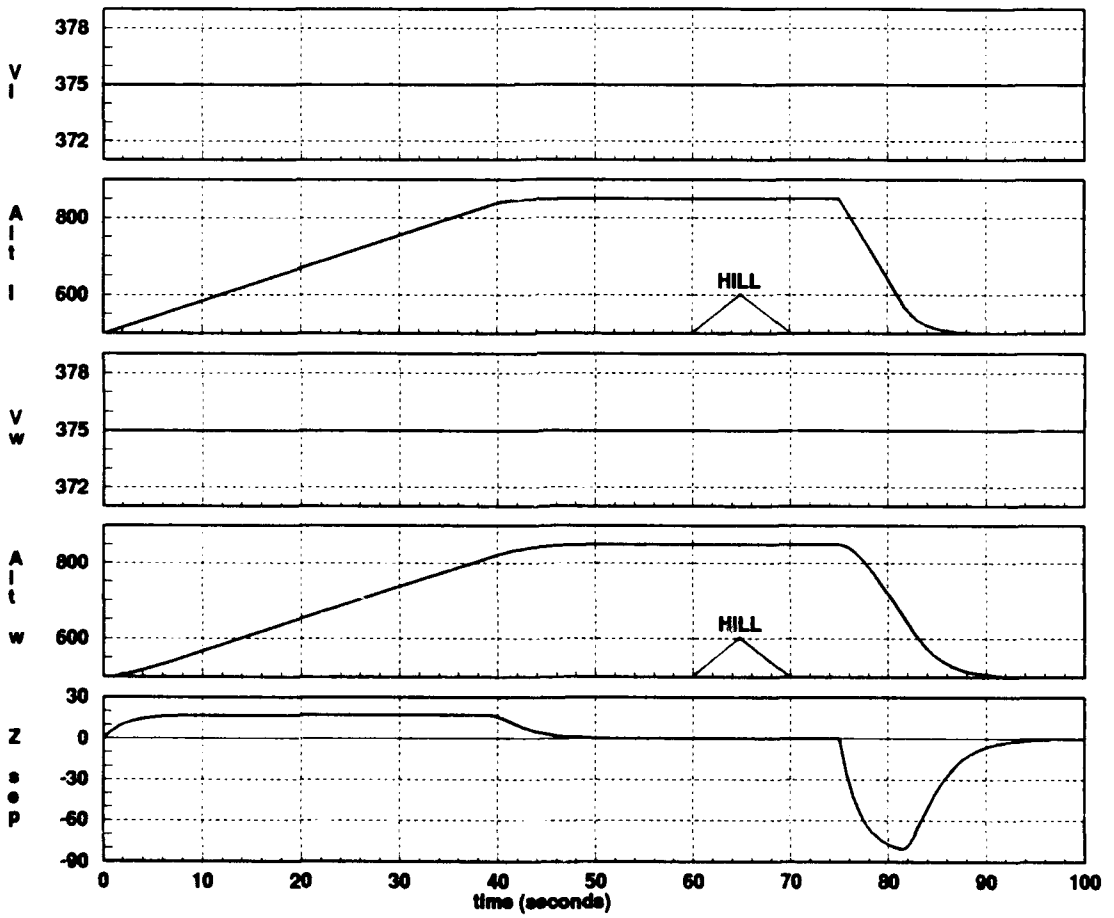

Figure C.9. Time Response for a Terrain Avoidance Maneuver

Appendix D. **Review of Results**

A review of the results given in Chapter V - Appendix C shows that zero steady state error is obtained for all tests. However, transient responses depend upon the configuration of the formation system. A formation system comprised of dissimilar aircraft in which the lead aircraft has a performance capability which is superior to that of the wing leads to larger transient responses. This is particularly evident for large commanded inputs such as a 45 degree heading change. The time responses are more apt to reach saturation for this type of formation system configuration. A formation comprised of dissimilar aircraft in which the lead aircraft has a degraded performance capability compared to that of the wing aircraft leads to smaller transient responses. A comparison of the 45 degree heading input in Chapter V with that in Appendix B illustrates this point. A formation control system comprised of similar aircraft with superior performance capability produces smaller transients than a configuration with a superior lead aircraft and inferior wing aircraft. A formation control system comprised of similar aircraft with degraded performance capability produces smaller transients than a configuration with an inferior lead aircraft and a superior wing aircraft.

Bibliography

1. Blakelock, John H. *Automatic Control of Aircraft and Missiles* (Second Edition). John Wiley and Sons, Inc., 1991.
2. Brentnall, B. "The Joint Tactical Information Distribution System (JTIDS)," *IEEE Transactions on Information Theory, 18*: 1-12 (1975).
3. D'Azzo, John J., and Constantine Houpis. *Linear Control System Analysis and Design.* NY: McGraw-Hill, 1988.
4. Geiselhart, R. *A Simulation Study of the Use of JTIDS in Tactical Missions*, Aeronautical Systems Division Technical Report 81-5014. Wright-Patterson AFB OH, September 1981.
5. Harrison, Scott. *Throughput and Delay Characteristics for a Slow-Frequency Hopped Aircraft-to-Aircraft Packet Radio Network.* MS Thesis, AFIT/GCS/ENG/90M-01. School of Engineering, Air Force Institute of Technology (AU), Wright-Patterson AFB OH, March 1990.
6. Hartley, Gerald A. *Automatic Formation Control of Full-Scale Aircraft Targets*, Naval Weapons Center Technical Publication 6670. Naval weapons Center, China Lake CA, September 1985.
7. Pachter, Meir. Professor. Personal interviews. School of Engineering, Air Force Institute of Technology (AU), Wright-Patterson AFB, OH, March through November 1991.
8. Porter, B. and A. Bradshaw. "Design of Linear Multivariable Continuous-Time Tracking Systems," *Int. J. Syst. Sci, 5*: 1155-1164 (1974).
9. Porter, B. and A. Bradshaw. "Singular Pertubation Methods in the Design of Tracking Systems Incorporating Inner-Loop Compensators and High-Gain Error-Actuated Controllers," *Int. J. Syst. Sci, 12*: 1193-1205 (1981).
10. Rohs, Paul. *A Fully Coupled, Automated Formation Control System for Dissimilar Aircraft in Maneuvering, Formation Flight.* MS Thesis, AFIT/GE/ENG/91M-03. School of Engineering, Air Force Institute of Technology (AU), Wright-Patterson AFB OH, March 1991.
11. Smitchens, Aivars. Program Manager, Intraformation Positioning System Program, Flight Controls Division, Flight Dynamics Laboratory. Personal Interviews. Wright Laboratories, Wright-Patterson AFB OH, March 1991 - April 1991.
12. Wellinger, D. *Army Formation Flight Study: Final Report, Report Number 6*, Contract Number DA-36-039-AMC-03367(E). Burlington, Massachusetts: Radio Corporation of America, Defense Electronic Products, Aerospace Systems Division, February 1965.